APPENDIX D
Hydraulics and Hydrology Analysis
For the Cat Island Chain
GREEN BAY HARBOR DMMP

APPENDIX D
Hydraulics and Hydrology Analysis
For the Cat Island Chain
Green Bay Harbor DMMP

Table of Contents

1.0 INTRODUCTION AND BACKGROUND 1
2.0 DATA GATHERING 2
2.1 Bathymetry 2
2.2 GIS Data Sets 7
2.3 Sediment & Water Characteristics 7
2.3.1 Green Bay Lake Bottom Sediment Samples 7
2.3.2 Total Suspended Sediment Samples 7
2.3.3 Lake Levels and Storm Surge 7
2.3.4 Wave Data 9
2.4 Vegetation Survey 12
3.0 GEOMORPHIC ASSESSMENT 12
4.0 PHYSICAL MODEL STUDY 28
4.1 Model Objectives 28
4.2 Model Facilities, Design and Construction 28
4.3 Overview of Model Testing Program 31
4.4 Model Material Characteristics 32
4.5 Key Model Results 35
4.5.1 Beaches 35
4.5.2 Revetments 42
4.6 Model Scale Effects and Interpretation 46

APPENDIX D
Hydraulics and Hydrology Analysis
For the Cat Island Chain
Green Bay Harbor DMMP

Table of Contents

5.0 WAVE GENERATION AND TRANSFORMATION MODELING..... 49
5.1 Wave Generation Modeling..... 49
5.2 Wave Transformation Modeling 53
5.2.1 Extreme Event Simulations 54
5.2.3 Growing Season Event Simulations 55
6.0 HYDRODYNAMIC ANALYSIS 58
6.1 MIKE 21 Hydrodynamic Model 58
6.2 Surge Event Simulations 59
6.3 Dredge Sand Beach Sections 65
7.0 MODELING TOTAL SUSPENDED SOLIDS..... 67
7.1 Introduction..... 67
7.2 Model Approach, Setup and Inputs 67
7.2.1 Modeling Approach 67
7.2.2 MT Model Parameters..... 68
7.2.3 Incoming Sediment From Rivers 69
7.2 Selection of Testing Scenarios 70
7.3 Model Testing and Calibration..... 71
7.4 Model Results 72
7.5.1 Individual Island Tests..... 73
7.5.2 All Islands..... 73
7.5.3 All Island with Shore Connection..... 74
7.5 Interpretation of Findings 74

1.0 Introduction and background

This appendix is a comprehensive hydrologic analysis that is an excerpt of the *Design Development Report on the Cat Island Chain Restoration* prepared by Baird & Associated for the Army Corps of Engineers, dated 2005.

The Cat Island Chain is located in Green Bay, Wisconsin. In the early 1970's the Cat Island Chain was severely eroded leaving a series of shoals mostly below low water datum. The US Army Corps of Engineers, US Fish & Wildlife and Brown County plan to restore the island chain.

The benefits of restoring the islands are threefold:

- Creating the conditions for re-establishment of emergent and submerged aquatic vegetation southwest of the Cat Island Chain;
- Providing capacity for placement of clean dredge spoils of Green Bay Federal Shipping Channel dredging activities;
- Restoring habitat associated with the islands.

A concept evaluation and initial design development report (Baird, 2002) was performed by Baird & Associates. The 2002 report documents conceptual coastal design of the islands, construction issues, and recommendations for subsequent phases. An initial report titled Cat Island Geomorphic Analysis (Baird, 2003) was also issued as part of Phase A of this study. The 2003 report included documentation regarding obtaining hydrographic survey data and a geomorphic analysis of shorelines along the southern edge of Green Bay.

This report was also completed by Baird & Associates and its purpose is to document design development activities completed since the 2003 report for the restoration of the Cat Island Chain. The information in this report supersedes that of the 2003 report. This report is divided into the following sections:

- Data Gathering
- Physical Modeling
- Numerical Modeling of Waves, Hydrodynamics and Sediment Transport
- Geomorphic Assessment
- Vegetation Stability Analysis

2.0 Data gathering

2.1 Bathymetry

Bathymetry of the study area from 1943 was obtained from the NOAA GeoDAS digital survey DVD and also a 1997 US Army Corps of Engineers Survey. To complement the available data, Baird & Associates contracted Spatial Data Surveys, LLC, Verona, WI, to perform Topographic/bathymetric survey of the study area during September and October 2003. The survey was conducted using GPS RTK and Coastal Oceanographics' Hypack data collection survey techniques. Figure 2.1 shows a general overview and elevations of the south Green Bay area and Figure 2.2 shows the new survey data points as well as the 1943 survey data. In this figure the yellow line encompasses an overlapping area between the two surveys.

Additional topographic survey information was obtained from Brown County, WI. This information provided elevation detail for Long Tail Point.

Figure 2.3 shows a number of selected profiles across the survey area and Figure 2.4 shows their corresponding elevations. It may be seen that Cat Island is now a submerged feature below the 0.0 ft contour (see Profiles B through H). The area between Cat Island and Long Tail Point has mostly a constant depth of about 8 ft with the exception of the old dredge spoil mounds intersected by Profile F. Profile F also skirts the edge of the navigation channel and Profile G and H cross the channel. Profiles G and H also cut across Frying Pan shoal.

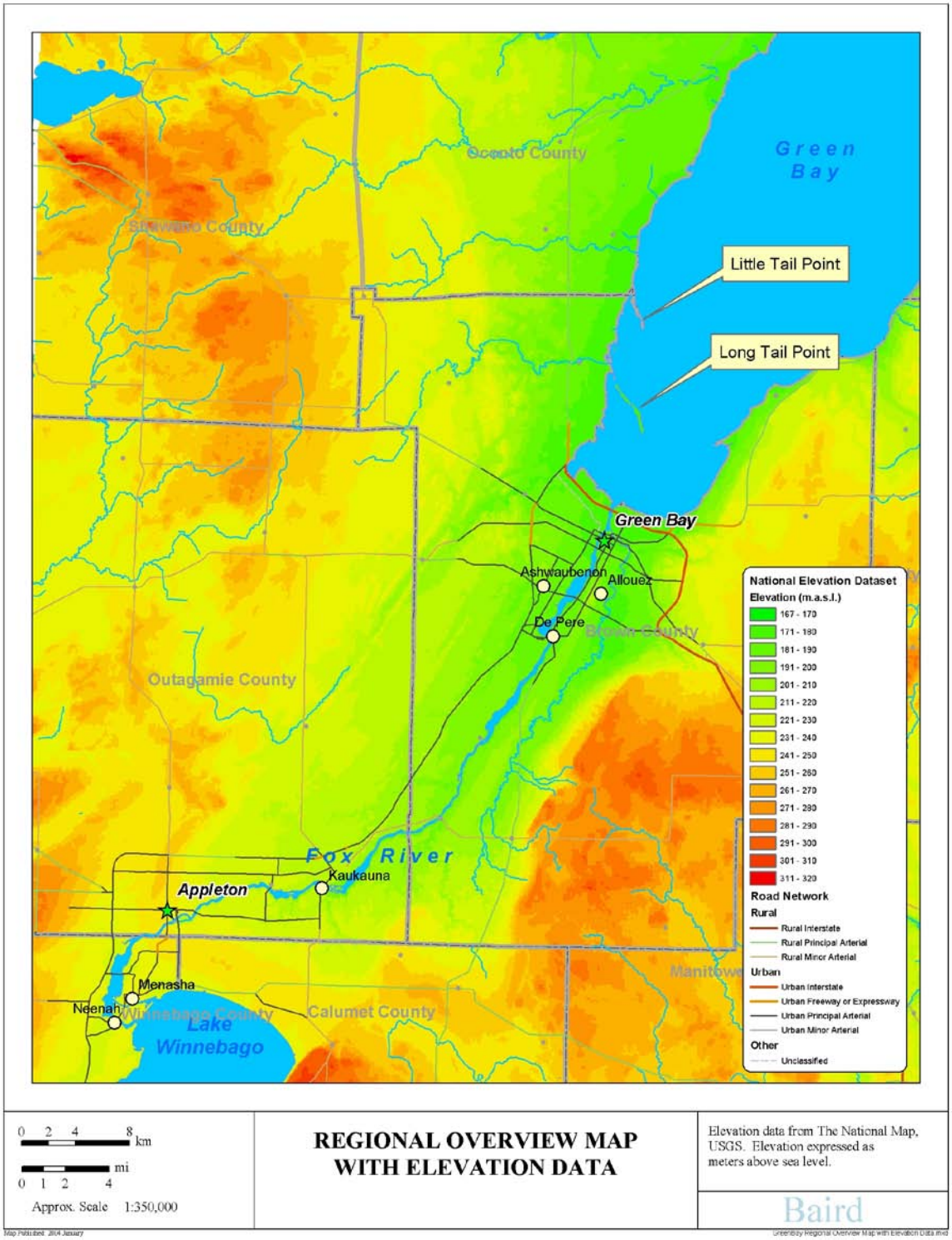

Figure 2.1 – Regional Overview Map with Elevation Data

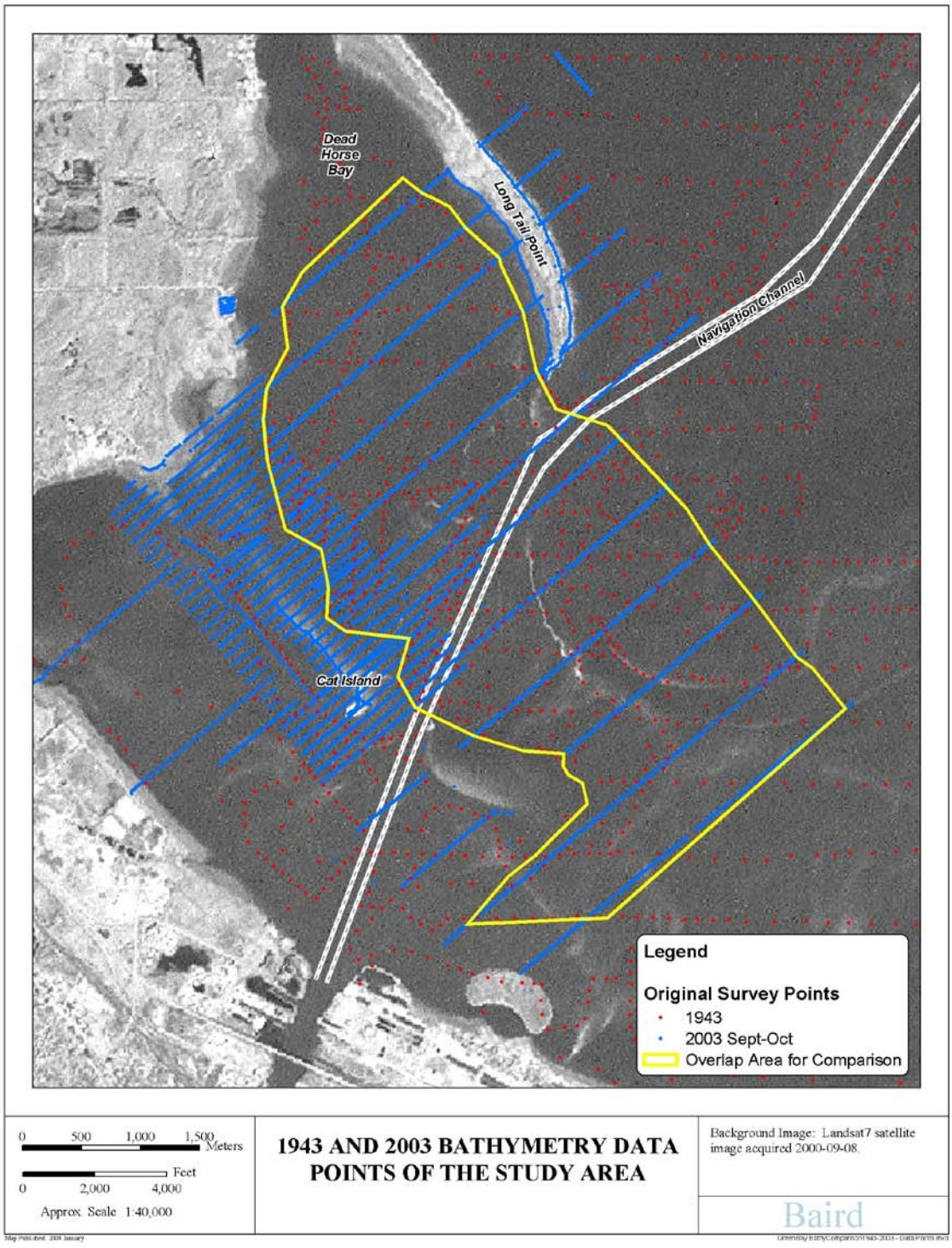

Figure 2.2 – 1943 and 2003 Bathymetry Data

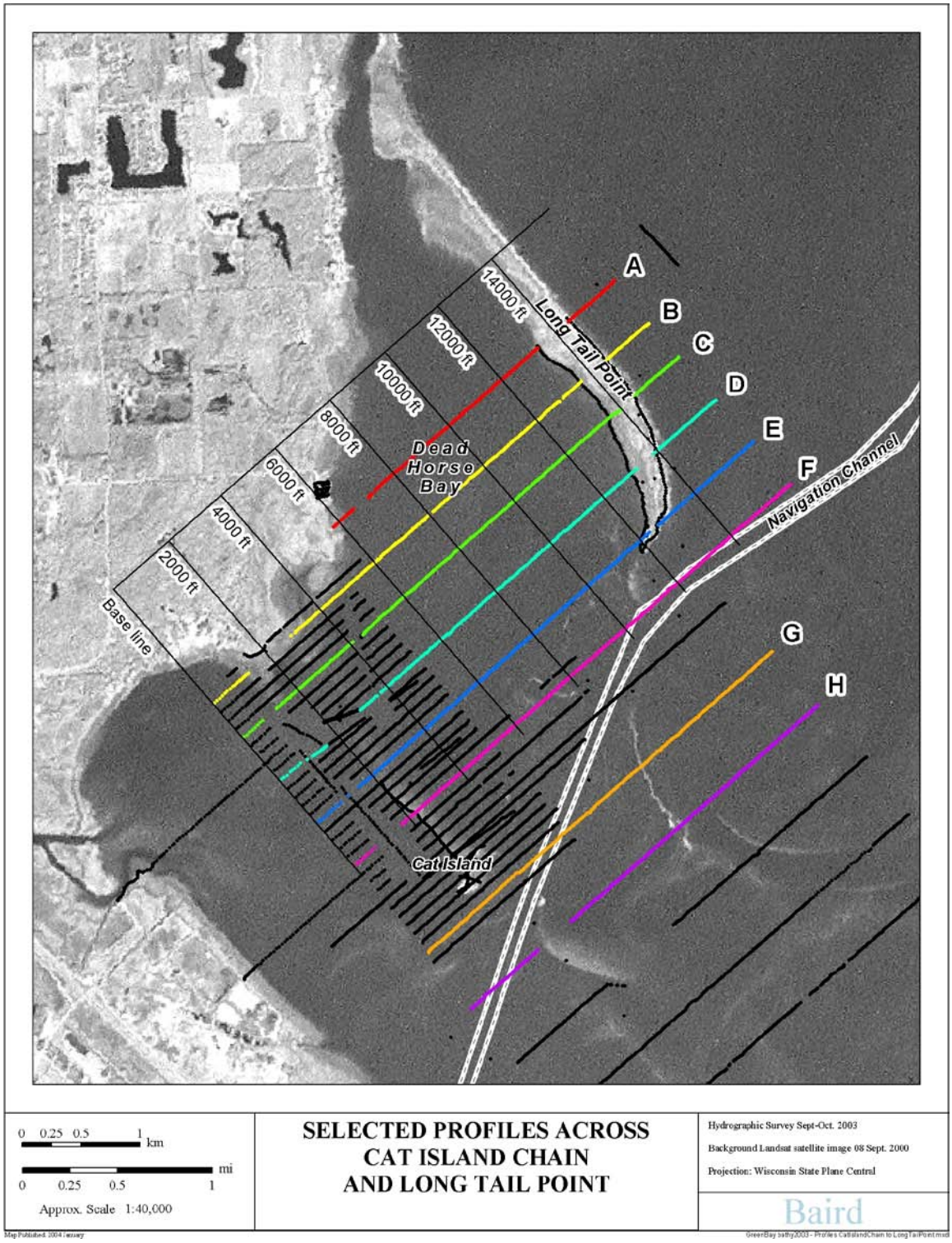

Figure 2.3 – Selected Profiles Across Cat Island Chain and Long Tail Point

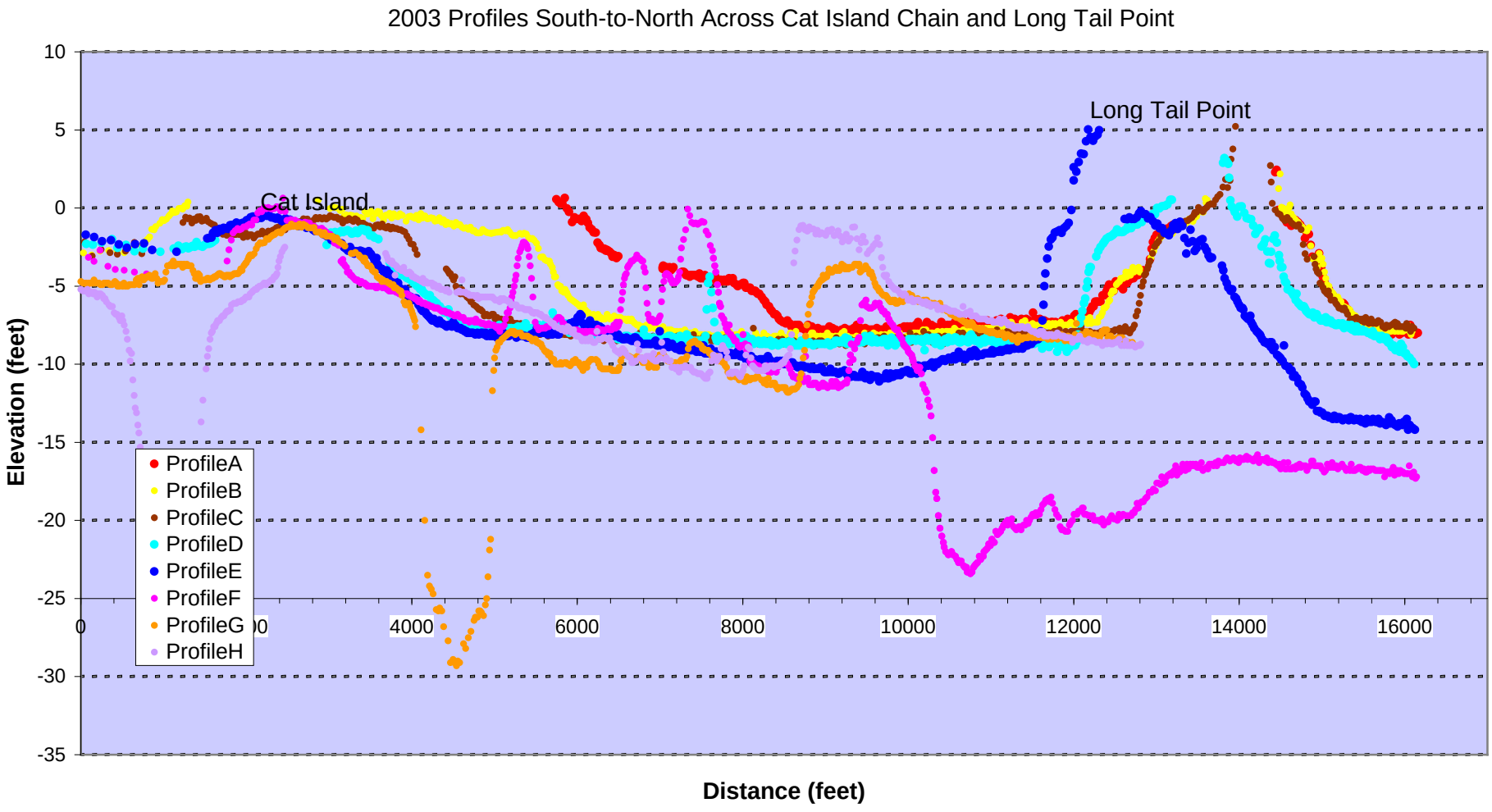

Figure 2.4 – 2003 Survey Profiles

2.2 GIS Data Sets

Historic air photos were acquired from the USGS EROS Data Center. The oldest available set was seven air photos captured on 28 June 1938 at a scale of 1:20,000. These were scanned at a resolution of 1200 dots per inch producing a nominal ground resolution of 0.5 meters. The photos were georegistered to within 10 meters using existing imagery as ground control.

Another set of historic air photos was available, captured on 11 May 1965 by the US Navy at an altitude of 20,000 feet, producing a 1:40,000 scale photo. These were scanned at a resolution of 1200 dots per inch producing a nominal ground resolution of 0.85 meters. The photos were georegistered to within 10 meters using existing imagery as ground control.

1992 Digital Orthophotos were purchased from the USGS, with a ground resolution of 1.0 meter.

Additionally, Landsat imagery was acquired from a variety of sources, including downloads from the University of Maryland's Global Land Cover archive. The imagery dates were 1988-05-17, 1989-09-18, 1999-07-27, and 2000-09-08.

2.3 Sediment & Water Characteristics

2.3.1 Green Bay Lake Bottom Sediment Samples

Acquisition and testing of sediment samples from the Green Bay Federal Channel were completed by Dodson-Stilson Inc. (DSI) between May 12 and 15, 1998. The sampling was completed to assess environmental impacts regarding possible disposal sites of the dredged material from the channel. Sampling sites and laboratory results can be found in the DSI report (DSI, 1998).

Several lake bottom samples were obtained during the hydrographic survey commissioned by Baird in 2003. Sample locations and grain size distribution curves are located in Appendix A.

2.3.2 Total Suspended Sediment Samples

Total Suspended Sediment (TSS) samples were collected by the Green Bay Metropolitan Sewerage District at several locations on the bay as part of the State of the Bay assessment. This sample information was utilized in the sediment transport analysis discussed in Section 7.0.

2.3.3 Lake Levels and Storm Surge

Water levels at Green Bay vary in response to long-term and seasonal variations in climate (as defined by monthly mean lake levels), as well as in response to specific storm events (i.e. localized, short-term storm surges associated with strong NE winds). Statistical analyses of water level data recorded by NOAA at Green Bay were undertaken in order to estimate extreme water levels by return period. This included a combined probability analysis of annual maximum (AMAX) lake levels (based on Lake Michigan gauge network data from 1918-2001) and annual maximum storm surges (based on analyses of hourly water level data at Green Bay from 1970-2002) using the HYDSTAT software package. The results of these analyses are summarized in Table 2.1.

Table 2.1
Extreme High Water Levels at Green Bay

Return Period (years)	Lake Level (ft LWD)	Storm Surge (ft)	Combined Water Level (ft LWD)
2	+2.1	2.2	+4.5
5	+3.2	2.8	+5.7
10	+3.8	3.3	+6.4
25	+4.3	4.1	**+7.1**
50	+4.6	4.7	+7.6
100	**+4.9**	**5.5**	+8.1
200	+5.1	6.3	+8.5
Max. on Record	**+4.9 (Oct. 1986)**	**5.5 (Dec. 3, 1990)**	**+7.3* (Apr. 9, 1973)**

*Note: water level gauge malfunctioned during Apr. 9, 1973 storm prior to peak surge; USGS (1976) suggests peak level of +7.3 ft LWD during this storm

The peak water level on record (estimated at +7.3 ft LWD) occurred during a severe storm event on April 9, 1973, with an estimated return period in the order of 30 years. This event caused severe flooding in Green Bay, with estimated property damage in the order of $6 million (Keillor, 1986), and resulted in severe erosion of the Cat Island chain. The mean lake level during this event was +3.6 ft LWD, with an estimated storm surge of 3.7 ft above the mean lake level for a peak elevation of 7.3 ft above LWD. Higher lake levels and larger storm surges are possible and have occurred. For example, Lake Michigan reached a record high of +4.9 ft LWD in October 1986, while a storm surge of 5.5 ft occurred at Green Bay during a storm on December 3, 1990. The estimated 100-year design water level, considering the combined occurrence of lake levels and surges, is +8.1 ft

LWD. This is almost one foot higher than the peak water level that occurred during the storm of April 9, 1973.

2.3.4 Wave Data

In order to obtain data for calibration of wave models used for design, two wave gauges were deployed. One gauge was located northeast of Long Tail Point, and the other northeast of Cat Island. A map depicting the gauge locations is shown in Figure 2.5.

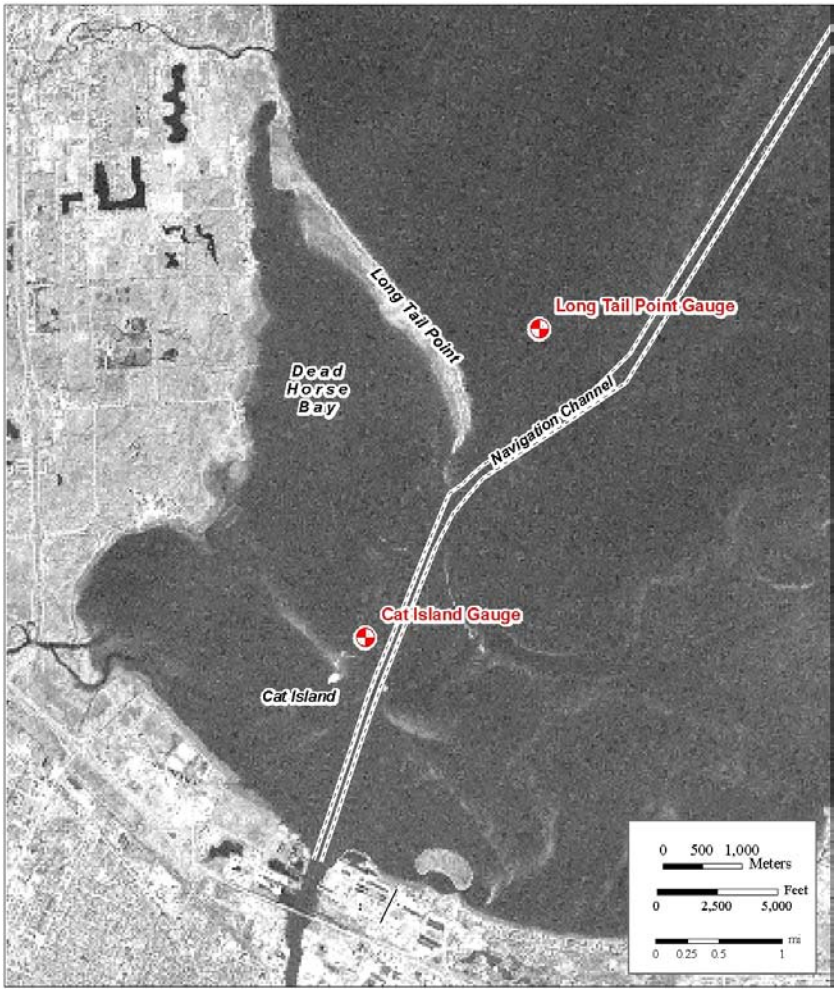

Figure 2.5 - Location of Wave Gauges

The wave gauges were deployed from March 25 to May 19, 2004. They were installed before total ice breakup in the upper bay in order to capture any large NE events that may have occurred immediately after the ice breakup. Ice breakup throughout the entire bay was estimated by satellite images to occur between April 6 and April 13, 2004. The gauges used were bottom mounted pressure gauges. Pressure records were transformed into wave records by linear wave theory. Graphs depicting the results of

the wave gauge records for the Long Tail Point Gauge and Cat Island Gauge are displayed respectively in Figures 2.6 and 2.7.

The largest wave height on record was approximately 0.8 m for the Long Tail Point Gauge and 0.3 m for the Cat Island Gauge. Although an extreme event was not observed during the deployment period, a better level of calibration was obtained through scaling of the winds used in the hindcast to determine design conditions. This is covered in further detail in Section 5.0.

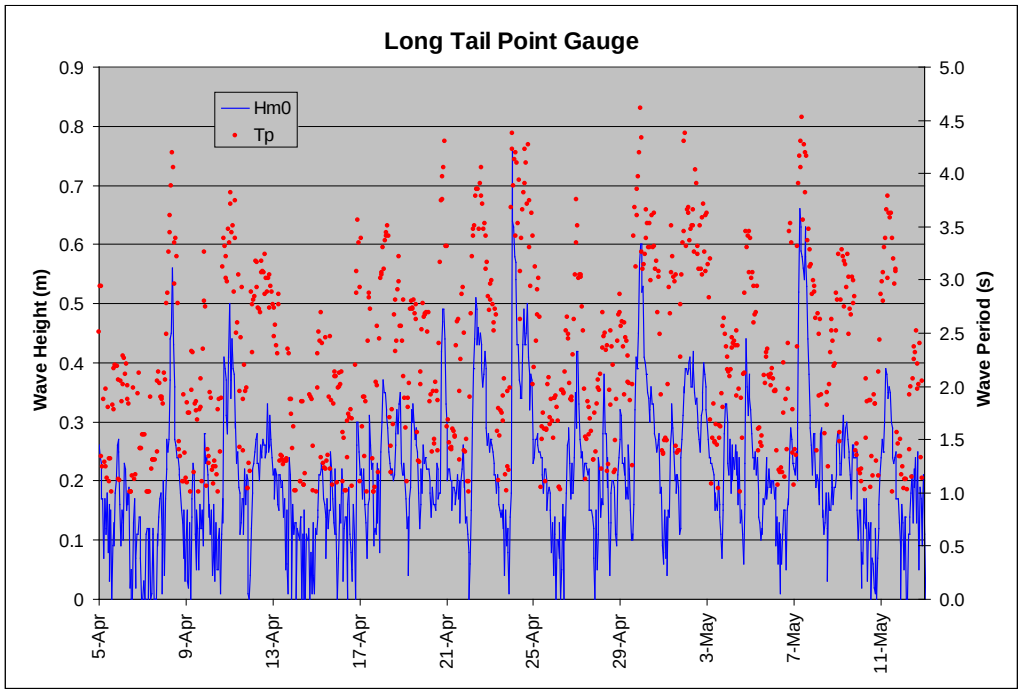

Figure 2.6 - Long Tail Point Wave Gauge Record

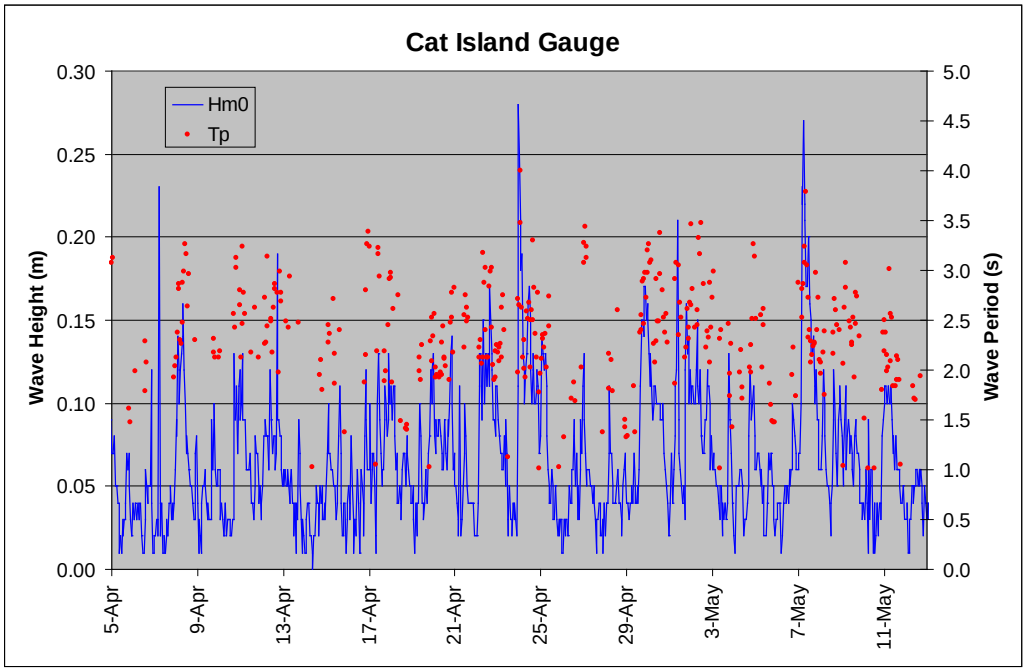

Figure 2.7 - Cat Island Wave Gauge Record

In addition to wind generated waves, ship generated waves were also observed at the site. As a ship passes by the Cat Islands through the shipping channel, the water is lowered around the islands. After the ship passes, a series of waves travel by the islands. Figure 2.8 displays a time series of a ship passing by the Cat Islands.

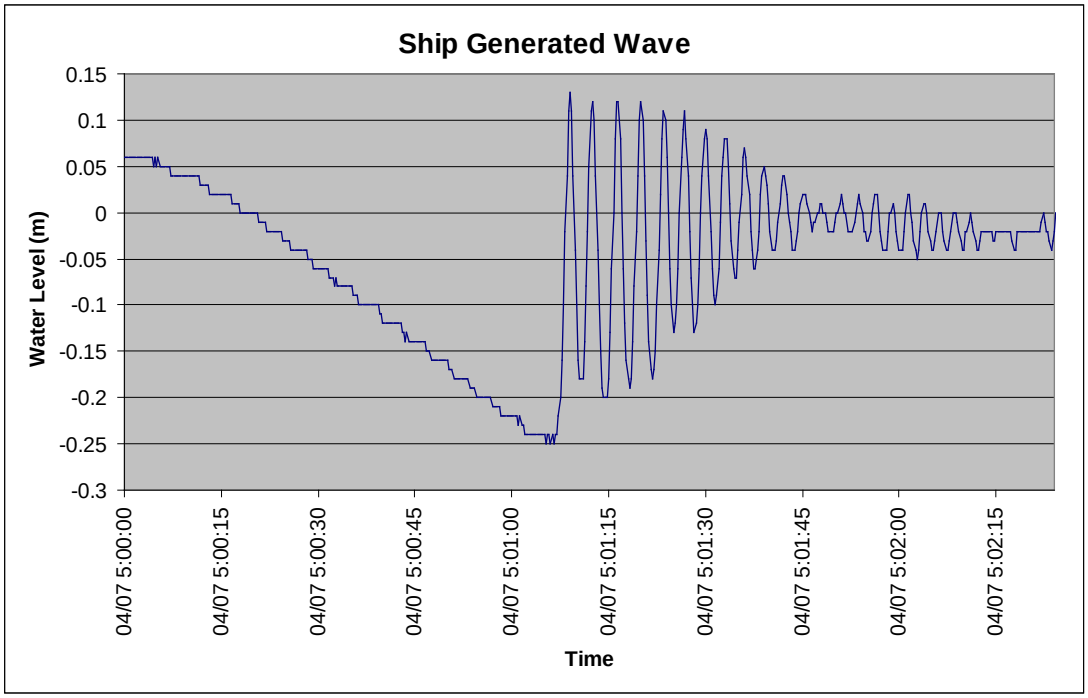

Figure 2.8 – Ship Wave at Cat Island

2.4 Vegetation Survey

USFW staff completed a reconnaissance survey of the vegetation communities on Long Tail Point to provide an indication of the role of wave exposure (see US exposed side) and land elevation on type of vegetation. The photos and their locations are provided in Appendix B.

3.0 Geomorphic Assessment

Three sets of air photos from June 28, 1938, May 11, 1965 and May 6, 1992 together with a Landsat 7 image from September 8, 2000 (15m resolution, Panchromatic Band 8) were georegistered in GIS to investigate the morphologic change on the lower part of Green Bay over past 60 years. Four series of shorelines were traced from the above photos in ArcMap. If the shoreline was not distinctive, it was not digitized.

Brown County contracted with Aerometric, Inc. of Sheboygan, WI to produce on orthophoto dataset, derived from 1" = 840' scale aerial photography that was flown in the spring of 2000. It was flown to provide six-inch ground resolution (or pixel) digital orthophotography coverage. This photo data were obtained subsequent to the completion of the geomorphic analysis and therefore have only be used as backdrop for various analyses and figures and not in the shoreline change assessment. The development of the orthophotography also resulted in the production of spot elevations and 2-foot elevation contours that were used along Long Tail Point to understand the Point's profile shape as part of the vegetation analysis (see Section 8 of this report).

Figure 3.1 shows the four digitized shorelines overlaid on the 1938 air photo. There are three distinct morphological features to consider in south Green Bay area: 1) Little Tail Point, 2) Long Tail Point and 3) Cat Island chain. The geomorphic history of these features has a geologic time scale. The fact that each feature is associated with a river (Little Suamico River, Suamico River and Duck Creek, respectively) suggests the possibility that they have been formed in part from the sediments delivered to the bay by these rivers. On the other hand, there is a smaller mirror image of Long Tail Point on the west side of the bay (Frying Pan Shoal) which indicates that these features might be the remnants of old coastal dunes/berms. Combined with isostatic rebound (in this area the land/lake bed is actually sinking at about 6 cm/century – see Baedke et al, 2004), rising or static levels on Lake Michigan over the past 5,000 years has resulted in gradual shifting of south shore of Green Bay towards the south due to gradual inundation. Figure 3.2 is the satellite image of Green Bay and indicates that similar features also exist on the west shores of the bay further north of the study area. As all the sediment is expected to move along the west and east shorelines of the bay and

deposit at its south end, it is possible that coastal dunes were established and then washed out at different stages of this long-term relative water level rise.

The area around Little Tail Point is shown in Figure 3.3. A number of longshore bars are observed around Little Tail Point indicating the sandy nature of this feature. Comparison of the four traced shorelines indicates that Little Tail Point has been relatively stable over the past 60 years. It should be mentioned that the location of each shoreline should be interpreted considering its corresponding lake level. The monthly mean level in Lake Michigan for June 1938, May 1965 and September 2000 was 176.28 m, 175.94 m and 176.09 m, respectively. The 1938, 1965 and 2000 shorelines therefore correspond to relatively low lake levels and can be compared relatively well without the need for water level correction. The mean lake level reached 176.53 m in May 1992 and explains why the Little Tail feature is narrow in the 1992 air photo. The 2003 hydrographic survey around Long Tail Point indicates a bottom slope of 1/100 on the north side and 1/200 on the south side of Long Tail. The corresponding information for Little Tail Point is not available but it is reasonable to assume they are similarly mild. Therefore, every 10 cm change in the water level roughly results in 30 m change in the dry (out of water) width of these spit features.

Figure 3.4 shows the traced shorelines on 1965 air photo. This is at the time of historic low water levels in Lake Michigan and therefore the three features are very prominent. Figures 3.5 and 3.6 show Cat Island and Long Tail Point in detail, respectively. It may be seen that there was little change in Cat Island between 1938 and 1965. The remnants of Cat Island in 1992 and 2000 images also do not indicate any change in their position. This may be attributed to the relatively calm wave climate in the area derived from the sheltering effect of Long Tail Point. Figure 3.5 also shows the dramatic demise of the Duck Creek wetland area after 1965 and most likely linked to the disappearance of the Cat Island chain in 1973.

Figure 3.6 shows the historic shorelines of Long Tail Point superimposed on the 1965 air photo. Again the 1938, 1965 and 2000 shorelines indicate that this area has experienced only minor changes over past 60 years. This is contrary to the findings of the previous report of October 31, 2002 in which, based on comparison between 1992 air photo and 1943 NOAA navigation chart, it was concluded that Long Tail Point has migrated inshore at a rate of 4 m/year in the last 60 years. The NOAA chart was compared to the present air photos in GIS and it was found that the boundaries of Long Tail Point shown in this chart are fairly rough and inaccurate (it is a navigation chart mostly concerned with the alignment of the navigation channel, which was indeed accurate).

In Figure 3.6 the shoreline of May 1992 reveals a gap between Long Tail Point and the shore (see also Figure 3.9). This is because of the higher water level at this time (176.53 m) when a section of the middle of the Tail was also submerged. This is very interesting, because the monthly mean water level in April 1973, when a storm is

believed to have destroyed Cat Island, was 177.1 m, i.e. about 60 cm above the May 1992 level. Adding the wave setup and surge to this high water level, it is likely that most of Long Tail Point was also submerged during this storm.

Figures 3.7 and 3.8 show the traced shorelines at Little Tail Point and Long Tail Point, respectively, on a Landsat 7 image taken in July 1999. The mean water level in this month was 176.41 m, which is very close to that of May 1992. It may be seen that the shoreline of 1992 (yellow line) closely follows the 1999 image in both figures indicating that the two features were fairly stable during the seven-year period of 1992 to 1999. Figure 3.8 shows Long Tail Point area shorelines on 1992 air photo, while Figure 3.10 shows the complete traced shorelines on Landsat image of September 2000.

The change in lakebed elevations determined by comparing bathymetry data of 1943 and 2003 is shown in Figure 3.11. The comparison is limited in accuracy because of the coarse grid spacing. Therefore, local areas of large erosion/deposition may be inaccurate and misleading. It may be seen that apart from areas along the navigation channel (related to small shifts in the channel alignment) there have not been any well-defined and significant changes in the bathymetry of the area. Most of the values are in the range of 1 to 2 feet, which is the expected accuracy of the present analysis, and therefore not very conclusive. In the lee of Long Tail Point there is a clear trend of deposition, presumably from sediment that is transported southward past the distant end of Long Tail Point. Also, between Cat Island and Long Tail Point there is a series of rises probably related to dredge spoil mounds from channel dredging. In general, it may be concluded that the area between Long Tail Point and Cat Island has been relatively stable over the past 60 years. The lakebed to the east of the navigation channel shows an overall erosion trend, possibly due to the channel intercepting a net westerly/southwesterly transport.

Figure 3.12 shows the lakebed change in the immediate vicinity of the former Cat Island Chain between the 1997 US Army Corps of Engineers hydrographic survey and the recent 2003 survey completed by Baird. It is evident that there has been very little change in the lakebed and that it may be considered relatively stable for this six-year period. A review of the two isolated areas of erosion and deposition revealed that these are probably not real and instead related the fact the lines for the two surveys were not coincident (i.e. one survey caught the hole between the old central and west islands and the other did not, and similarly one caught the edge of the remnant Cat Island and the other did not).

The stability of Long and Little Tail Points implies that there is a balance between incoming and outgoing sediment transport resulting in no change in morphology. In other words, the spit features are in dynamic equilibrium. This dynamic equilibrium will be maintained only as long as the incoming sediment supply matches the outgoing transport beyond the distal ends of the Points. In turn, this requires that supplies from local rivers and shoreline erosion be maintained. The stability of these features also

implies that wave overwash and related transgression of the features is a relatively infrequent.

In the previous report (October 2002) part of the dredge volumes from the navigation channel (adjacent to Long Tail Point) was linked to a southeastwardly longshore transport along Long Tail Point. The observation of a large area of deposition in the lee of the distal end of the Point would appear to confirm this hypothesis. Also, although it is not so evident for Long Tail Point (primarily because the 1938 air photo does not cover the distal end of the point and the water level during the 1965 photo was low), it is evident that the distal end of Little Tail Point is extending with time as one might expect. Certainly, the position of the old lighthouse at the end of Long Tail Point (located well north of the current distal end of the Point), the geomorphic similarity of this feature, and the fact that there is lake bed sedimentation (and significant dredging in this area of the navigation channel) all point to the ongoing extension of Long Tail Point towards the southeast. With time this is likely to lead to increased dredging requirements for the navigation channel in this area (providing no additional mitigative measures are undertaken).

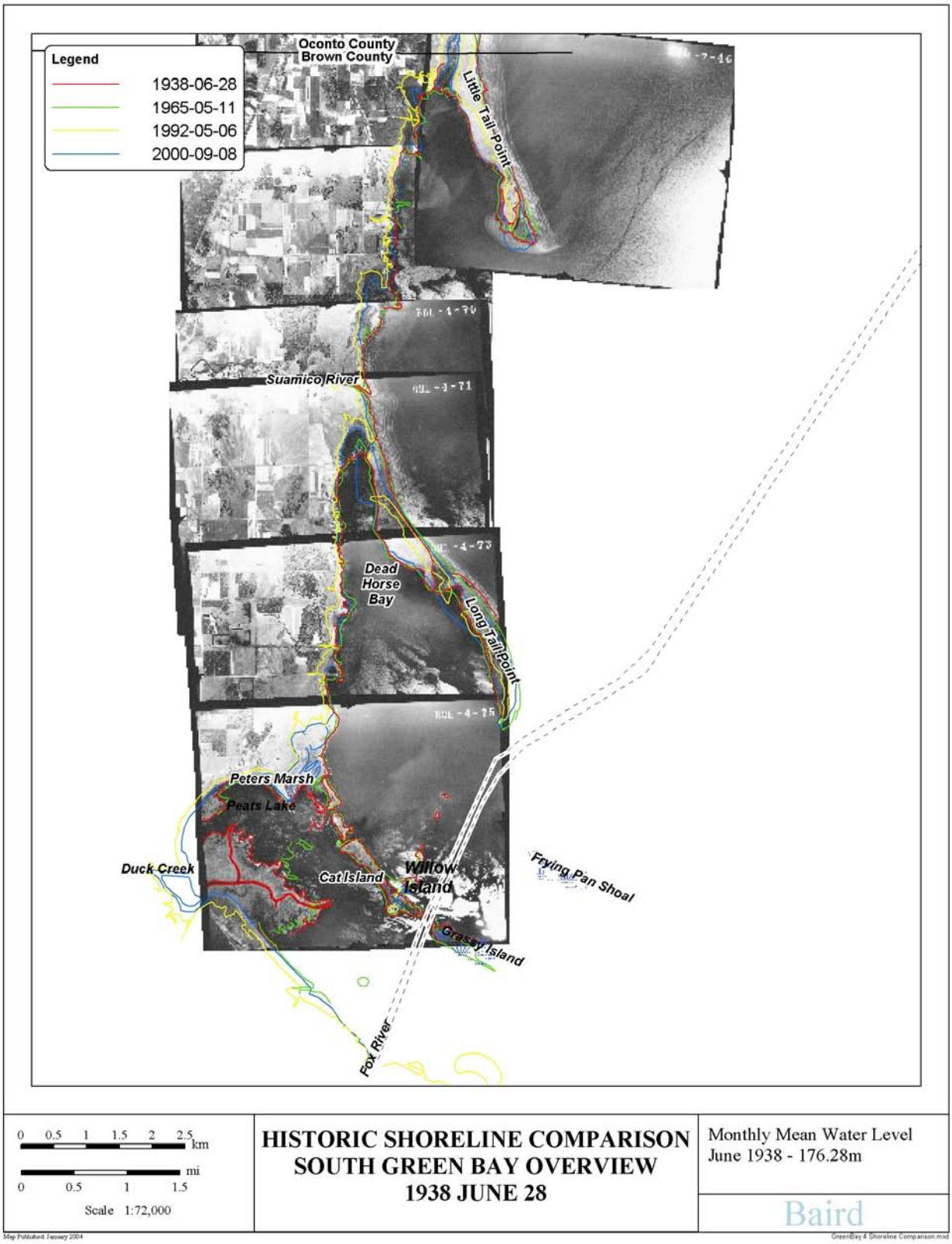
Legend
1938-06-28
1965-05-11
1992-05-06
2000-09-08
Oconto County
Brown County
Little Tail Point
Suamico River
Dead Horse Bay
Long Tail Point
Peters Marsh
Peats Lake
Duck Creek
Cat Island
Willow Island
Frying Pan Shoal
Grassy Island
Fox River
0 0.5 1 1.5 2 2.5 km
0 0.5 1 1.5 mi
Scale 1:72,000
HISTORIC SHORELINE COMPARISON
SOUTH GREEN BAY OVERVIEW
1938 JUNE 28
Monthly Mean Water Level
June 1938 - 176.28m
Baird

Figure 3.1

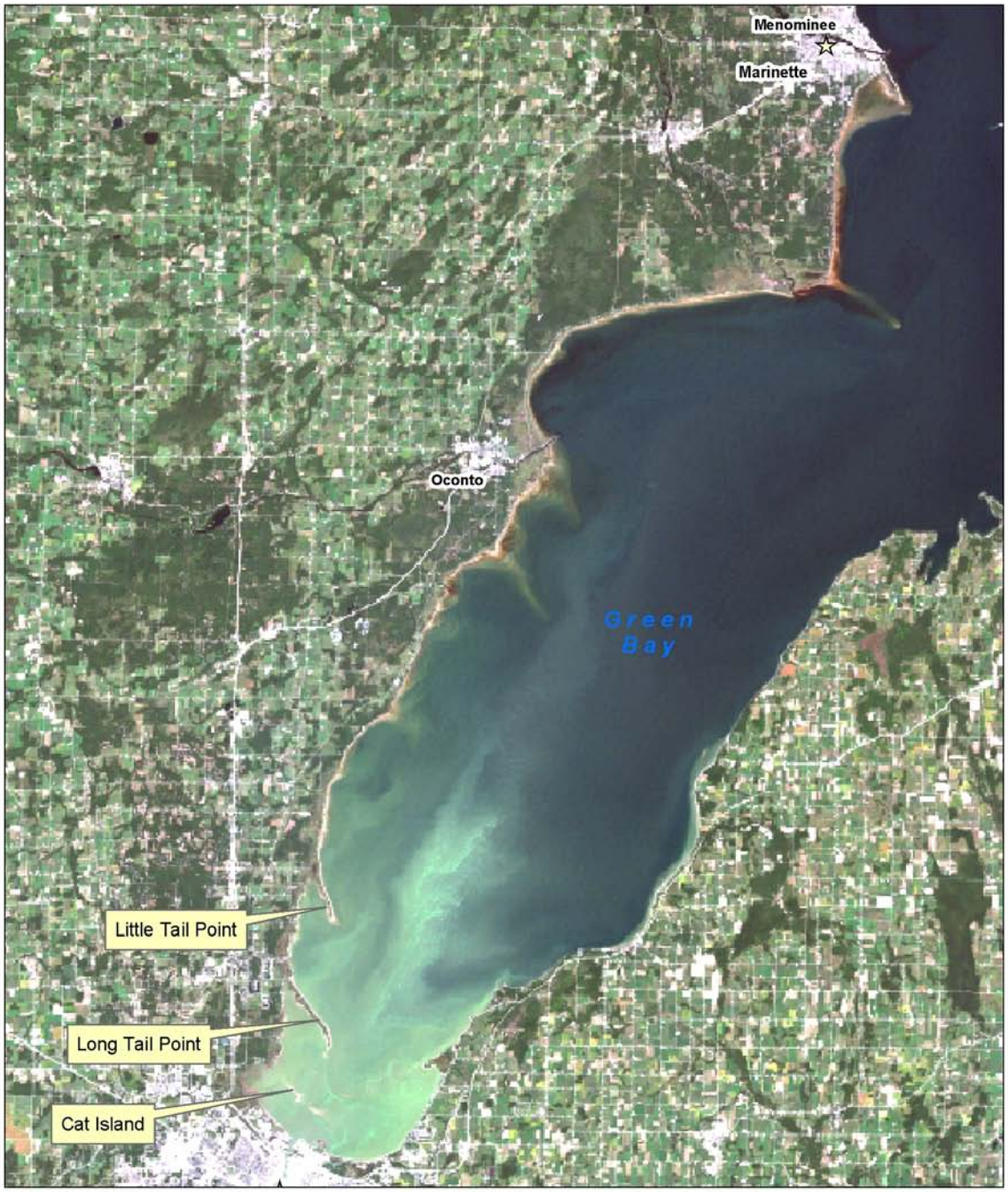

0 2 4 8 km

0 1 2 4 mi

Approx. Scale 1:300,000

SATELLITE IMAGE OF GREEN BAY AND THE STUDY AREA

Landsat 7 Satellite:
08 September 2000,
True Color (Bands 3-2-1),
Histogram Equalize, 2 Std. Dev.

Baird

Map Published: 2004 January

GreenBay Landsat Images - 2000-09-08.mxd

Figure 3.2

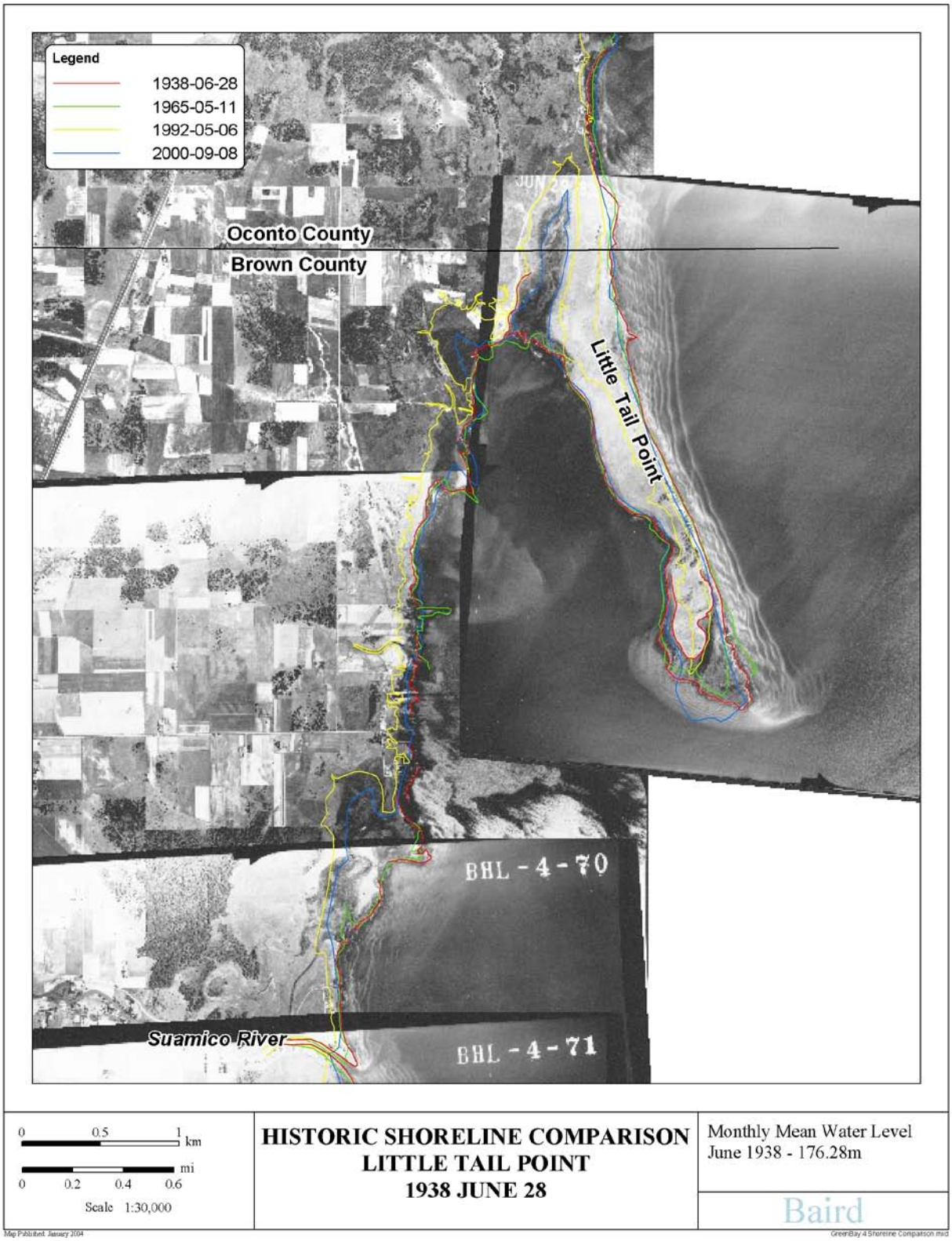
Legend
1938-06-28
1965-05-11
1992-05-06
2000-09-08
Oconto County
Brown County
Little Tail Point
BHL - 4 - 70
Suamico River
BHL - 4 - 71
0 0.5 1 km
0 0.2 0.4 0.6 mi
Scale 1:30,000
HISTORIC SHORELINE COMPARISON
LITTLE TAIL POINT
1938 JUNE 28
Monthly Mean Water Level
June 1938 - 176.28m
Baird
Map Published: January 2004
GreenBay 4 Shoreline Comparison.mxd

Figure 3.3

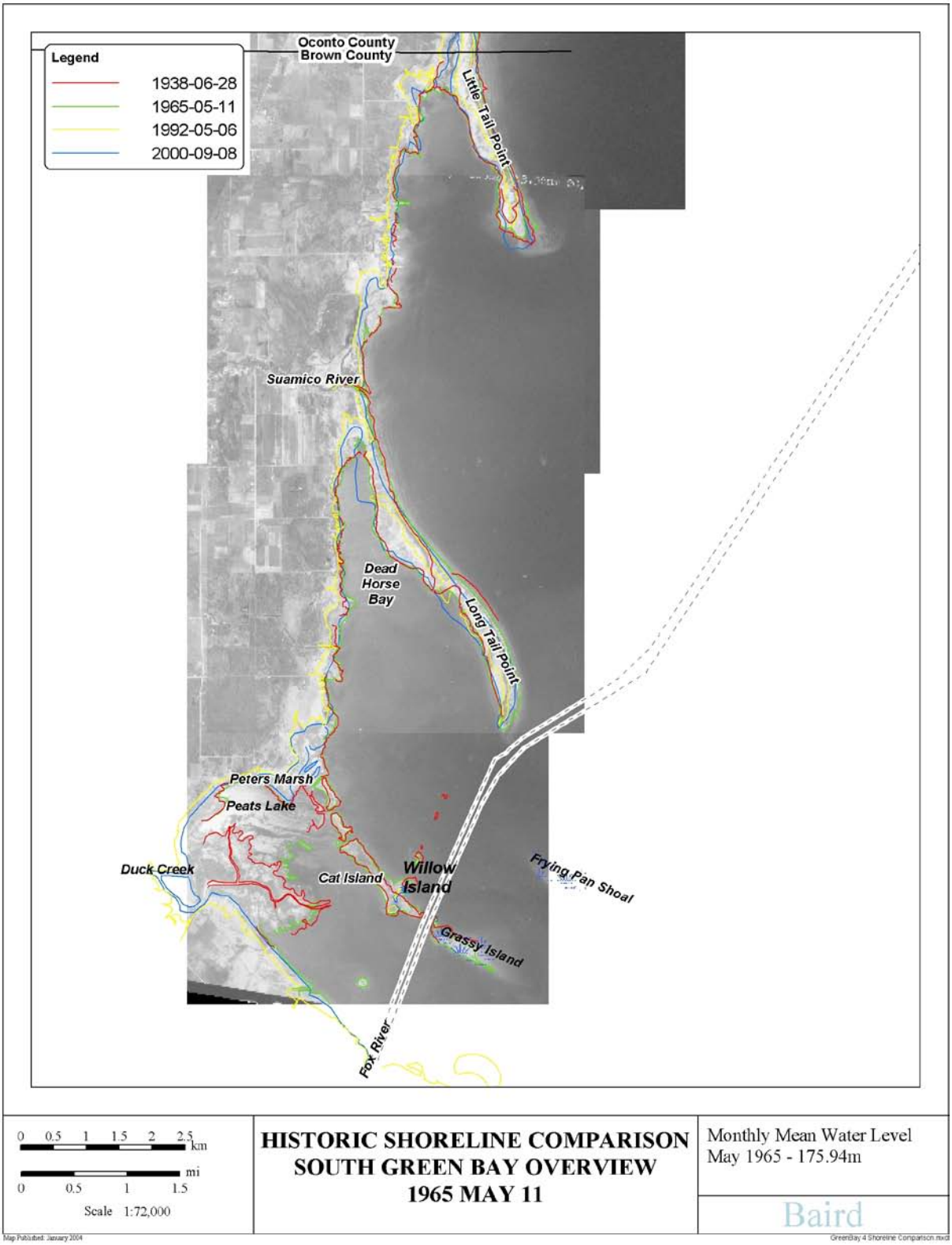
Legend
1938-06-28
1965-05-11
1992-05-06
2000-09-08
Oconto County
Brown County
Little Tail Point
Suamico River
Dead Horse Bay
Long Tail Point
Peters Marsh
Peats Lake
Duck Creek
Cat Island
Willow Island
Frying Pan Shoal
Grassy Island
Fox River
0 0.5 1 1.5 2 2.5 km
0 0.5 1 1.5 mi
Scale 1:72,000
HISTORIC SHORELINE COMPARISON
SOUTH GREEN BAY OVERVIEW
1965 MAY 11
Monthly Mean Water Level
May 1965 - 175.94m
Baird
Map Published: January 2004
GreenBay 4 Shoreline Comparison.mxd

Figure 3.4

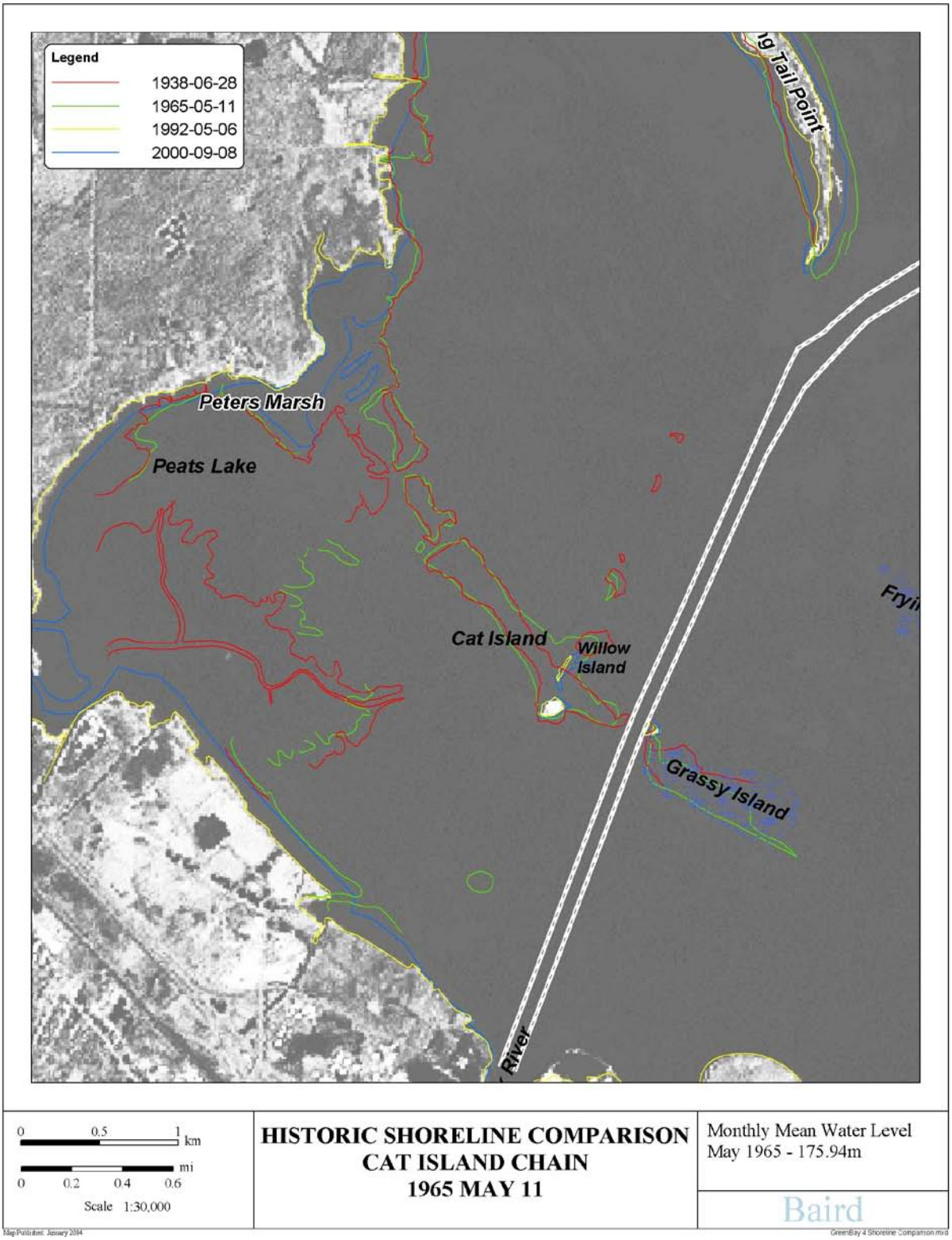
Legend
1938-06-28
1965-05-11
1992-05-06
2000-09-08
Peters Marsh
Peats Lake
Cat Island
Willow Island
Grassy Island
Tail Point
0 0.5 1 km
0 0.2 0.4 0.6 mi
Scale 1:30,000
HISTORIC SHORELINE COMPARISON
CAT ISLAND CHAIN
1965 MAY 11
Monthly Mean Water Level
May 1965 - 175.94m
Baird

Figure 3.5

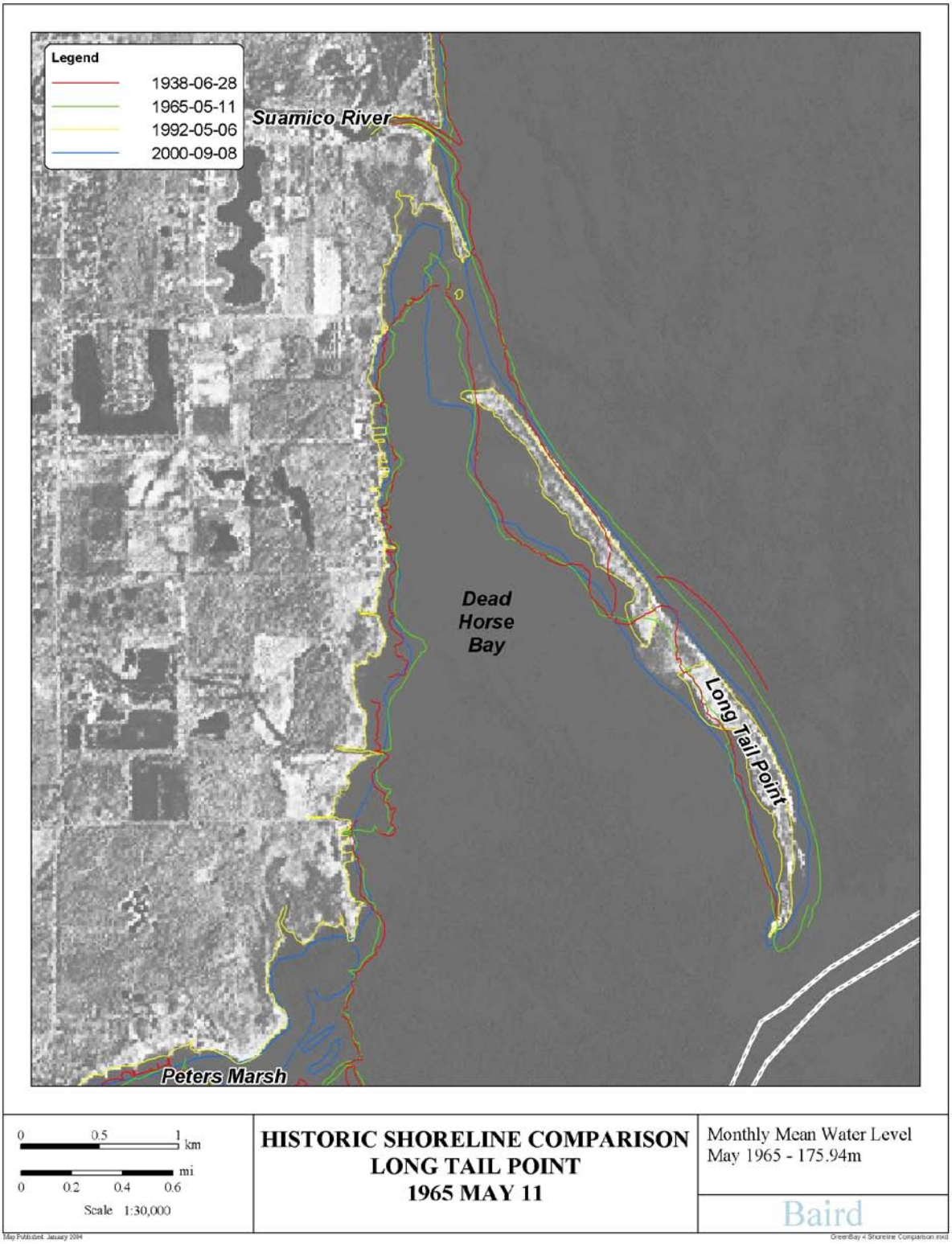
Legend
1938-06-28
1965-05-11
1992-05-06
2000-09-08
Suamico River
Dead Horse Bay
Long Tail Point
Peters Marsh
0 0.5 1 km
0 0.2 0.4 0.6 mi
Scale 1:30,000
HISTORIC SHORELINE COMPARISON
LONG TAIL POINT
1965 MAY 11
Monthly Mean Water Level
May 1965 - 175.94m
Baird

Figure 3.6

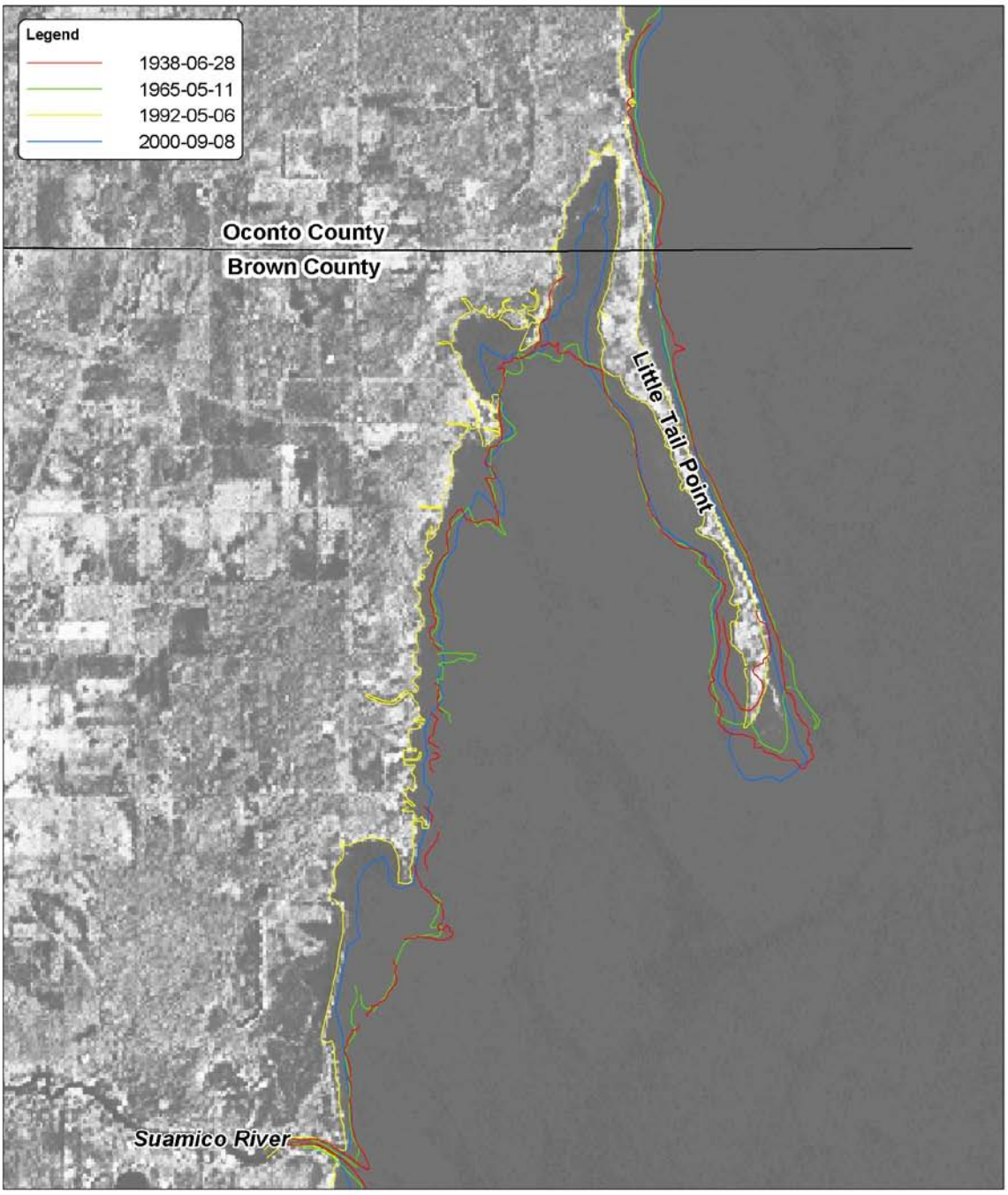

0 0.5 1 km

0 0.2 0.4 0.6 mi

Scale 1:30,000

HISTORIC SHORELINE COMPARISON
LITTLE TAIL POINT
LANDSAT - 1999 JULY 27

Monthly Mean Water Level
July 1999 - 176.41m

Baird

Map Published: January 2004

GreenBay 4 Shoreline Comparison.mxd

Figure 3.7

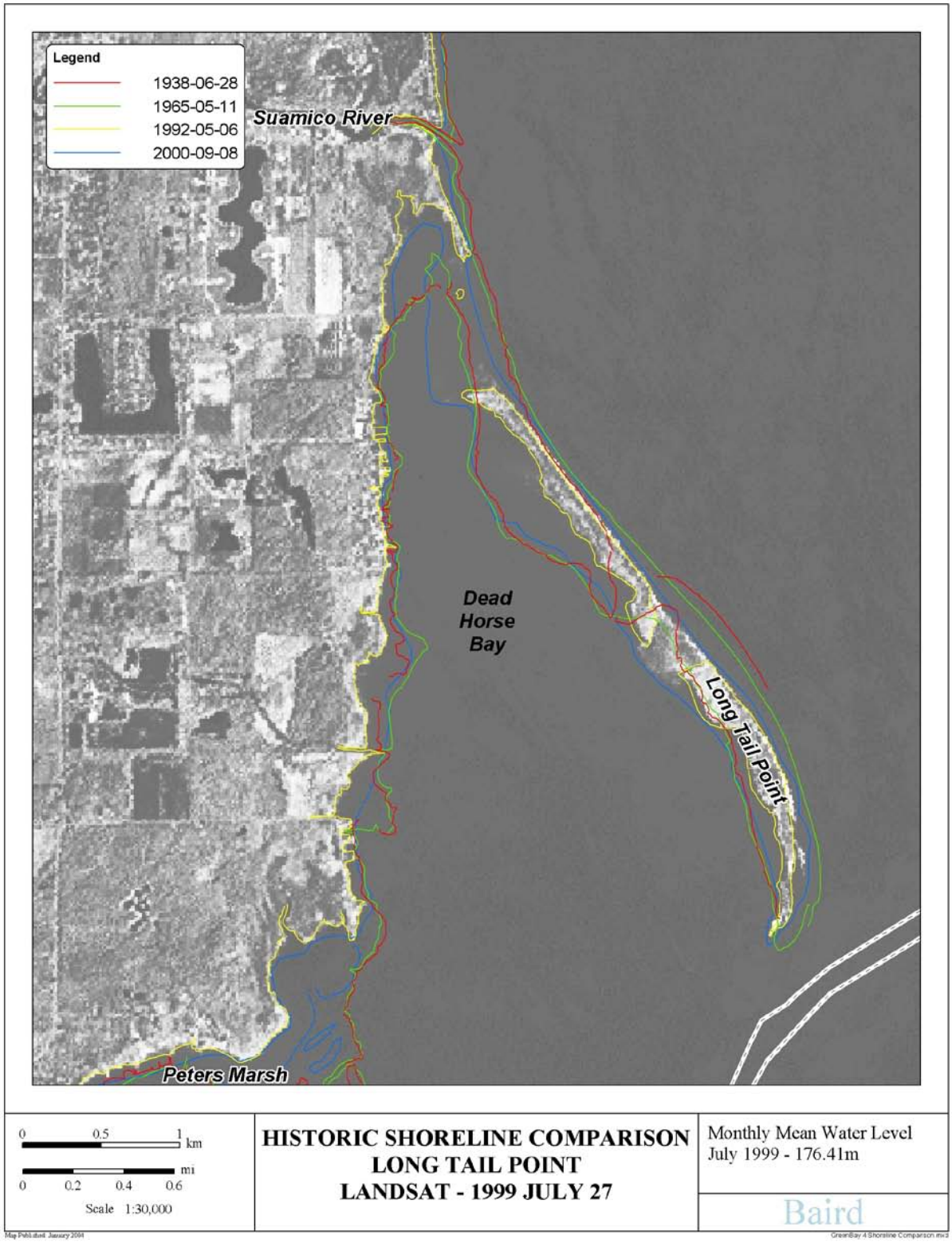
Legend
1938-06-28
1965-05-11
1992-05-06
2000-09-08
Suamico River
Dead Horse Bay
Long Tail Point
Peters Marsh
0 0.5 1 km
0 0.2 0.4 0.6 mi
Scale 1:30,000
HISTORIC SHORELINE COMPARISON
LONG TAIL POINT
LANDSAT - 1999 JULY 27
Monthly Mean Water Level
July 1999 - 176.41m
Baird

Figure 3.8

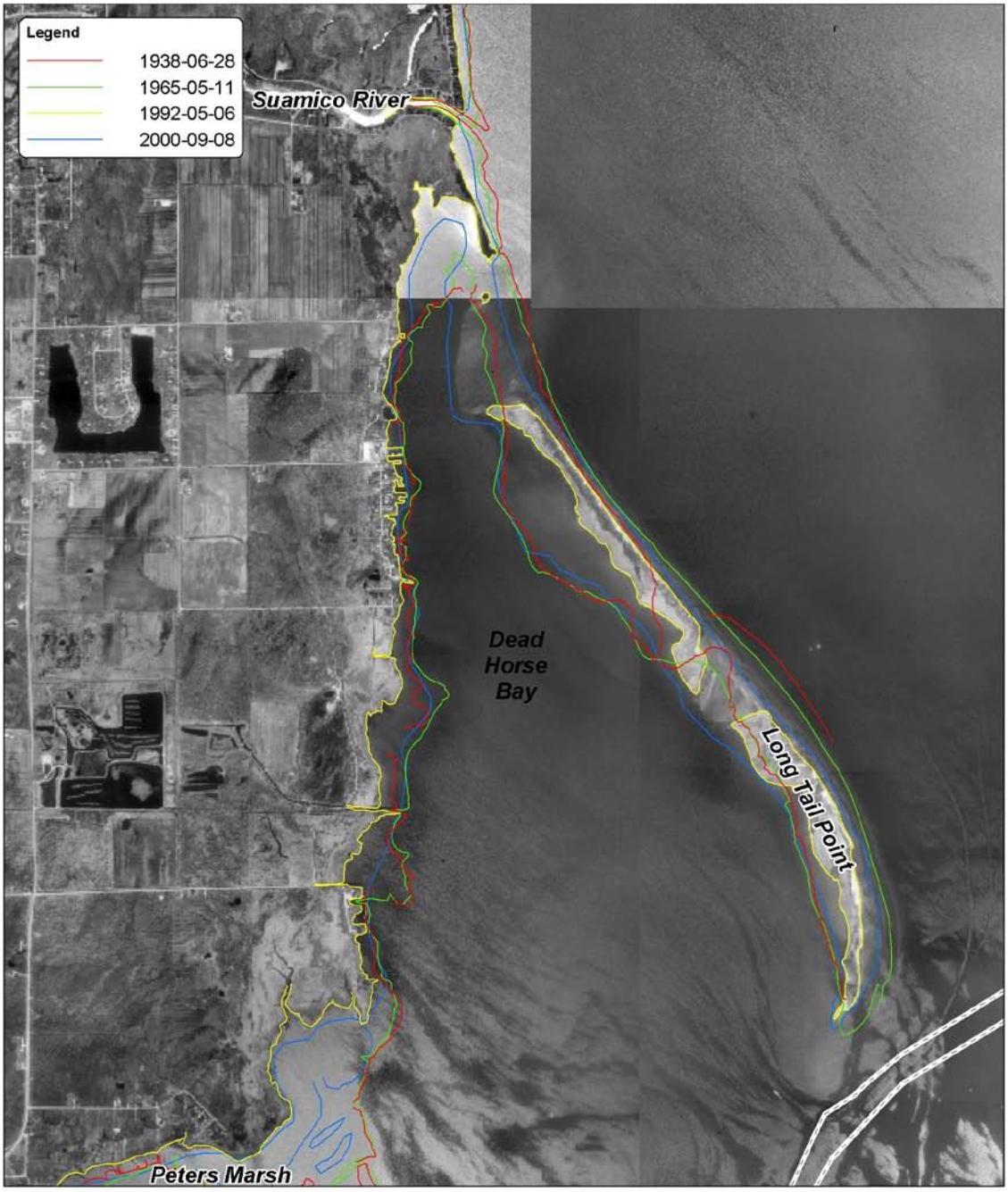

0 0.5 1 km

0 0.2 0.4 0.6 mi

Scale 1:30,000

HISTORIC SHORELINE COMPARISON
LONG TAIL POINT
1992 MAY 06

Monthly Mean Water Level
May 1992 - 176.53m

Baird

Map Published: January 2004

GreenBay 4 Shoreline Comparison.mxd

Figure 3.9

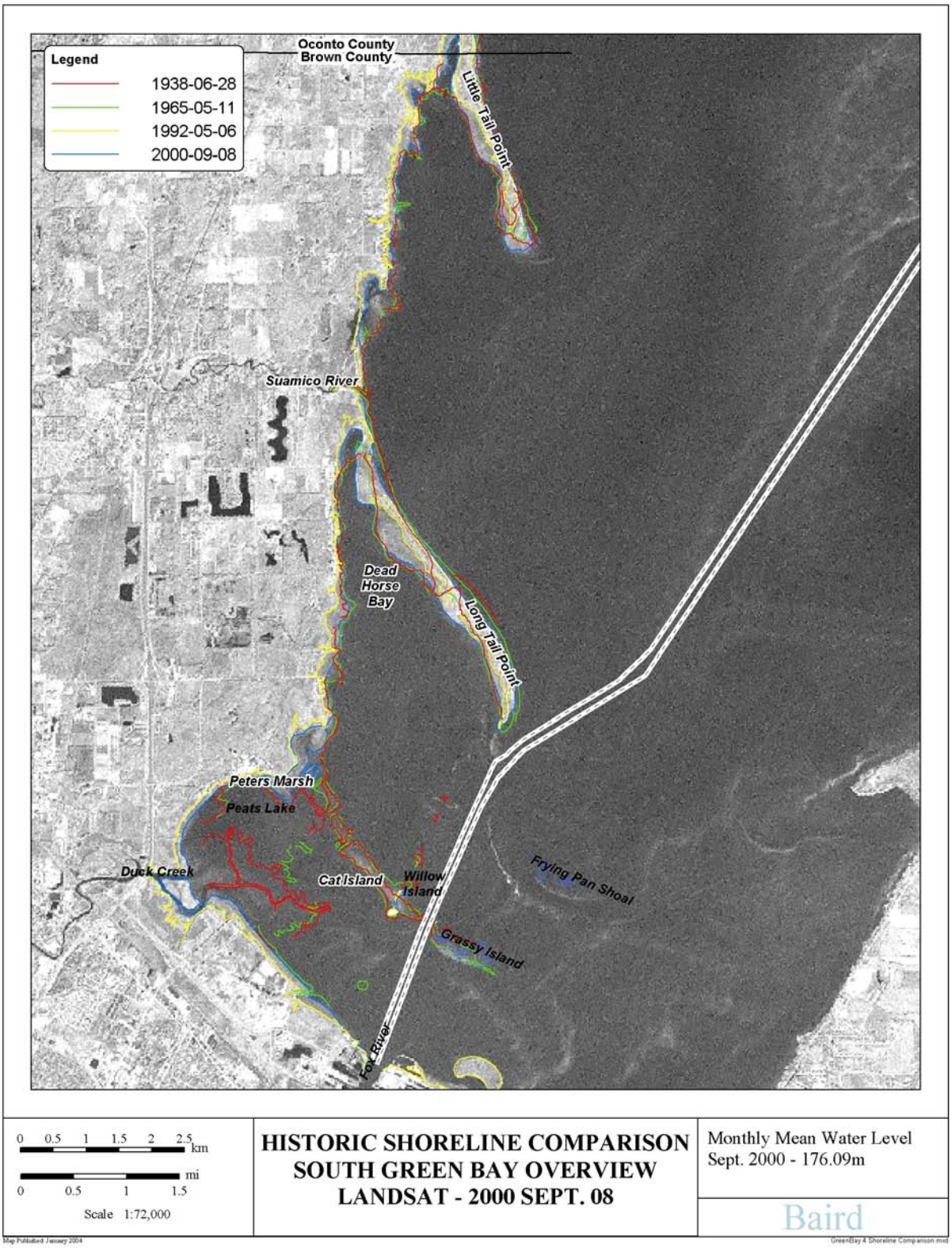
Legend
1938-06-28
1965-05-11
1992-05-06
2000-09-08
Oconto County
Brown County
Little Tail Point
Suamico River
Dead Horse Bay
Long Tail Point
Peters Marsh
Peats Lake
Duck Creek
Cat Island
Willow Island
Frying Pan Shoal
Grassy Island
Fox River
0 0.5 1 1.5 2 2.5 km
0 0.5 1 1.5 mi
Scale 1:72,000
HISTORIC SHORELINE COMPARISON
SOUTH GREEN BAY OVERVIEW
LANDSAT - 2000 SEPT. 08
Monthly Mean Water Level
Sept. 2000 - 176.09m
Baird

Figure 3.10

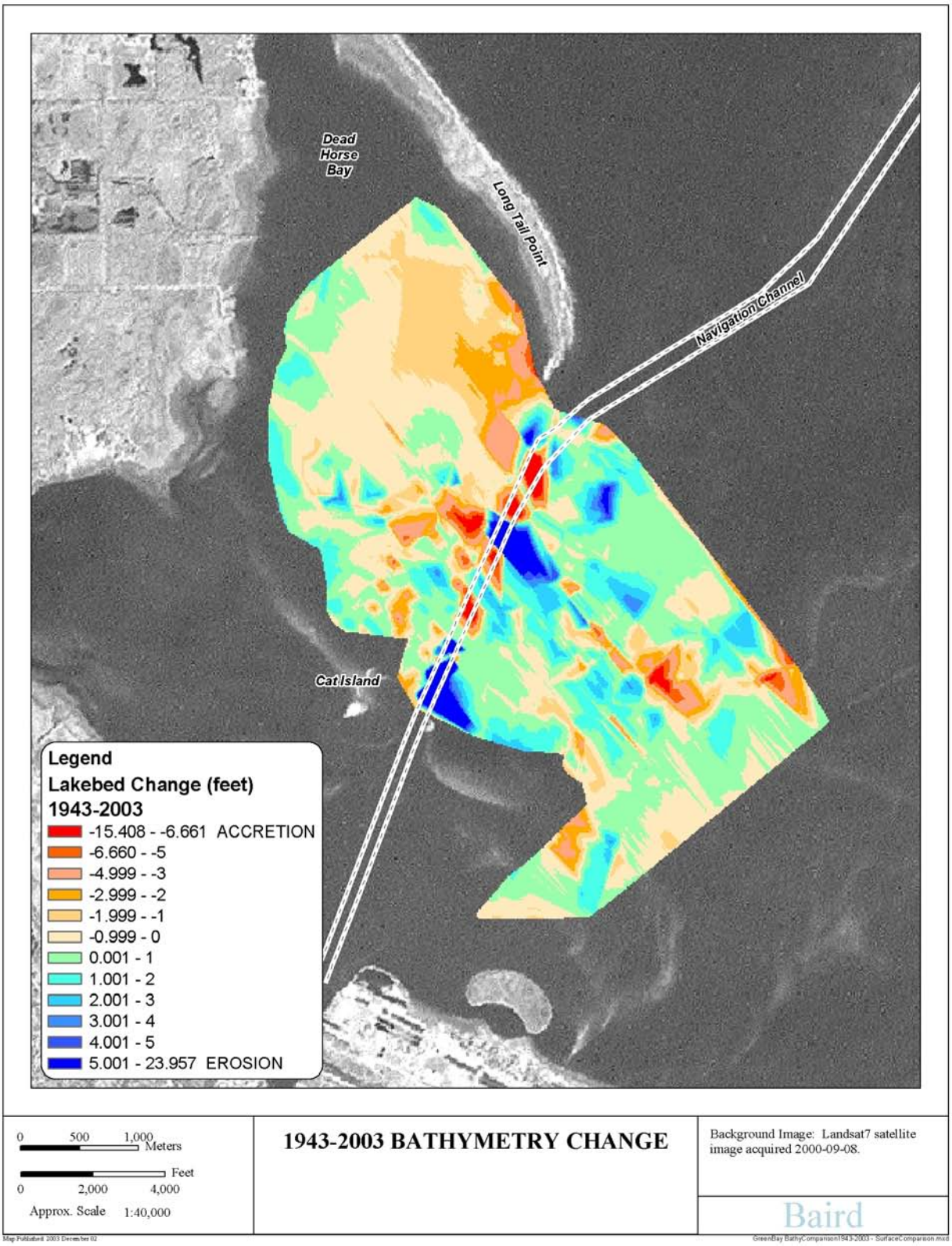
Dead Horse Bay
Long Tail Point
Navigation Channel
Cat Island
Legend
Lakebed Change (feet)
1943-2003
-15.408 - -6.661 ACCRETION
-6.660 - -5
-4.999 - -3
-2.999 - -2
-1.999 - -1
-0.999 - 0
0.001 - 1
1.001 - 2
2.001 - 3
3.001 - 4
4.001 - 5
5.001 - 23.957 EROSION
0 500 1,000 Meters
Feet
0 2,000 4,000
Approx. Scale 1:40,000
1943-2003 BATHYMETRY CHANGE
Background Image: Landsat7 satellite image acquired 2000-09-08.
Baird

Figure 3.11

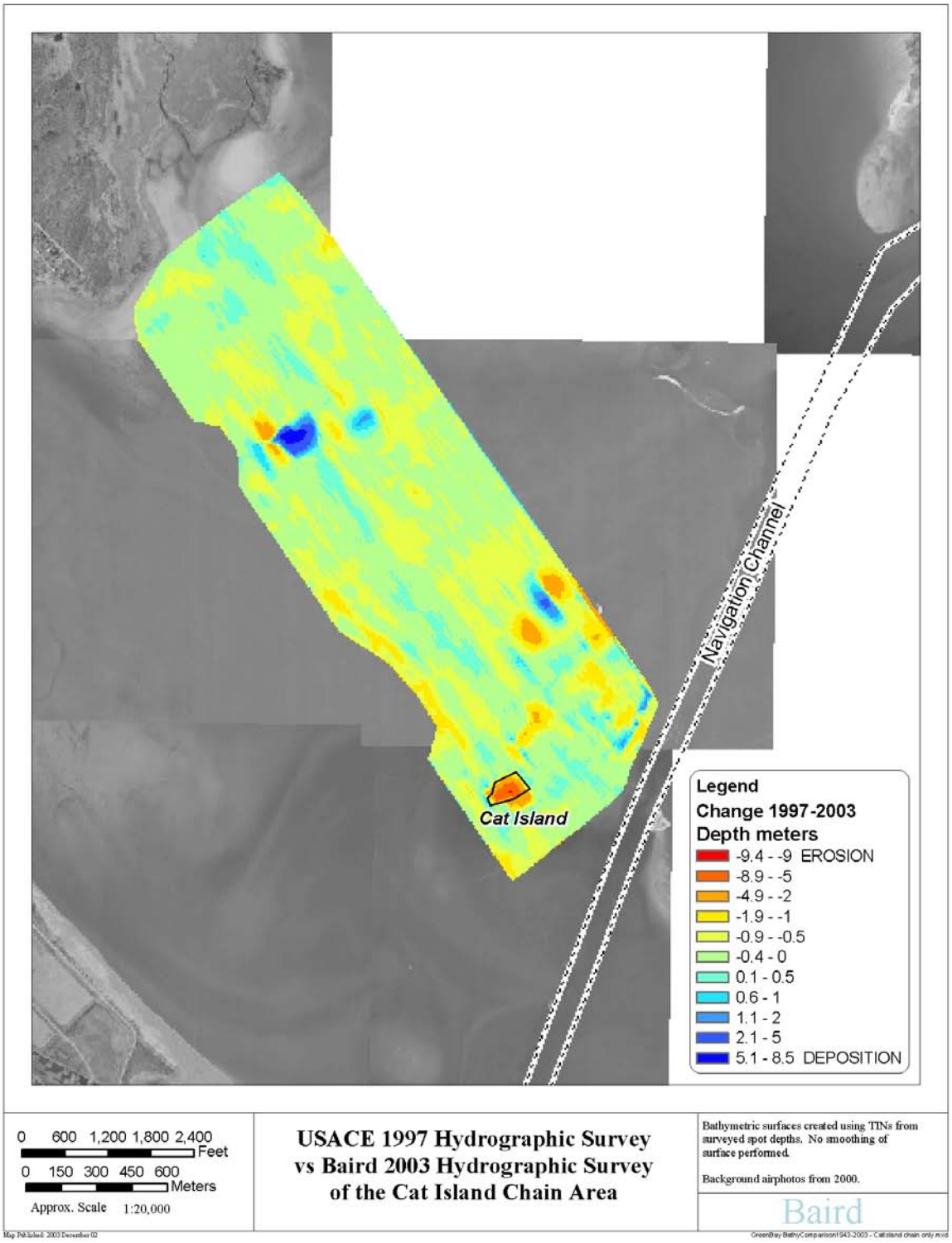
Navigation Channel
Cat Island
Legend
Change 1997-2003
Depth meters
-9.4 - -9 EROSION
-8.9 - -5
-4.9 - -2
-1.9 - -1
-0.9 - -0.5
-0.4 - 0
0.1 - 0.5
0.6 - 1
1.1 - 2
2.1 - 5
5.1 - 8.5 DEPOSITION
0 600 1,200 1,800 2,400 Feet
0 150 300 450 600 Meters
Approx. Scale 1:20,000
USACE 1997 Hydrographic Survey
vs Baird 2003 Hydrographic Survey
of the Cat Island Chain Area
Bathymetric surfaces created using TINs from surveyed spot depths. No smoothing of surface performed.
Background airphotos from 2000.
Baird

Figure 3.12

4.0 Physical model study

4.1 Model Objectives

The primary objective of the physical model investigation was to provide detailed information to support the development and optimization of designs for the island perimeter/containment structures considering the range in exposure to wave action around the islands, as well as the characteristics of locally available construction materials (sands, gravels and rock). In particular, the model investigation focused on the following processes:

- Revetment stability and overtopping;
- Beach profile response and overtopping.

4.2 Model Facilities, Design and Construction

The model was undertaken in the 47 by 200 ft Coastal Wave Basin (CWB) at the Canadian Hydraulics Centre of the National Research Council in Ottawa, Canada. The CWB is equipped with a computer controlled wave generator (WM14) that can simulate irregular wave conditions with significant wave heights (Hs) of up to 0.5 to 1 ft depending on the water depth and wave period.

The geometric scale of the Cat Island model was set at 1:10 based on consideration of several factors, including:

- Model wave generation capabilities versus design wave conditions (refer to Section 4.0);
- Availability of model materials (sands, gravels and crushed rock) to simulate anticipated construction materials (refer to Section 9.0);
- Desire to simulate a number of different beach materials and revetment designs;
- Desire to work at as large a scale as possible (to minimize model scale effects).

The adopted model layout is shown in Figures 4.1 and 4.2, and included five different test sections, including three beaches and two revetments. The model test sections were constructed on existing bathymetry in the CWB, which provided a reasonable representation of the flat lakebed slope to the NE of the proposed Cat Island chain. The depth at the toe of the beach and revetment sections was –2 ft CD, which is similar to the average lakebed elevation along the NE limit of the proposed island chain. A range in beach fill materials and revetment designs were tested under a range in water levels and wave conditions, as summarized in Section 4.3.

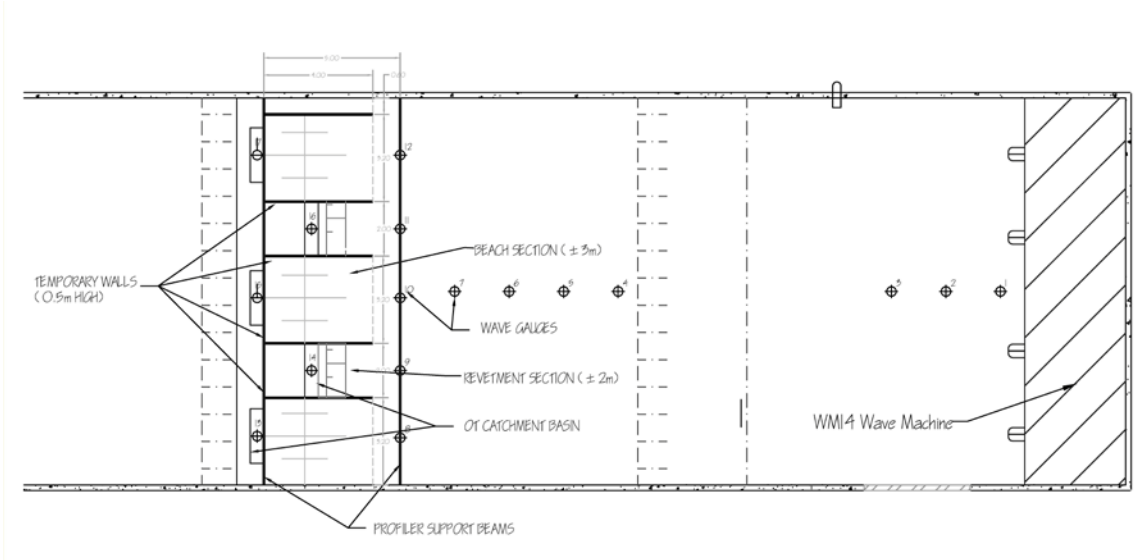

Figure 4.1 – Model Layout

Figure 4.2 – Overview of Model Beaches, Revetments and Instrumentation

The model instrumentation included 12 wave gauges; five wave overtopping catchments/gauges and an electro-mechanical profiler. The wave gauges provide a measure of wave conditions at selected locations in the model (refer to Figures 4.1 and 4.2), while the wave overtopping catchments/gauges provide a measure of the volume/rate of water overtopping the crest of each beach and revetment section (refer

to Figure 4.3). Samples were measured at each wave and overtopping gauge for every model test condition, with a 20 minute (prototype) sample duration and a 25 Hz (model) sampling frequency. CHC's GEDAP software was used to reduce and analyze these data. Standard zero crossing and spectral analyses were undertaken to define representative wave parameters at each wave gauge (including Havg, $H_{1/3}$, $H_{1/10}$, H_{max}, T_{avg}, $T_{1/3}$, H_{mo}, T_p, etc.), while customized analyses procedures were developed and utilized to define representative wave overtopping rates.

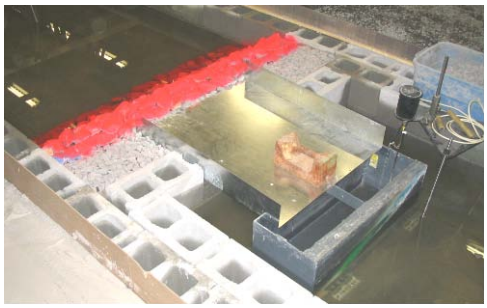

Figure 4.3 – Wave Overtopping Catchments/Gauges

The profiler (refer to Figure 4.4) was used to measure profile development on the beaches throughout each test series. Profiles were measured at two locations across each test section, with various graphical presentations used to assess ongoing profile development and to compare the profile response of different beach fill materials. The profiler was also used in some tests to measure the profile response of the revetment structures. In addition, visual observations of revetment armor layer stability were made throughout the testing program in order to define damage patterns/levels.

Figure 4.4 – Electro-Mechanical Profiler

4.3 Overview of Model Testing Program

Four separate test series were run in order to assess the performance of different beach fill materials and revetment designs. Tables 4.1 provides a summary of the basic design parameters for the five test sections in each test series, while Table 4.2 provides a summary of the range in test conditions in each test series. In general, beach fill materials were placed to an elevation of +8 to +9 ft CD with a front slope of 6:1 (horizontal:vertical), while the revetments were constructed with various riprap armor layers placed to an elevation of +9 to +10.5 ft CD with a front slope of 1.5:1 (specific exceptions are noted in Table 4.1).

Table 4.1 – Details of Model Test Sections

Test Series	Beach 1	Revetment 1	Beach 2	Revetment 2	Beach 3
A	Stone Dust	Conventional (16-20" riprap, +10.0 ft CD)	Pea Gravel	Conventional (25-32" riprap, +10.5 ft CD)	Silica Sand
B	Stone Dust	Conventional (16-20" riprap, +10.0 ft CD, 2:1 slope)	Pea Gravel	Conventional (25-32" riprap, +10.5 ft CD)	Silica Sand
C	Stone Chip	Conventional (9-18" riprap, +9.5 ft CD)	Pea Gravel (with sand berm at toe)	Conventional (14-20" riprap, +9.0 ft CD	Concrete Sand
D	Stone Chip (1.5:1 slope)	Berm (9-18" riprap, +10 ft CD)	Pea Gravel (1.5:1 slope)	Berm (9-11" riprap, +10.0 ft CD)	Filter Sand

Table 4.2 – Model Test Conditions

Test Series	Water Levels (ft CD)	Wave Conditions		No. of Beach Profile Sets	No. of Revetment Profile Sets	Overtopping Measurements
		Hs/Tp	Total Duration			
A	+4, +5	1.8ft/4s to 3.7ft/6s	15 hrs (model)	8	As-built only	Revetments only
B	+7	1.0ft/2s to 4.6ft/6s	5 hrs (model)	5	None	Beaches & revetments
C	+4, +6	1.8ft/4s to 4.3ft/7s	11 hrs (model)	5	4	Beaches & revetments
D	+4, +6, +7	1.9ft/4s to 4.7ft/7s	15 hrs (model)	7	7	Beaches & revetments

The characteristics of the different beach fill and revetment armor materials tested are presented in the following section of this report.

4.4 Model Material Characteristics

Most of the beach fill materials used in the Cat Island tests were aggregates (natural or crushed) available from local quarries. Two commercial/industrial grade silica sands (a fine sand used extensively at CHC for mobile bed model tests, and a coarse "filter" sand available from a local pool supply store) were also used.

Stone materials for the revetment filter and armor layers were mixed from pre-sorted stockpiles available at CHC (in 1/8" size increments from 1 to 2"), as well as crushed "clear" stone products available from local quarries.

Grain size distributions (GSDs) were measured on samples of each beach fill and revetment armor material. Standard sieve tests were used to define the GSDs for the model beach fill materials (refer to Figure 4.5), while individual stone weights were measured to define the GSDs for the model armor materials (refer to Figure 4.6).

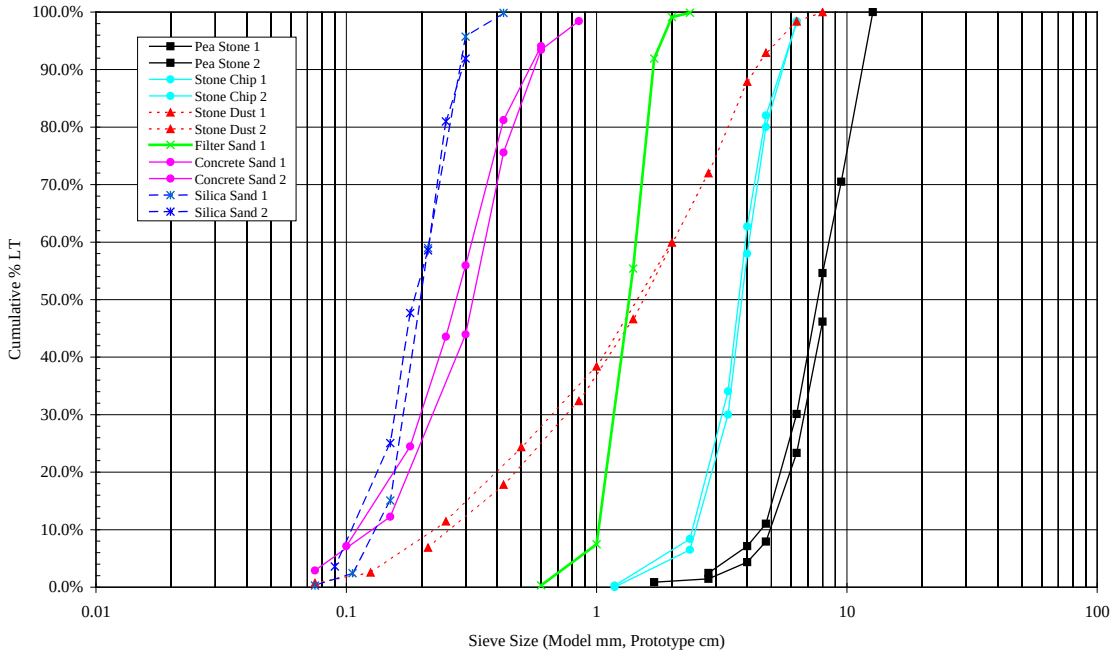

Figure 4.5 – Model Beach Fill Materials – Sample GSDs

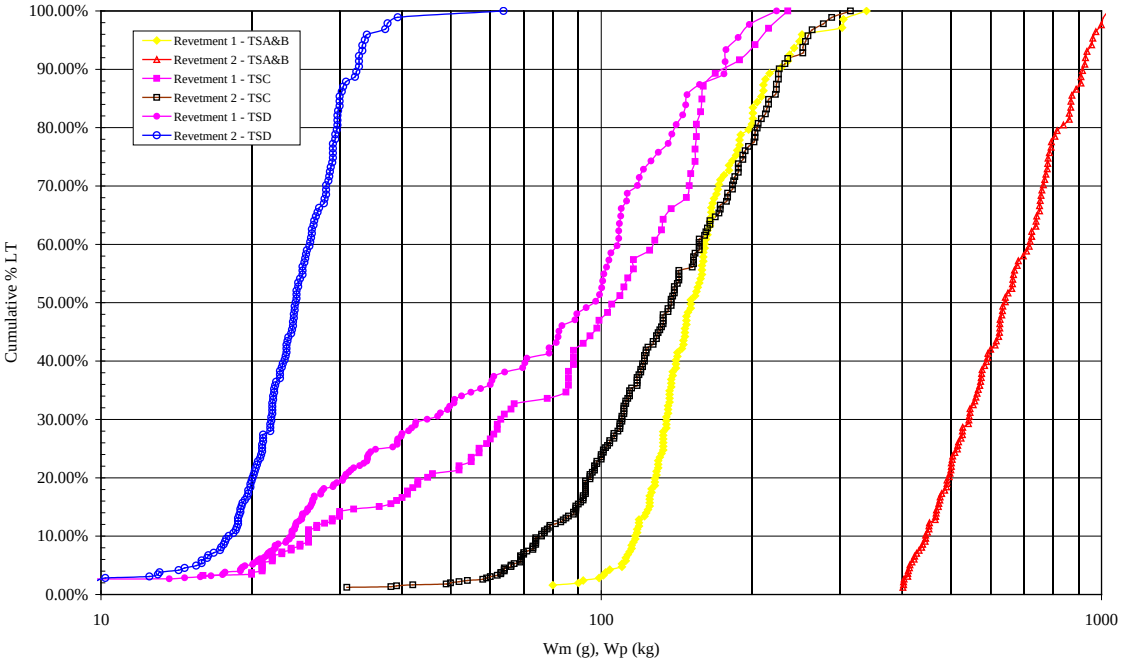

Figure 4.6 – Model Armor Stone Materials – Sample GSDs

The beach fill and armor stone gradation characteristics are also summarized in Tables 4.3 and 4.4 respectively. The armor stone gradations were measured by stone weight (Table 4.4a), but are also presented by "equivalent" stone size (Table 4.4b).

Table 4.3 – Beach Fill Material Characteristics

Material Description	Sieve Size (Model mm, Prototype cm)			D90/D10
	D10	D50	D90	
Silica Sand	0.12	0.19	0.29	2.4
Concrete Sand	0.13	0.30	0.55	4.2
Filter Sand	1.0	1.3	1.7	1.7
Stone Dust	0.25	1.5	4.25	17
Stone Chip	2.5	3.8	5.5	2.2
Pea Gravel	4.8	8.0	11.5	2.4

Table 4.4a – Armor Stone Characteristics by Weight

Material Description	Stone Weight (Model g, Prototype kg)			W90/W10
	W10	W50	W90	
Revetment 1 – TS A&B	120	150	230	1.9
Revetment 2 – TS A&B	445	640	920	2.1
Revetment 1 – TS C & D	25	100	175	7.0
Revetment 2 – TS C	75	140	225	3.0
Revetment 2 – TS D	18	25	33	1.8

Table 4.4b – Armor Stone Characteristics by Equivalent Size

Material Description	Equivalent Stone Size* (Prototype inches)			D90/D10
	D10	D50	D90	
Revetment 1 – TS A&B	16	17.5	20	1.2
Revetment 2 – TS A&B	25	28	32	1.3
Revetment 1 – TS C & D	9.5	15	18.5	1.8
Revetment 2 – TS C	14	17	20	1.4
Revetment 2 – TS D	8.5	9.5	10.5	1.2

*Note: equivalent stone size assumes stone density = 165 lbs/ft^3, shape factor = 1.15 (angular)

The model materials generally exhibit narrow grading, with the exception of the stone dust beach fill (Beach 1 in TSA & B) and one widely graded armor (Revetment 1 in TS

C & D). In general, the model materials are representative of prototype materials that are readily available, or can be easily produced, by quarries in the vicinity of Green Bay (and trucked to the site) or around the north end of Lake Michigan (and shipped to the site on self-unloaders). For example, the filter sand, stone chip and pea gravel beach fills represent 3/8-3/4", 1-2.5" and 2-4" materials respectively, which roughly correspond to Michigan Limestone's G-1, E-1 and 2B products (refer to Section W, and Figure W.1). Considering riprap and armor stone, at least one local quarry stocks a 6-12" product. However, larger materials would likely be specifically produced for this project.

As noted earlier, it may be possible to process shot rock or quarry run materials to produce suitable beach fill and riprap materials for this project. For example, the material could be passed over an 8" grizzly, with material smaller than 8" being used as beach fill (additional processing to remove fines might be required) and material larger than 8" being used as riprap. The feasibility of this approach requires more detailed information on the characteristics of shot rock and quarry run materials produced at local quarries.

4.5 Key Model Results

4.5.1 Beaches

4.5.1.1 Profile Development

As noted earlier, a detailed understanding of beach profile development was one of the key objectives of the Cat Island physical model. Beach profile development was measured for six different beach fill materials under wave conditions up to Hs/Tp = 4.7 ft/7 at water levels ranging from +4 to +7 ft CD. The model beach fill materials had median grain sizes ranging from 0.2 to 8 mm (0.2 to 8 cm, or 1/16 to 3", prototype), with all but one being narrowly graded (refer to GSDs presented in Figure 3.5 and Table 4.3).

As noted earlier, the model beaches were constructed to an initial elevation of +8 to +9 ft CD, with a 6:1 front slope, and were then exposed to progressively increasing wave conditions at a water level of +4 ft CD, followed by similar tests at one or more higher water levels (up to +7 ft CD). For example, the profile development test sequences used in Test Series C and D are presented in Table 4.5, with corresponding profiles measured on the concrete sand (TSC), filter sand (TSD), stone chip (TSD) and pea gravel beaches (TSC and D) presented in Figures 4.7 to 4.10. It is noted a berm of silica sand was placed in front of the toe of the pea stone beach in TSC to simulate the deposition of fine sediment that might naturally occur at the site. In addition, it is noted that the stone chip and pea gravel beaches were placed at a steep slope (angle of repose ~1.5:1) in TSD; all other tests were done with an initial beach slope of ~6:1.

Table 4.5 – Test Sequence for Test Series C and D

WL (ft CD)	Hso* (ft)	Tp (s)	Hs* (ft)	Duration (hrs)	TS C Profile #	TS D Profile #
As-Built Profiles					001	001
+4	2.0	4	1.9	~6	002	002
+4	3.9	6	3.1	~12	003	003
+6	3.2	6	3.2	~6	004	004
+6	4.2	6	4.0	~6	Not tested	005
+6	6.0	6	4.1	~6	005	006
+7	6.2	6	4.7	~6	Not tested	007

*Note: Hso at wave generator (d = -9 ft CD), Hs at test section (d = -2 ft CD)

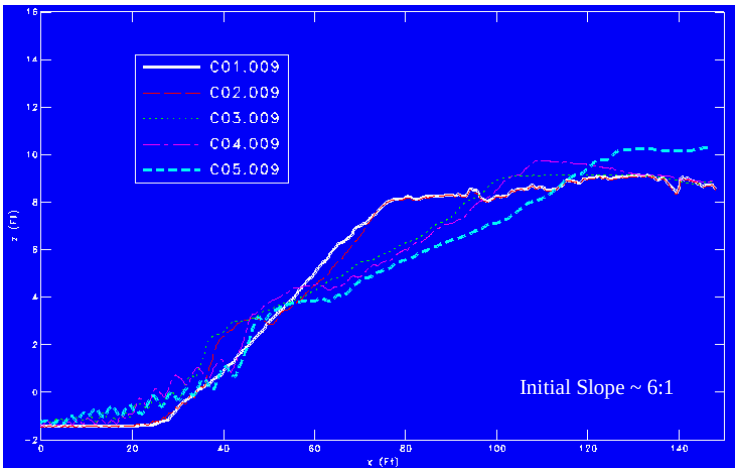

Figure 4.7 – Concrete Sand Beach – Sequential Profiles through TSC

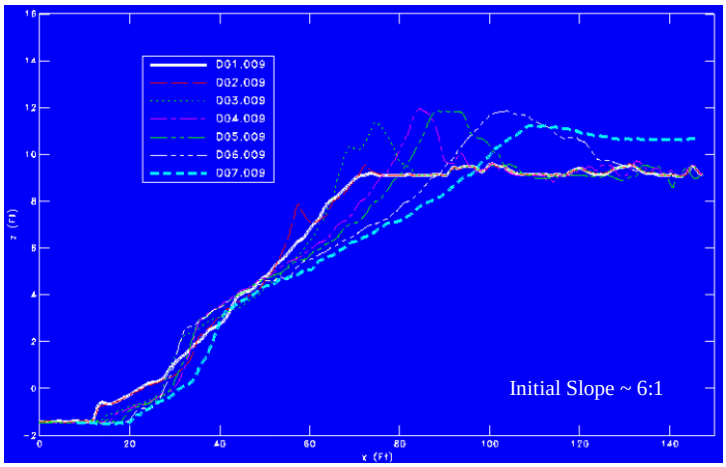

Figure 4.8 - Filter Sand Beach – Sequential Profiles through TSD

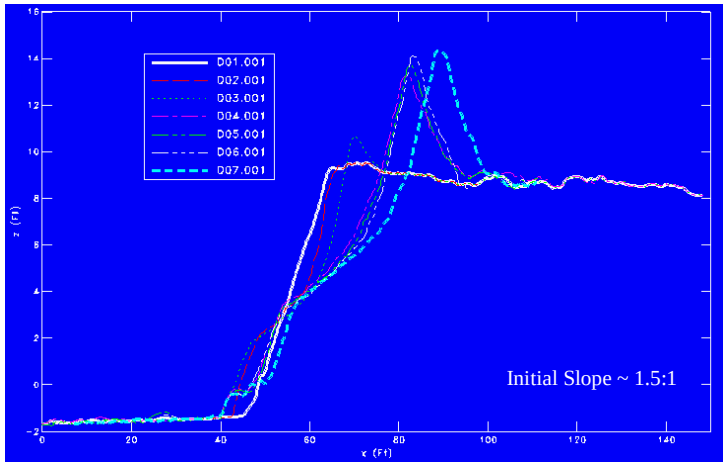

Figure 4.9 – Stone Chip Beach – Sequential Profiles through TSD

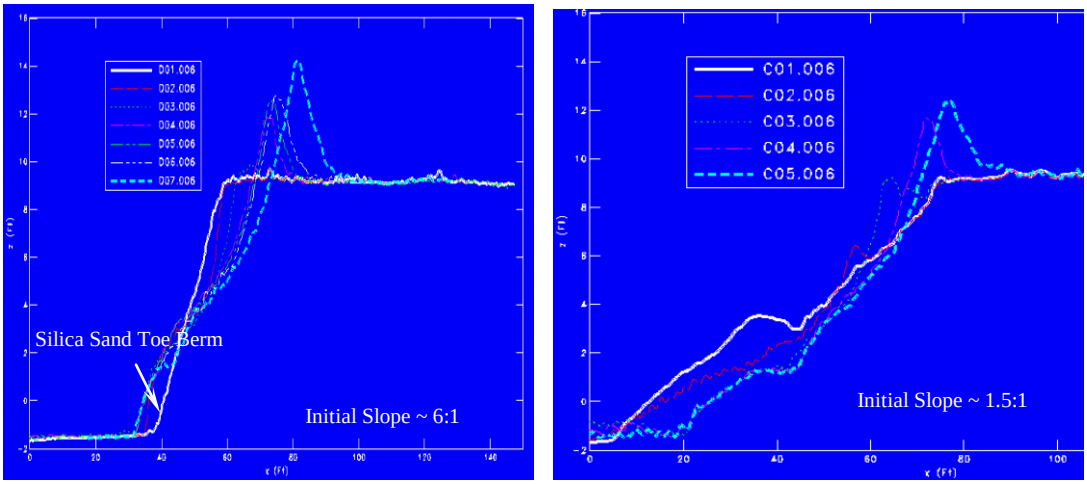

Figure 4.10 – Pea Stone Beach – Sequential Profiles through TSC and TSD

These results show progressive recession of the beach face in response to increasing wave action, and the development of a significant storm berms on the coarser beach fill materials (up to an elevation as high as +14 ft CD). The profile response of the silica sand and stone dust beaches tested in TSA/B was generally similar to that of the concrete sand shown in Figure 4.7, with flatter slopes and less pronounced berm development than the coarser materials.

Figure 4.11 presents a comparison of beach profiles measured for all six beach fill materials following exposure to storm wave conditions (approximately 12 hours at Hs ~ 3.1 ft, Tp ~ 6 s) at a moderately high water level (+4 ft CD). Results for three of the beach fill materials following a shorter duration (6 hrs) of more severe storm waves (Hs ~ 4 ft, Tp ~ 6 s) at a higher water level (+6 ft CD) are presented in Figure 4.12.

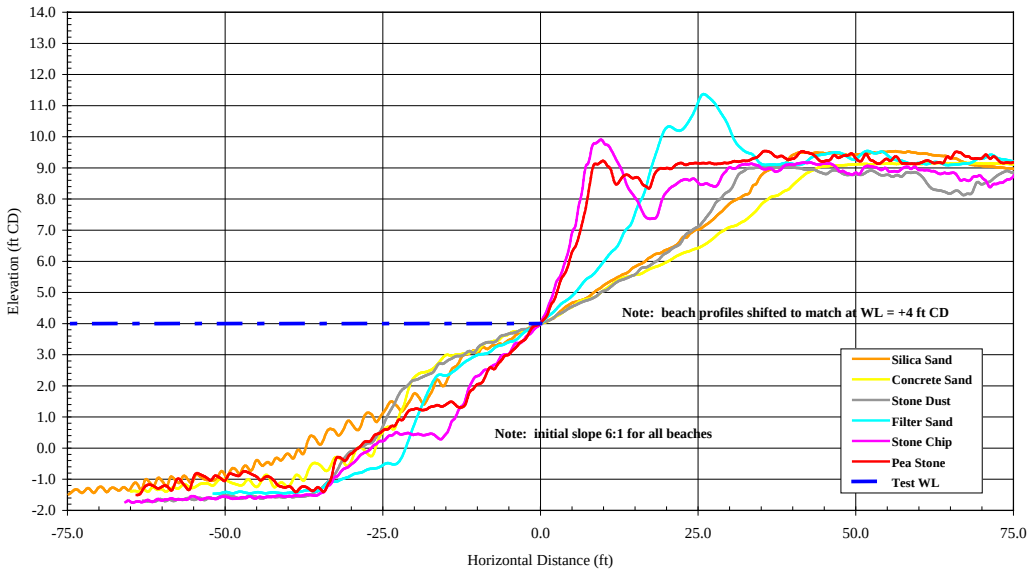

Figure 4.11 – Comparison of Model Beach Profiles
(after ~ 12 hours at Hs/Tp ~ 3.1 ft/6s at WL = +4 ft CD)

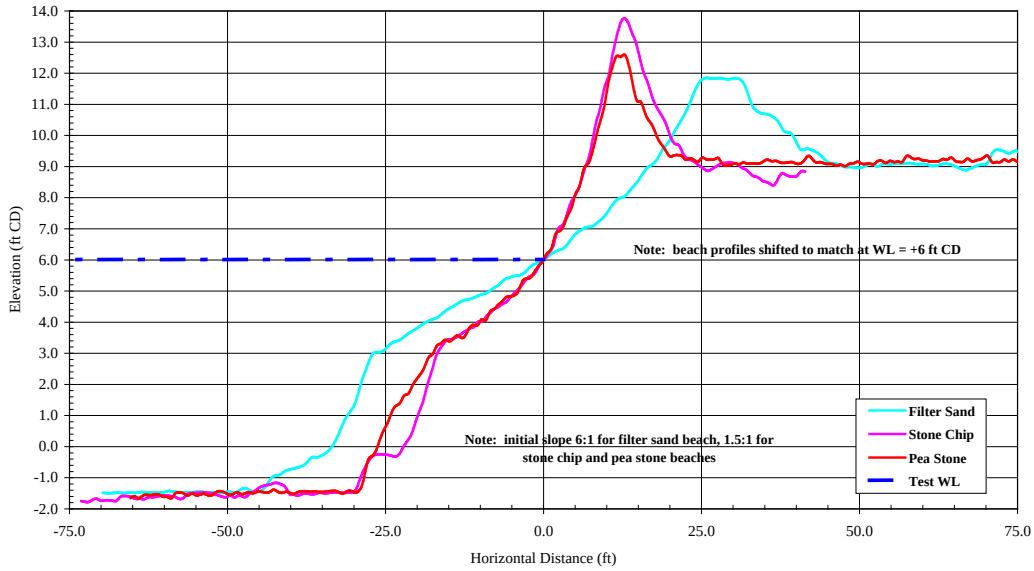

Figure 4.12 – Comparison of Model Beach Profiles
(after ~ 6 hours at Hs/Tp ~ 4 ft/6s at WL = +6 ft CD)

It is noted that there was some variation in beach profile across the width of each test section following any given test condition. For example, the peak berm elevations varied by up to +/-1 ft across the width of each test section following any given test condition.
The stone dust beach profile showed considerable variability, likely due to the wide gradation of this material and spatial variability in the material characteristics. It is interesting to note that similar variations were noted by Bradbury and McCabe (2003) in their tests of mixed sand/gravel beaches.

In any event, the model beach profile measurements generally show two characteristic profile types. The first profile type is characterized by a relatively flat slope, without a significant "storm berm", and was exhibited by the two model sands (silica sand and concrete sand) and stone dust beaches. The second profile type is characterized by a relatively steep slope, with a significant storm berm, and was exhibited by the two coarsest materials (stone chip and pea stone). This is a classic gravel beach profile, as previously schematized by van der Meer (1988) and Powell (1990). The filter sand beach profile falls in between these two profile types.

The difference between these two profile types is attributed to the beach fill material characteristics. Specifically, the silica sand, concrete sand and stone dust materials include a significant proportion of fine material (<1 mm) and have relatively low porosity/permeability, while the stone chip and pea stone materials have no fines and high porosity/permeability. Not surprisingly, the first group of materials exhibits a profile shape typical of sandy beaches, while the second group of model materials

exhibits a profile shapes typical of gravel/shingle/cobble beaches. The filter sand appears to fall within a transition zone between these two profile types, with an intermediate slope and moderate berm development.

Repeat tests were done with the stone chip and pea stone beaches with initial front slopes of 6:1 and 1.5:1. In addition, repeat tests were done with the pea stone beach without and with a wedge of fine sand placed in front of the toe of the beach to simulate the impact of contamination of a gravel beach with sand. No significant differences were noted in the resulting beach profiles following an extended exposure to storm wave conditions.

4.5.1.2Wave Overtopping

Wave overtopping of the beaches (and revetments) was measured throughout TSB through D using an overtopping catchment channel and basin (refer to Figure 3.3), with the water level in the catchment basin measured by a capacitance gauge continuously through each one hour (prototype) duration sample. Figure 3.13 presents a typical time series of overtopping data (catchment basin water level versus time) for the three beaches and two revetments under a particular test condition. These data show a number of overtopping "events" (rapid rise in water level) associated with the arrival of "groups" of larger waves at each structure.

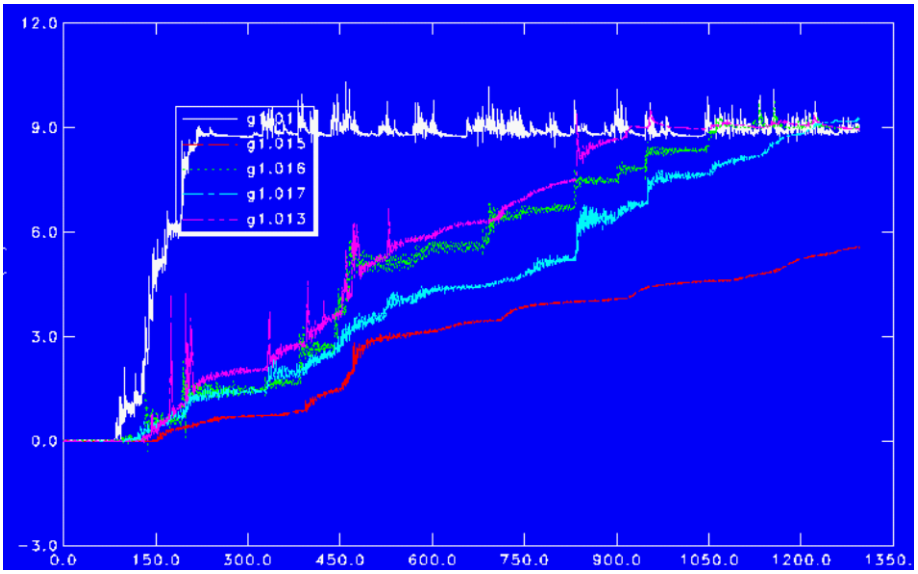

Figure 4.13 – Typical Time Series of Overtopping Data
(Water Level in Catchment Basin versus Time)

These data were subsequently analyzed in order to estimate the mean wave-overtopping rate over each 1-hour (prototype) duration sample, as well as the peak "instantaneous"

overtopping rates within each sample (maximum values averaged over durations of 1*Tp and 3*Tp, where Tp is the peak wave period of the test wave condition). Figure 4.14 presents the overtopping data for the different model beaches, with the mean wave overtopping rate ($m^3/s/m$) plotted as a function of the relative freeboard, F/Hs (F = beach crest height above still water level, Hs = significant wave height at structure toe).

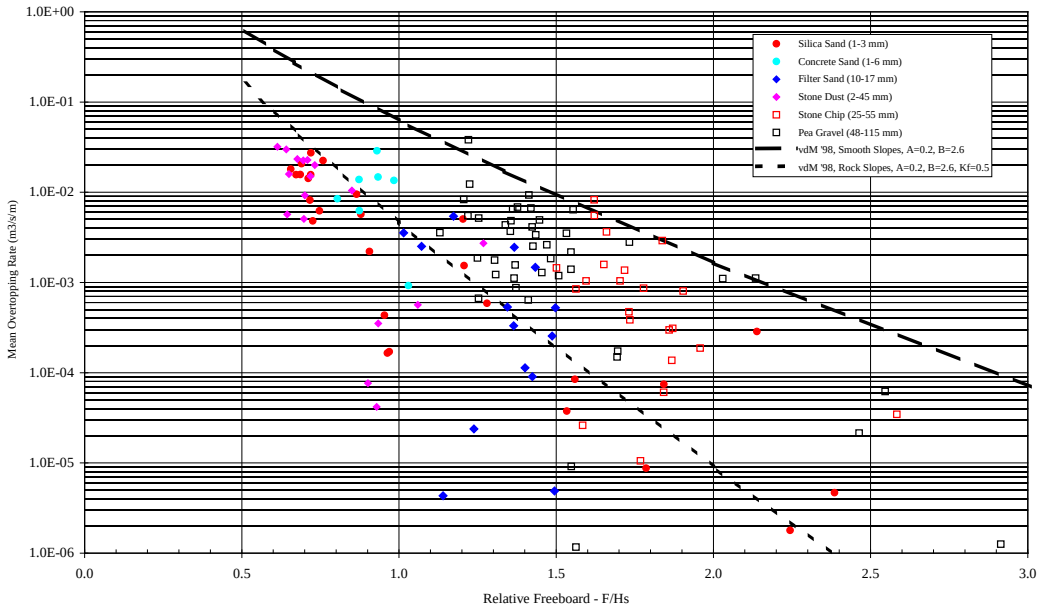

Figure 4.14 - Beach Overtopping Data – Mean OT Rate vs. F/Hs

The model results show considerable scatter, which is typical of model overtopping measurements, as noted by Goda (1985). However, some trends are apparent in the data, with the coarser (and more porous) beach fill materials (stone chip and pea gravel - open symbols in Figure 4.14) generally having higher overtopping rates at any particular value of the relative freeboard parameter. The dashed lines shown in the figure are based on the empirical prediction model of van der Meer (1998) for non-breaking waves on smooth and rock slopes. The higher smooth slope prediction provides an upper bound limit for the model results, as defined by the measurements on the coarser beach fill materials. The lower rock slope prediction provides a mid-range estimate of the results for the other beach fill materials.

The higher overtopping rates noted above for the coarser beach fill materials is somewhat misleading, in that these materials develop a higher storm berm, and therefore have a higher relative freeboard, than the finer materials under any given test condition. Figure 4.15 presents a subset of the beach overtopping data (extreme waves at WL = +6 ft CD), with the mean overtopping rate plotted as a function of the incident wave height at the toe of the beach.

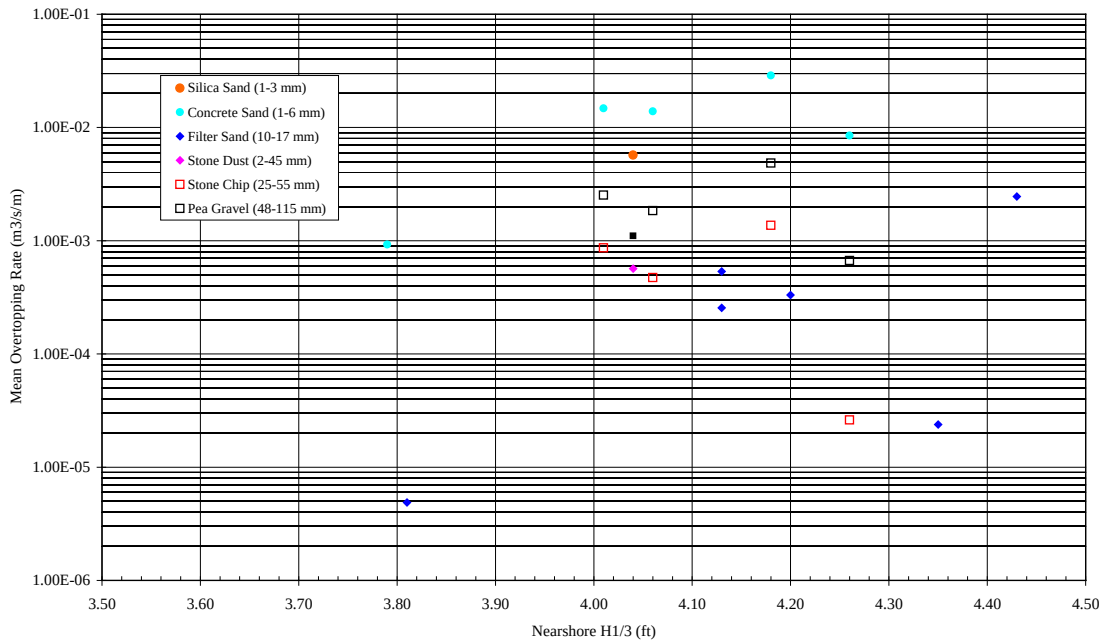

Figure 4.15 – Beach Overtopping Data - Mean OT Rate vs. Hs

This plot demonstrates that the mean wave-overtopping rate is higher for the finer sand beaches than for the coarser gravel beaches under similar wave and water level conditions. This trend is attributed to the combination of the reduced permeability, flatter slope and lower crest of the sand beaches.

4.5.2 Revetments

4.5.2.1Armour Layer Stability

The revetments in Test Series A and B were "conventional" design concepts, with two layers of armor stone placed over a filter layer and core. The structures were constructed with a crest elevation of approximately +10 ft CD, with the fill behind the crest of the structure protected by a filter stone "splash pad" (nominally 10"). Two different armor stone gradations were tested, including 16-20" and 24-32" size ranges (refer to Figure 4.6 and Table 4.4). For comparison purposes, Hudson equation calculations (refer to USACE, 2001) for the 20 and 100 year design wave heights (Hs = 3.3 and 3.9 ft respectively) give armor stone sizes (D50) of 16" and 19" respectively.

The larger armor gradation was stable under all test conditions (up to and exceeding the 100 year design wave at a water level of +7 ft CD), with the exception of one stone that was displaced landward from the crest by severe wave overtopping. Figure 4.16 shows this revetment following TSB.

Figure 4.16 - Conventional Revetment with 24-32" Armor Layer after TSB

The smaller armor gradation suffered minor damage during the 20-year design wave condition with structure slopes of 1.5:1 (TSA) and 2:1 (TSB), with increasing damage under more severe conditions. Figure 4.17 shows the revetment following TSB.

Figure 4.17 - Conventional Revetment with 16-20" Armor Stone After TSB

Severe wave overtopping was observed/measured on both structures during tests at high water levels (+6 to +7 ft CD), but no significant damage to the crest was noted due to the protection provided by the splash pad. Overtopping is discussed in more detail in the following section.

"Berm" type design concepts were assessed in Test Series C and D, with a wider layer of riprap placed directly over the core (i.e. no filter layer). Two graded ripraps were tested, including 9-18" and 14-20", as well as a smaller, more narrowly graded, riprap (8-10"). These structures were constructed with berm widths of 7 to 20 ft at an elevation of +9 to +10 ft CD. The core stone fill material behind the berm crests was left unprotected. Sequential profiles were measured to document changes in the profile under progressively more severe waves and water levels. Figures 4.18 to 4.20 show the measured profile response for the three riprap gradations (refer to Table 4.5 for a summary of test conditions).

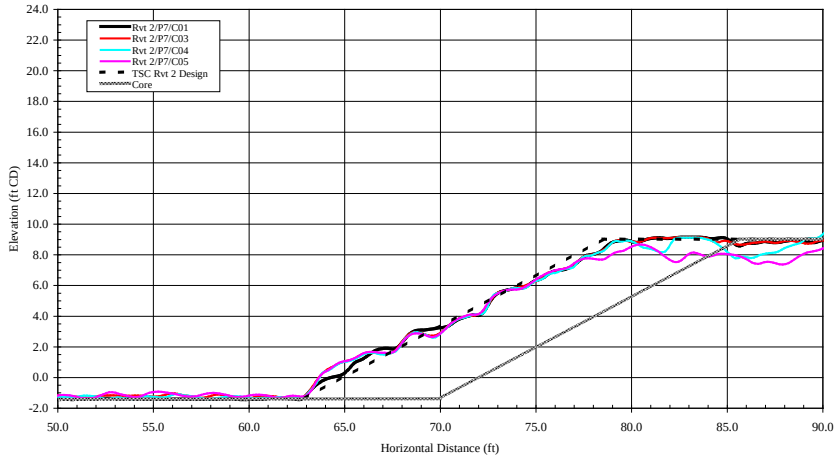

Figure 4.18 – Berm Revetment Profile Response - 14-20" Riprap, TSC

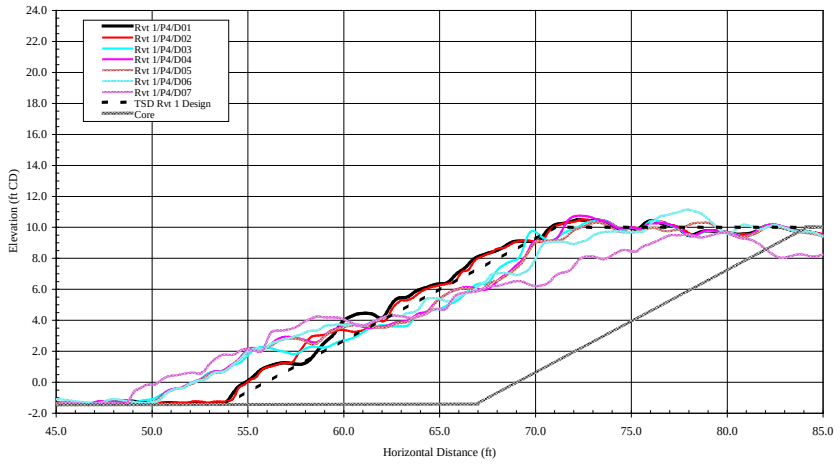

Figure 4.19 – Berm Revetment Profile Response - 9-18" Riprap, TSD

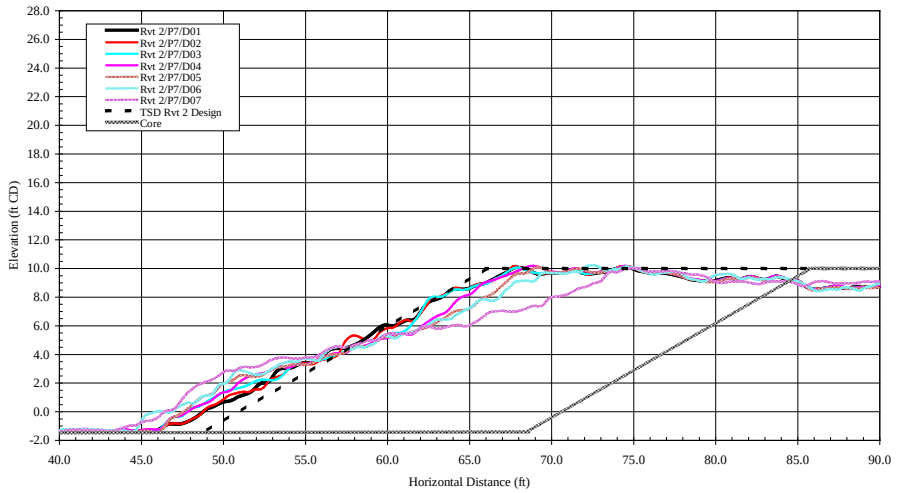

Figure 4.20 – Berm Revetment Profile Response – 8-10" Riprap in TSD

No significant profile development was noted on the largest riprap material (14-20") under wave conditions up to and exceeding the 100-year design event. However, severe overtopping during storm waves at water levels of +6 ft CD and higher caused erosion of the unprotected fill material behind the riprap berm, with subsequent landward displacement of stone from the berm crest. The onset of profile development in the two smaller riprap materials occurred at Hs ~ 3 ft, which is similar to the 20 year design condition. In general, these results show the initial stages of development of an "S-shaped" profile that is similar to, but less pronounced than, that of the gravel beach profiles presented earlier. As noted above, severe overtopping during storm waves at high water levels caused erosion of the fill material behind the riprap berms, with subsequent landward displacement of stone from the berm crest in some cases. This damage mechanism was not observed on the revetment with the widest berm (20 ft). Wave overtopping of the revetment structures is discussed in more detail below.

4.5.2.2Wave Overtopping

Wave overtopping of the revetments was measured throughout TSA through D using an overtopping catchment channel and basin (refer to Figure 4.3), with the water level in the catchment basin measured by a capacitance gauge continuously through each one-hour (prototype) duration sample (refer to Figure 4.13 for example). Data reduction and analyses procedures were similar to those described earlier for the beach overtopping data. Figure 4.21 presents the mean wave-overtopping rate ($m^3/s/m$) plotted as a function of the relative freeboard, F/Hs (F = structure height above still water level, Hs = significant wave height at structure toe) for the different revetment structures.

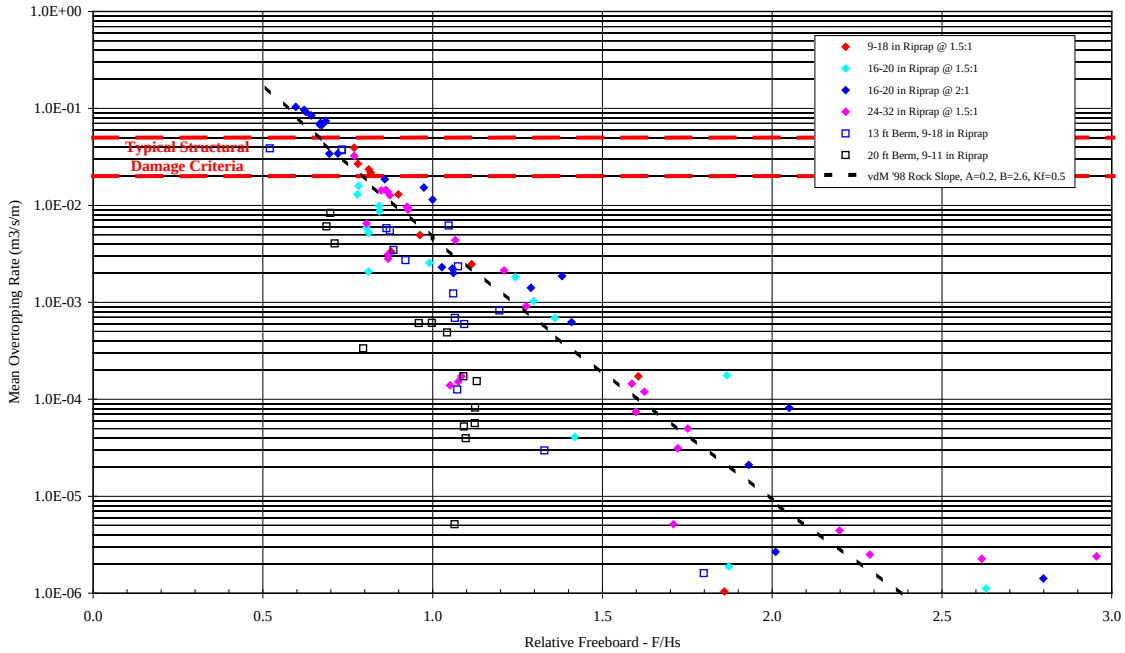

Figure 4.21 – Revetment Overtopping Data – Mean OT Rate vs. F/Hs

Again, there is considerable scatter in the overtopping data. However, the empirical approach of van der Meer (1998) for rock slopes provides a reasonable mid-range estimate of the model measurements on the conventional revetment designs. Further, the test results indicate that the berm structures (open symbols in figure) have lower overtopping rates than the conventional structures; this is attributed to the increased width and porosity of the berms.

Published information (for example, Besley/HRW, 1999; USACE, 2001; OCDI, 2002) suggests that structural damage due to wave overtopping can be expected for mean wave overtopping rates in the order of 0.02 to 0.05 $m^3/s/m$ (0.2 to 0.5 $ft^3/s/ft$ or greater). This range is highlighted by the red dashed lines in Figure 4.21. The model results (measured overtopping rates, as well as visual observations) indicate that damage (to the crest and adjacent fill) due to wave overtopping can be expected for F/Hs $> \sim$ 0.75 to 1.0. This result is generally consistent with Baird's experience with physical model investigations of other coastal structures.

4.6 Model Scale Effects and Interpretation

As noted earlier, "scale effects" are inherent in any physical model, as the viscosity (and surface tension) of the water is not scaled properly (there is no practical alternative to water as the model fluid), thereby leading to exaggerated viscous (and surface tension) forces in the model. In addition, other model effects, such as the absence of wind, must be considered in the interpretation/application of model results. The

following paragraphs provide a brief summary of these issues with respect to revetment stability, wave runup/overtopping and beach profile response.
Considering the stability of rubblemound structures such as revetments and breakwaters, Dai and Kamel (1969) indicate that viscous scale effects (due to a change in wave-induced flow characteristics within the core from turbulent in prototype to laminar in the model) may be significant for Reynolds Numbers (Re) of less than 30,000 ($Re = D*\sqrt{gH}/v$, where D = armor size, g = gravitational acceleration, H = wave height and v = kinematic viscosity of water). However, more recent research (Owen and Briggs, 1986) suggests that this limit may be as low as 3,000 to 8,000. In any event, it is generally agreed that these scale effects result in conservative results, with damage to the armor layer being exaggerated in the model. Considering the revetment structures modeled in this study, the armor layer Reynolds Number is 20,000 or greater under the design wave conditions, so no significant scale effects are anticipated with respect to stability.

Considering wave runup and overtopping, a literature review indicates considerable differences in opinion regarding scale effects in physical models. For example, de Wall et al (1996) suggest that model scale effects (due to incorrectly scaled viscosity and surface tension, as well as the absence of wind in the model) may be significant at low overtopping rates (i.e. models underestimate spray/splash overtopping), but insignificant at high overtopping rates (i.e. models accurately simulate green water/sheet flow overtopping). More recently, Pearson et al (2002) found no significant difference between small and large-scale measurements of wave overtopping on vertical walls. On the other hand, the OPTICREST project (see de Rouck et al, 2001) indicates that actual wave runup levels on prototype sloping structures are underestimated by small-scale model results, which infers that wave overtopping may be underestimated as well. However, at this time, given the large scatter in the model overtopping results (typical of such tests, as noted by Goda, 1985), the uncertainty related to scale effects, and the relatively large model scale, no adjustment to the overtopping rates has been applied.

Considering the beaches, it is noted that “mobile bed” models of coastal processes (i.e. sediment transport, beach profile response, etc.) may be subject to significant scale effects, as the flow and sediment transport regimes may be different in model and prototype. The development of model scaling relationships for mobile bed models (and the quantification of model scale effects) has been (and continues to be) the subject of extensive research by international hydraulics laboratories, with various sediment scaling relationships having been proposed by different researchers. However, there is no generally accepted sediment scaling methodology in widespread use at this time.

In general, fine-grained sediments cannot be scaled down geometrically, as the required model sediment would be cohesive (i.e. silt or clay), with a completely different response to hydrodynamic flows than the cohesionless prototype sediment (for example, a 1:10 scale model of 0.3 mm (medium) sand would require 0.03 mm silt). Rather,

very fine sand (and/or lightweight sediment) is generally used in mobile bed models, with characteristic response parameters for the model sediment (such as fall velocity, critical shear stress or some other sediment "mobility" parameter) scaled to prototype and used to estimate the corresponding prototype grain size. Clearly, larger scale models result in reduced scale effects, but even the large scale (1:10) model used for Cat Island cannot simulate the response of sand beaches without some scale effects. Table 4.6 below presents estimated prototype sediment sizes (D50) for the Cat Island model beach fill materials based on several scaling approaches, including geometric (i.e. 1:10 model scale), fall velocity (based on Hallermeier, 1981), critical shear stress (based on Shields curve, after van Rijn, 1984) and flow regime (laminar/turbulent) within porous media (based on Jensen and Klinting, 1983).

Table 4.6 – Model Beach Fill Scaling – Various Methods

Model Material	Model D50 (mm)	Scaled D50 (Prototype mm)			
		Geometric	Fall Vel.	Shear Vel.	Flow Regime*
Silica Sand	0.19	1.9	0.6	1.8	0.5-1.7
Concrete Sand	0.30	3.0	0.9	2.1	0.9-2.6
Filter Sand	1.3	13	13	8.4	6-12
Stone Dust	1.5	15	15	10	7-14
Stone Chip	3.8	38	38	34	25-38
Pea Gravel	8.0	80	80	80	60-80

*Note: flow regime estimate depends on assumed flow velocity within beach fill material

These results generally suggest the potential for significant scale effects (i.e. scaled prototype size is significantly different from that given by geometric scaling) for the finer grained model sediments, but limited to none for the coarser-grained model sediments. Given the presence of a significant proportion of fines in the model stone dust material, and the fact that the profile response of such a "mixed beach" is generally controlled by these fines, it too would be subject to scale effects.

For this project, the most important scale effect is related to the beach profile, with the actual beaches anticipated to have a flatter slope than the model beaches. Baird's extensive experience in beach modeling, design and monitoring, in particular comparisons of model and prototype beach profiles for several completed projects, indicates that prototype sand beaches will have swash zone slopes up to two to three times flatter than model sand beaches depending on model and prototype grain sizes, model scale, etc. Considering the Cat Island model, a factor of two is suggested to convert the model sand beach profiles into prototype sand or mixed (sand-gravel) beach profiles. However, the coarsest model beaches (stone chip and pea gravel) are believed to provide an accurate representation of actual profiles expected for geometrically scaled materials (i.e. clean gravel and cobble beaches).

In summary, no significant scale effects are anticipated with respect to revetment stability, wave overtopping or gravel/cobble beach profiles. However, actual sand beach profiles at Cat Island are likely to be significantly flatter than the sand beach profiles measured in the model. A factor of two adjustments has been applied to the model sand beach profiles based on comparisons of model and prototype beach profiles available from previous studies.

5.0 Wave Generation and Transformation modeling

5.1 Wave Generation Modeling

A preliminary assessment of the wave conditions in the vicinity of the project site was made during the initial phases of the study. The complexity of the generation process in a narrow fetch region and the wave transformation in the vicinity of the site required that additional analyses be carried out for final design. These analyses included the installation of wave recorders, as described in Section 2.2.4.

Following retrieval of the wave data from the pressure recorders, a numerical wave hindcast was carried out for the period of deployment. This hindcast, which used the numerical model WAVAD, included all of Green Bay and used winds recorded from the Green Bay Airport. WAVAD is a second generation, two-dimensional wave generation and propagation model, similar to the WISWAVE model used by the U.S. Army Corps of Engineers. The model was run at a 15-minute time step on a bathymetric grid with a 2 km grid spacing, as shown in Figure 5.1 (depths in meters).

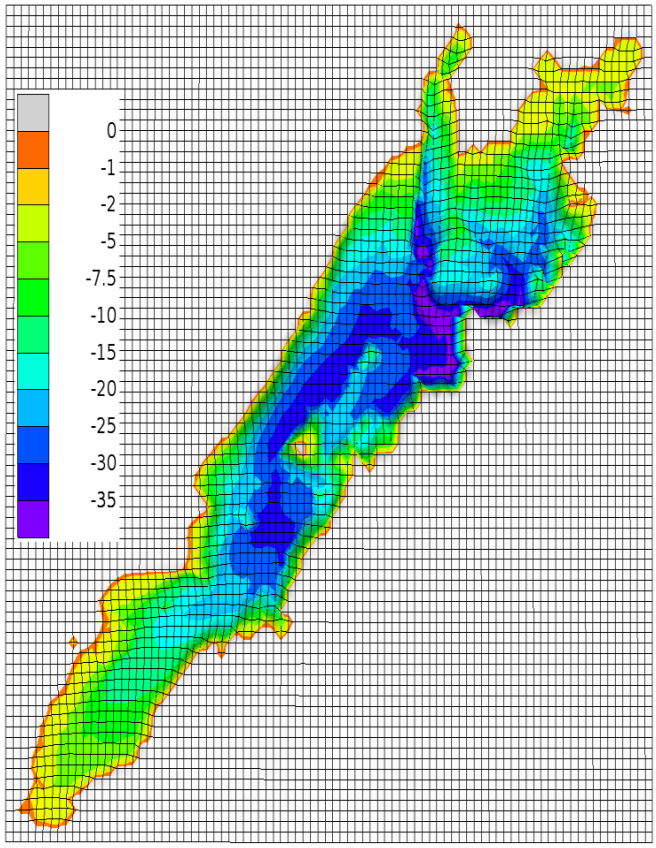

Figure 5.1 - Bathymetric Grid Used for the WAVAD Model.

Comparisons were first made between the gauge at Long Tail Point since this gauge has less influence from sheltering and other bathymetric effects compared to the inner gauge. The initial comparison showed a poor relationship between the hindcast data and the measured data. While there was typically some over-estimation of the waves, occasionally an underestimation occurred. This inconsistency lead to investigation of the wind data used for the study.

To better represent winds over Green Bay, a comparison was made between winds recorded at the airport and those recorded over the water at NOAA Buoy 45002. This comparison was carried out only for winds from the NE sector, since it is these winds that create significant waves at the site and these winds pass over the city of Green Bay before being measured at the airport. The analysis examined statistical wind trends during different thermal gradients over the lake (i.e. the air-water temperature difference measured at the buoy). Based on this analysis it was concluded that winds recorded at the airport during warm air and cold-water conditions (typical of the spring) were significantly higher than those that occurred over the lake. Conversely, warm water and cold air (typical of the fall or during sub-freezing air conditions in the spring) resulted in winds that are higher over the lake than those measured at the airport. Figure 5.2 shows the relationship between winds at the airport and winds over the lake

for two air-water temperature difference scenarios. These plots present the relationship between quantile levels (for instance 90 per cent, 99 per cent, etc.) for winds at the airport and the buoy that were measured concurrently.

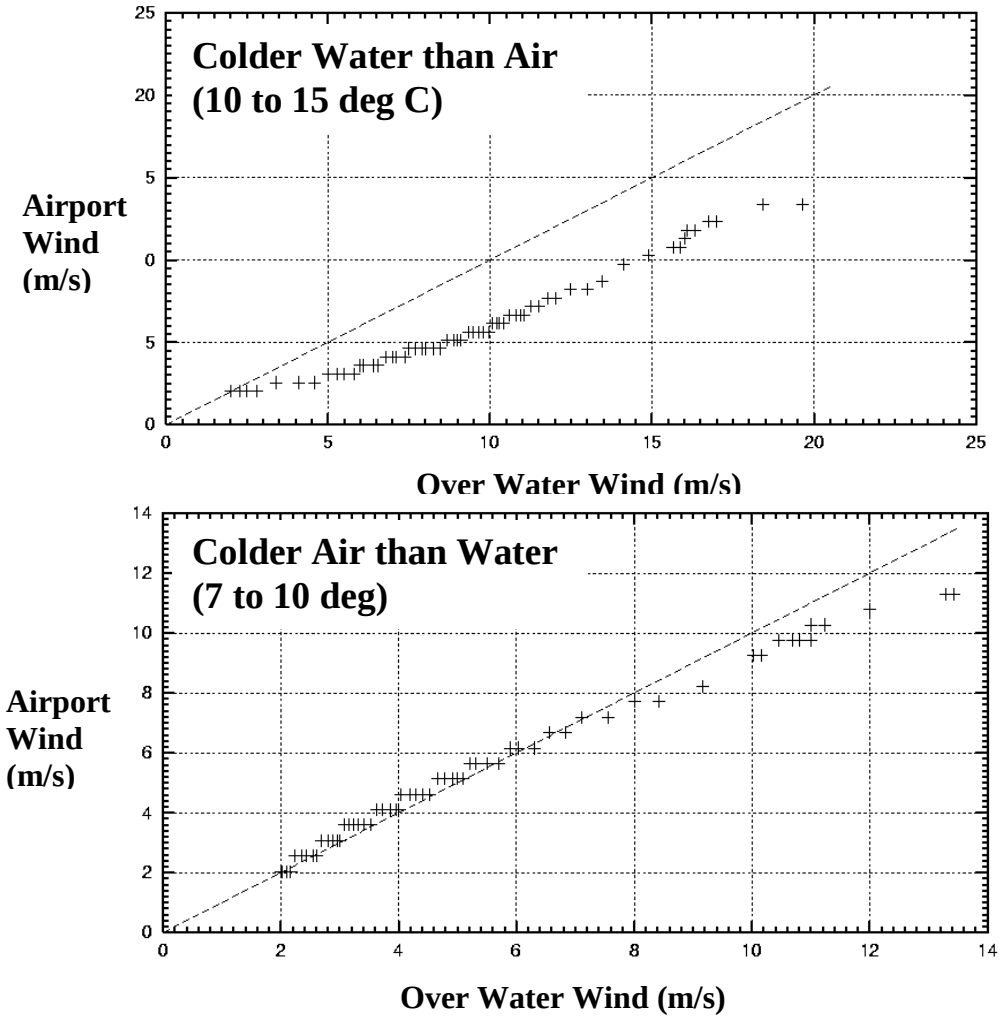

Figure 5.2 - Wind Speed Relationships for Different Air-Water Temperature Differences

From the relationship depicted in Figure 5.2 (and others not shown for other temperature gradients), correction factors were generated and these were applied to the wind conditions measured at the airport. The resulting Temperature Difference Scaled (TDS) winds then provided a set of wind data that were statistically similar to the winds recorded on the surface of Lake Michigan.

The hindcast was then re-run with the TDS winds and the results were substantially different. Figure 5.3 shows a comparison of the hindcast waves, using both sets of wind data as well as the measured data at Long Tail Point.

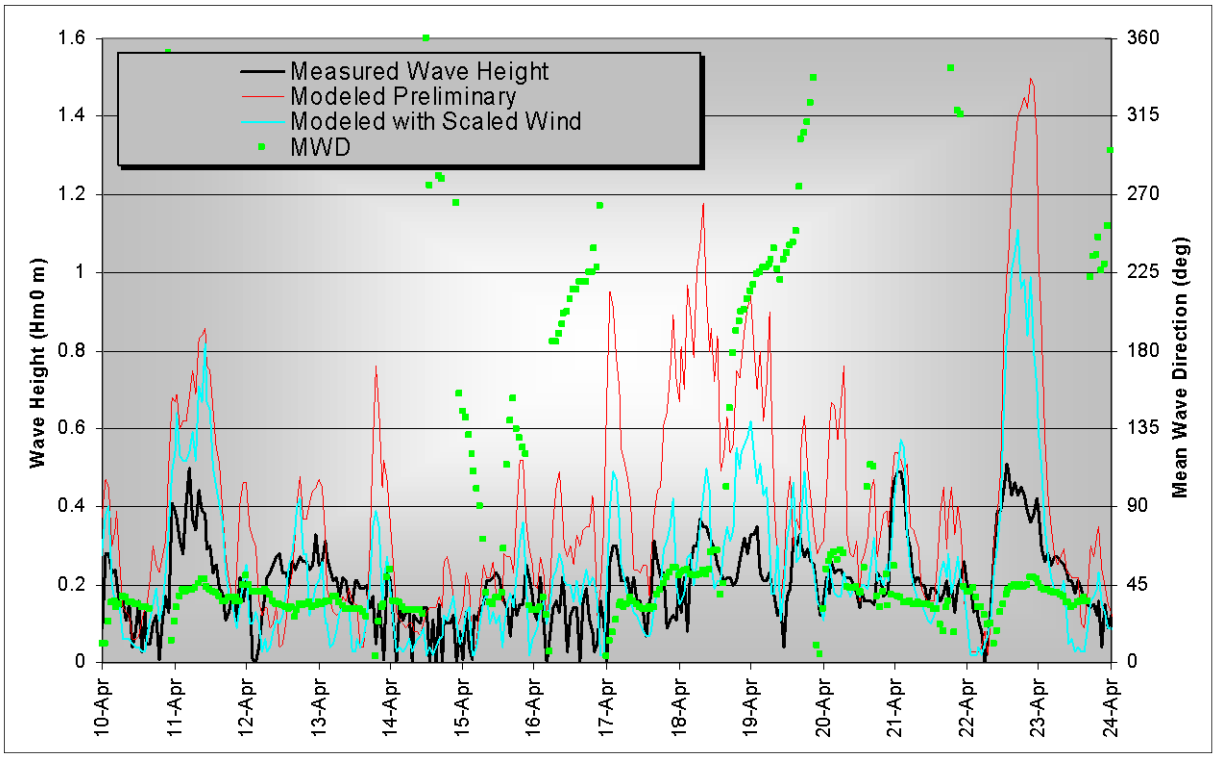

Figure 5.3 - Comparison of Hindcast Waves and Recorded Waves

A slight over-prediction of the waves at Long Tail Point remained after correction of the winds. Examination of a number of the larger events indicated that much of this over- prediction was due to refraction of the waves along the edge of the dredge channel as it transitioned towards the tip of the point. However, this wave transformation did not entirely explain the over prediction of the wave conditions. One approach to rectify this would have been to apply some sort of scale factor to the winds or waves in order to achieve a better match between the modeled and recorded waves. However, due to the fact that the field deployment did not measure any particularly large wave events, it was decided that reducing waves based on a scale factor was non-conservative and inappropriate since there was no assurance that the over-predicting seen for smaller wave events was consistent for larger wave events.

Following the adjustments to the winds during the calibration period (spring 2004), the same wind transformations were applied to the historical wind data and the hindcast was re-run for the period of record of the winds. This was done initially using Baird's parametric hindcast model and the listing of storm events was re-generated. From this list of events, the top 15 events were identified for further study and were then simulated in WAVAD.

Following the determination of the wave height at the offshore location, wave transformation modeling was required in order to determine the wave conditions at the position of the proposed islands

5.2 Wave Transformation Modeling

To determine detailed wave conditions at the site, the wave model STWAVE was implemented. STWAVE is a steady-state wave transformation model developed by the US Army Corps of Engineers capable of quantifying the effects of wave generation, shoaling, breaking, refraction and diffraction.

Bathymetry data as documented in Section 2, wind and wave conditions defined by the modeling in Section 4.1 are all used as input to the STWAVE model. A bathymetry grid was created with the parameters assigned in Table 5.1 was utilized in all of the STWAVE runs. Figure 5.4 displays a color map of the STWAVE bathymetry grid.

Table 5.1 - STWAVE Bathymetry Grid Parameters

Parameter	Value
Nx	329
Ny	335
Δx	50 m
Δy	50 m

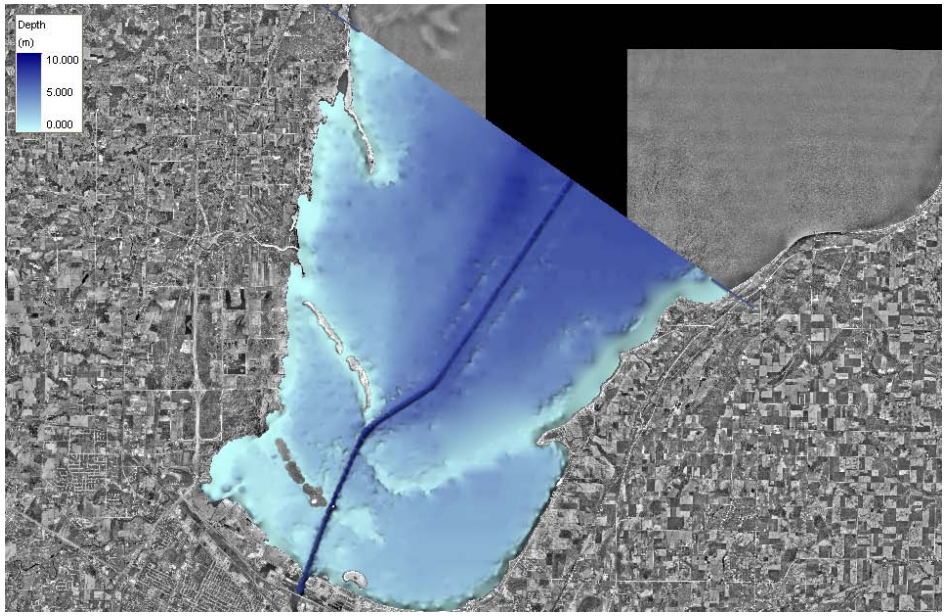

Figure 5.4 – Color Map of STWAVE Bathymetry Grid

5.2.1 Extreme Event Simulations

A series of extreme events were simulated using STWAVE to determine design conditions for the proposed Cat Island restoration plan. The top 20 events of record were used as input to the wave model. The results for the top event are displayed in Figure 5.5. All extreme event STWAVE model results are included in Attachment A.

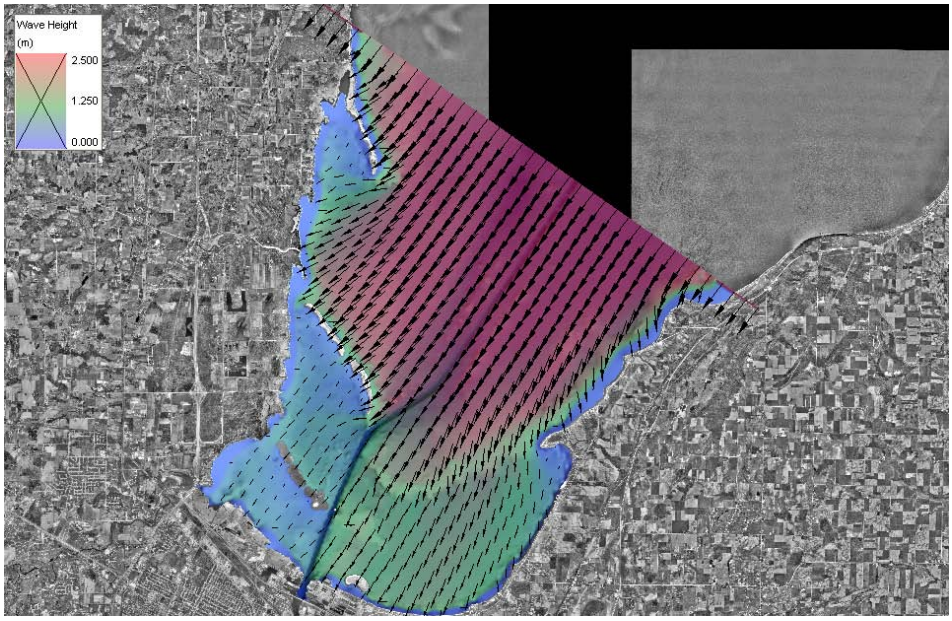

Figure 5.5 - STWAVE Results for NE Event (Ho = 2.7 m, Tp = 8.5 sec)

The results of the model for the extreme events were extracted and input into an extreme value analysis to obtain wave heights for various return periods for the islands. Table 5.2 documents the results of the analysis.

Table 5.2 - Wave Conditions by Return Period for Cat Island

Return Period (yrs)	Wave Height (m)
2	0.8
5	0.9
10	1.0
20	1.0
25	1.0
50	1.1
100	1.2
500	1.3

The 20-year event was chosen for design in the design development study. This relates to a 3.3 ft (1.0 m) wave, with a 6 second period.

On the southwest side of the islands, the SMB equation as documented in the 1977 Shore Protection Manual (USACE, 1977) was applied to determine a maximum wave height & period. Inputs to the calculation include a wind speed of 60 miles per hour, depth of 8 ft (lake bed elevation of –3 ft, LWD and high water of +5 ft, LWD), and a fetch of 2 miles. A design wave height and period of 2 ft and 4 seconds, respectively, was determined from the calculation.

5.2.3 Growing Season Event Simulations

A series of typical annual events were also simulated using the STWAVE model. The purpose of these runs was for use in the vegetation analysis documented in Section 8. The events approximated a range of average annual events that may occur in a typical growing season. Using the model output of wave heights, a grid of wave orbital velocities was calculated using linear wave theory. Figure 5.6 displays a typical growing season event simulation. Figures 5.7 and 5.8 show orbital velocities for existing and proposed conditions, respectively.

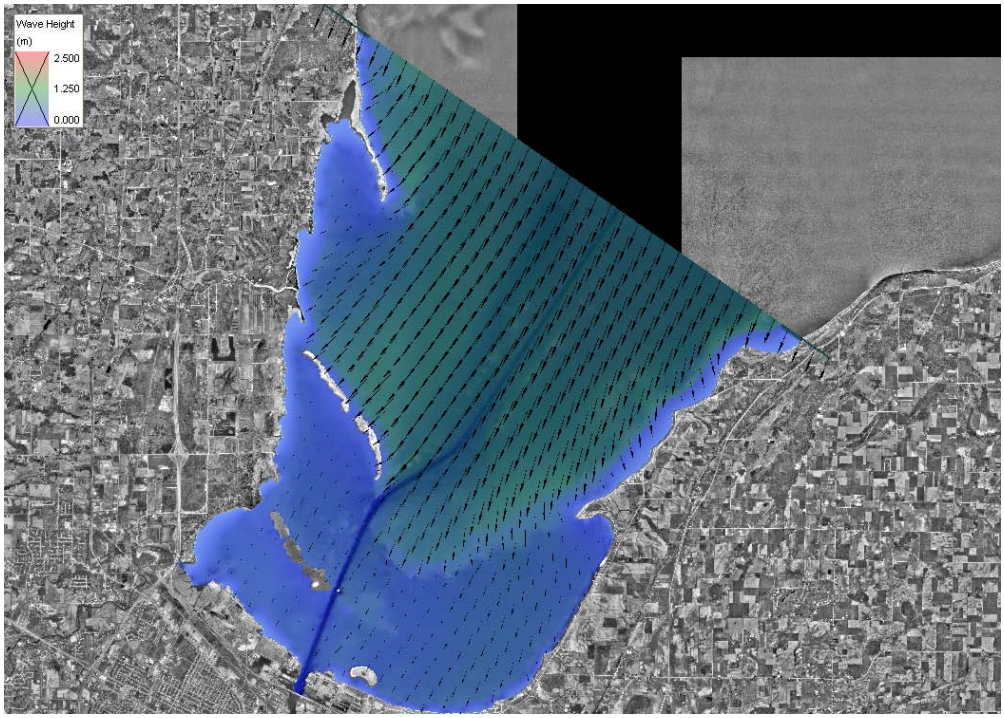

Figure 5.6 - STWAVE Results for Typical Growing Season Event (Ho = 1.3 m, Tp = 5.5 sec)

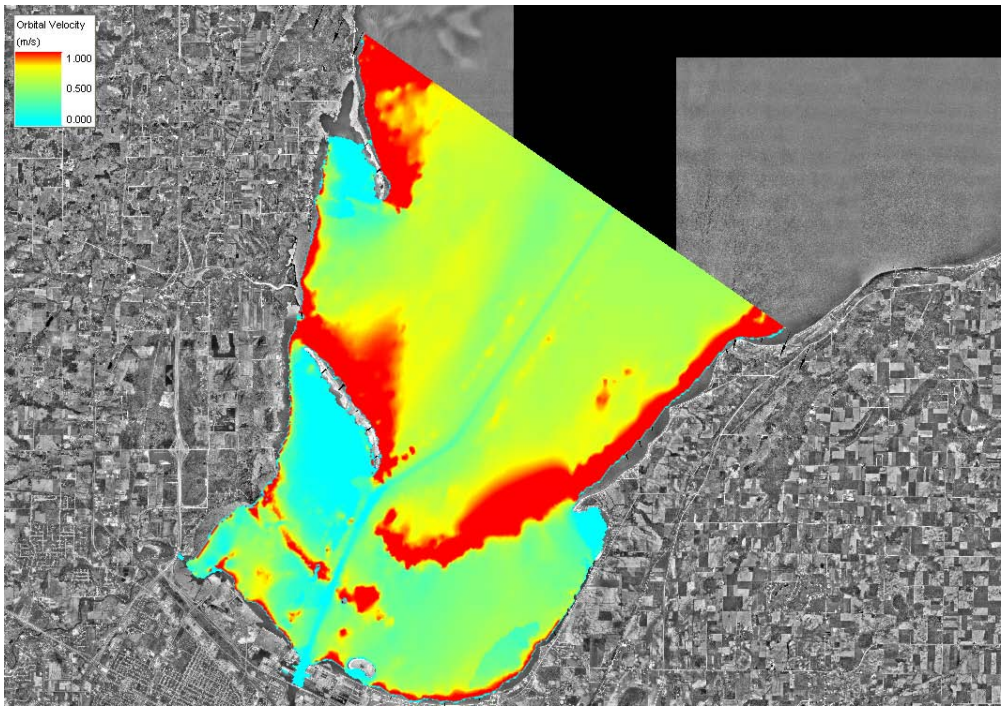

Figure 5.7 – Orbital Velocities - Existing Conditions (Ho = 1.3 m, Tp = 5.5 sec)

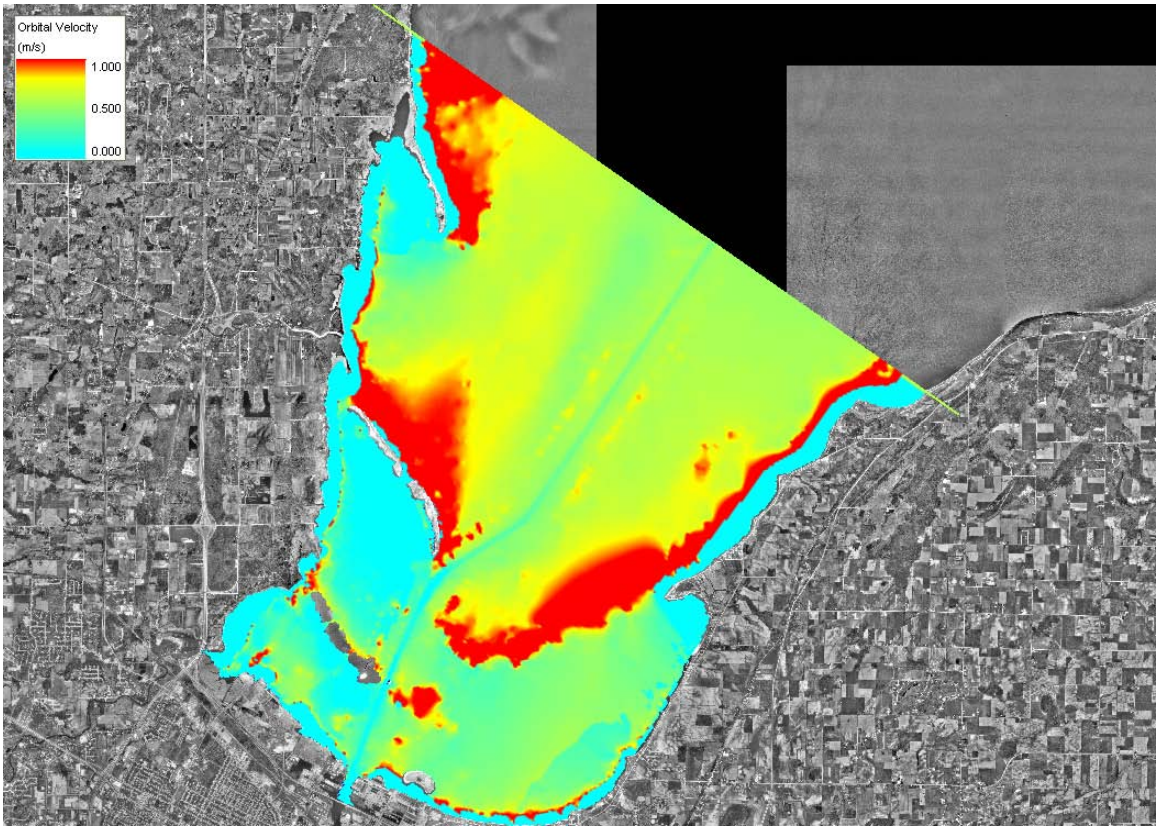

Figure 5.8 – Orbital Velocities - Proposed Conditions (Ho = 1.3 m, Tp = 5.5 sec)

6.0 Hydrodynamic analysis

6.1 MIKE 21 Hydrodynamic Model

A hydrodynamic analysis was performed to evaluate velocities around the proposed islands due to storm surge by wind. The hydrodynamic model was also used as the basis for TSS modeling (both river plume and local re-suspension by waves) as described in Section 7. Due to the orientation and geometry of the bay, the worst condition for storm surge at the Cat Islands is a strong northeasterly wind. The water level near the Cat Islands builds up and as the wind stops the water level seiches back down to the level before the storm. This phenomena is observed in the water level data obtained from NOAA gauge 9087079 Green Bay, Lake Michigan, WI. As the water level rises up and seiches downwards, water is pushed into and around the proposed layout of the Cat Islands. The analysis was performed to quantify the velocities around the proposed islands that may be observed during extreme events.

The HD module of the MIKE 21 modeling system was used for this analysis. Used as inputs to the model are the following:

- Detailed Bathymetry data for the entire Green Bay
- Wind Conditions from Green Bay, WI (NOAA Gauge 14898)
- Water Levels from Sturgeon Bay, WI (NOAA Gauge 9087072) and Port Inland, MI (NOAA Gauge 9087096)

The grids were created using a nesting system, to both cover a large area and cover the Cat Island area in great detail. The grids used had a range of mesh sizing of 500 m, 180 m, 60 m and 20 m. Details for each grid are displayed in Table 6.1. The grids are displayed in Attachment B.

Table 6.1 – Grid Parameters for Hydrodynamic Analysis

Grid Spacing	Nx	Ny
500 m	98	299
180 m	115	111
60 m	220	166
20 m	259	202

6.2 Surge Event Simulations

The NOAA Green Bay water level gauge was probed to find extreme and typical surge events. Four events were identified for use in analysis. The events chosen are displayed in Table 6.2.

Table 6.2 – Events chosen for Hydrodynamic Analysis

Date	Surge Height (ft)
December 3, 1990	5.5
April 15, 1993	3.8
April 20, 2000	3.5
May 18, 2000	2.0

The Green Bay NOAA water level gauge was used for calibration of the model. Each event compared to the gauge very well. Figures 6.1 through 6.4 display the results of the calibration analysis.

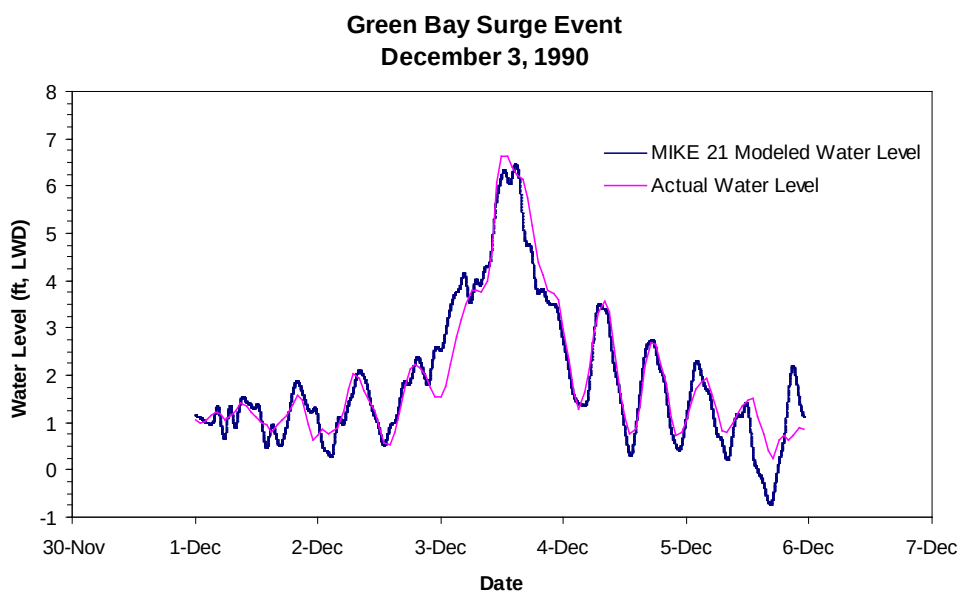

Figure 6.1 – December 3, 1990 Surge Model Results

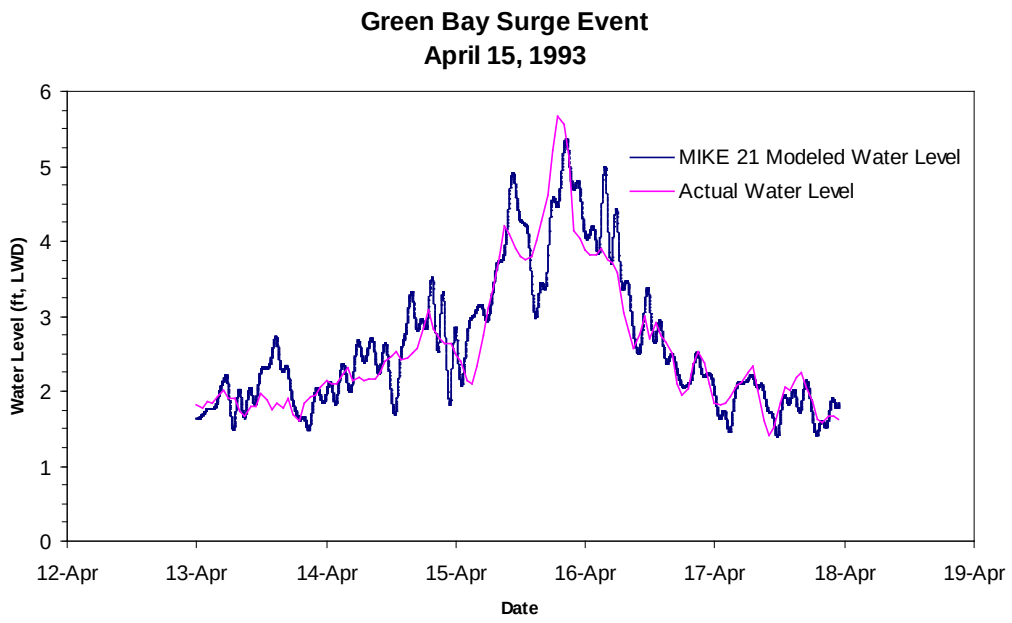

Figure 6.2 – April 15, 1993 Surge Model Results

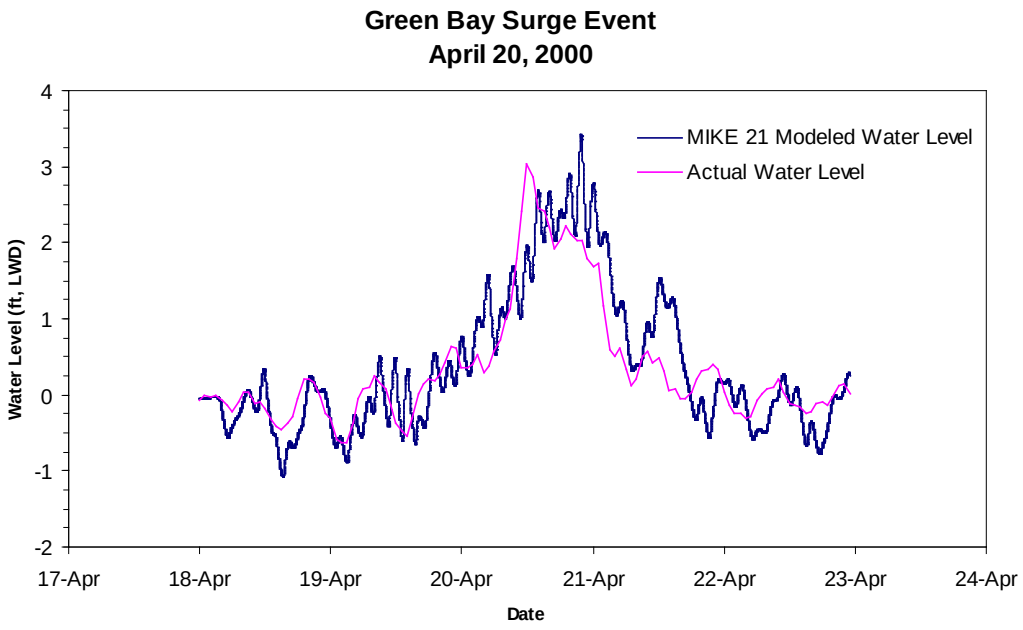

Figure 6.3 – April 20, 2000 Surge Model Results

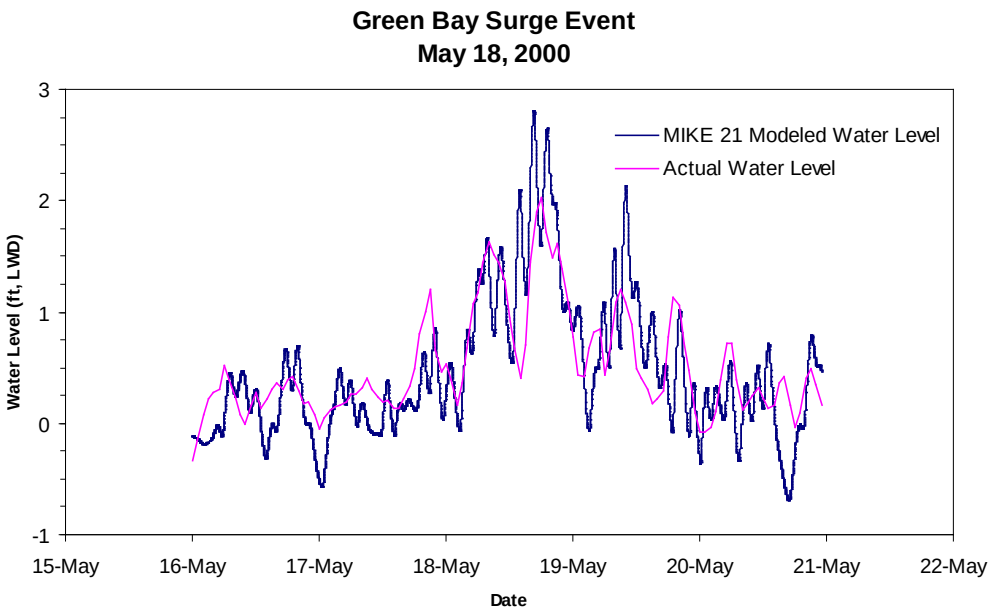

Figure 6.4 – May 18, 2000 Surge Model Results

After calibration, the four simulations were performed for each of the following conditions:

- Existing Conditions (no islands)
- Proposed Conditions (all 3 islands)
- Construction Worst Case Condition (all 3 islands, Access Road from shore to Central Island)

Bathymetric grids for the proposed islands and construction road conditions are displayed in Attachment B. The MIKE 21 Model was run for all 4 events and 3 bathymetric conditions. Figures 6.5 through 6.7 display model result velocity vector maps for the peak of the December 3, 1990 event for the three conditions. The peak velocity observed in the gaps was 0.4 m/s in the existing conditions, 0.7 m/s for the proposed conditions and 0.7 m/s for the construction road conditions. Figures 6.8 through 6.10 display velocities in the gaps for the December 3, 1990 event for the three conditions. Attachment B displays the gap velocities for the remaining event and condition combinations.

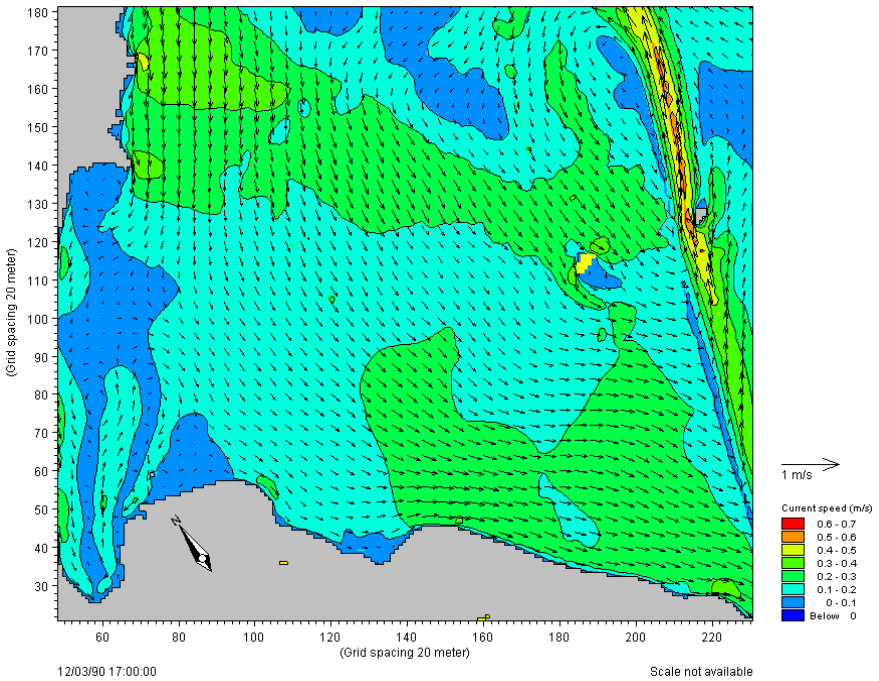

Figure 6.5 – December 3, 1990 Existing Conditions

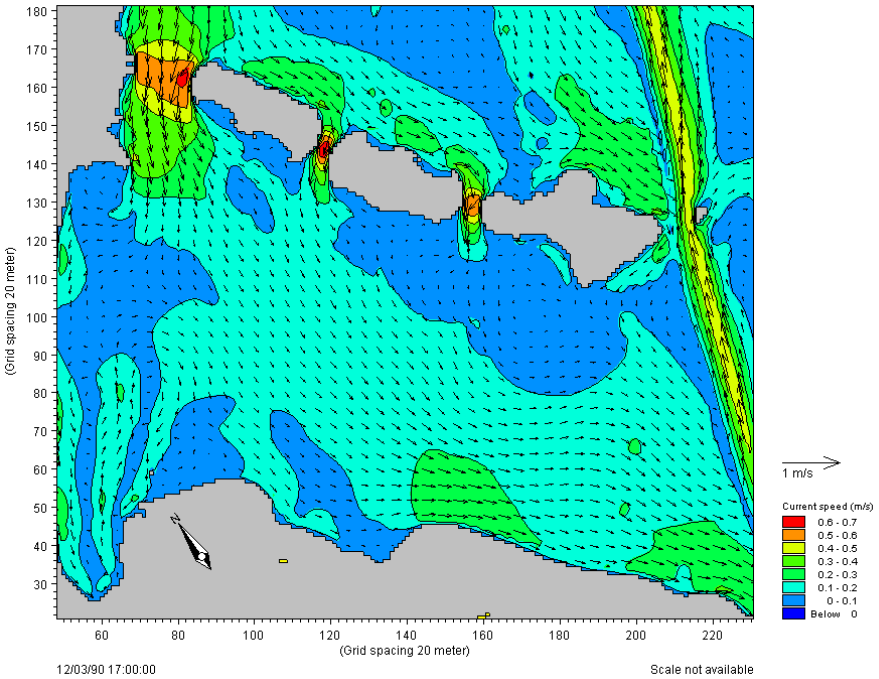

Figure 6.6 – December 3, 1990 Proposed Conditions

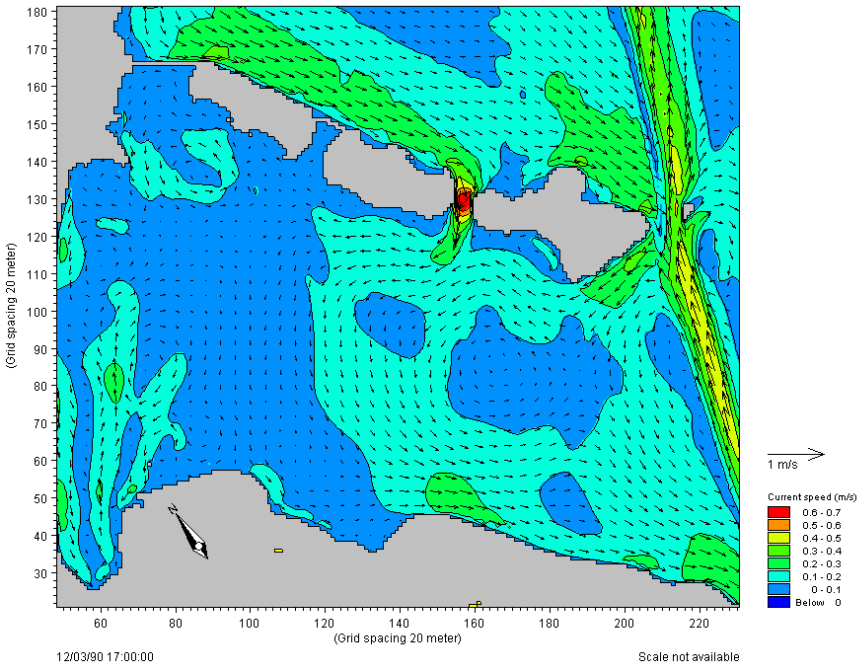

Figure 6.5 – December 3, 1990 Construction Road Conditions

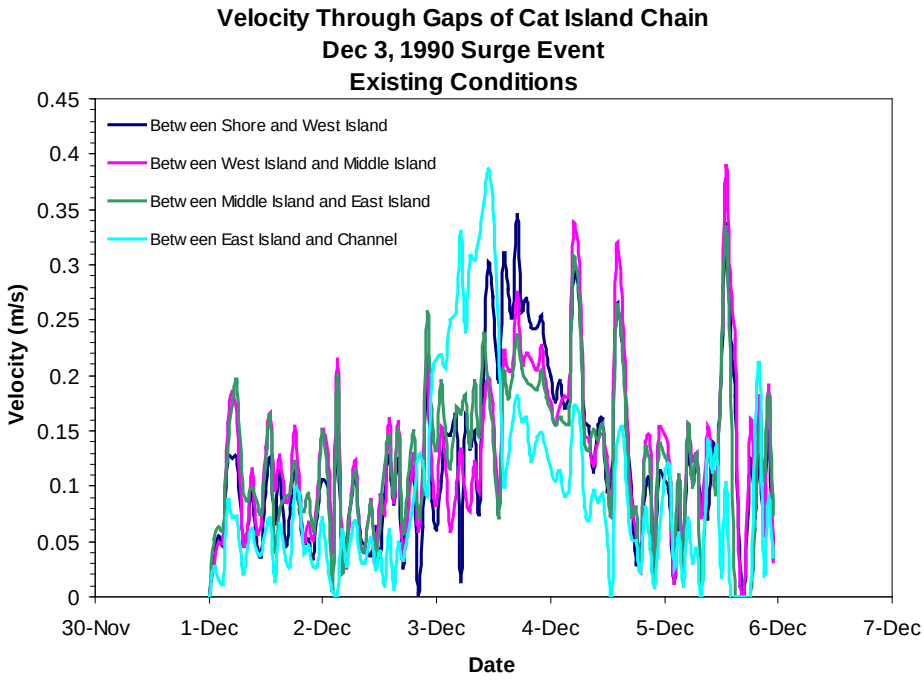

Figure 6.8 – Island Gap Velocities for Dec 3, 1990 Event – Existing Conditions

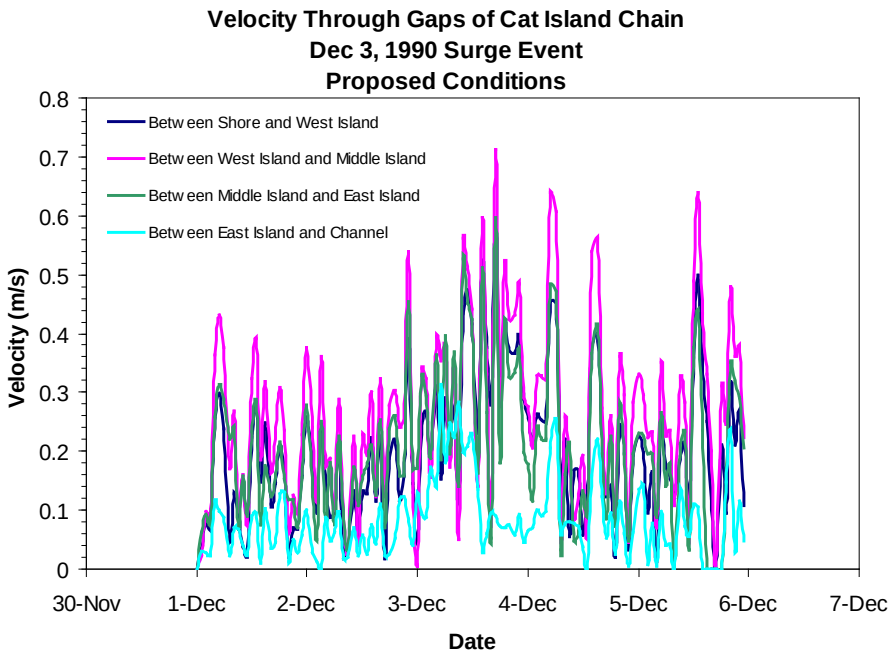

Figure 6.8 – Island Gap Velocities for Dec 3, 1990 Event – Proposed Conditions

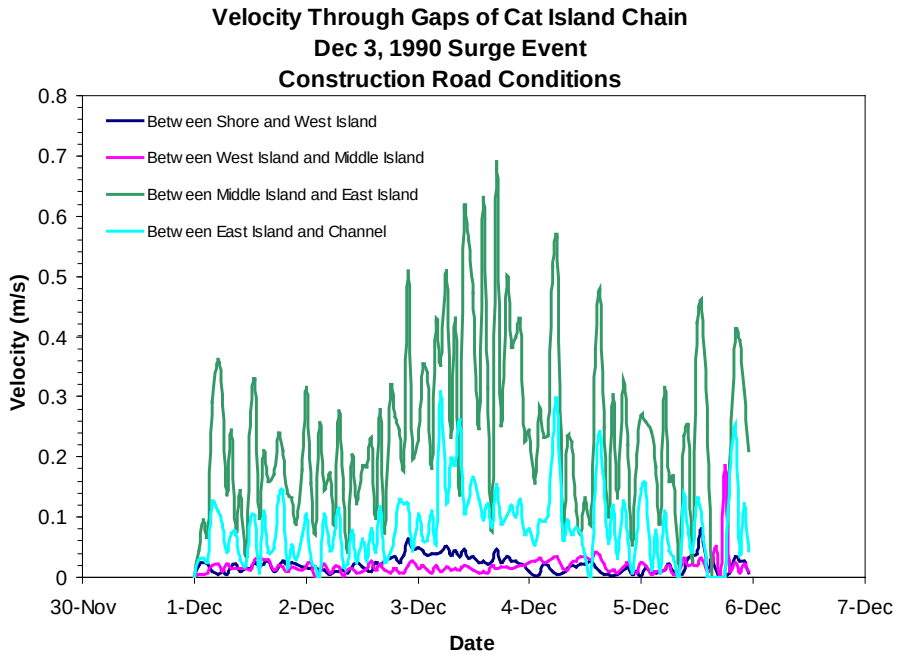

Figure 6.8 – Island Gap Velocities for Dec 3, 1990 Event – Construction Road Conditions

6.3 Dredge Sand Beach Sections

Along the southwest side of the proposed islands a flatter slope is anticipated, due to the fine sediments of the dredge sand material. The COSMOS numerical model of coastal processes was applied to investigate the cross-shore stability of fine sand beaches on the lee side of the islands. It is important to evaluate the stability of the dredged sand without protection on the lee side of the island during extreme wave attack. The COSMOS model is a deterministic profile model of coastal processes and simulates: wave transformation (shoaling, refraction, friction losses, breaking, wave decay and reformation, run-up and overtopping), hydrodynamics (longshore and cross-shore steady currents including undertow and non-linear orbital velocities) and erosion/sedimentation (considering bed and suspended load, erosion of glacial sediment and a consideration of erosion resistance surfaces).

For application to the lee side of the island, an extreme storm condition (24 hours with an Hs of 2 ft and a period of 3 s) was modeled for three different lake level scenarios corresponding to moderate to very high lake levels (+3, +4 and +5 ft LWD). The model tests were completed for two different assumptions on D50 of the dredged sediment (0.1 mm and 0.15 mm). The assumed initial nearshore/beach profile consisted of a slope of 1:200 below +2 ft and a graded 1:15 slope above +2 ft. The results, showing profile change for the 24-hour period, are shown in Figures 9.8 and 9.9. The results demonstrate that erosion of the upper and steeper 1:15 slope only commences for lake levels of +4 ft or greater. For the model test with a D50 of 0.15 mm the eroded sediment is transported no further than about 80 ft (25 m) beyond the toe of the steep slope (i.e. out onto the flatter slope beyond). For the test with the finer D50 of 0.1 mm, most of the sediment that is transported offshore is confined to within 100 ft (30 m) of the toe of the steep slope, however a small amount is transported further offshore. This numerical model estimates were used to develop the required length and form of the beach containing structures on the southwest side of the islands and also to confirm that losses of beach sediment from the islands would be minimal under extreme storm conditions.

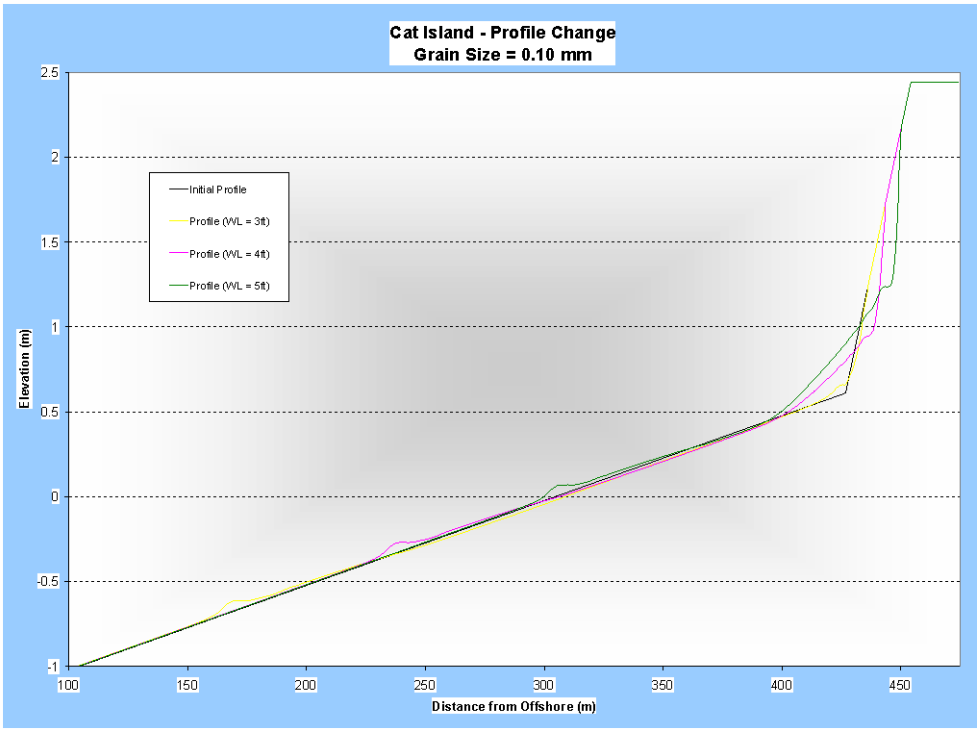

Figure 9.8 – Dredge Material Beach Section Profile Change (d = 0.10 mm)

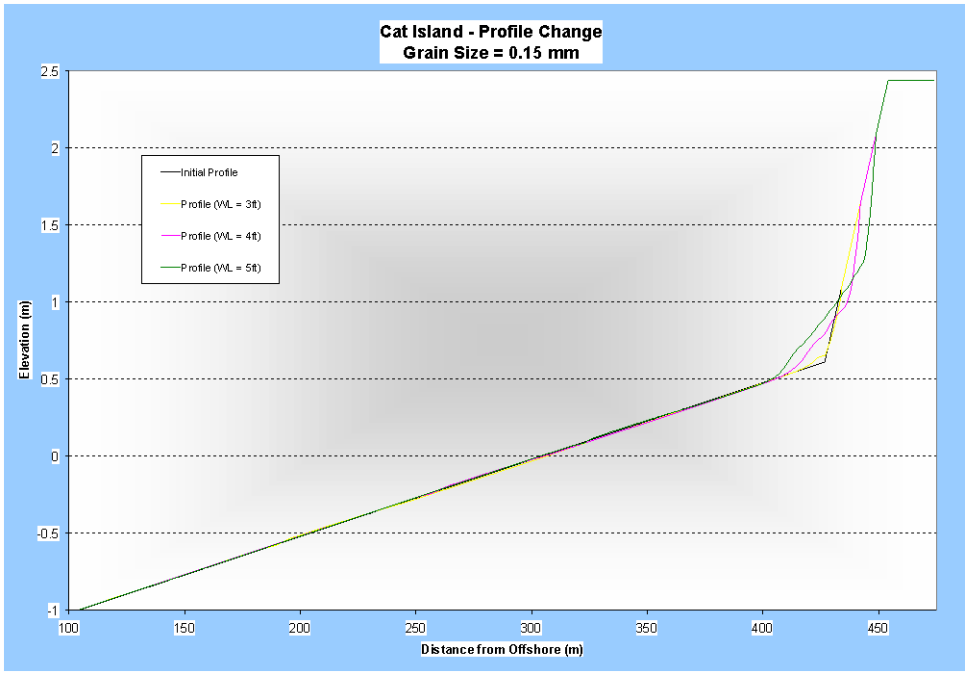

Figure 9.9 – Dredge Material Beach Section Profile Change (d = 0.15 mm)

7.0 Modeling Total Suspended Solids

7.1 Introduction

The primary purpose of the TSS modeling was to define the TSS and associated water clarity with and without the islands constructed. One of the primary goals of the restoration of the Cat Island Chain is to promote the re-establishment of aquatic vegetation in the areas of the mouth of Duck Creek, Peat's Lake and Peter's Marsh. Large areas of aquatic vegetation were lost after the sub-aerial part of the Cat Island Chain was washed away in 1973. It is assumed that one of the key current impairments to recovery of these areas of aquatic vegetation is less than ideal water clarity. Numerical models of waves, currents, sediment re-suspension and advection/dispersion of suspended sediment will be applied to representative conditions to evaluate the impact of the proposed islands on water clarity in the lee of the islands. In turn, these predictions will be used to evaluate the potential survivorship of aquatic vegetation with and without the islands in Section 8 of this report.

7.2 Model Approach, Setup and Inputs

7.2.1 Modeling Approach

The major causes of high TSS in Lower Green Bay are the sediment plumes from Fox River and Duck Creek and sediment re-suspension induced by waves and currents. These suspended sediments are carried by lake circulation driven by wind, surge, and waves as well as river flows. Since the wave-induced current component is generally smaller than wind driven current, and more localized, the currents generated by wave radiation stresses are neglected in this modeling assessment.

In order to account for the complicated dynamic conditions, a comprehensive numerical model system has been developed as shown in Figure 7.1. The system consists of the STWAVE model, the MIKE21 Hydrodynamic (HD) and Mud Transport (MT) models. The STWAVE model was used to simulate waves that are generated by wind with consideration of wave transformation and propagation in shallow waters (details on the STWAVE modeling are presented in Section 5). Wind and lake level data are required inputs for the STWAVE model.

MIKE21 was used to simulate hydrodynamics and sediment transport in the TSS assessment. It is a two-dimensional horizontal model employing a finite difference method. The MIKE21 model has been applied in thousands of locations around the world and is recognized as one of the most stable and reliable hydrodynamic models. There are two modules included in this modeling application:

- HD module – simulates water level fluctuation and currents in response to a variety of forcing functions in lakes, estuaries and coastal regions. The effects and facilities include bottom shear stress, wind shear stress, barometric pressure gradients, Coriolis force, momentum dispersion, sources and sinks, evaporation, flooding and drying and wave radiation stresses. It is the basic model for all other simulations.

- MT module – accounts for the erosion, transport and deposition of silt, mud and clay particles under the action of currents and waves. The module can be applied in two modes: multi-fraction mode and multi-layer mode. The multi-fraction mode enables the model to simulate the dynamics of multiple fractions of suspended sediment and is suitable for depositional environments. The multi-layer mode enables the model to simulate the evolution of, and interaction between, several bed layers and sediment re-suspension induced by waves. Generally, this mode is suitable for depositional and erosional environments.

The two modules are integrated in the MIKE21 software package that provides a convenient user interface for setup.

The inputs for the MIKE21 model include: a) river inflow and TSS from Fox River and Duck Creek, b) temporally varying wind speed and direction, and c) temporally varying mean lake level. Wave data generated by STWAVE are used as an additional input for the MT module. Coriolis force and drying process are also included in the modeling application.

Finally, the currents and sediment concentration calculated by the MIKE21 model and the orbital velocity calculated by STWAVE model are used as inputs to Baird in-house software - Spatial Data Analysis (SDA) for the aquatic vegetation analysis, which will be described in Section 8 in detail.

7.2.2 MT Model Parameters

All parameters for STWAVE are set as the same as described in Section 5, which are calibrated against the recorded waves. The MIKE21 model provides a variety of parameters for hydrodynamic and sediment transport simulation. Some of these parameters need to be adjusted through model calibration. All parameters for hydrodynamic simulation are described in Section 6 and have been calibrated with observed data. These parameters are directly used for this application. The major parameters associated with mud transport are:

- **Suspended sediment grain size** - MIKE21 doesn't provide a parameter to directly set the grain size of suspended sediment. Instead, it provides an adjustable coefficient for settling velocity, which is equal to settling velocity in clear and still water and can be completely determined by grain size. Two grain

sizes of 0.02 mm (fine silt) and 0.0027 mm (clay) were used for the model simulations. Clay is the dominant fraction of sediment discharged by the Fox River and Duck Creek and will be used for sediment plume modeling. Fine silt is representative of the sediment that can be easily re-suspended by waves from the lakebed. This class is used for the simulation of sediment re-suspension induced by waves;

- **Bed sediment materials** – MIKE21 with MT multi-layer mode uses a number of layers to describe bed soil materials. The physical properties of each layer are described by parameters such as critical shear stress, dry density, and erosion coefficient. Critical shear stress and erosion coefficient are the key parameters for the simulation of sediment re-suspension. Relatively, dry density is not as important as the others because it is used only for bed change calculations, which are not important for this project. In the model application, three layers with thickness of 0.5 m, 0.5 m, and 2 m are used to describe the lakebed sediment. Based on the available borehole logs, a median grain size of 0.15 mm (fine sand) is used to determine these parameters for all three layers as described below.

- **Critical shear stress for erosion** – Critical shear stress for erosion depends mainly on grain size and consolidation. The top layer is assumed to be a fresh deposit and no consolidation is considered. In that case, the critical shear stress can be determined using Shields' Curve, giving 0.12 Pa for 0.15mm sediment. Although the grain size for the second and third layers are assumed to be the same, consolidation should be considered. Using information from other studies, the critical shear stresses in the second and third layer are set as 0.20 and 2.5 Pa, respectively;

- **Erosion coefficient factor** - This is a calibration parameter and is initially set as the default value. The value is then adjusted through calibration. There is another parameter called erosion coefficient power for which the default value (1.0) is used.

7.2.3 Incoming Sediment From Rivers

The suspended sediment load from Fox River and Duck Creek is an important source for sediment plumes in the bay. The suspended sediment concentration must be provided for the modeling test as an input. Unfortunately, continuous long-term records of TSS at the two river mouths are not available for the model setup and simulation. Therefore, the available TSS sample data are used to develop relationships between TSS and discharge for both rivers as listed below:

- Sediment sampling data collected at USGS Gage at DePere (#04085059) between 1988 to 1990;

- Sediment sampling data collected at USGS Gage at Duck Creek Near Howard (#04072150).

The developed rating curves are shown in Figures 7.2 and 7.3 for Fox River for Duck Creek, respectively. The trend of increasing TSS with flow is obvious though the correlation of TSS and discharge is not the best (particularly for Duck Creek). Nevertheless, these developed rating curves are used to generate the time series TSS from the rivers using the continuously measured discharge data at the gages.

It should be noted that the TSS calculated by using the rating curves represents only abiotic component of suspended solid from the rivers. There is no information to determine biotic component from the river. Therefore, a constant fraction is used for the biotic component (see Science and Technical Advisory Committee, 2000) for vegetation analysis. The biotic component is not included in the model simulations.

7.2 Selection of Testing Scenarios

The objective of the modeling is to reproduce TSS patterns under extreme weather conditions during the growing season for aquatic vegetation (from April to November). As the selected models were not conducive to long-term and continuous model simulation it was necessary to define representative storm conditions for modeling.

The turbidity in Lower Green Bay is generally high during rainfall events and/or windstorms. During rainfall events, large river flows carry large amounts of suspended sediment into the bay and resulting in a widespread sediment plume. Generally, the rainfall events occur more frequently in the spring and summer seasons than the other seasons. Therefore, these events may have significant impacts on vegetation growth. Depending on wind direction, windstorms can create large waves on the bay that suspend sediment from the lakebed resulting in high turbidity in the bay. Additionally, high wind speed during windstorms can generate strong lake circulation and surges that will enhance the advection of sediment. Therefore, the selection of representative storm events is based on three factors:

- Flow discharge and incoming TSS from Fox River – representing rainfall events on the Fox River Watershed;

- Wind speed and direction in the bay – representing windstorms on Green Bay;

- Lake level variation – representing storm surges in Green Bay;

Five extreme events were selected to represent distinctive scenarios as described in the following table.

Table 7.1 The Selected Five Events for Model Simulations

Runs	Date	Wind		Fox River		Duck Creek		Major Dynamics
		Speed (km/h)	Direction (deg)	Discharge (m^3/s)	TSS (mg/l)	Discharge (m^3/s)	TSS (mg/l)	
1	7/17/1993	20	E	481	140	40	30	River Flow
2	6/22/1996	28	NE	453	130	25	184	River Flow
3	3/31/1998	55	NE	453	120	40	30	River Flow + Wind
4	9/4/2000	47	NE	283	50	0.1	10	Wind
5	4/28/2002	54	NNE	354	70	20	23	Wind + Surge

The table lists the peak wind speed, dominant wind direction, maximum flow discharge, and TSS for each event. The model period for each event is generally 2 days to 15 days depending on how fast the model reaches stability. Model Runs 1 and 2 represent rainfall storm events during which the water clarity in Lower Green Bay is mainly impaired by sediment plumes discharged from the two rivers. Run 3 represents a scenario of heavy rain and high waves. Run 4 represents a wind storm (and wave) event and Run 5 represents a windstorm with large surge (large lake level rise).

7.3 Model Testing and Calibration

The model calibration was performed for Runs 1, 2 and 4 with measured TSS, when available. A number of the TSS measurements at fixed stations (see locations in Figure 7.4) have been regularly made during the summer season (from June to September) since 1986. These valuable data are used for model calibration. Unfortunately, the TSS measurements were generally conducted after storms for safety purposes (i.e. to avoid being on the bay in vessels when waves were highest) whereas the modeling focused on the peak conditions of the storms. Therefore, the model periods for these three runs have been extended to cover the measurement period. The available measured data do not cover the model periods for both Runs 3 and 5 and therefore these two runs were not directly calibrated.

The comparisons of modeled to measured TSS are shown in Figure 7.5 to 7.7 for Runs 1, 2, and 4, respectively. The modeled TSS is shown by full color shading with a TSS gradation of 20 mg/l. The measured TSS at the stations is plotted as a dot filled with appropriate color using the same gradation as the modeled TSS. Therefore, the measured TSS agrees well with the modeled TSS if the color inside a dot is the same as the surrounding color. It is evident that the modeled TSS generally agrees well with the measured TSS for the stations #22, #23, #32, and #26. Note that these four stations are most representative of the project site – the area of anticipated aquatic vegetation restoration. However, the modeled TSS at Station #25 is generally lower than the measured TSS. This may result from the fact that the lakeside open boundary condition

in the model was assumed to have no incoming sediment flux from the other part of the bay, which is probably incorrect at least in some conditions.

Figure 7.7 shows the TSS levels determined by the University of Wisconsin (UW) from a satellite image as well (in smaller dots). The colors of the dots show the inferred TSS levels and are the same as the color scale used for the modeled and directly measured TSS. It is seen that the modeled TSS generally agrees with the estimated TSS from the satellite image. However, the modeled TSS is higher near the navigation channel and lower near the shores when compared to the TSS estimated by UW from the satellite image. Apart from numerical model inaccuracy, the discrepancy may result from satellite image analysis because the bands (or color channels) that are sensitive to water turbidity are also sensitive to water depth (and reflection from the lake bed). Generally, the approach using satellite image to determine the TSS may over-predict TSS in shallow water and under-predict TSS in deep water. The discrepancy between the predicted and inferred TSS levels from the satellite image may also result from inaccurate representation of the TSS load discharged from the Fox River.

In summary, the numerical model results reproduce the TSS patterns in the dynamic circumstances of rainfall events and windstorms reasonably well in the area of anticipated aquatic vegetation restoration. This calibrated model is next used to predict the TSS levels after the construction of the proposed islands, as described below.

7.4 Model Results

The calibrated model is used to predict flow and TSS patterns after the construction of the proposed east, central, and west islands. The model simulation runs include five selected events combined with the following five island configurations:

- East island;
- Central island;
- West island;
- All islands - a combination of all three islands;
- All islands together with an access road linking the west island to the shore.

Together with the existing conditions, more than 30 model runs were performed for this assessment. The model runs for each configuration used the same boundary conditions and the same model parameters as those for the existing conditions simulation. Therefore, the model results are fully comparable. Considering that all three islands may be eventually constructed within 2 to 3 years, this section will focus on the model

results for the configurations of all islands and all islands with the access road. All the results are presented in Attachment C.

7.5.1 Individual Island Tests

Each individual island could possibly exist on its own during the construction period, although all three islands may be constructed within 2 to 3 years. The objective of modeling each the different cases is to provide the hydrodynamic and TSS information for possible construction conditions. Since individual islands, on their own, may not have significant impact on TSS patterns, only Run 4 (high wave-induced re-suspension of lake bed sediment) is described here. The model results for other runs are shown in Attachment C.

The TSS patterns at the peak speed wind speed are shown in Figures 7.8 to 7.11 for existing condition, east island, central island, and west island, respectively. (The model runs were dynamic and only snapshots of the results are presented here, animations of the results are provided in Attachment C on CD). It is evident that the east and central islands, on their own, do not have a significant impact on the TSS pattern in the lee of the islands. However, the construction of the west island, on its own, can reduce TSS in the sheltered area. This result suggests that it would be best to begin construction with the west island, particularly if it takes many years to construct all three islands.

7.5.2 All Islands

The TSS patterns at the maximum TSS or wind speed for all five selected events are shown in Figures 7.12 to 7.26. For each event, there are three figures to depict the TSS patterns with the existing condition, all islands, all islands with the access road for comparison purposes.

Runs 1 and 2 represent rainfall storm scenarios and the sediment plume from the rivers is main contributor for high TSS in Lower Green Bay. The TSS patterns for the current circumstance and after the construction of three islands are shown in Figures 7.12 to 7.13 for Run 1 and in Figures 7.15 to 7.16 for Run 2, respectively. The construction of all islands causes a slight increase or decrease of the TSS in the lee of islands, depending on the direction of lake circulation. The TSS is slightly reduced after the construction if the lake circulation is counterclockwise as depicted in Run 1 (see Figures 7.12 and 7.13). Otherwise, the TSS is only slightly increased after the construction when the lake circulation is clockwise as depicted in Run 2 (see Figures 7.15 and 7.16). This may result from changes to the circulation patterns caused by the construction of the islands.

The TSS patterns for Runs 3, 4 and 5 are shown in Figures 7.17 to Figure 7.26. Through the comparison of these figures, the water clarity in the lee of three islands is

significantly improved after the construction of the islands. However, the TSS near the shore is still high, which probably results from the existence of the gap between the west island and the shore. This suggests that the access road linking the west island and the shore (or subsequently, a series of islands and dense aquatic vegetation after the road is removed) is necessary to restore the vegetation growth near the shore and inside this gap towards the southwest.

In summary, the construction of three islands will significantly reduce the TSS levels associated with wave and current induced sediment re-suspension but will have no significant influence (positive or negative) on the TSS levels that are derived from sediment plumes discharged from the rivers.

7.5.3 All Island with Shore Connection

As mentioned above, the existence of gap between the west island and the shore results in high TSS along the shore (see Figure 7.25). It is necessary to build the road to block the sediment transport along the shore. Clearly, after the construction of connection, the water clarity in Peat Lake and Peter's Marsh is significantly improved in most cases (see Figures 7.14, 7.20, 7.23, and 7.26). However, the connection road may trap the sediment plume if the lake circulation is clockwise as seem by comparing Figure 7.16 and Figure 7.17.

7.5 Interpretation of Findings

On the basis of model investigations for a variety of island configurations, the following conclusions can be made:

- The construction of all islands can tremendously reduce TSS level associated with wave and current induced sediment re-suspension in the lee of the islands during windstorms. It will significantly improve water clarity and promote the re-establishment of aquatic vegetation;

- The construction of the islands will not significantly change the TSS levels associated with sediment plumes from the Fox River during rainfall events. Depending on the direction of lake circulation, the TSS level in the lee of islands will be slightly higher or lower. If the lake circulation is counterclockwise, the TSS levels are reduced;

- After the construction of the three islands without an access road to shore, high TSS is found along the shore into the lower bay emanating from the gap between the west island and the shore. This suggests that flow through the gap should be blocked or significantly impeded. This could be achieved through construction of an access road during construction and possibly through a series of islands and dense aquatic vegetation after construction (i.e. when the access

road is no longer required). The model test results indicate that the access road can effectively block such longshore sediment transport and the water clarity in Peats Lake and Peter's Marsh is significantly improved;

- The access road linking the west island to the shore may cause a problem by trapping the sediment plume from Fox River when the lake circulation is clockwise. The frequency of occurrence for this situation is low and this condition would have naturally occurred when the islands and a dense marsh to the west of the islands existed prior to the early 1970s;

- The construction should commence at the access road, proceeding to the west island, and then central and east islands. This construction sequence will provide the greatest reduction TSS levels in the lower bay during the construction.

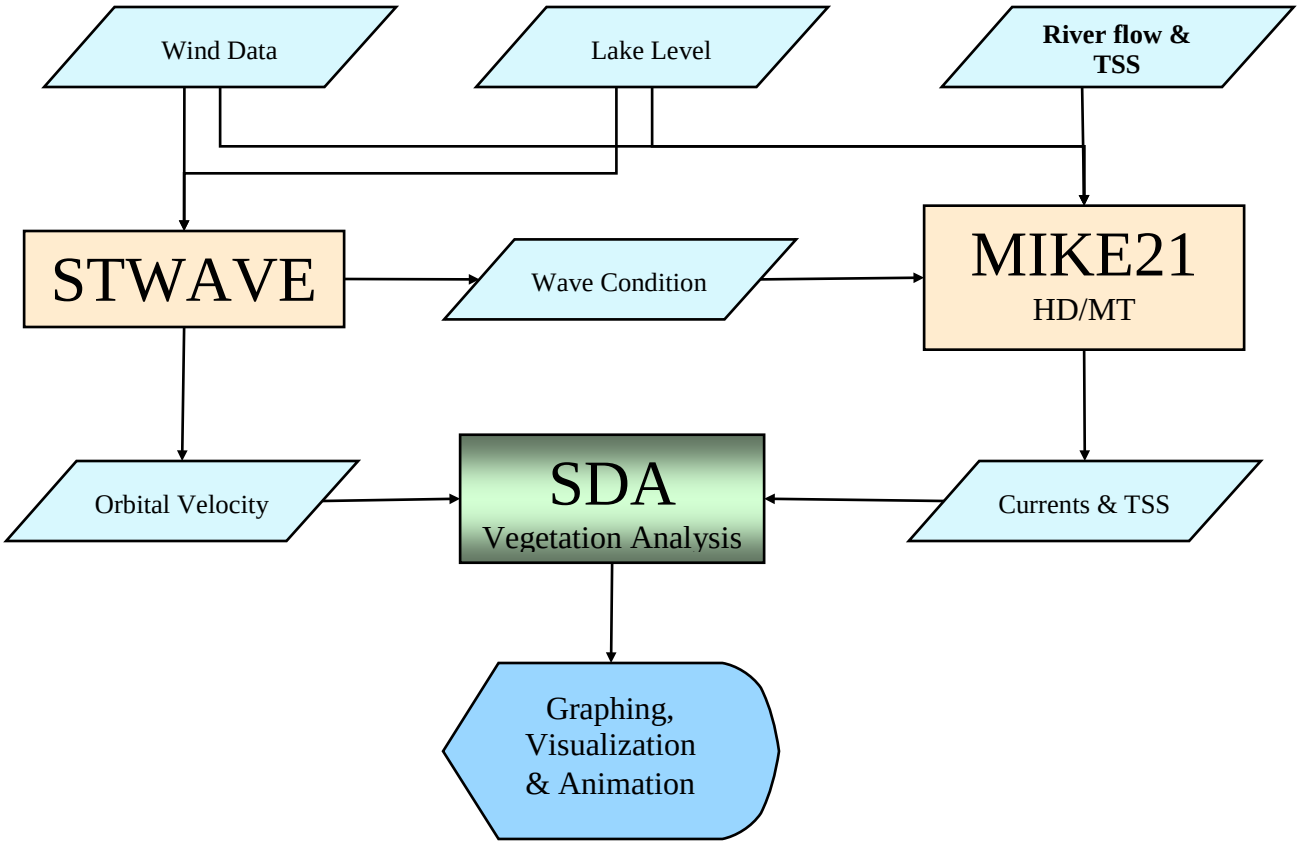

Figure 7. 1 Model System for TSS and Vegetation Analysis

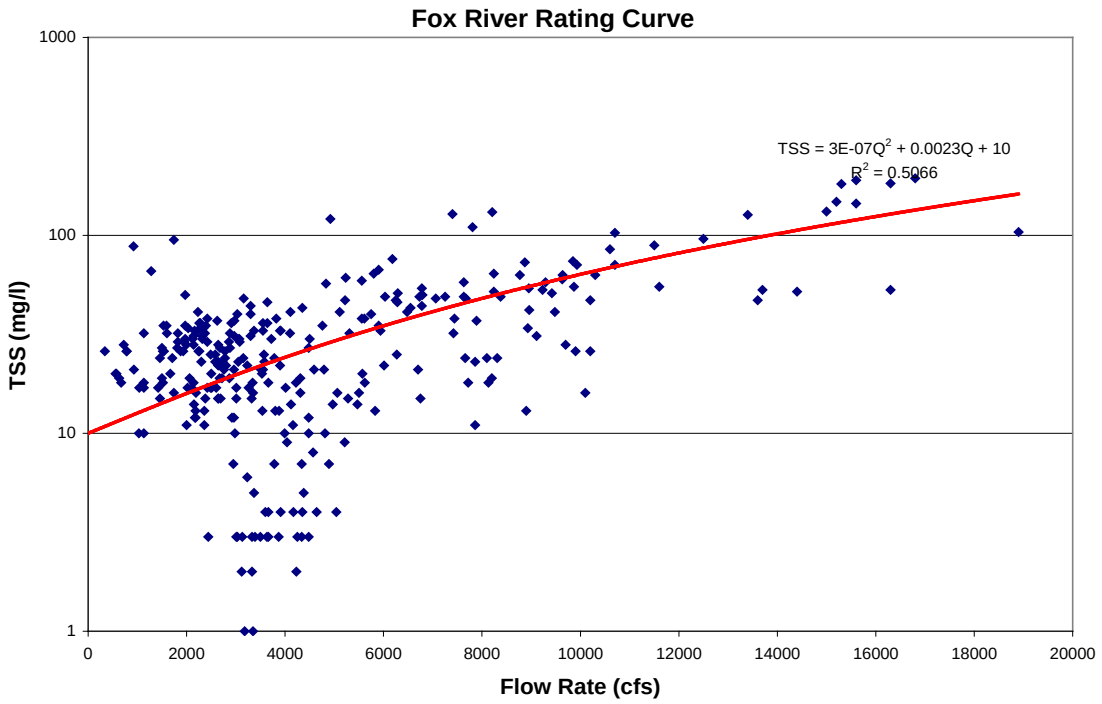

Figure 7. 2 Rating Curve of TSS for the Fox River (Using DePere Station Information)

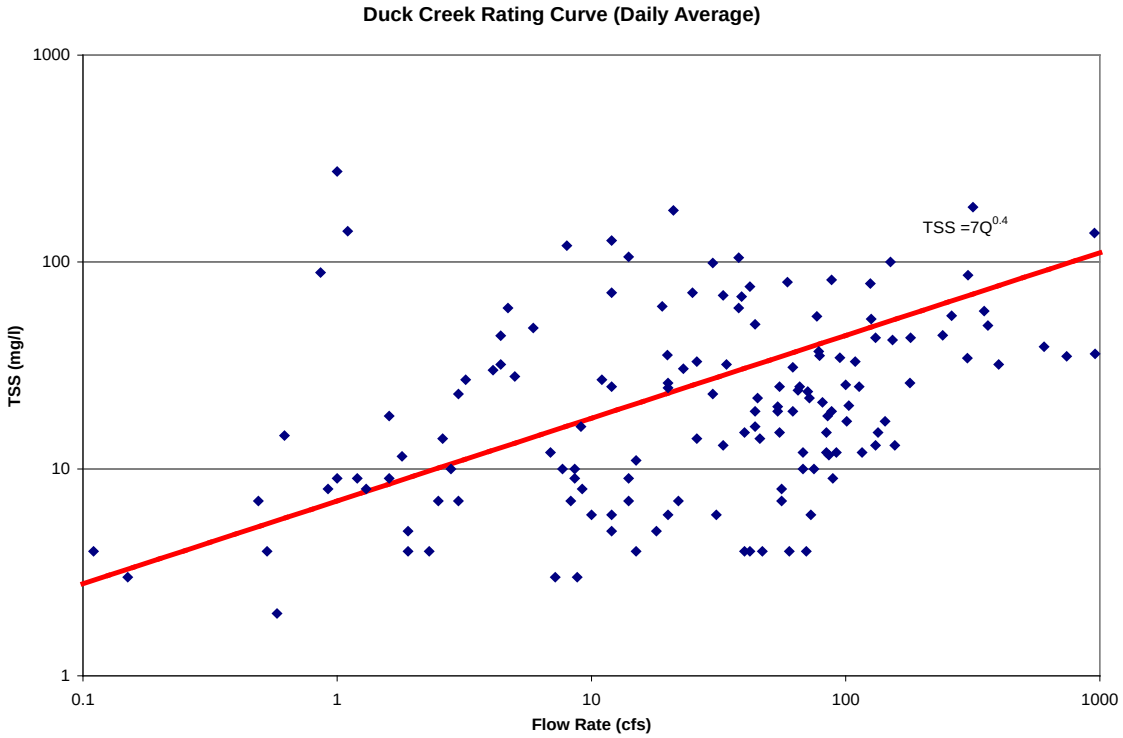

Figure 7 3 Rating Curve of TSS for Duck Creek

Figure 7.4 Locations of Water Sampling Stations

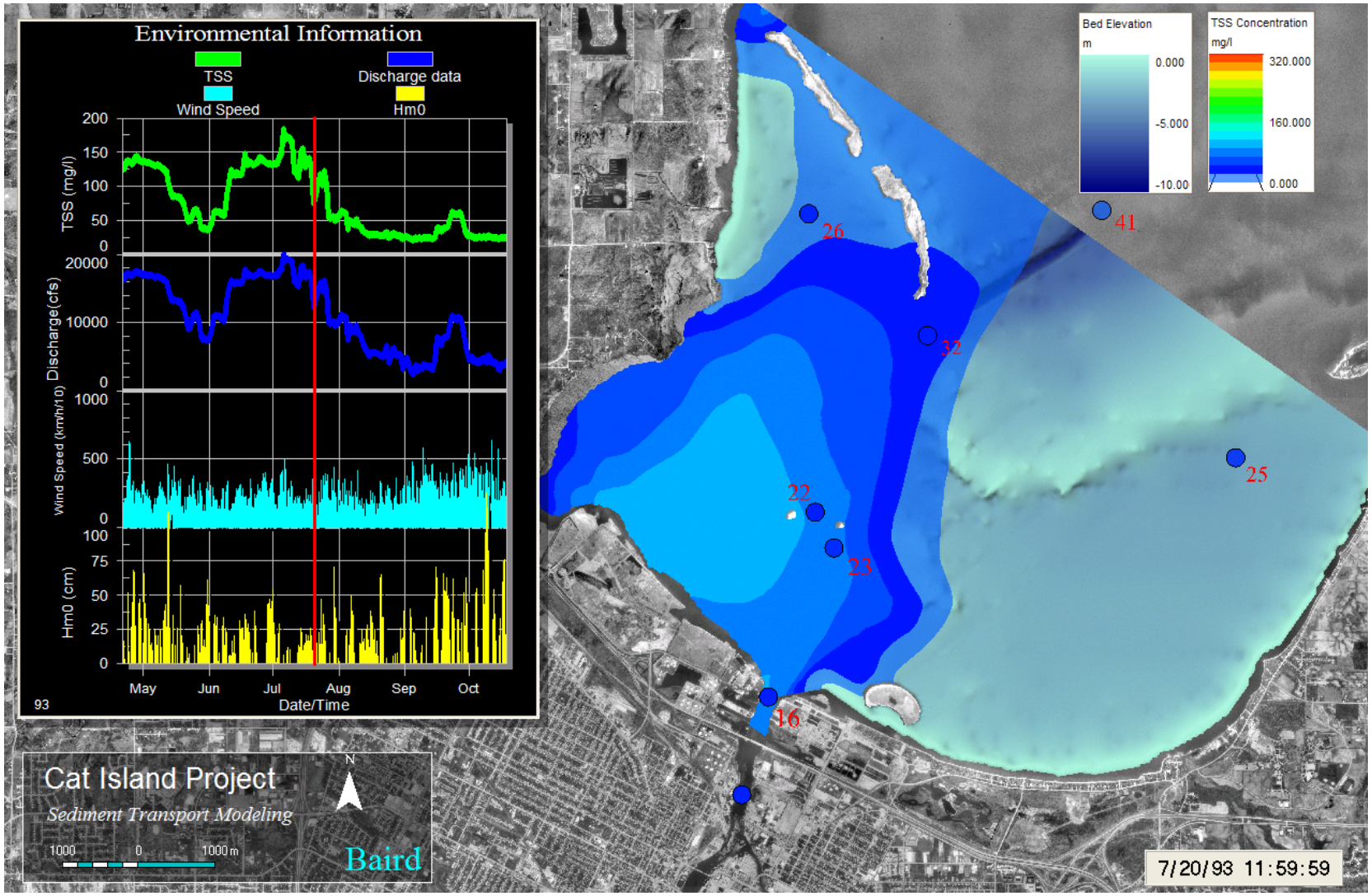

Figure 7.5 Model Calibration for Run 1

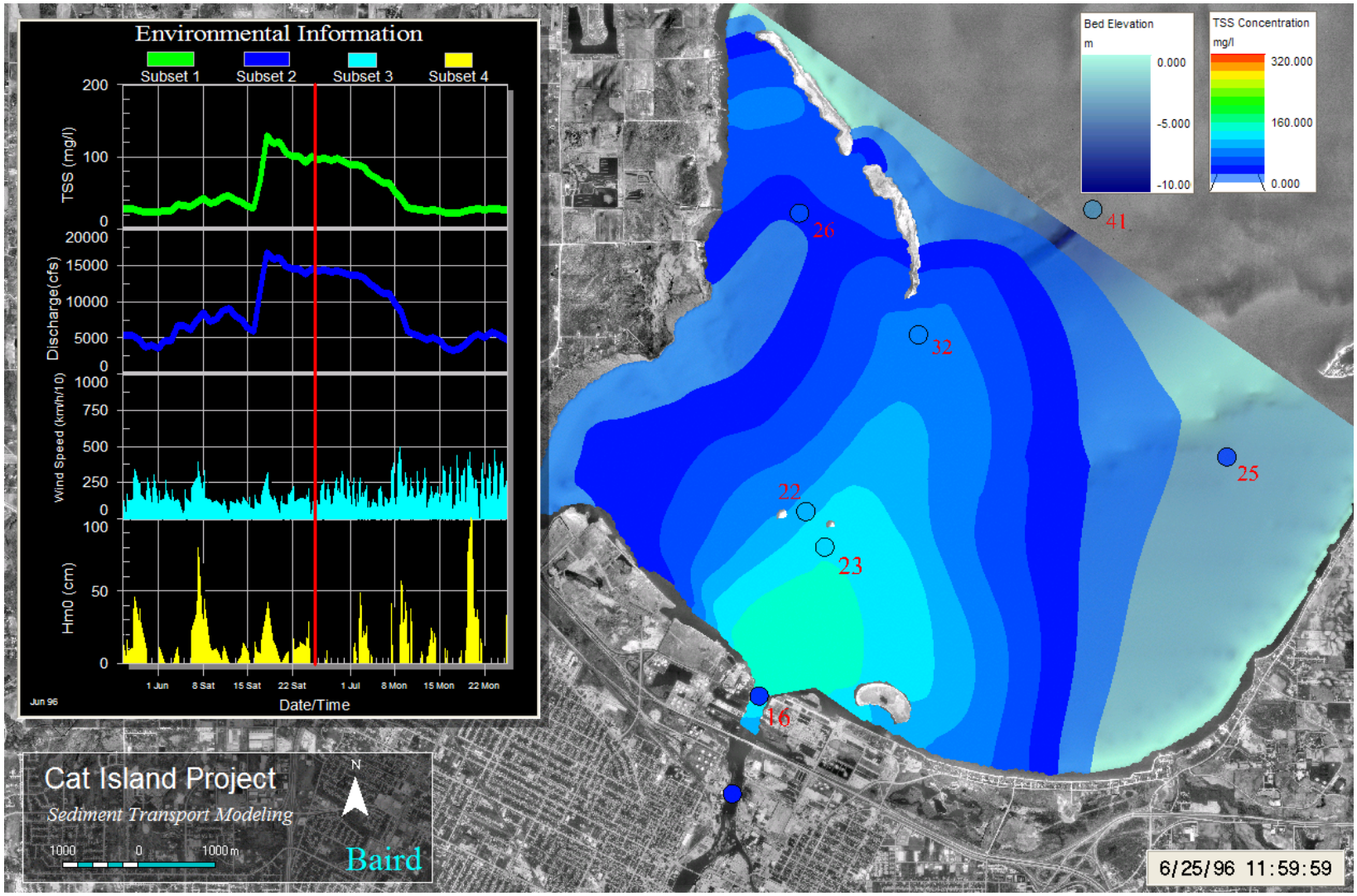

Figure 7.6 Model Calibration for Run 2

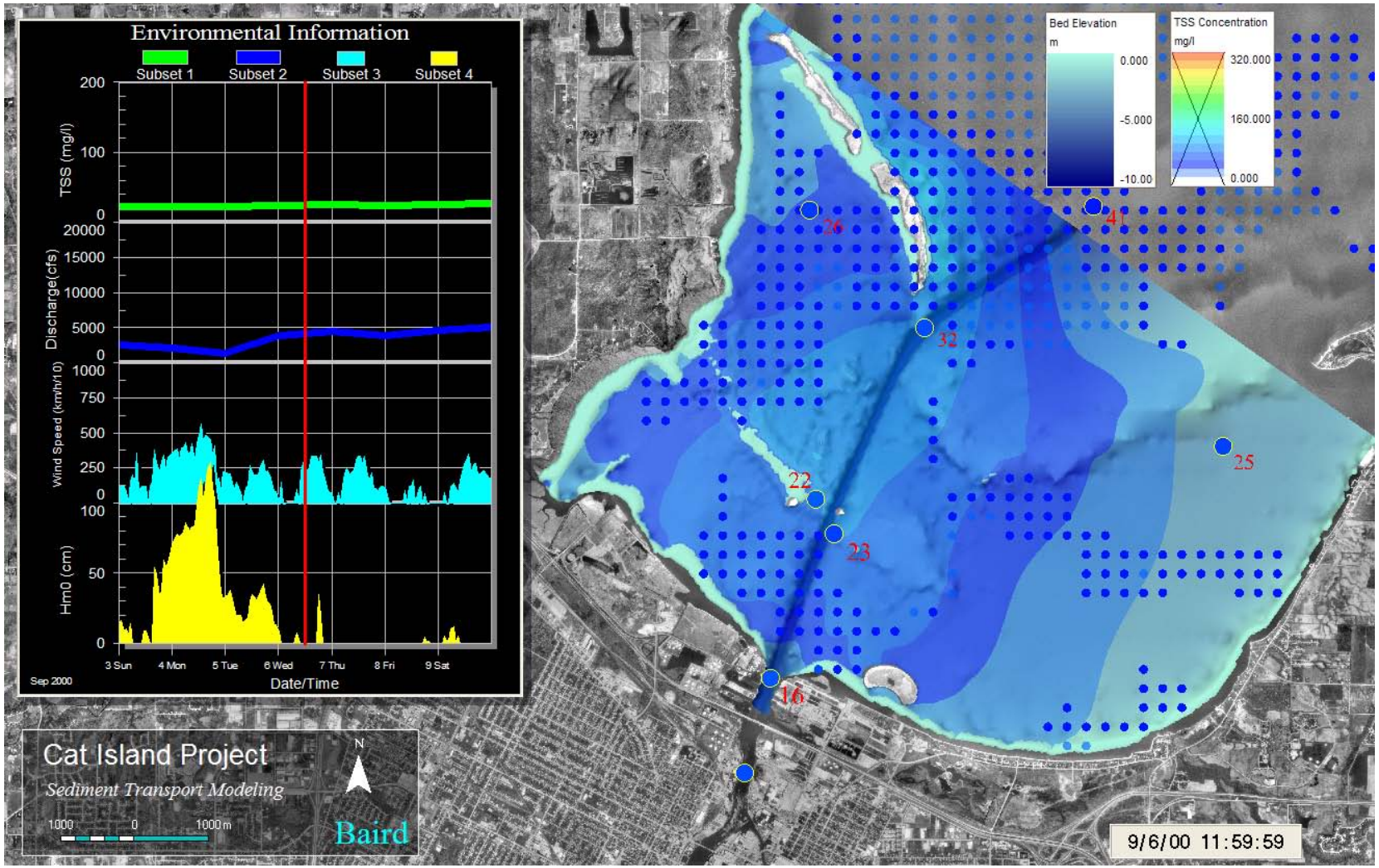

Figure 7.7 Model Calibration for Run 4

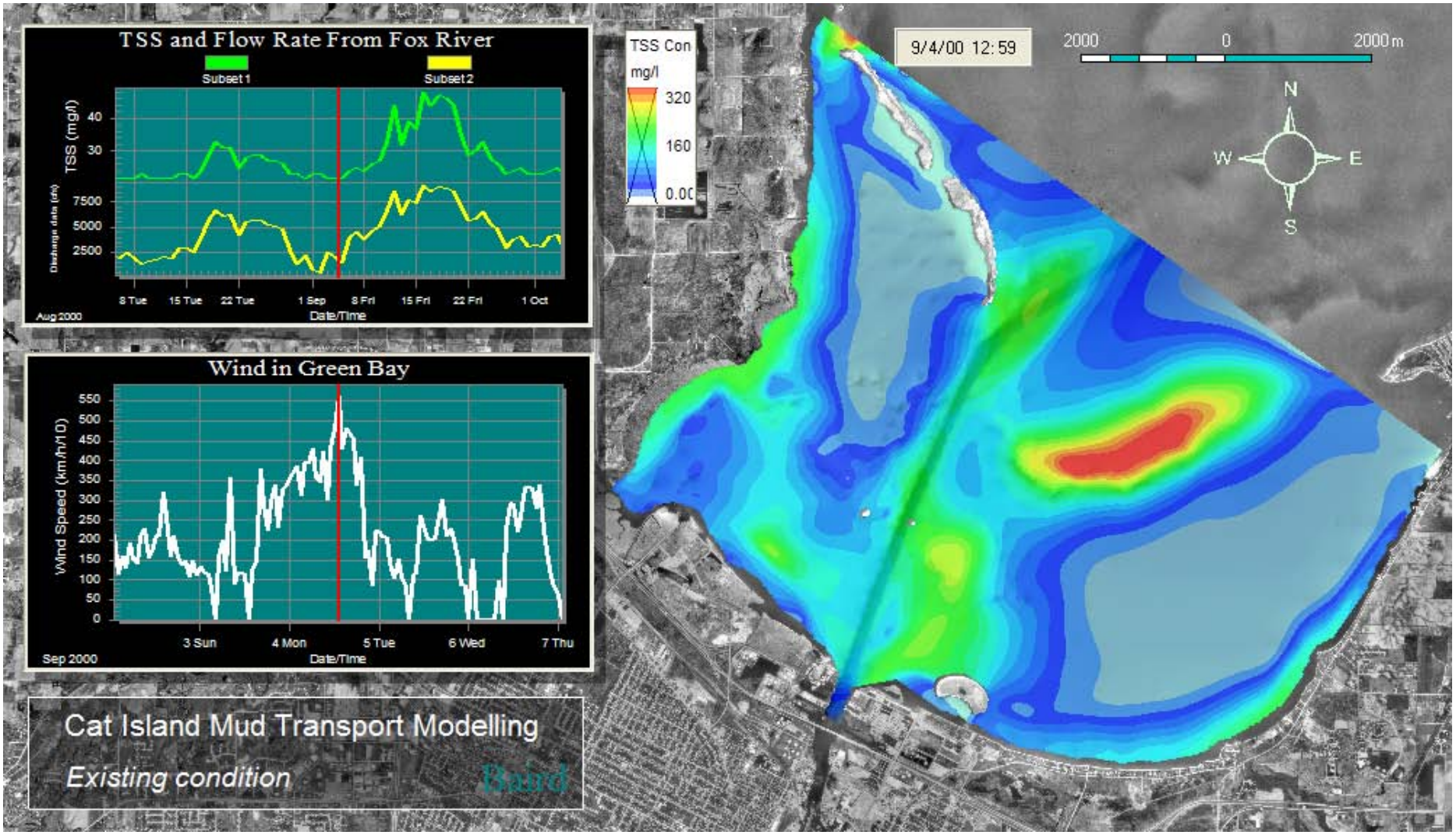

Figure 7.8 TSS Pattern for Run 4 - Existing Condition

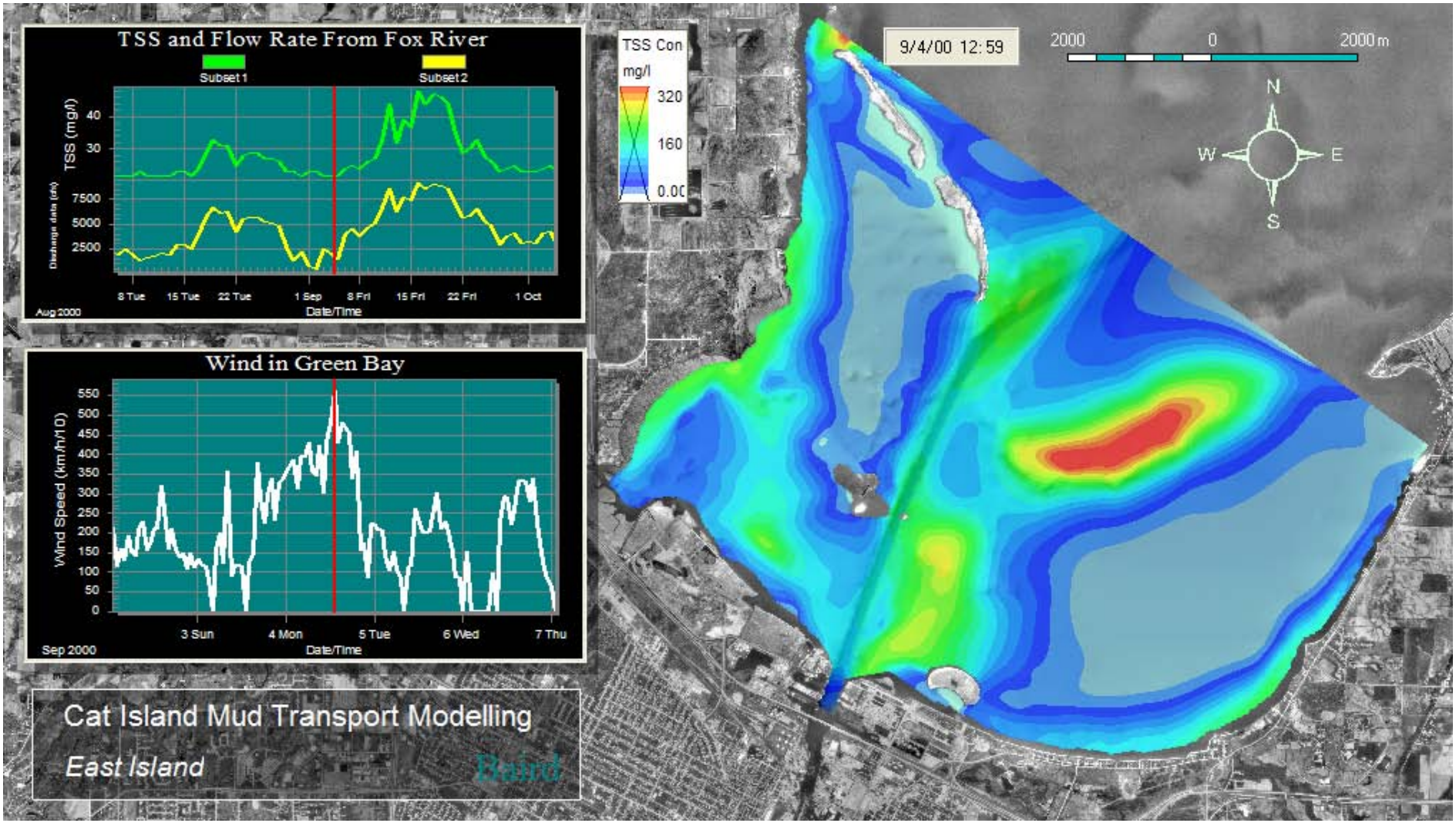

Figure 7.9 TSS Pattern for Run 4 - East Island

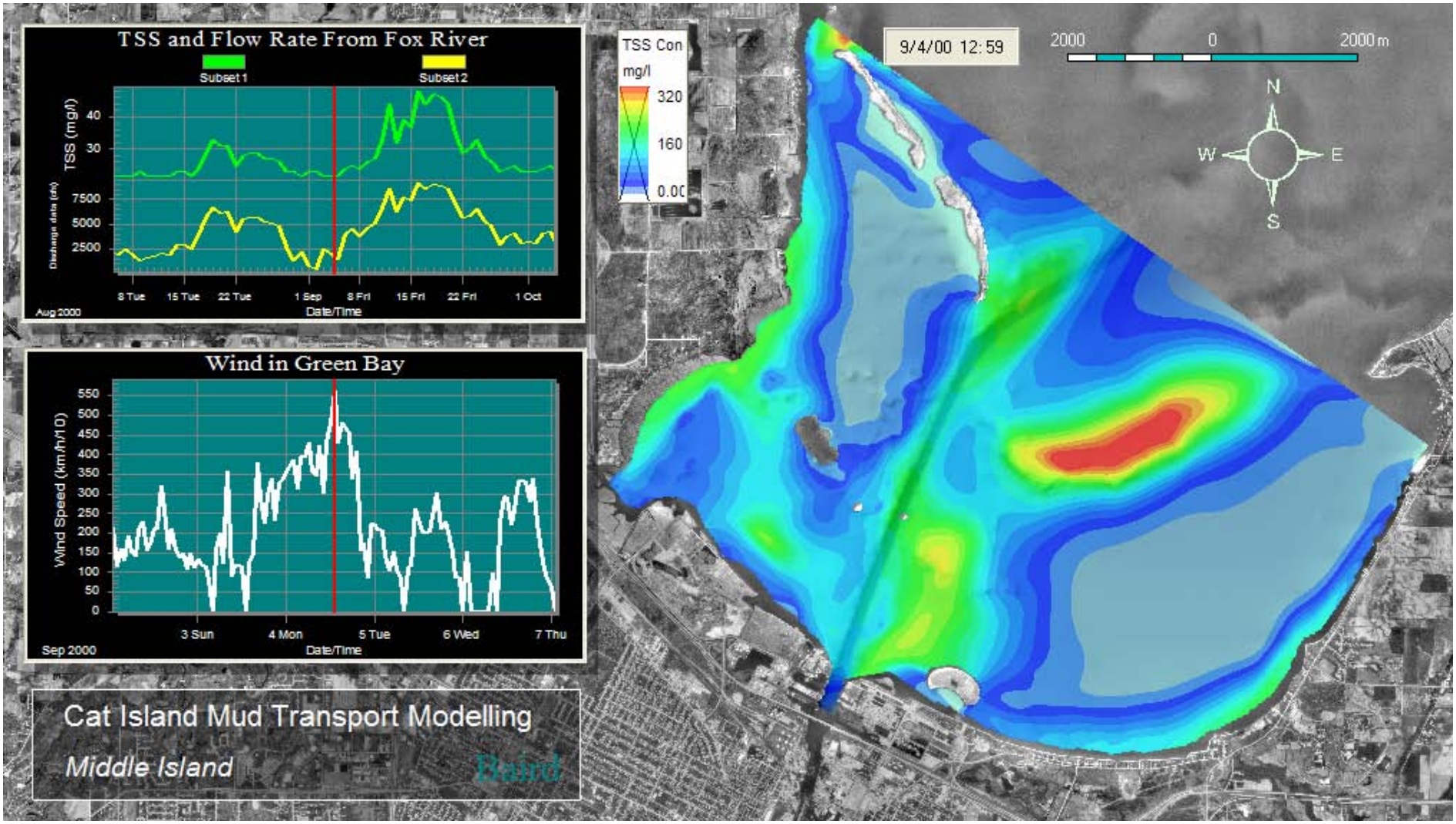

Figure 7.10 TSS Pattern for Run 4 - Central Island

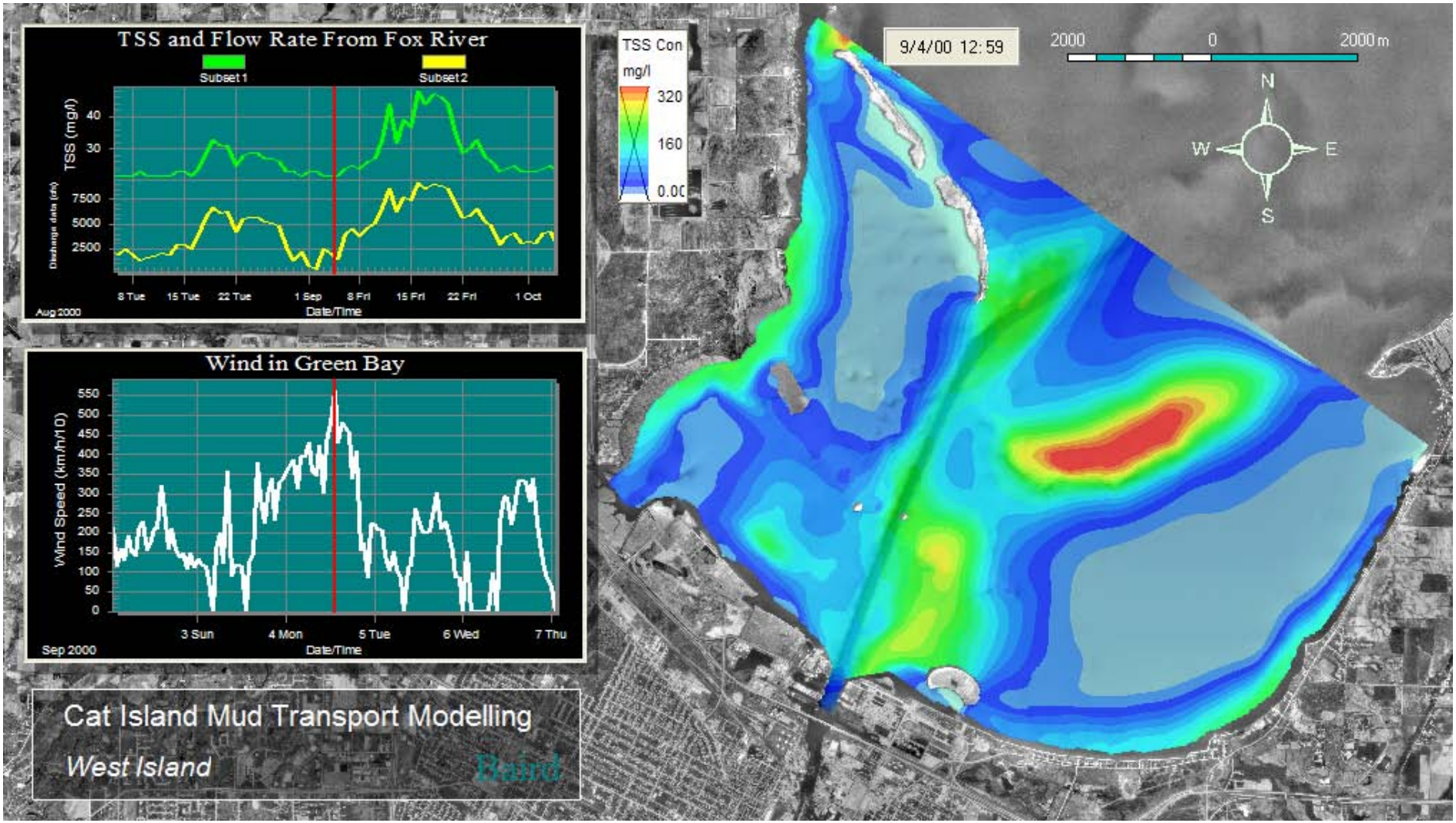

Figure 7.11 TSS Pattern for Run 4 - West Island

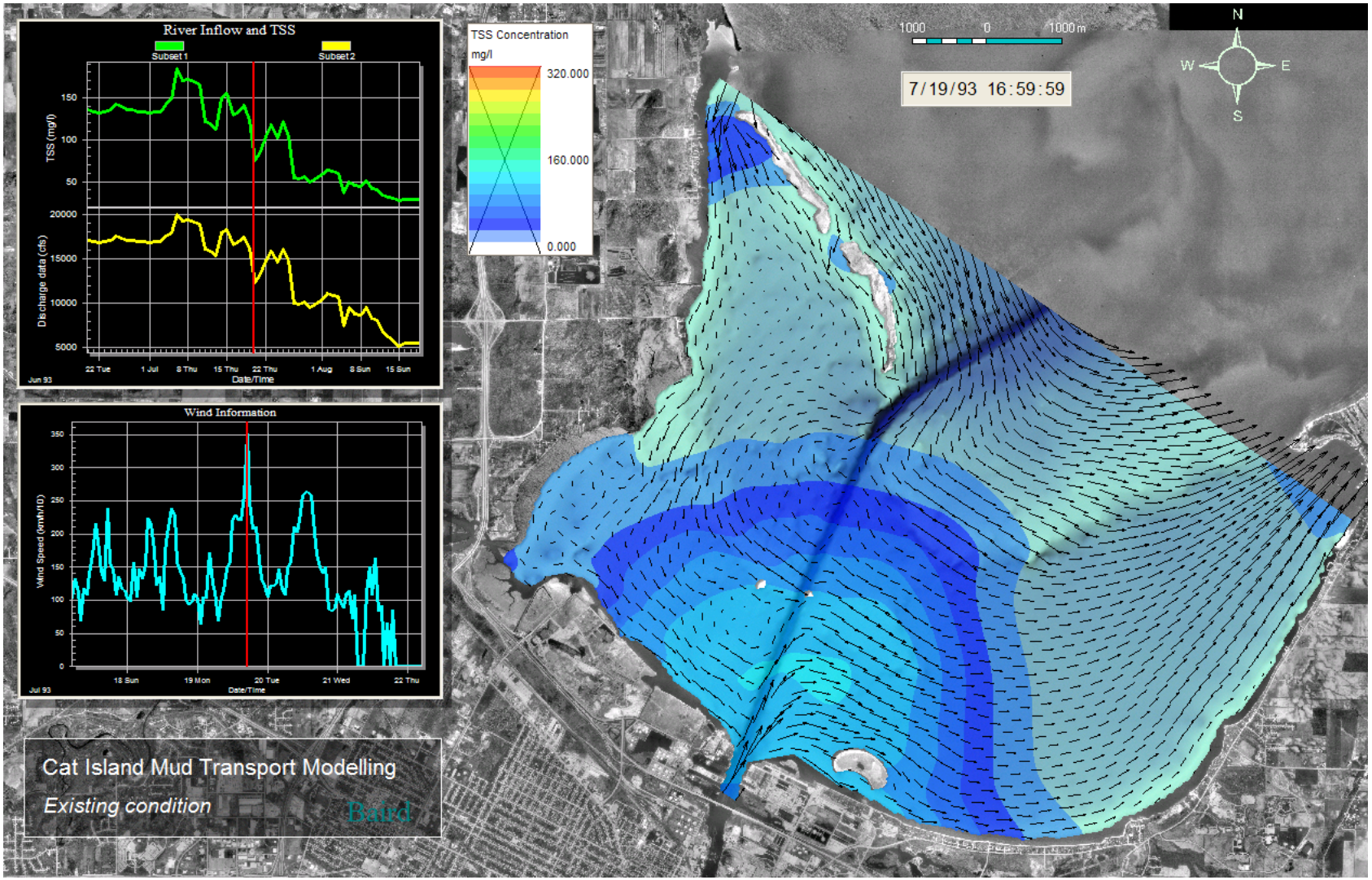

Figure 7.12 TSS and Flow Patterns for Run 1 - Existing Condition

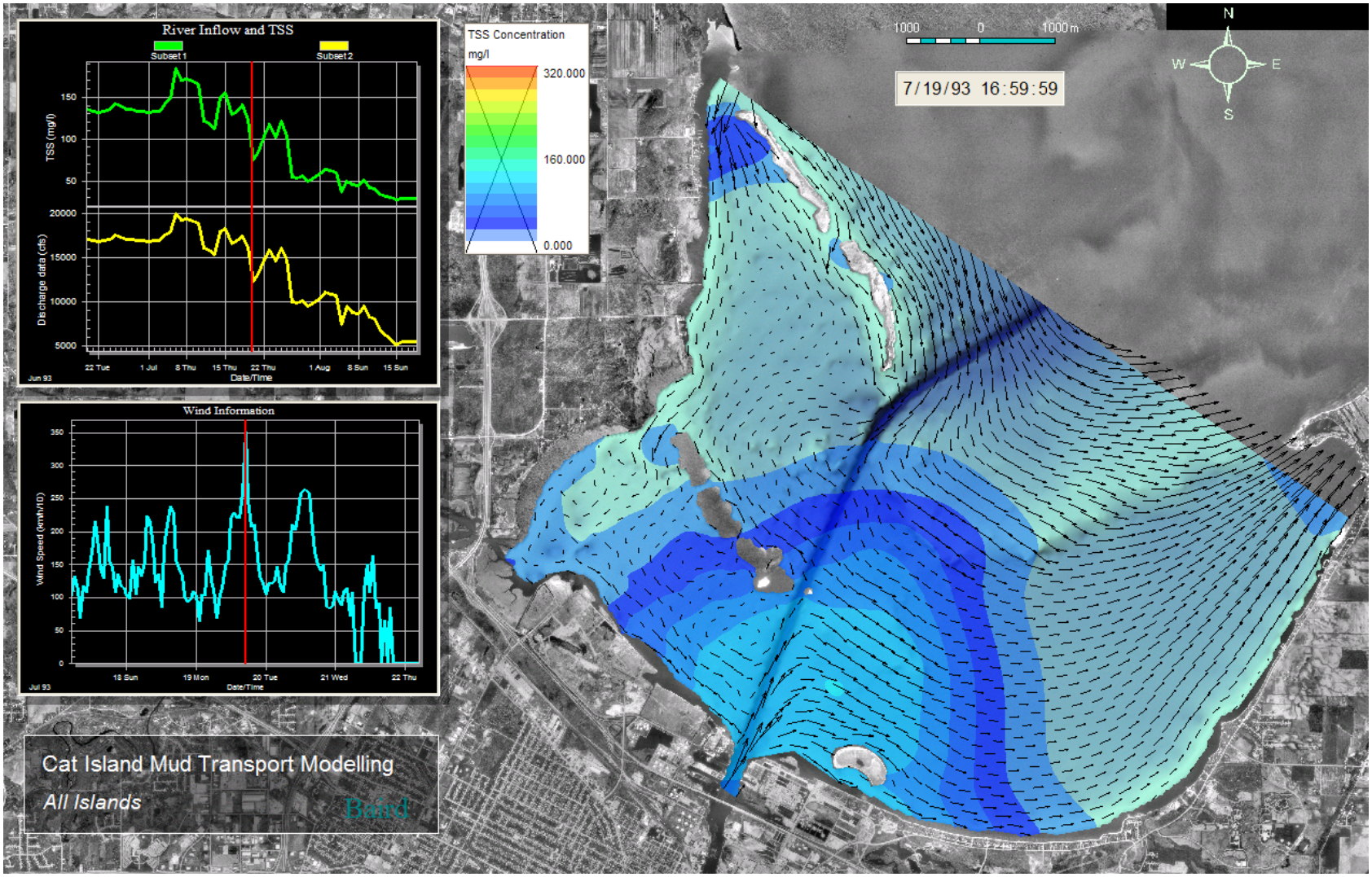

Figure 7.13 TSS and Flow Patterns for Run 1 - All Islands

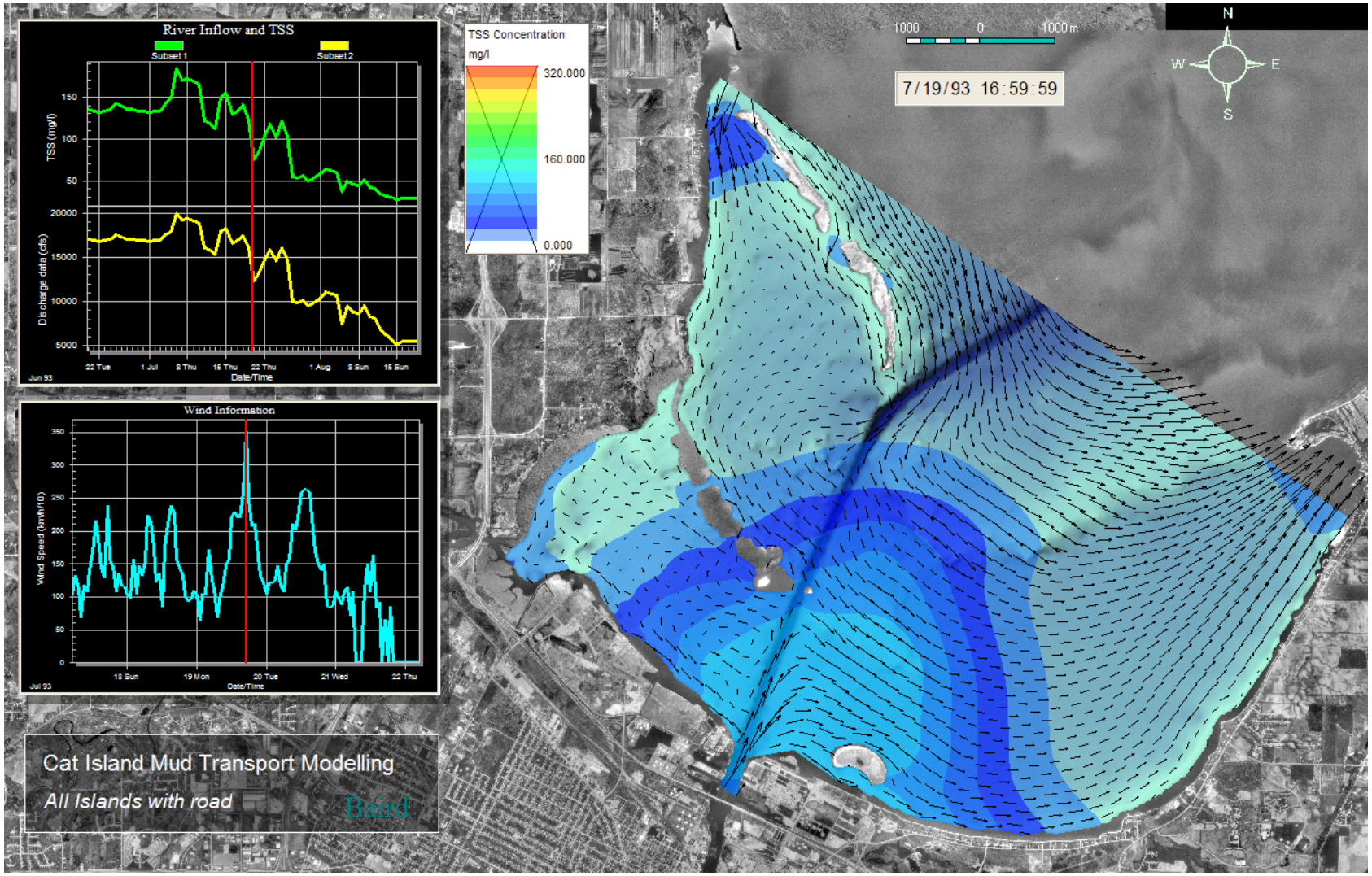

Figure 7.14 TSS and Flow Patterns for Run 1 - All Islands with Roads

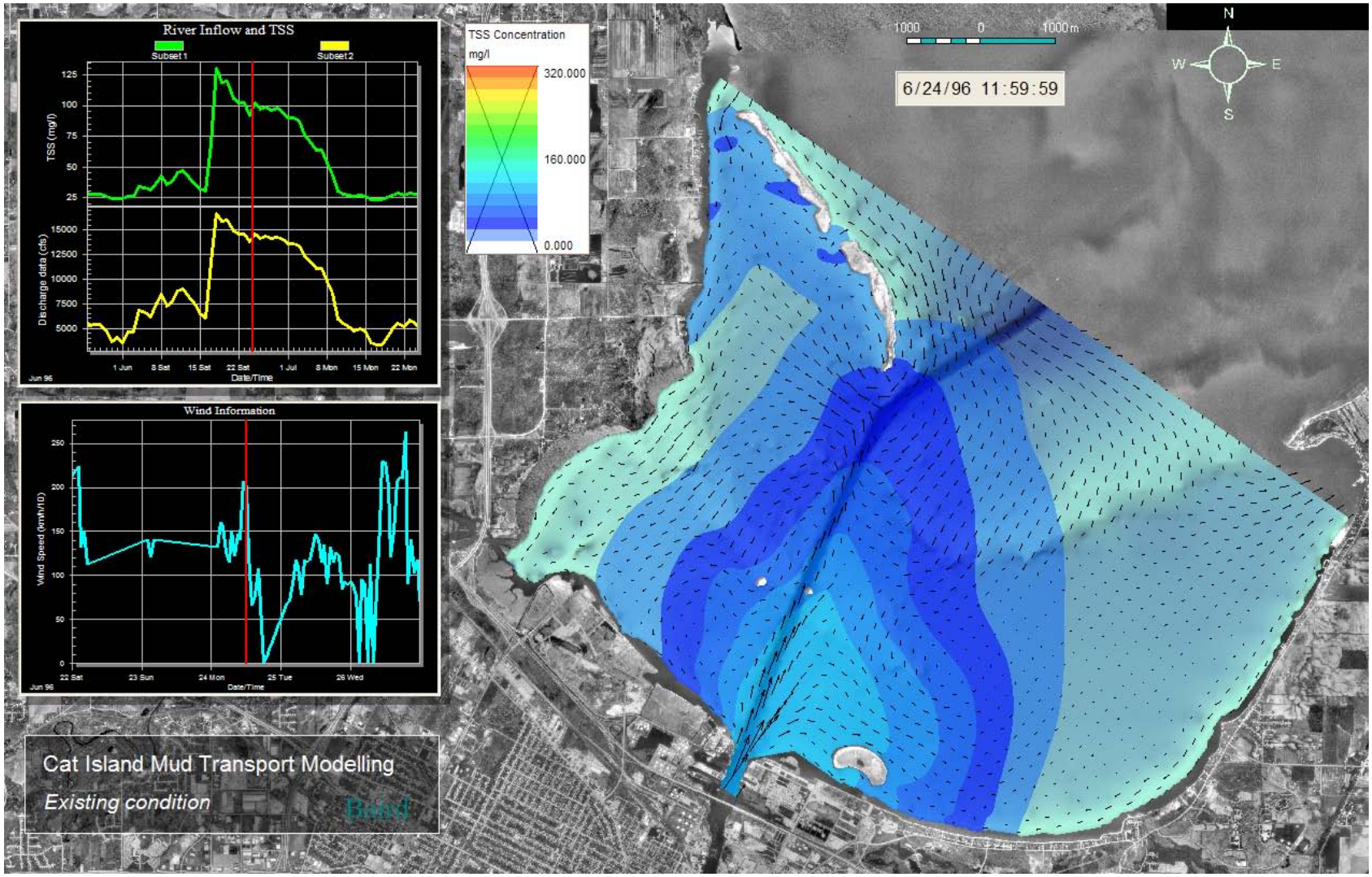

Figure 7.15 TSS and Flow Patterns for Run 2 - Existing Condition

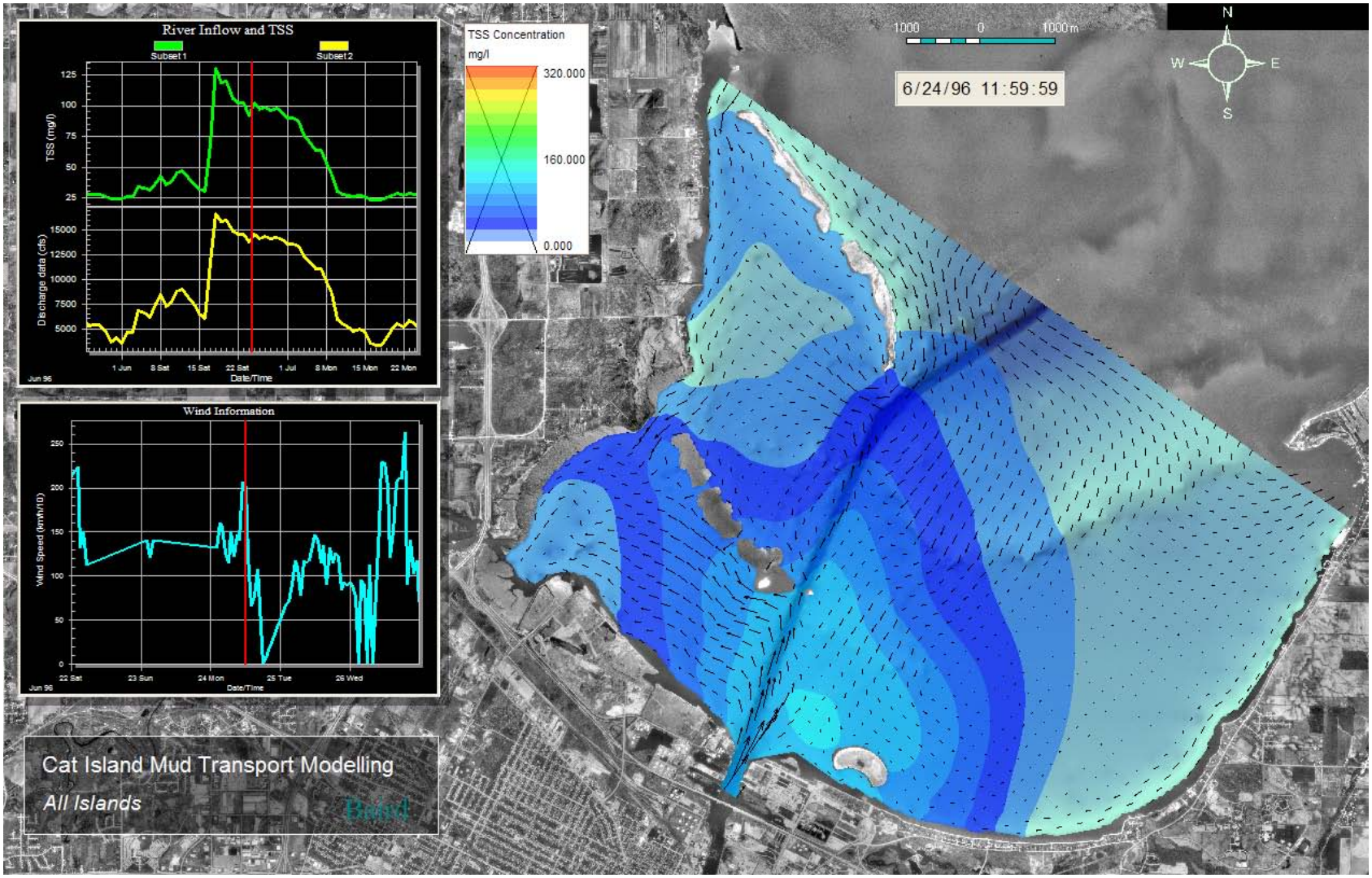

Figure 7.16 TSS and Flow Patterns for Run 2 - All Islands

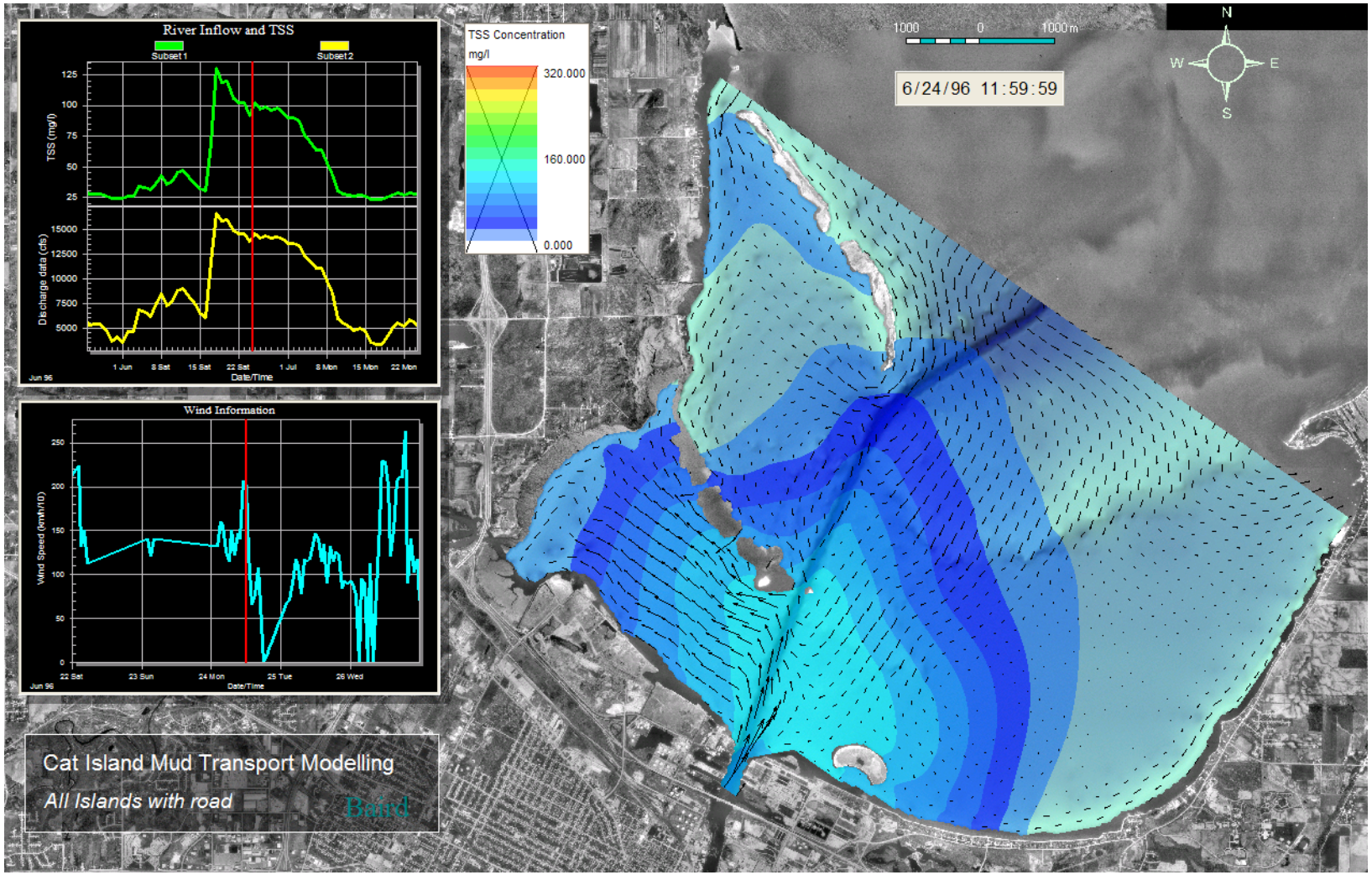

Figure 7.17 TSS and Flow Patterns for Run 2 - All Islands with the Access Road

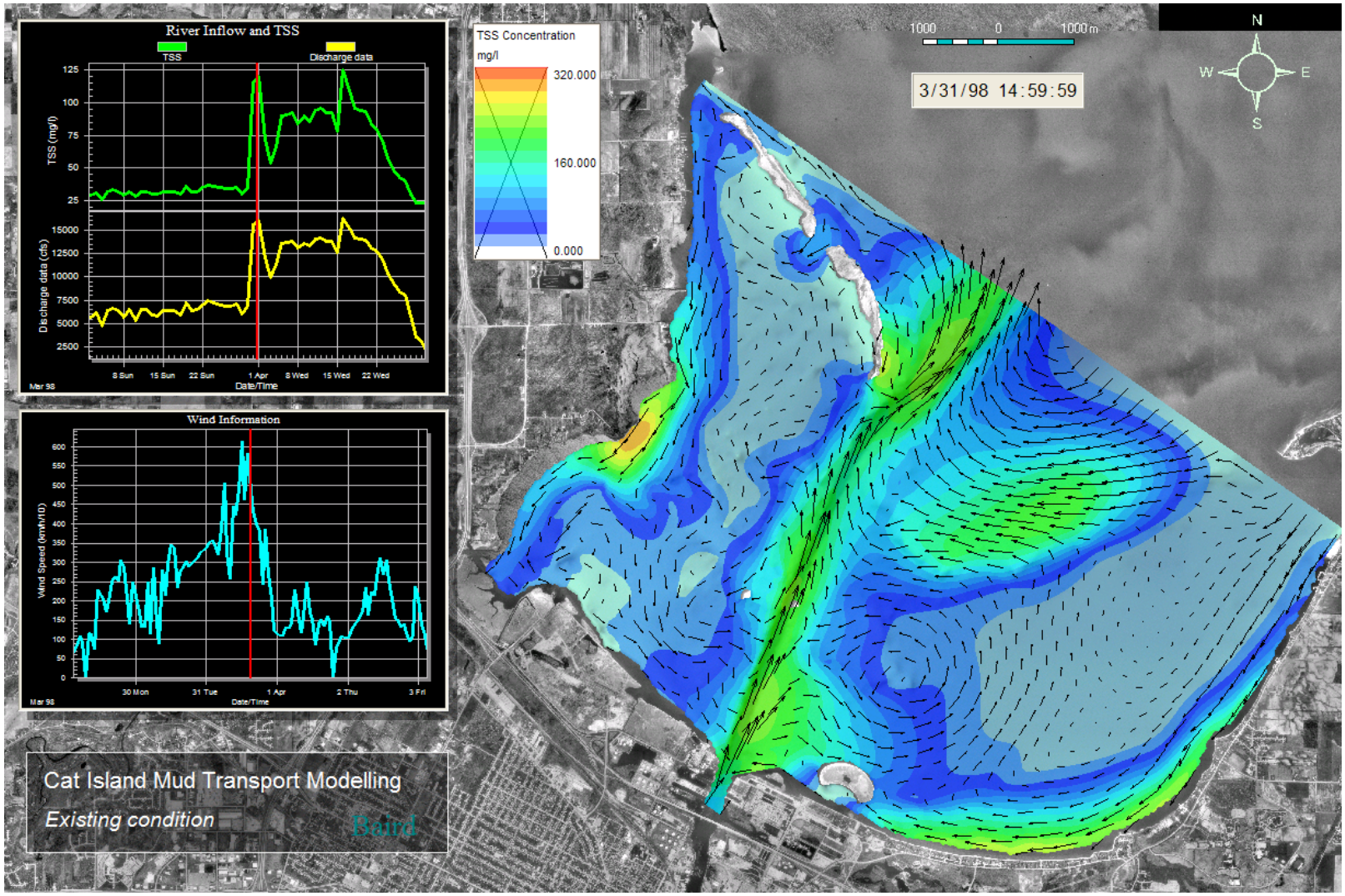

Figure 7.18 TSS and Flow Patterns for Run 3 - Existing Conditions

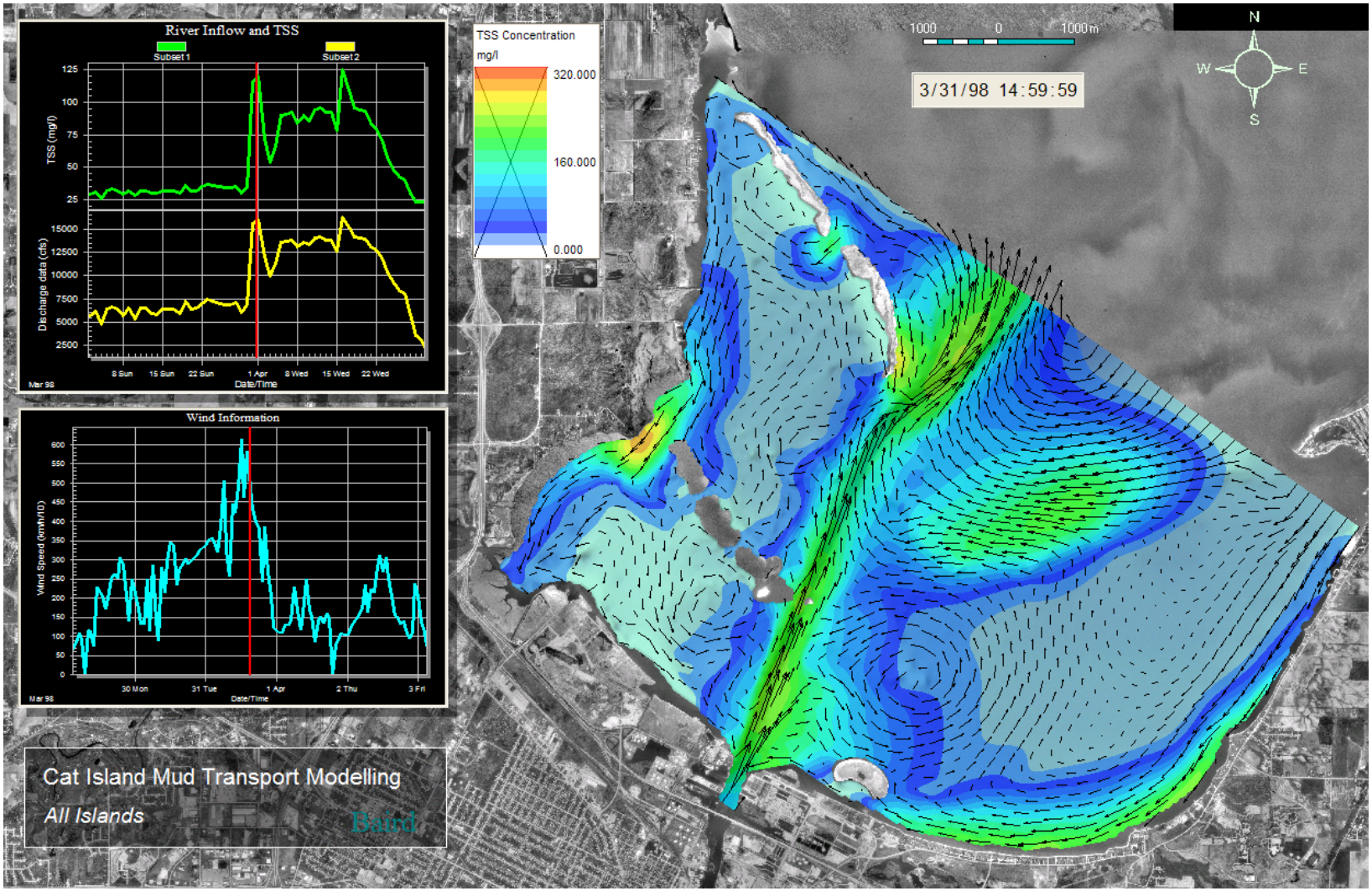

Figure 7.19 TSS and Flow Patterns for Run 3 - All Islands

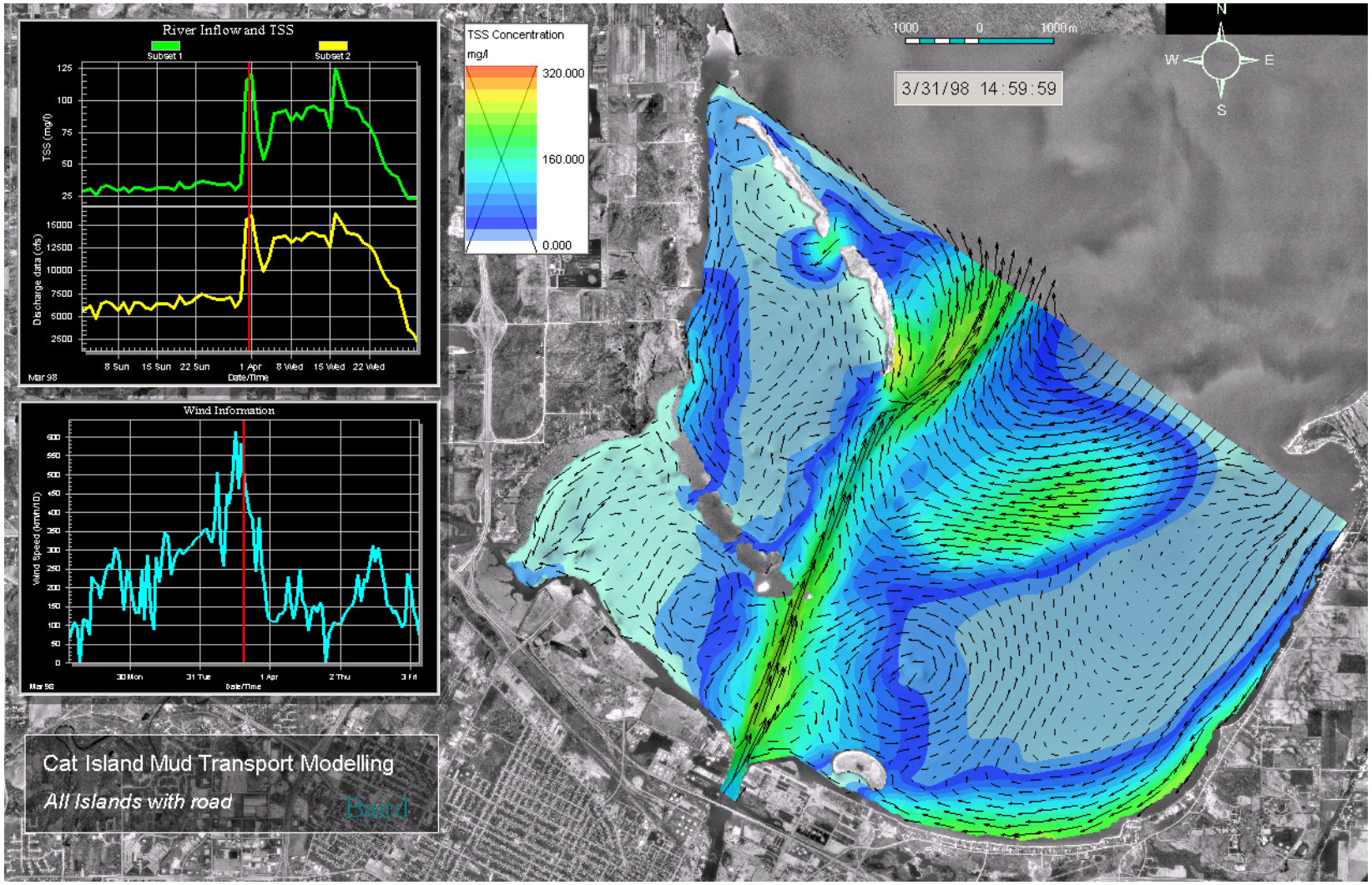

Figure 7.20 TSS and Flow Patterns for Run 3 - All Islands with the Access Road

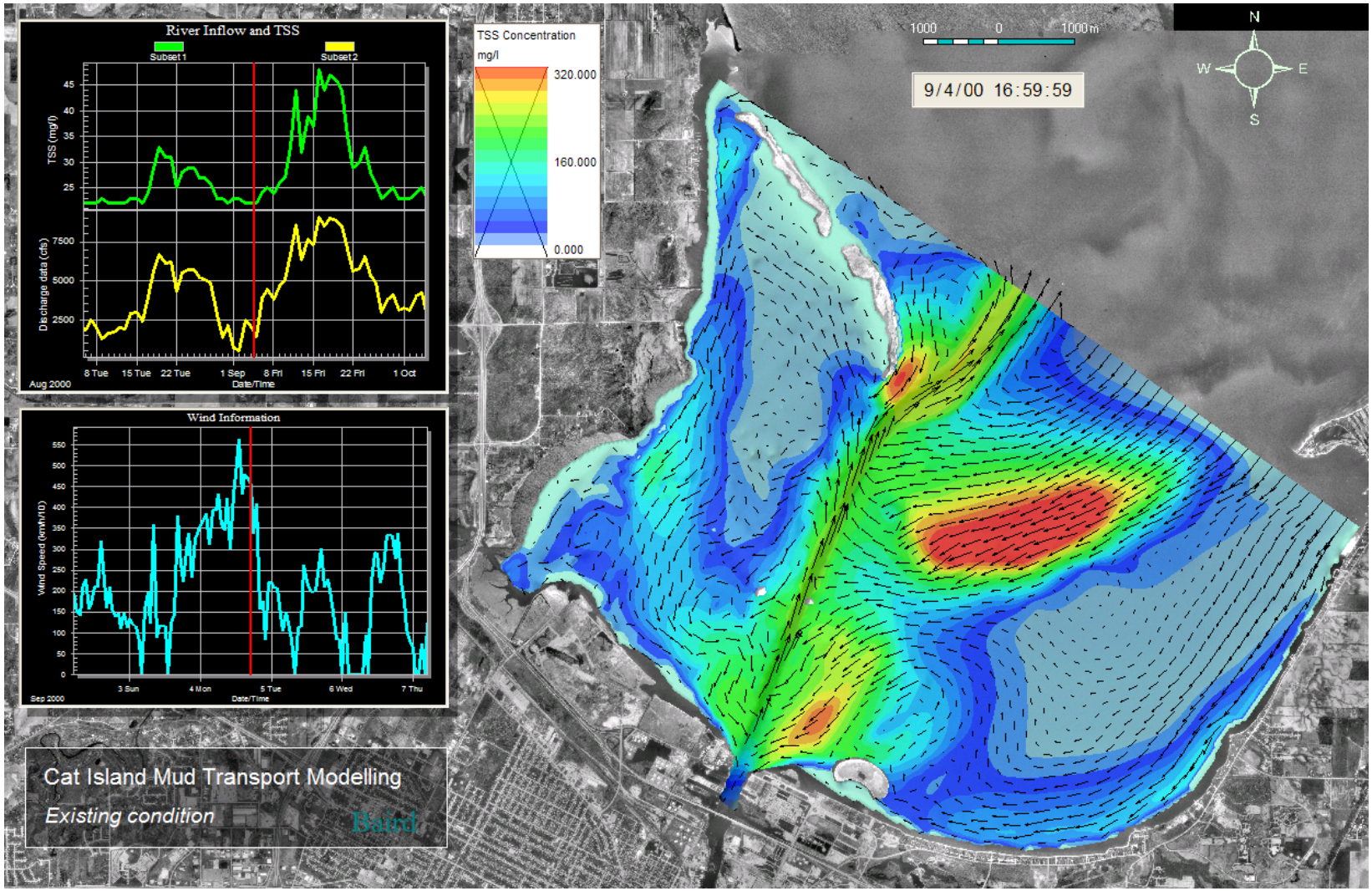

Figure 7.21 TSS and Flow Patterns for Run 4 - Existing Conditions

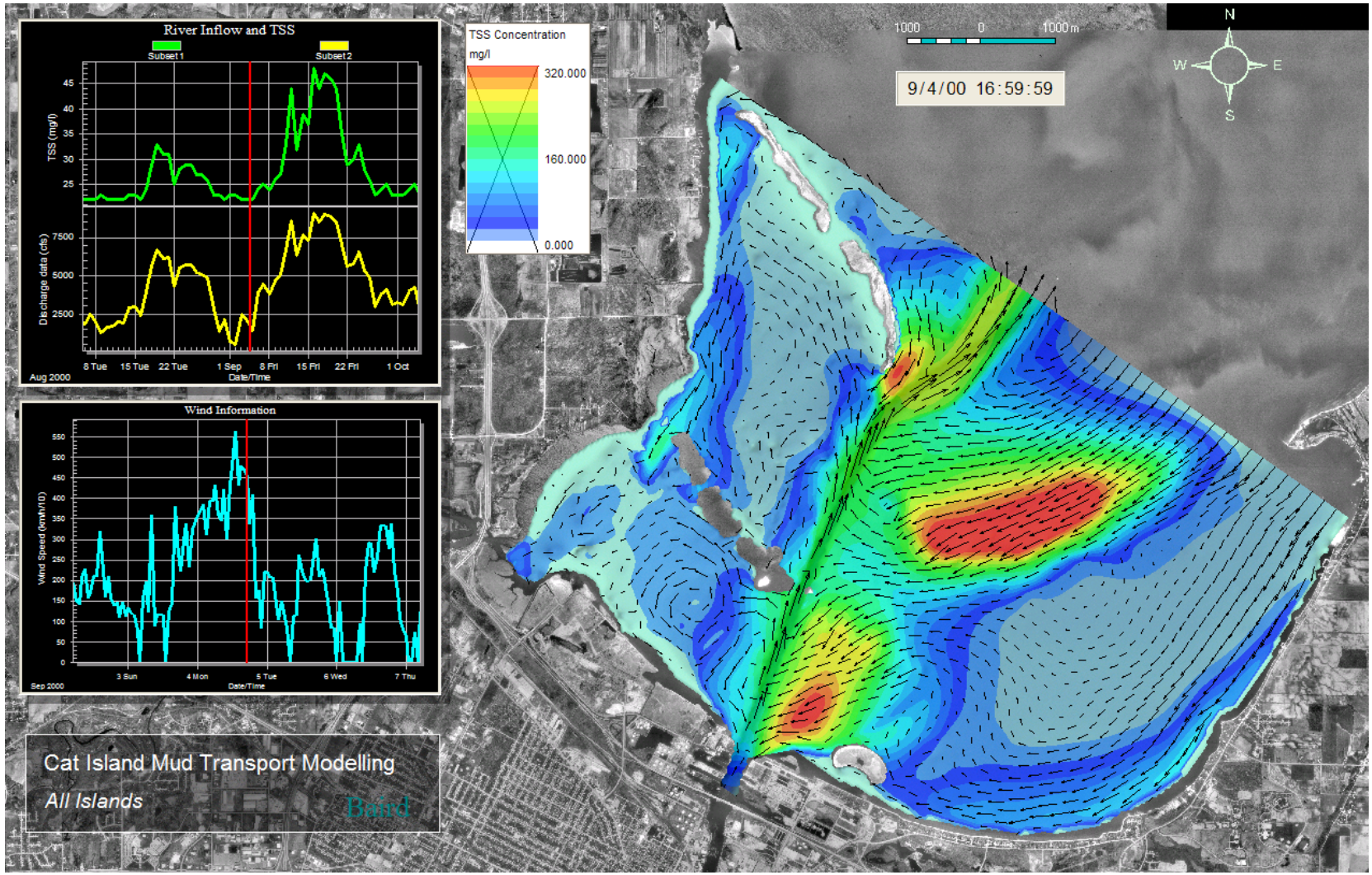

Figure 7.22 TSS and Flow Patterns for Run 4 - All Islands

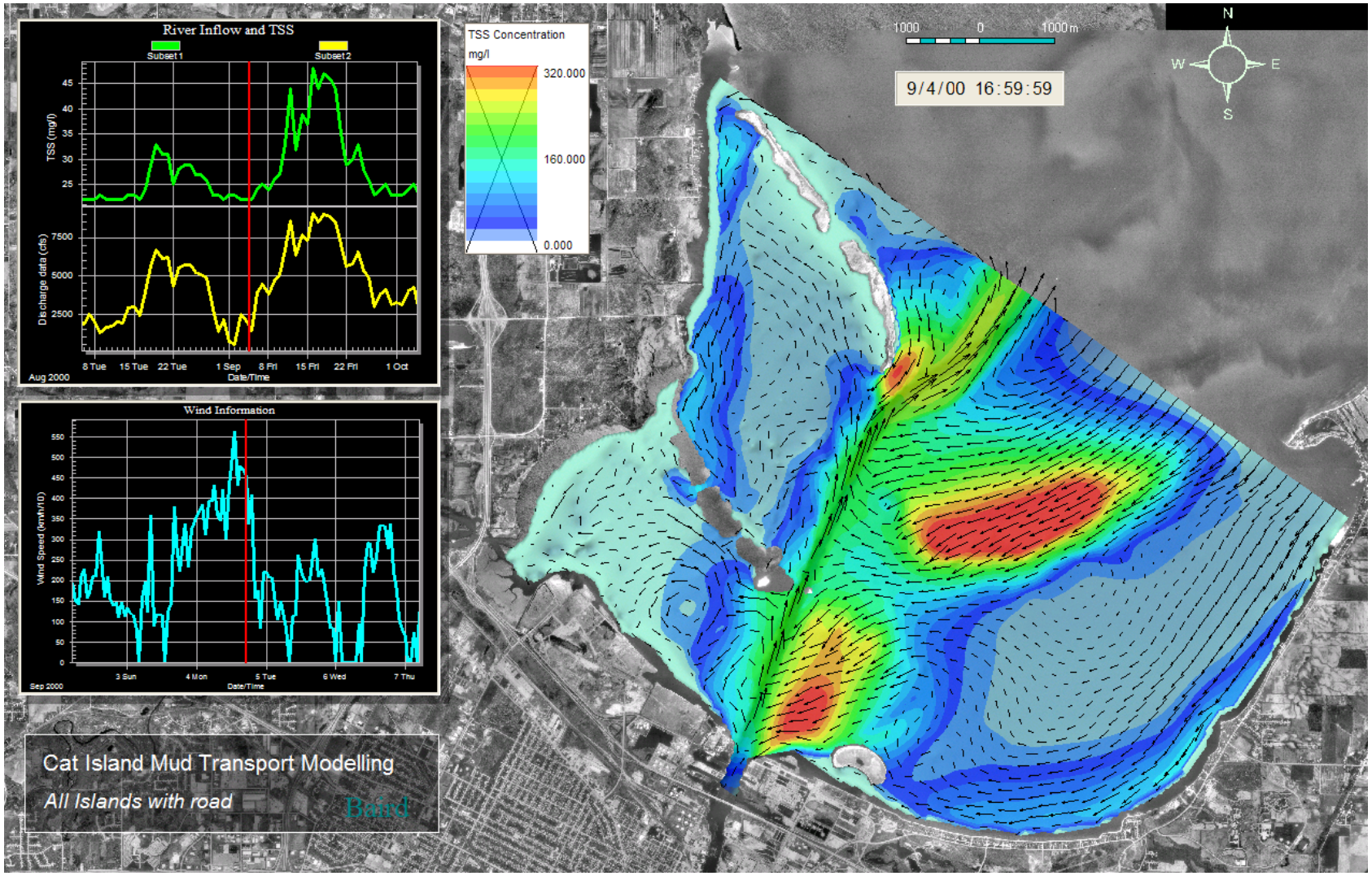

Figure 7.23 TSS and Flow Patterns for Run - All Islands with the Access Road

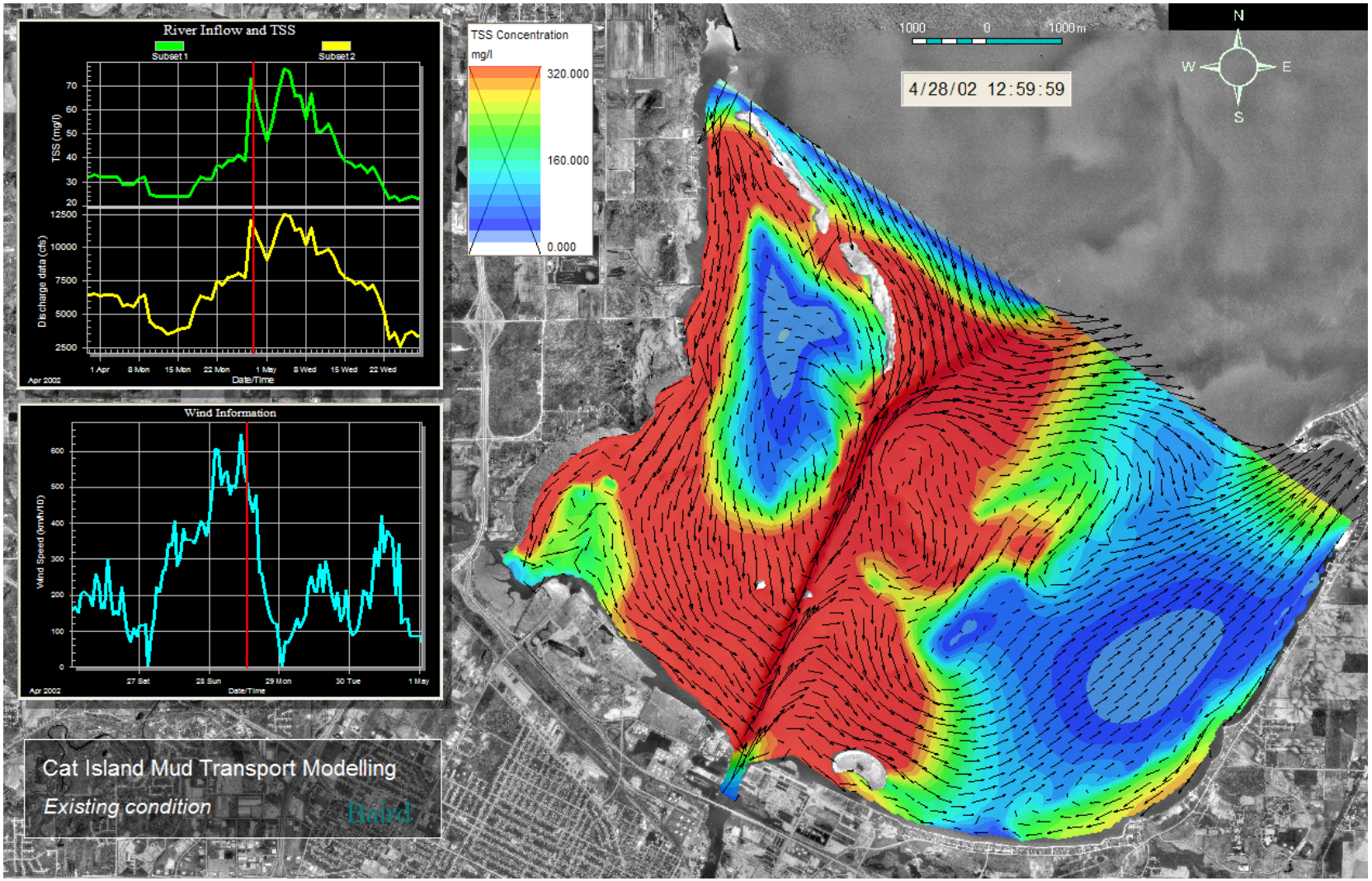

Figure 7.24 TSS and Flow Patterns for Run 5 - Existing Condition

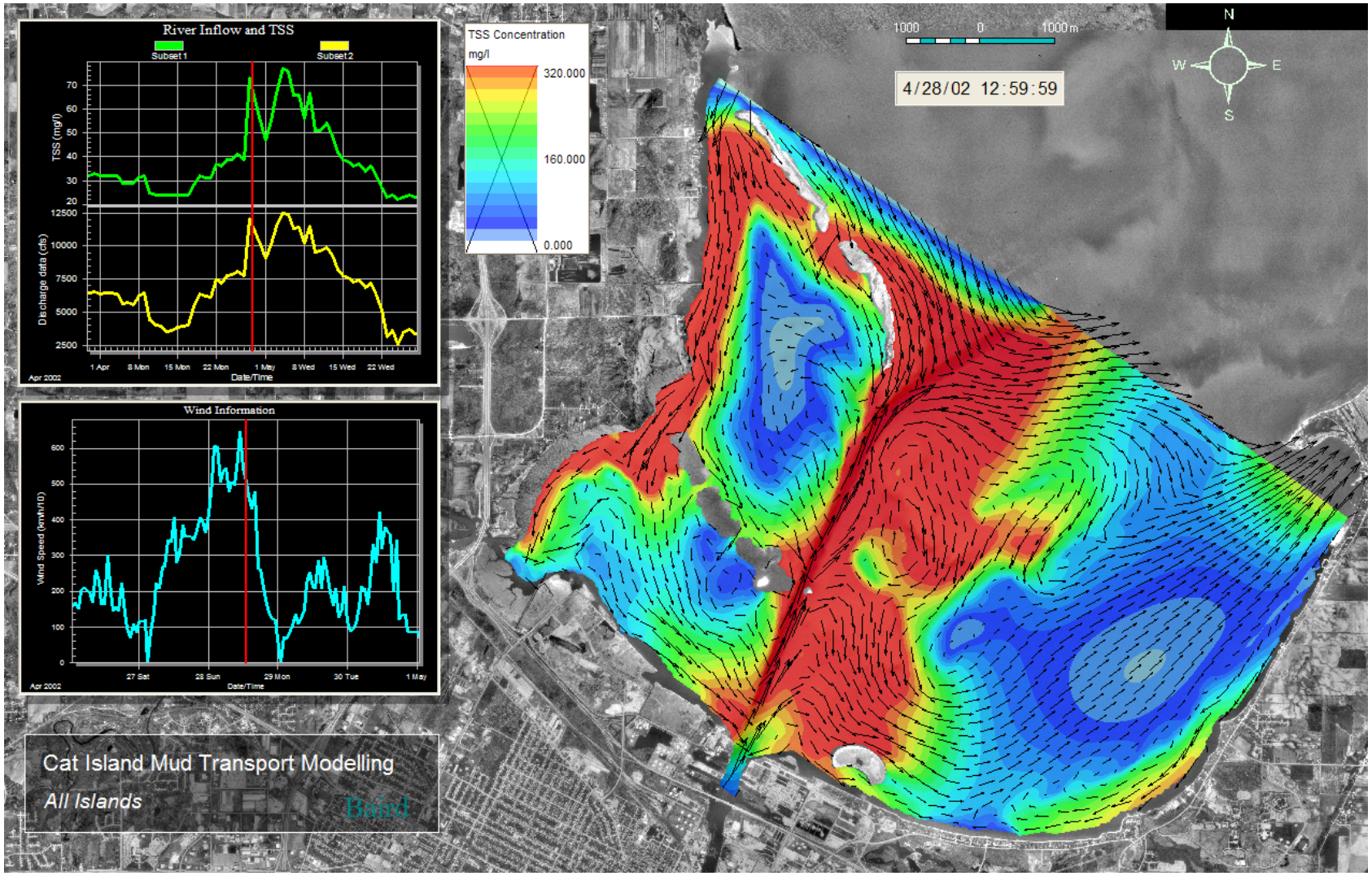

Figure 7.25 TSS and Flow Patterns for Run 5 - All Islands

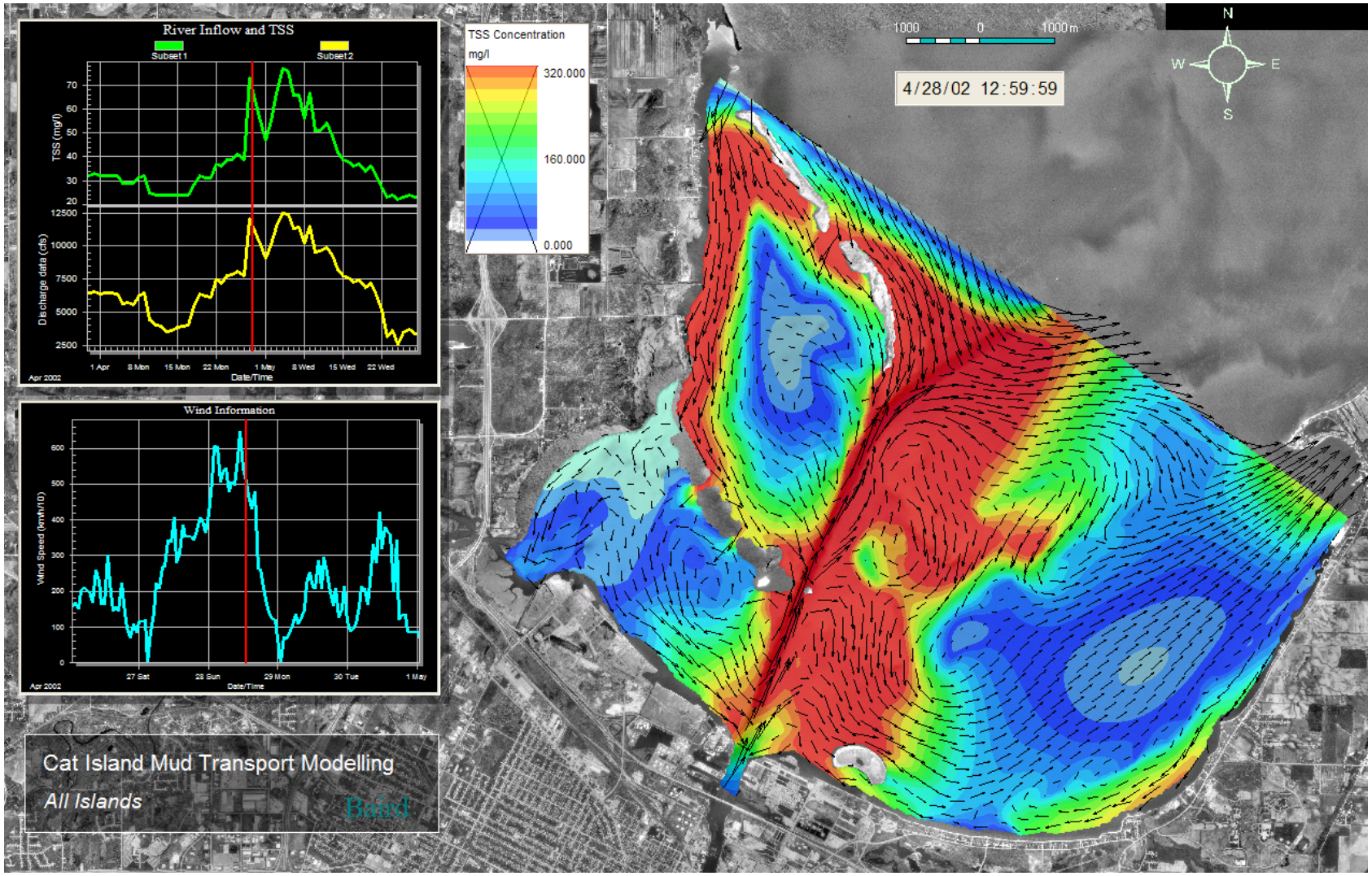

Figure 7.26 TSS and Flow Patterns for Run 5 - All Islands with the Access Road

Attachment A
Wave Transformation Modeling

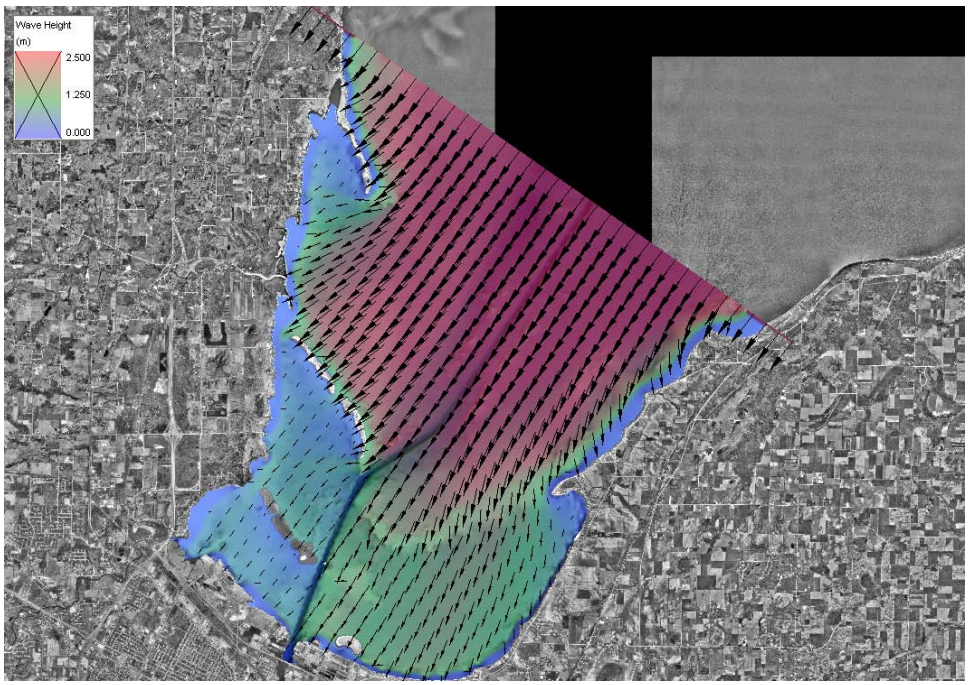

Ho = 2.7 m, Tp = 8.5 sec, Wave Dir = 38, Wind = 23 m/s, Wind Dir = 35

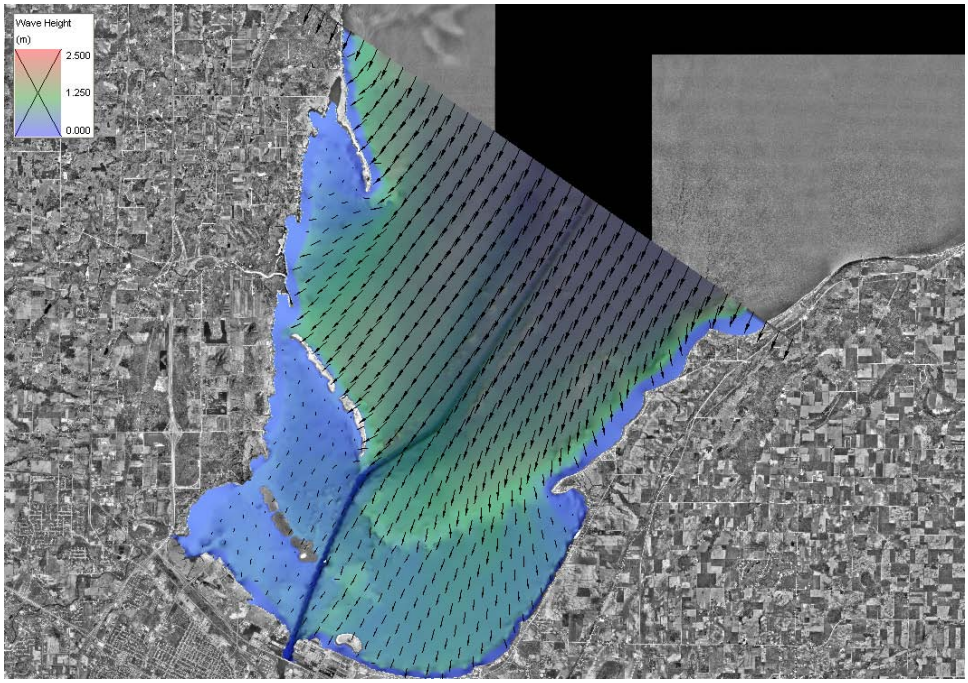

Ho = 1.7 m, Tp = 6.1 sec, Wave Dir = 24, Wind = 13 m/s, Wind Dir = 5

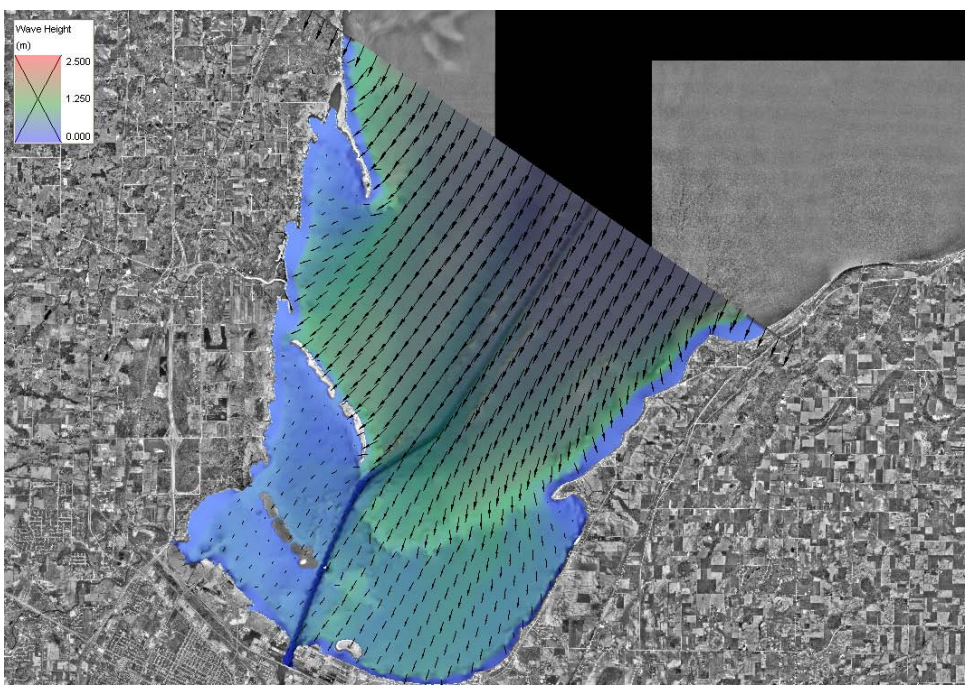

Ho = 1.7 m, Tp = 6.1 sec, Wave Dir = 24, Wind = 13 m/s, Wind Dir = 25

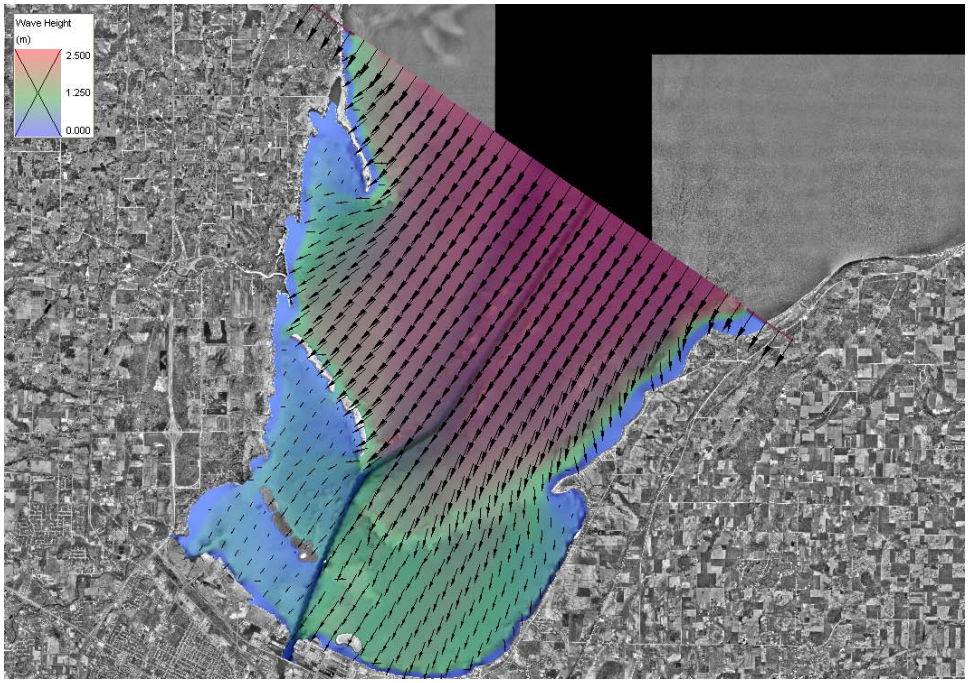

Ho = 2.5 m, Tp = 7.0 sec, Wave Dir = 33, Wind = 21 m/s, Wind Dir = 30

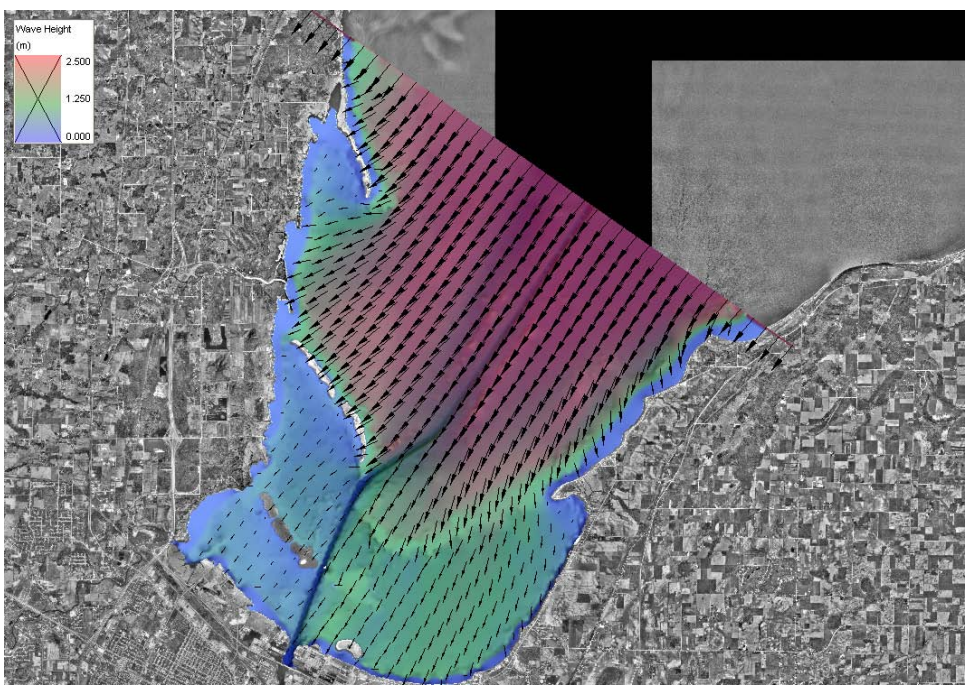

Ho = 2.4 m, Tp = 7.7 sec, Wave Dir = 40, Wind = 20 m/s, Wind Dir = 35

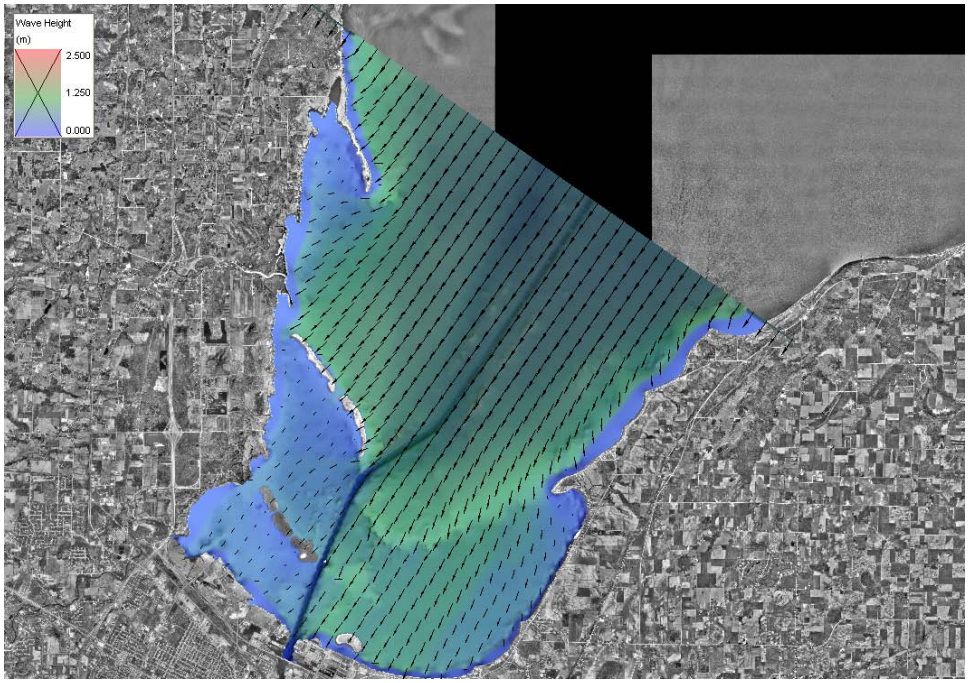

Ho = 1.4 m, Tp = 4.8 sec, Wave Dir = 35, Wind = 15 m/s, Wind Dir = 35

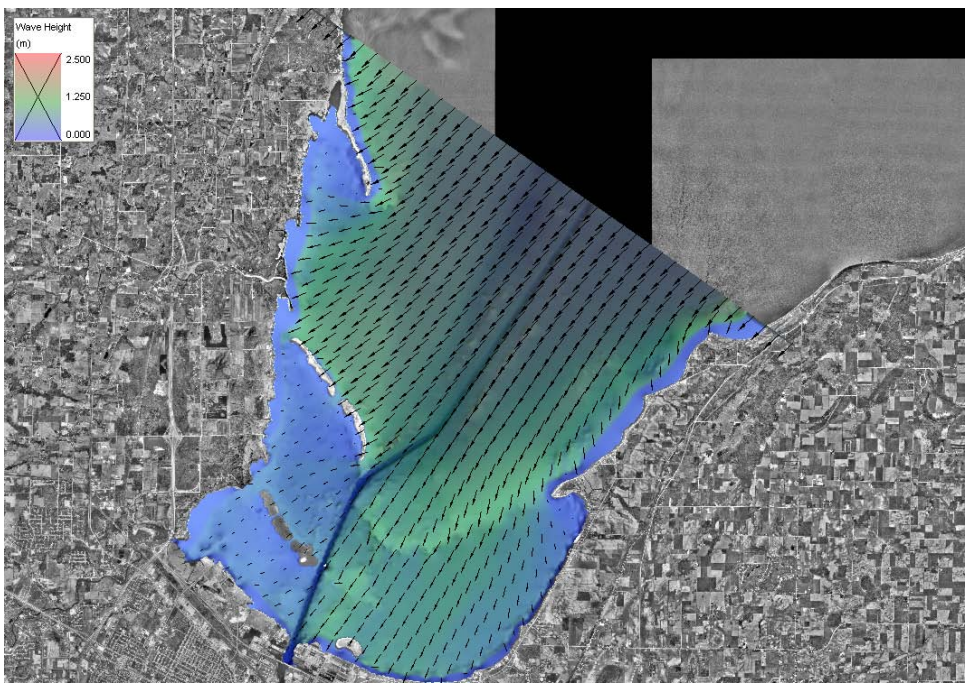

Ho = 1.6 m, Tp = 5.9 sec, Wave Dir = 47, Wind = 12 m/s, Wind Dir = 55

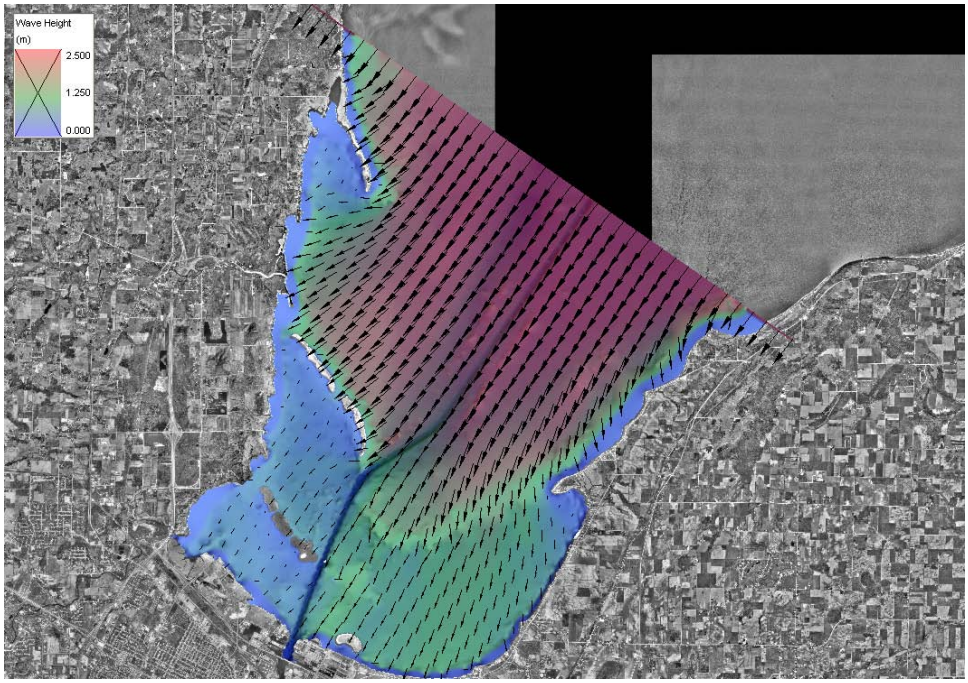

Ho = 2.3 m, Tp =7.9 sec, Wave Dir = 38, Wind = 18 m/s, Wind Dir = 30

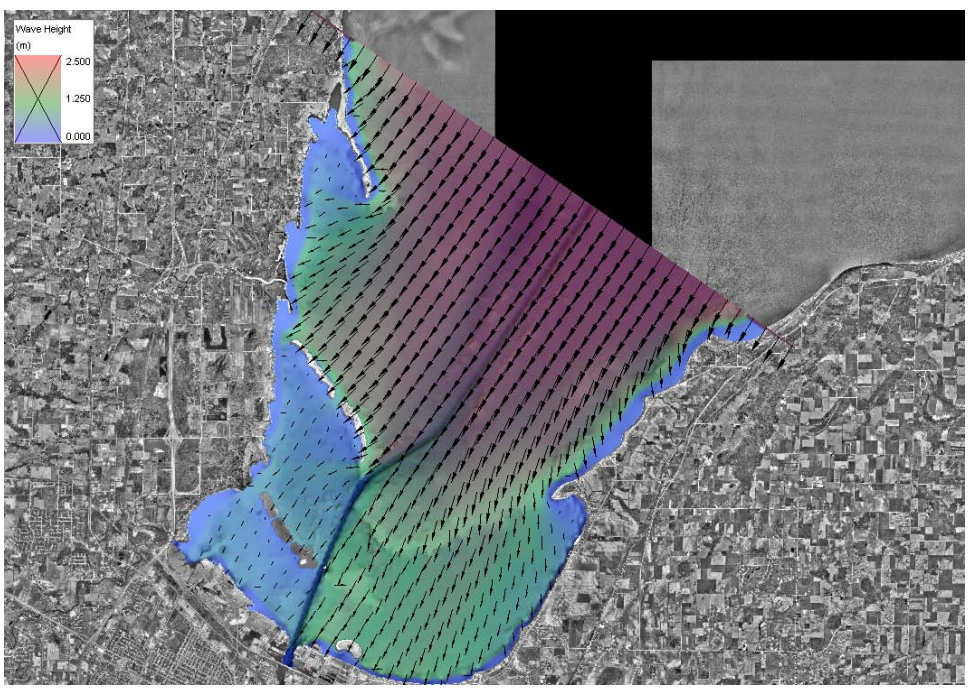

Ho = 2.2 m, Tp = 6.9 sec, Wave Dir = 32, Wind = 18 m/s, Wind Dir = 25

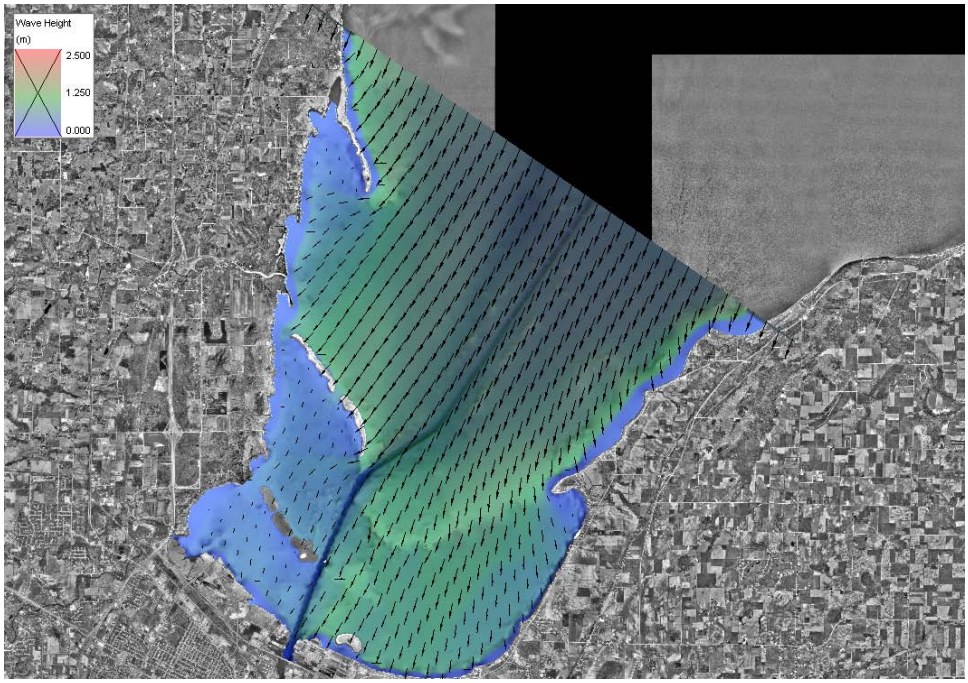

Ho = 1.5 m, Tp = 5.4 sec, Wave Dir = 22, Wind = 15 m/s, Wind Dir = 5

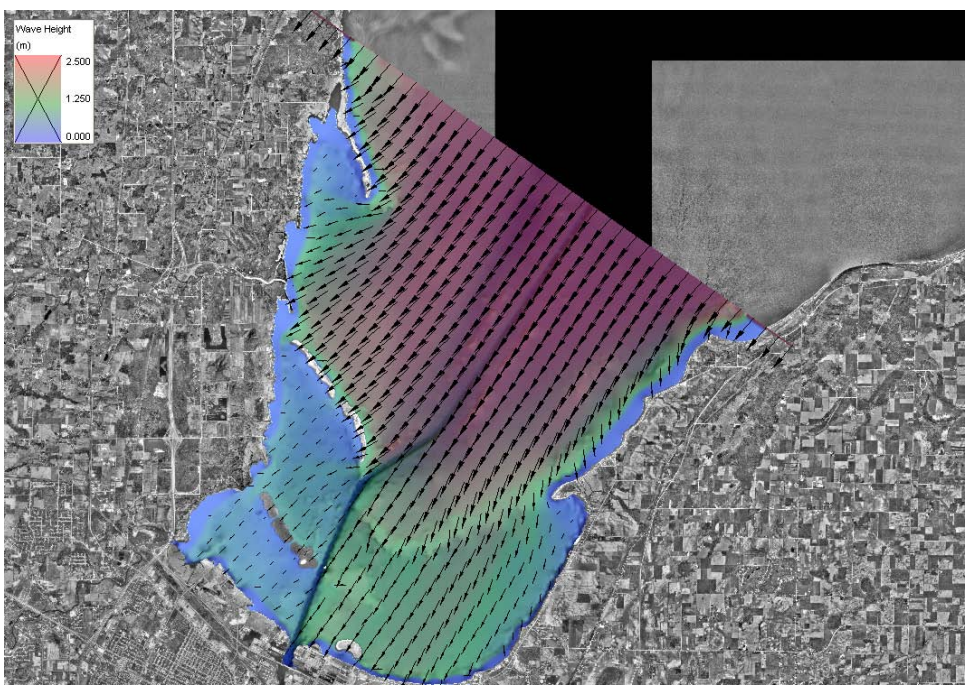

Ho = 2.2 m, Tp = 6.7 sec, Wave Dir = 41, Wind = 22 m/s, Wind Dir = 45

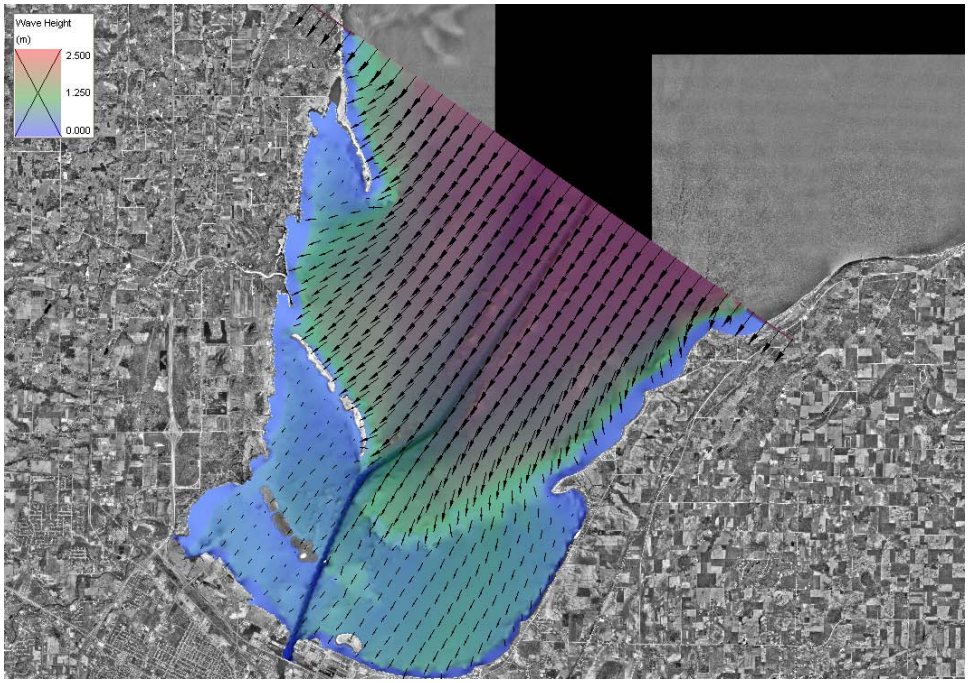

Ho = 2.2 m, Tp = 6.5 sec, Wave Dir = 38, Wind = 18 m/s, Wind Dir = 35

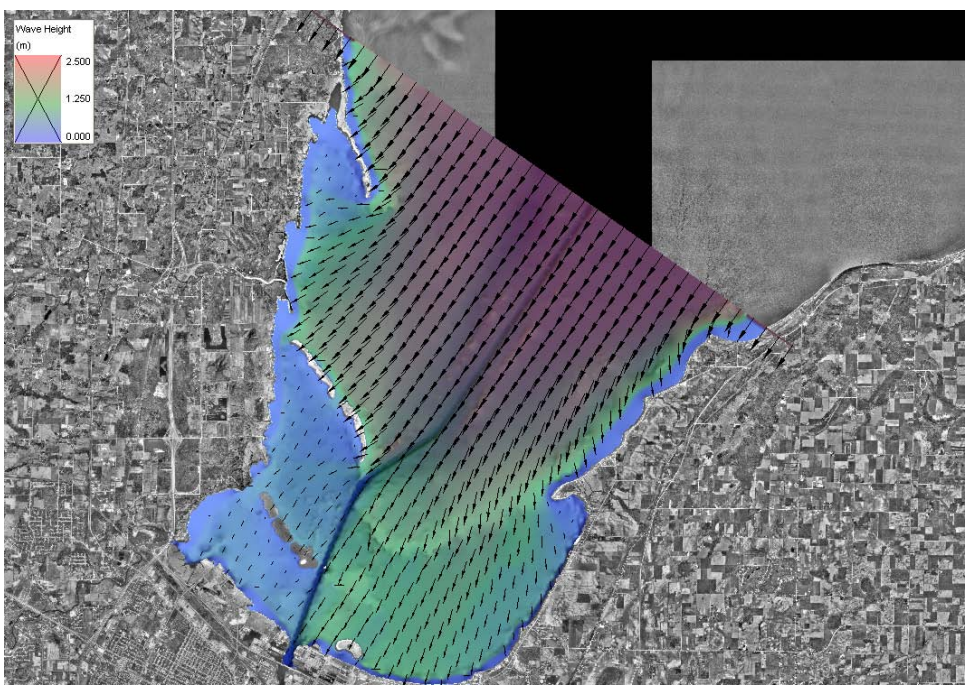

Ho = 2.1 m, Tp = 6.6 sec, Wave Dir = 35, Wind = 16 m/s, Wind Dir = 25

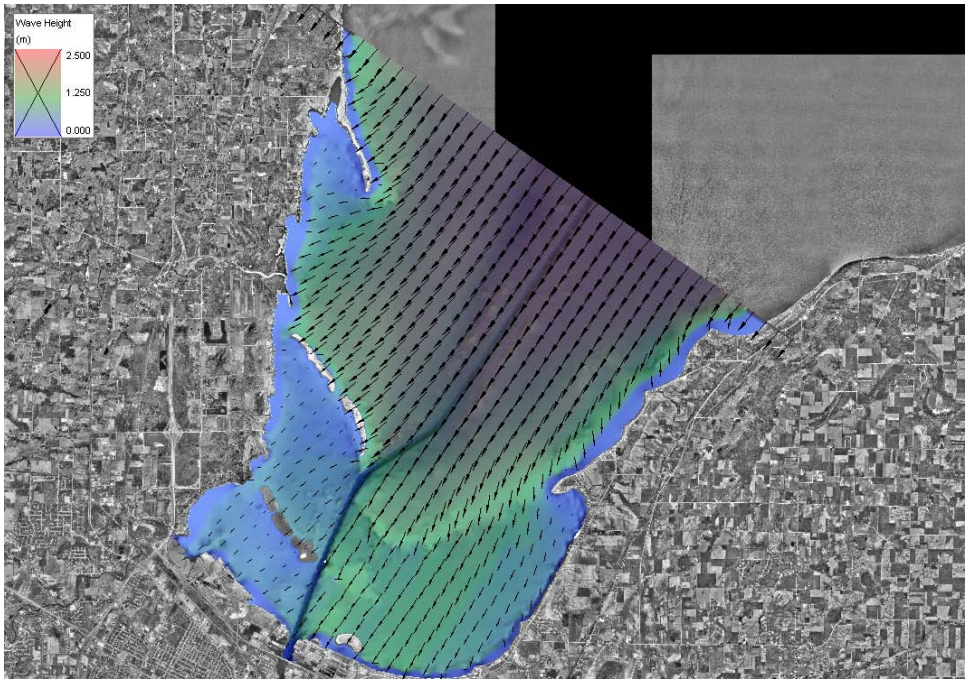

Ho = 1.8 m, Tp = 5.8 sec, Wave Dir = 40, Wind = 18 m/s, Wind Dir = 45

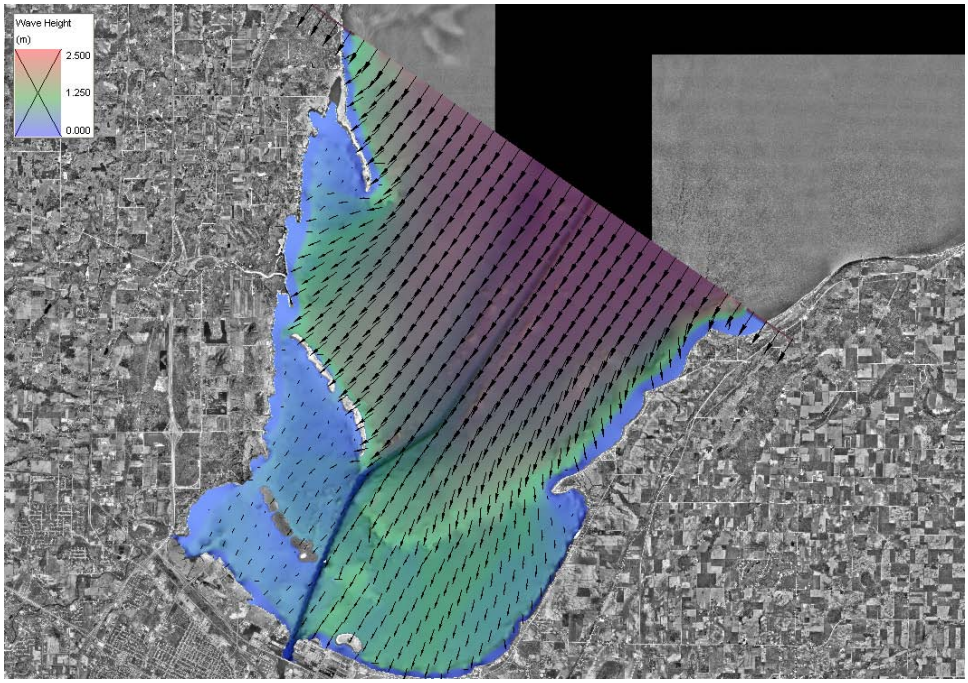

Ho = 2.1 m, Tp = 6.4 sec, Wave Dir = 33, Wind = 16 m/s, Wind Dir = 25

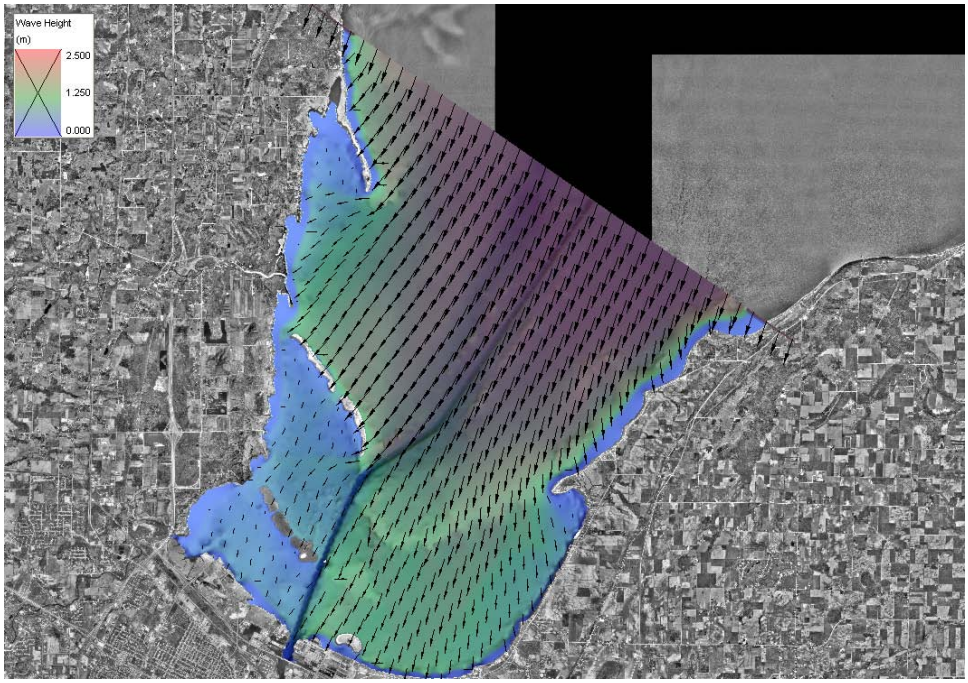

Ho = 1.9 m, Tp = 6.0 sec, Wave Dir = 20, Wind = 18 m/s, Wind Dir = 5

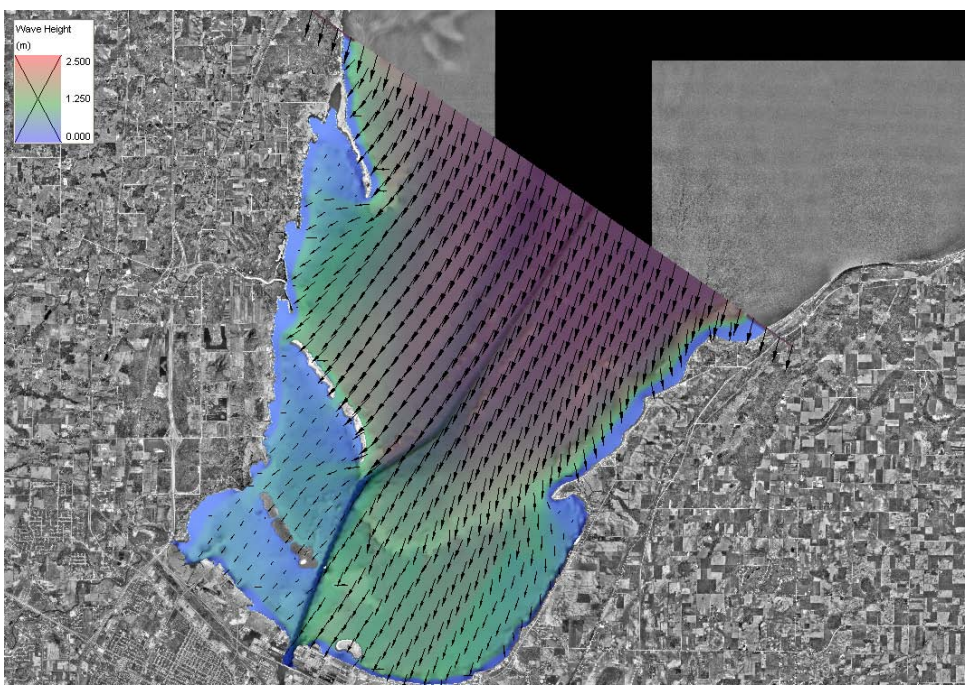

Ho = 2.0 m, Tp = 6.3 sec, Wave Dir = 15, Wind = 20 m/s, Wind Dir = 35

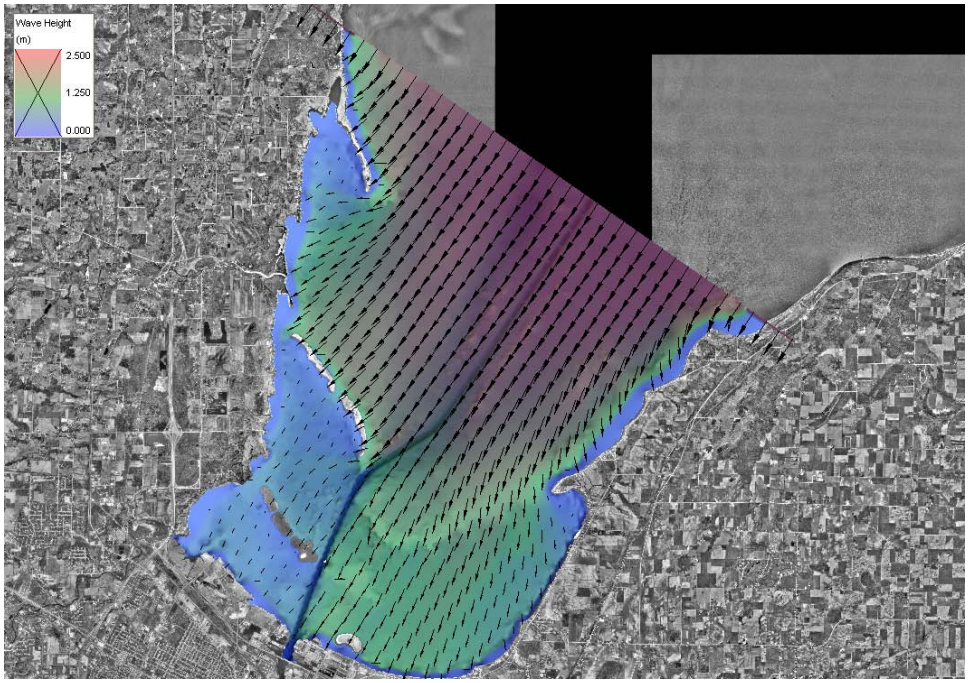

Ho = 2.1 m, Tp = 6.5 sec, Wave Dir = 33, Wind = 17 m/s, Wind Dir = 25

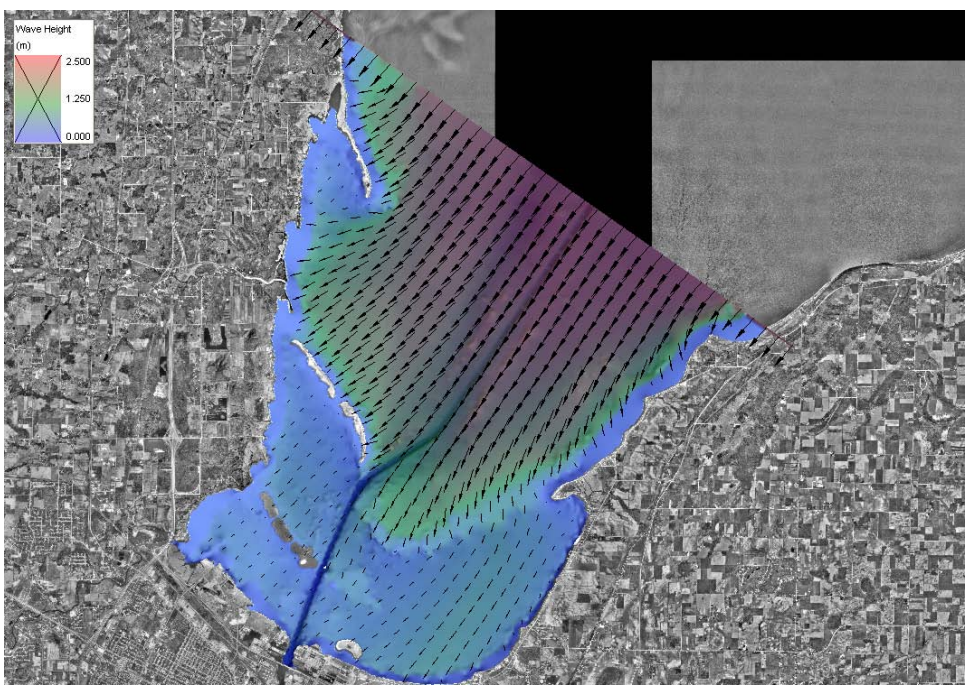

Ho = 2.1 m, Tp = 6.6 sec, Wave Dir = 41, Wind = 18 m/s, Wind Dir = 45

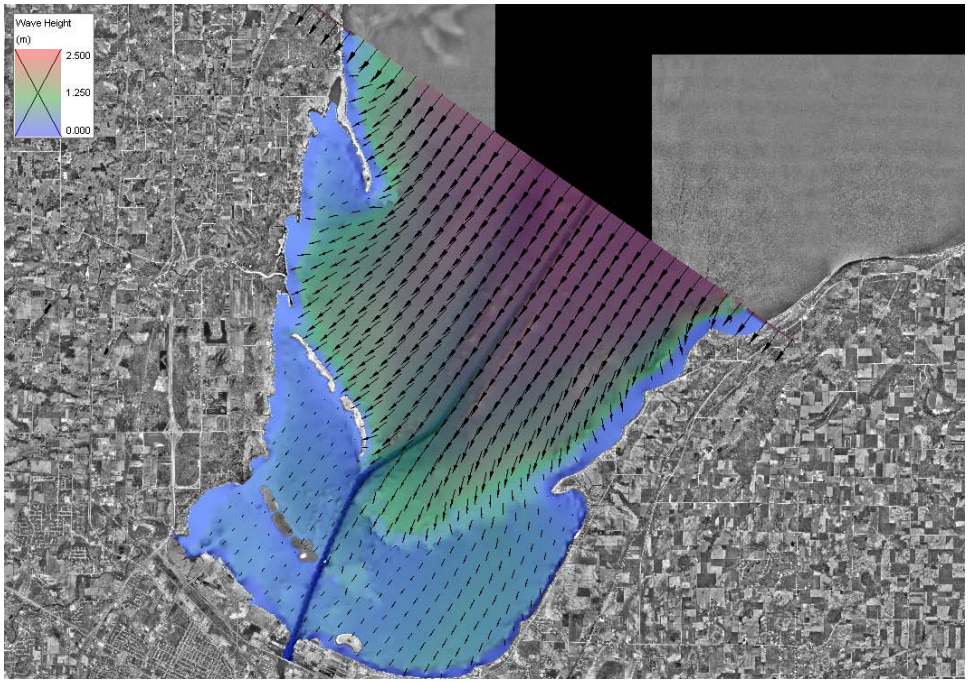

Ho = 2.1 m, Tp = 6.6 sec, Wave Dir = 38, Wind = 16 m/s, Wind Dir = 35

Attachment B
Hydrodynamic Modeling

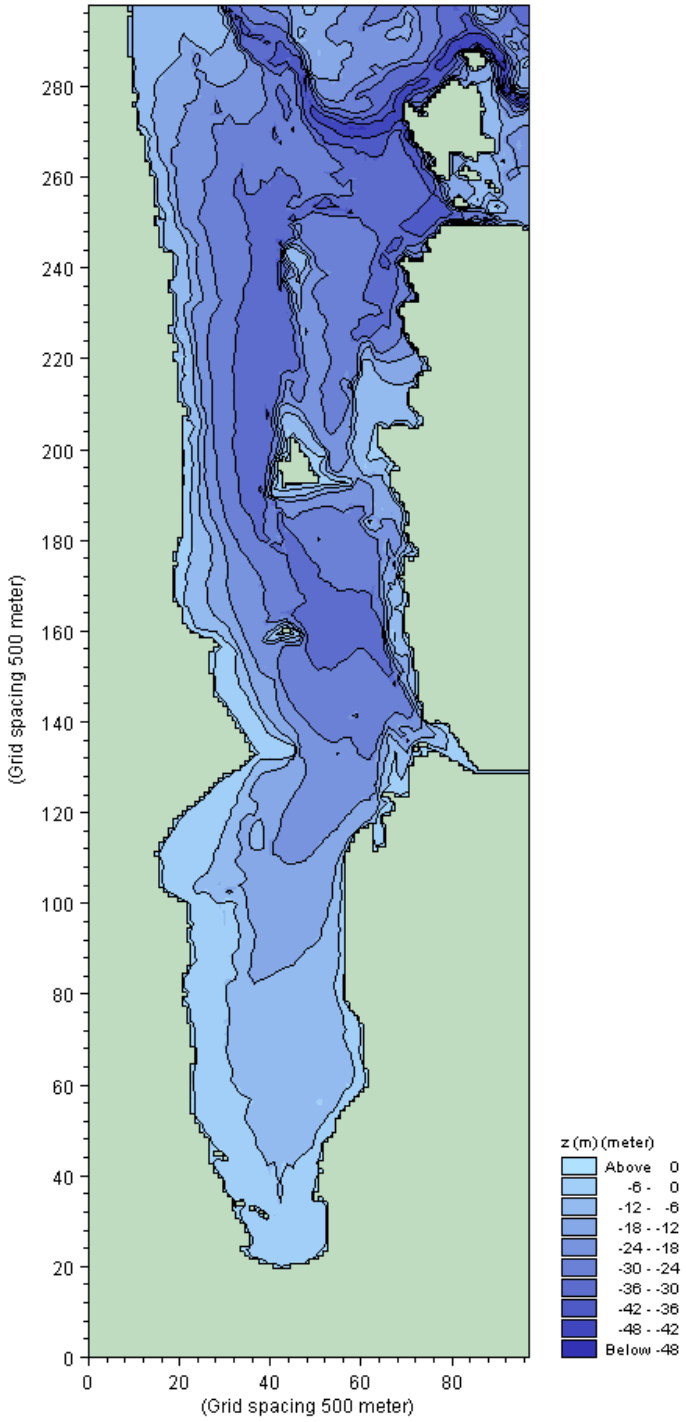

500 m Bathymetric Grid

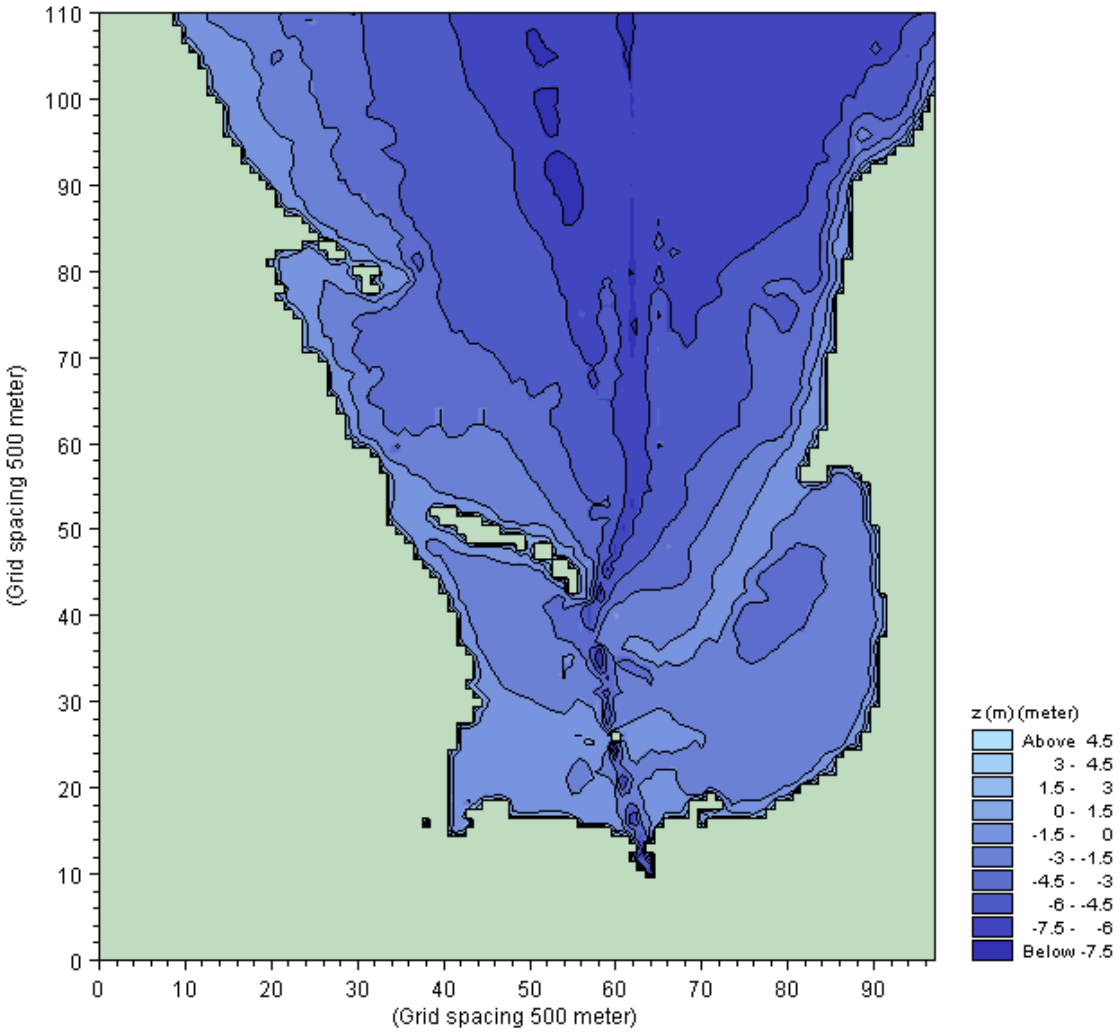

180 m Bathymetric Grid

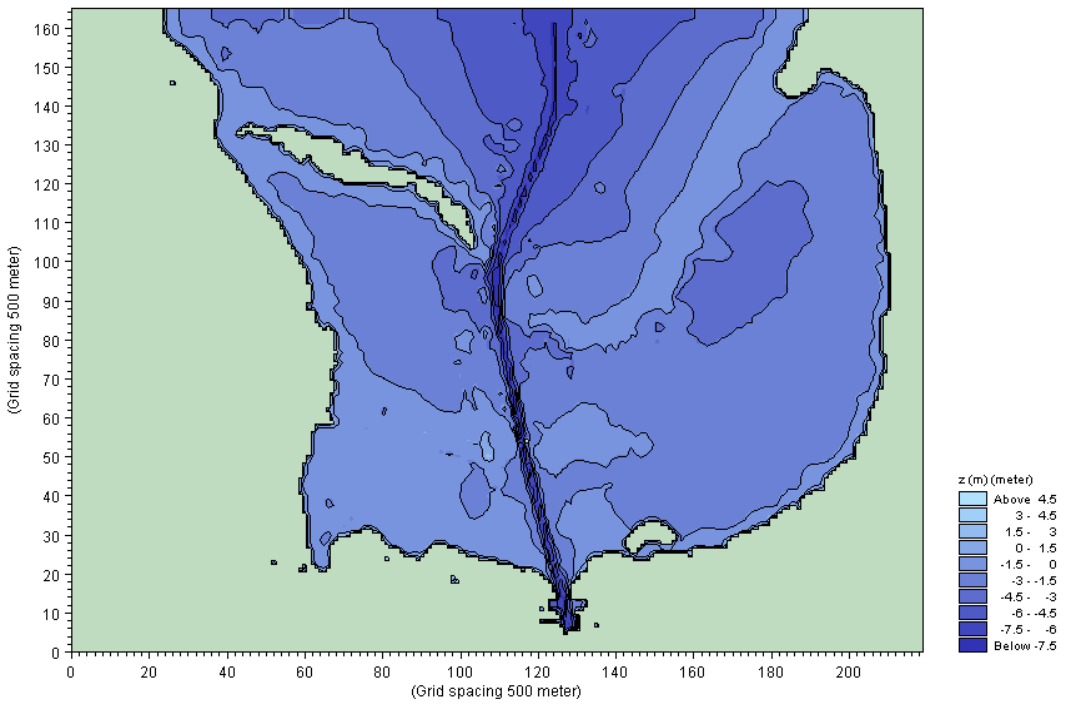

60 m Bathymetric Grid

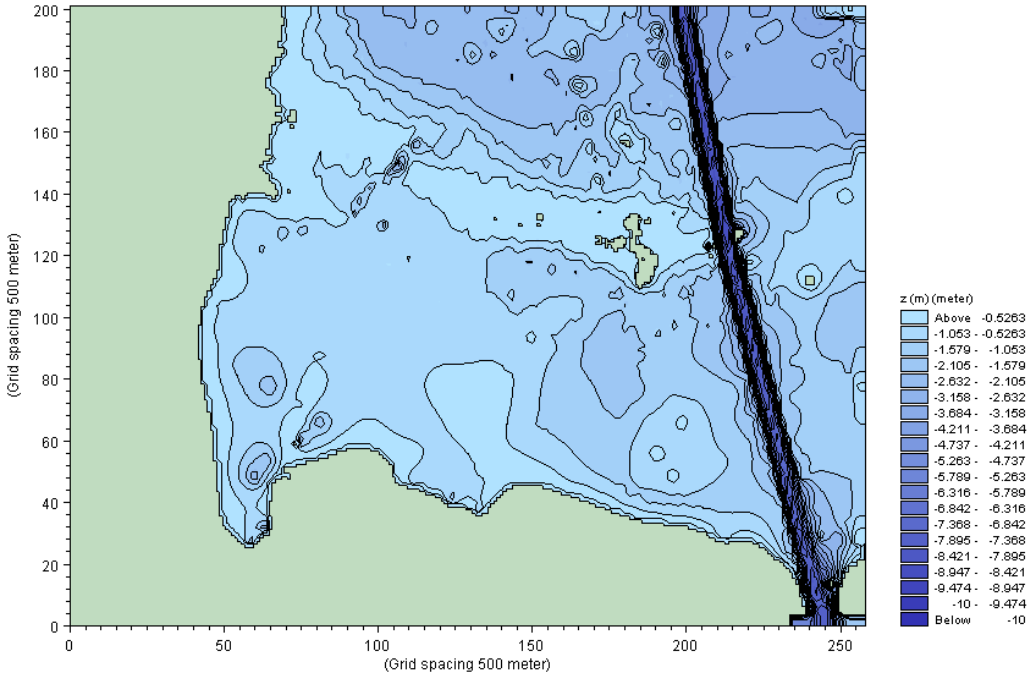

20 m Bathymetric Grid – Existing Conditions

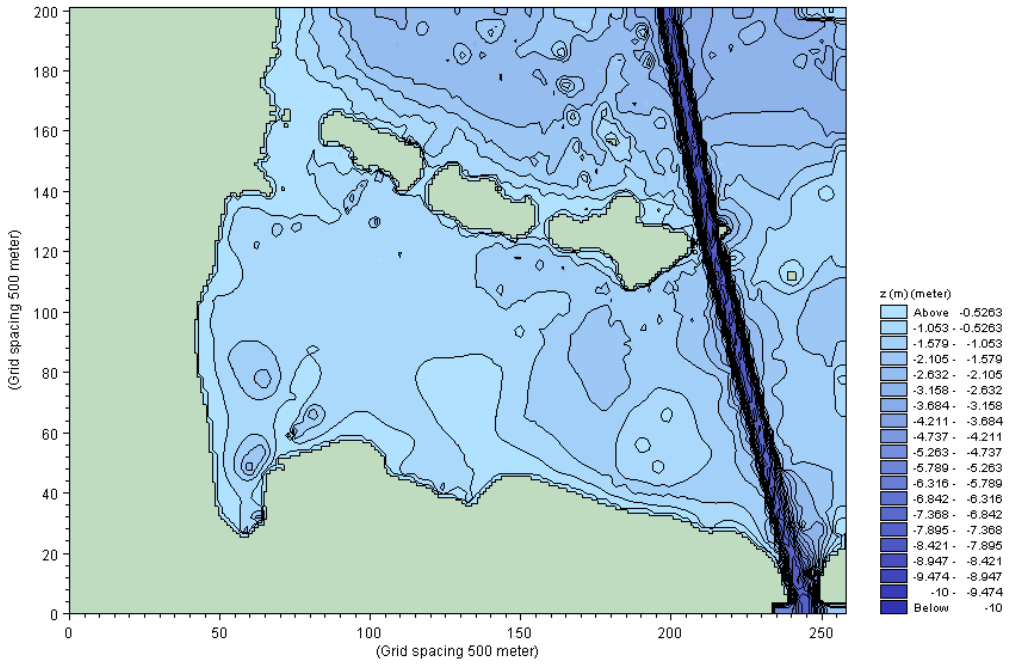

20 m Bathymetric Grid – Proposed Conditions

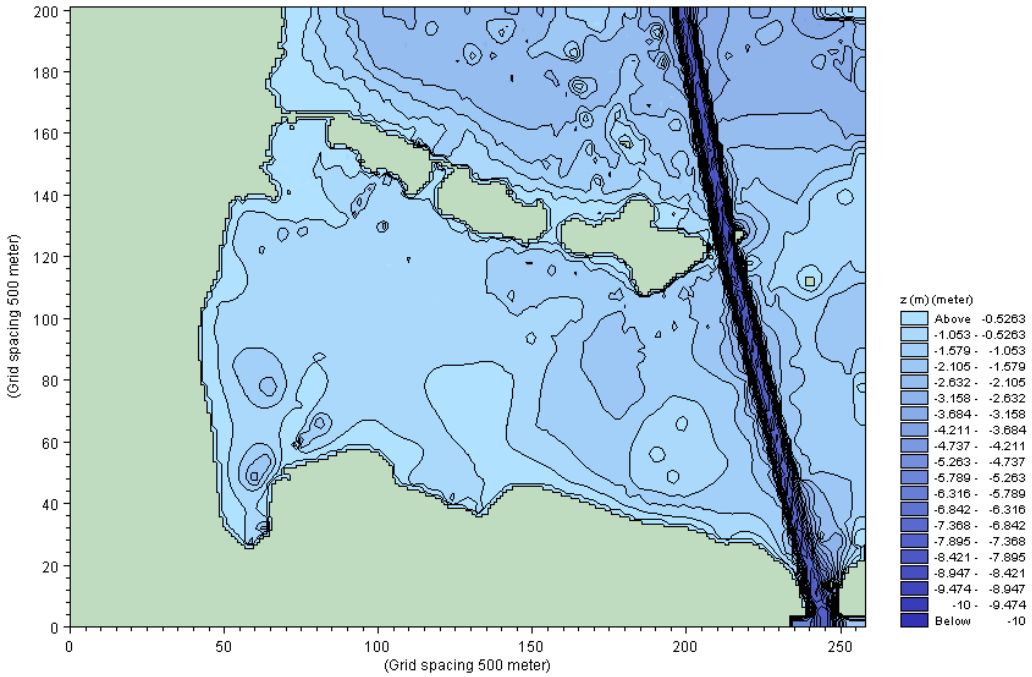

20 m Bathymetric Grid – Construction Road Conditions

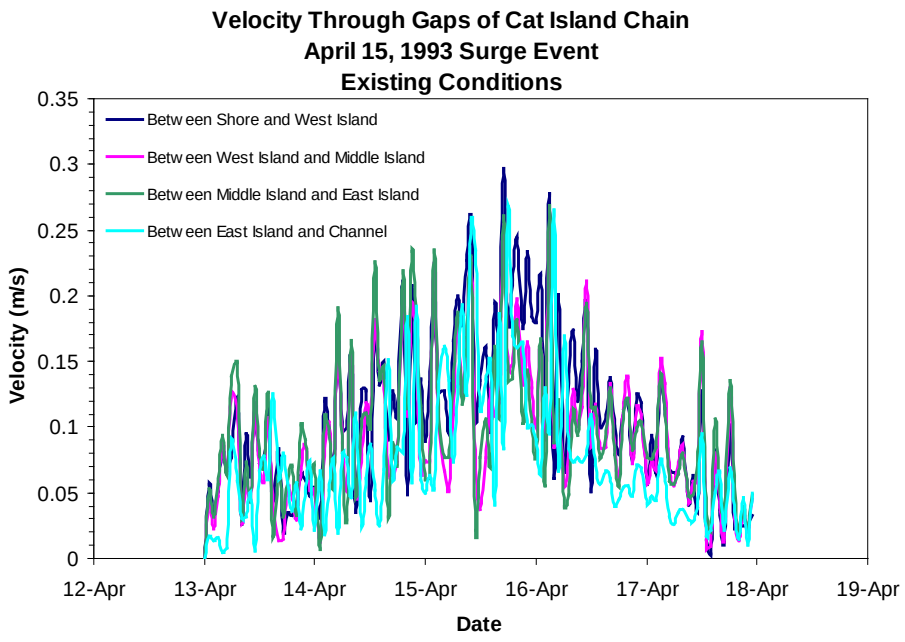
Velocity Through Gaps of Cat Island Chain
April 15, 1993 Surge Event
Existing Conditions
Between Shore and West Island
Between West Island and Middle Island
Between Middle Island and East Island
Between East Island and Channel
Velocity (m/s)
0.35
0.3
0.25
0.2
0.15
0.1
0.05
0
12-Apr
13-Apr
14-Apr
15-Apr
16-Apr
17-Apr
18-Apr
19-Apr
Date

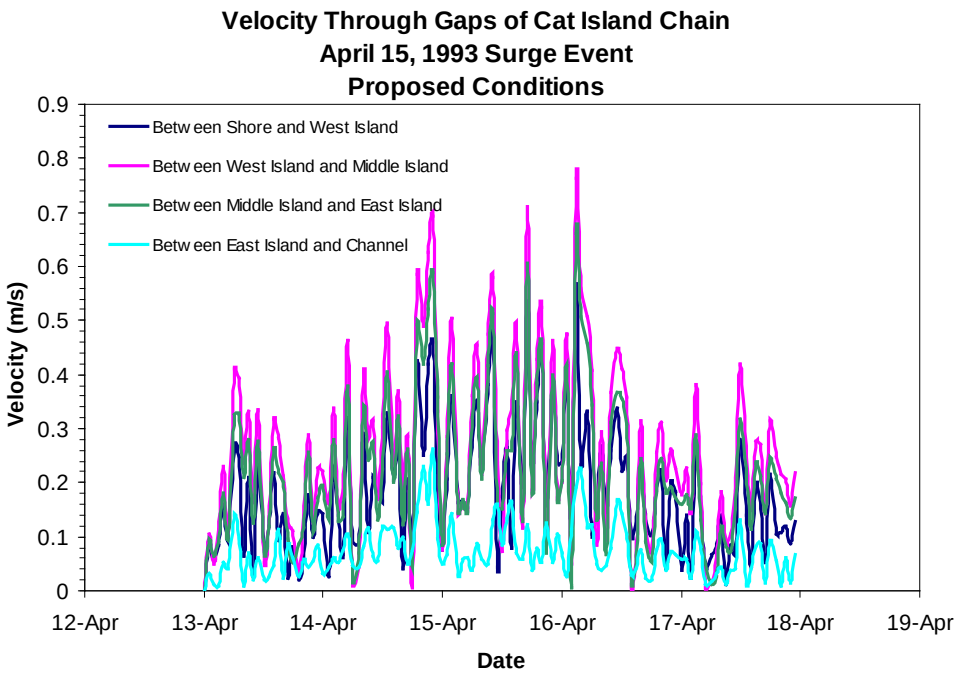
Velocity Through Gaps of Cat Island Chain
April 15, 1993 Surge Event
Proposed Conditions
Between Shore and West Island
Between West Island and Middle Island
Between Middle Island and East Island
Between East Island and Channel
Velocity (m/s)
0.9
0.8
0.7
0.6
0.5
0.4
0.3
0.2
0.1
0
12-Apr
13-Apr
14-Apr
15-Apr
16-Apr
17-Apr
18-Apr
19-Apr
Date

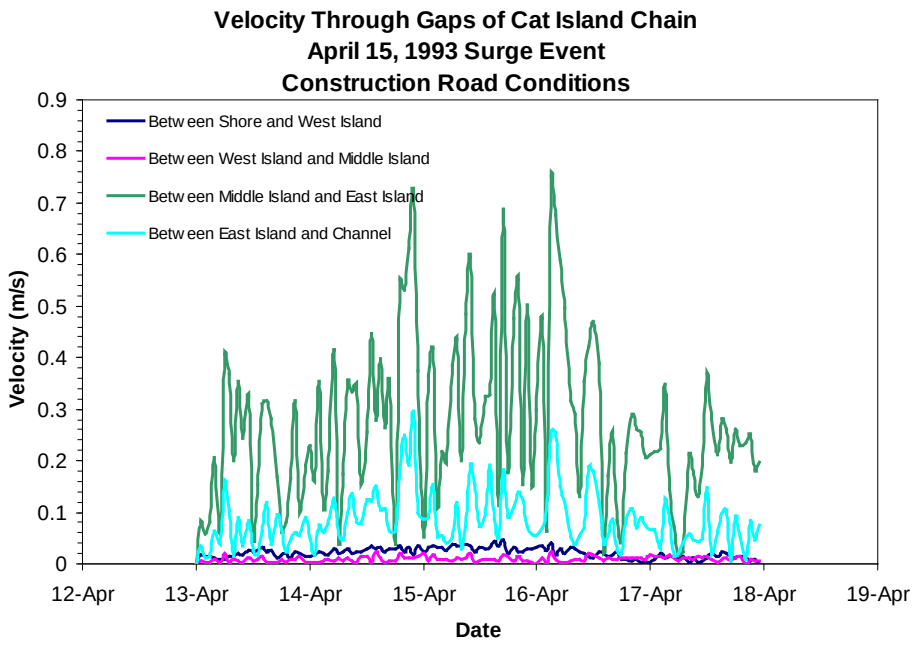
Velocity Through Gaps of Cat Island Chain
April 15, 1993 Surge Event
Construction Road Conditions
Between Shore and West Island
Between West Island and Middle Island
Between Middle Island and East Island
Between East Island and Channel
Velocity (m/s)
0.9
0.8
0.7
0.6
0.5
0.4
0.3
0.2
0.1
0
12-Apr
13-Apr
14-Apr
15-Apr
16-Apr
17-Apr
18-Apr
19-Apr
Date

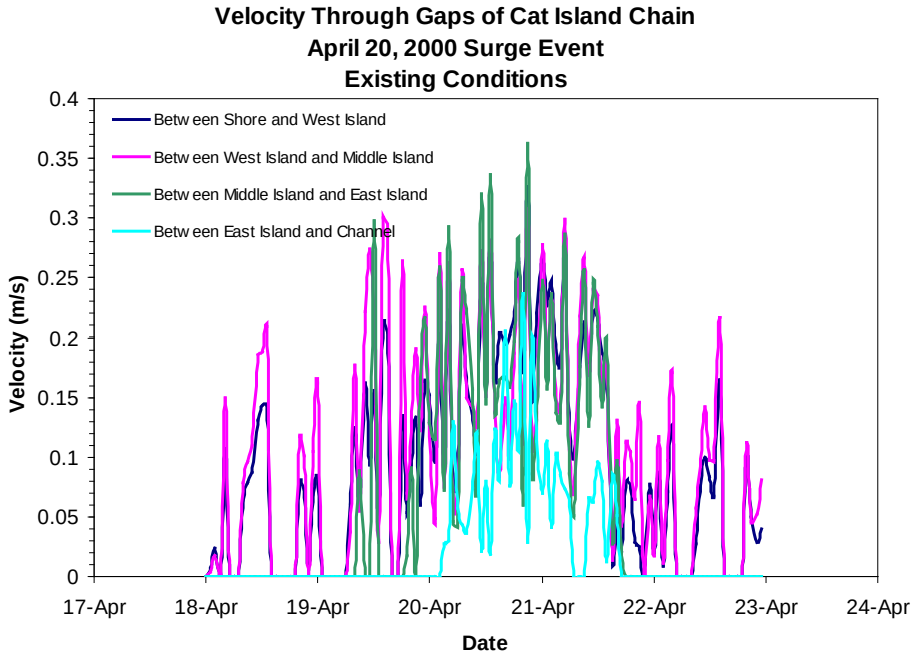
Velocity Through Gaps of Cat Island Chain
April 20, 2000 Surge Event
Existing Conditions
Between Shore and West Island
Between West Island and Middle Island
Between Middle Island and East Island
Between East Island and Channel
Velocity (m/s)
0.4
0.35
0.3
0.25
0.2
0.15
0.1
0.05
0
17-Apr
18-Apr
19-Apr
20-Apr
21-Apr
22-Apr
23-Apr
24-Apr
Date

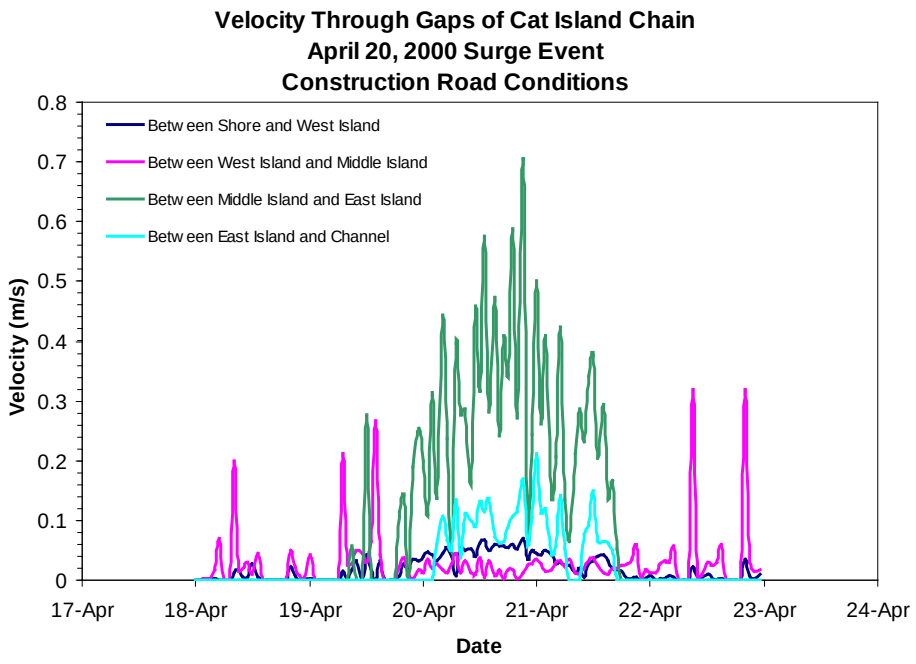
Velocity Through Gaps of Cat Island Chain
April 20, 2000 Surge Event
Construction Road Conditions
Between Shore and West Island
Between West Island and Middle Island
Between Middle Island and East Island
Between East Island and Channel
Velocity (m/s)
0.8
0.7
0.6
0.5
0.4
0.3
0.2
0.1
0
17-Apr
18-Apr
19-Apr
20-Apr
21-Apr
22-Apr
23-Apr
24-Apr
Date

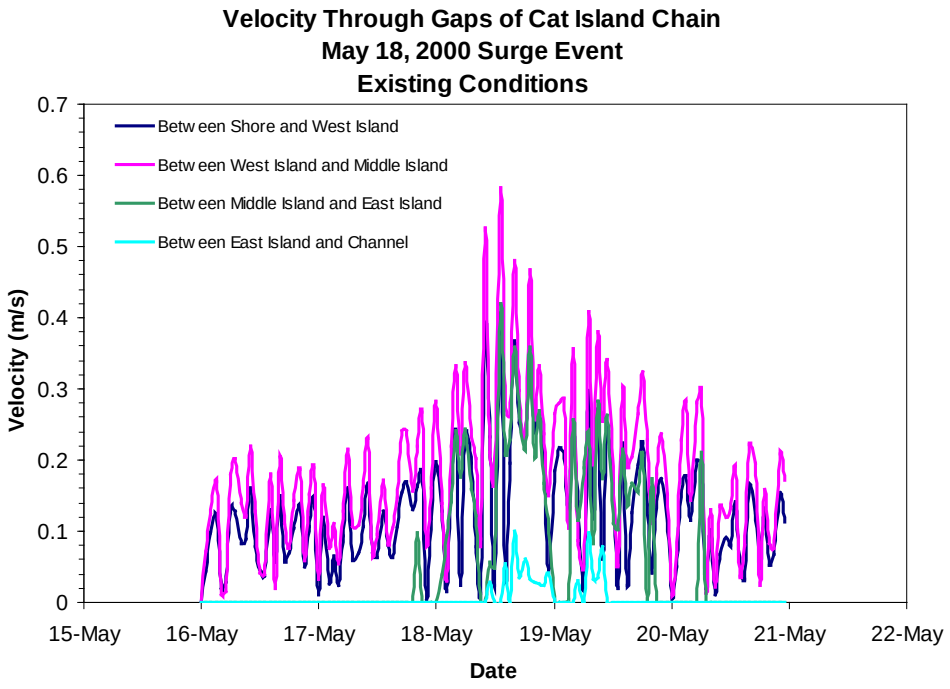
Velocity Through Gaps of Cat Island Chain
May 18, 2000 Surge Event
Existing Conditions
Between Shore and West Island
Between West Island and Middle Island
Between Middle Island and East Island
Between East Island and Channel
Velocity (m/s)
0.7
0.6
0.5
0.4
0.3
0.2
0.1
0
15-May
16-May
17-May
18-May
19-May
20-May
21-May
22-May
Date

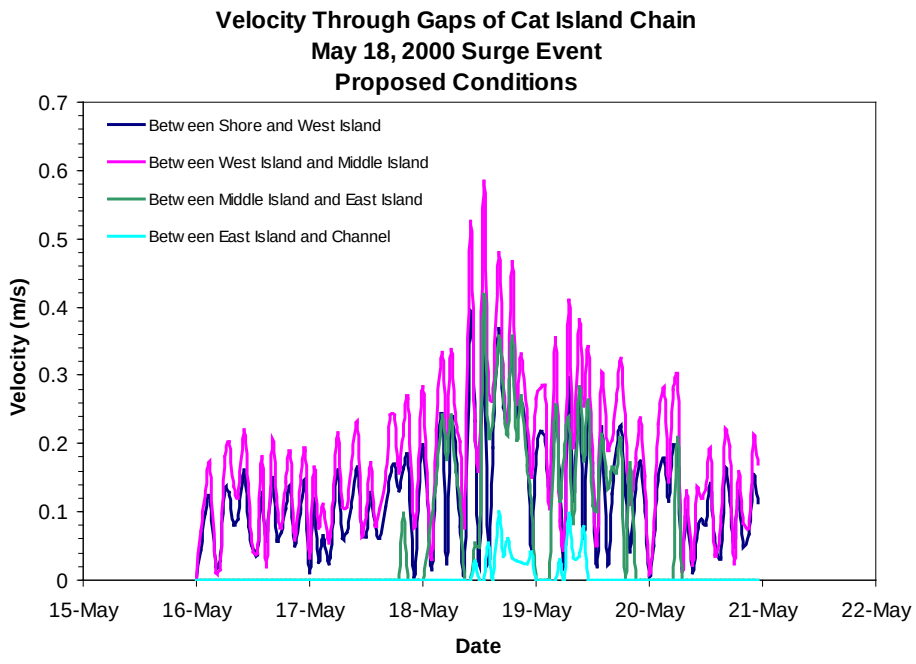
Velocity Through Gaps of Cat Island Chain
May 18, 2000 Surge Event
Proposed Conditions
Between Shore and West Island
Between West Island and Middle Island
Between Middle Island and East Island
Between East Island and Channel
Velocity (m/s)
0.7
0.6
0.5
0.4
0.3
0.2
0.1
0
15-May
16-May
17-May
18-May
19-May
20-May
21-May
22-May
Date

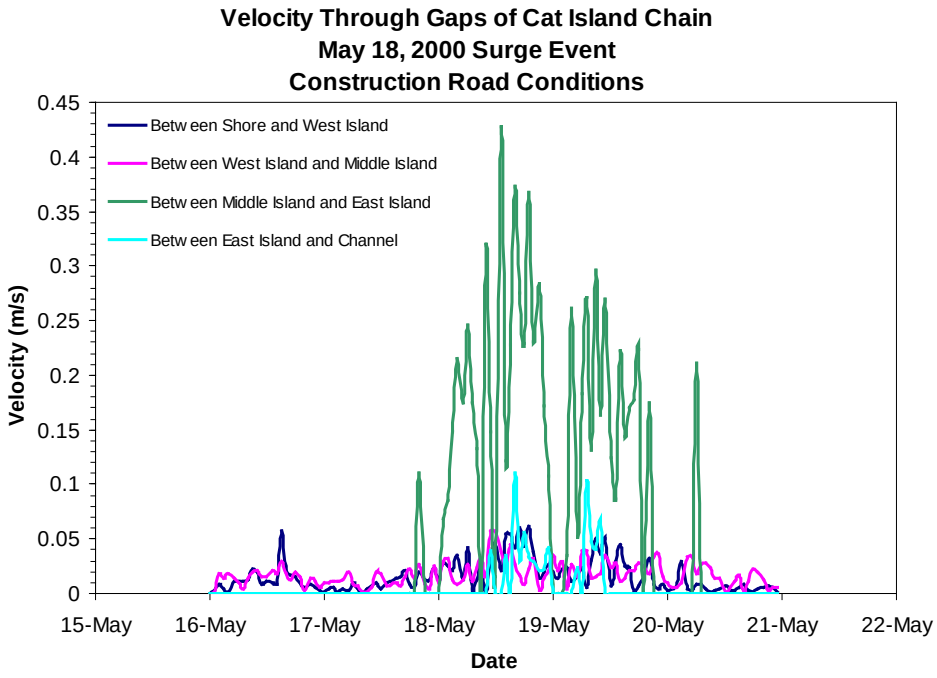
Velocity Through Gaps of Cat Island Chain
May 18, 2000 Surge Event
Construction Road Conditions
Between Shore and West Island
Between West Island and Middle Island
Between Middle Island and East Island
Between East Island and Channel
Velocity (m/s)
0.45
0.4
0.35
0.3
0.25
0.2
0.15
0.1
0.05
0
15-May
16-May
17-May
18-May
19-May
20-May
21-May
22-May
Date

Attachment C
Suspended Sediment Modeling

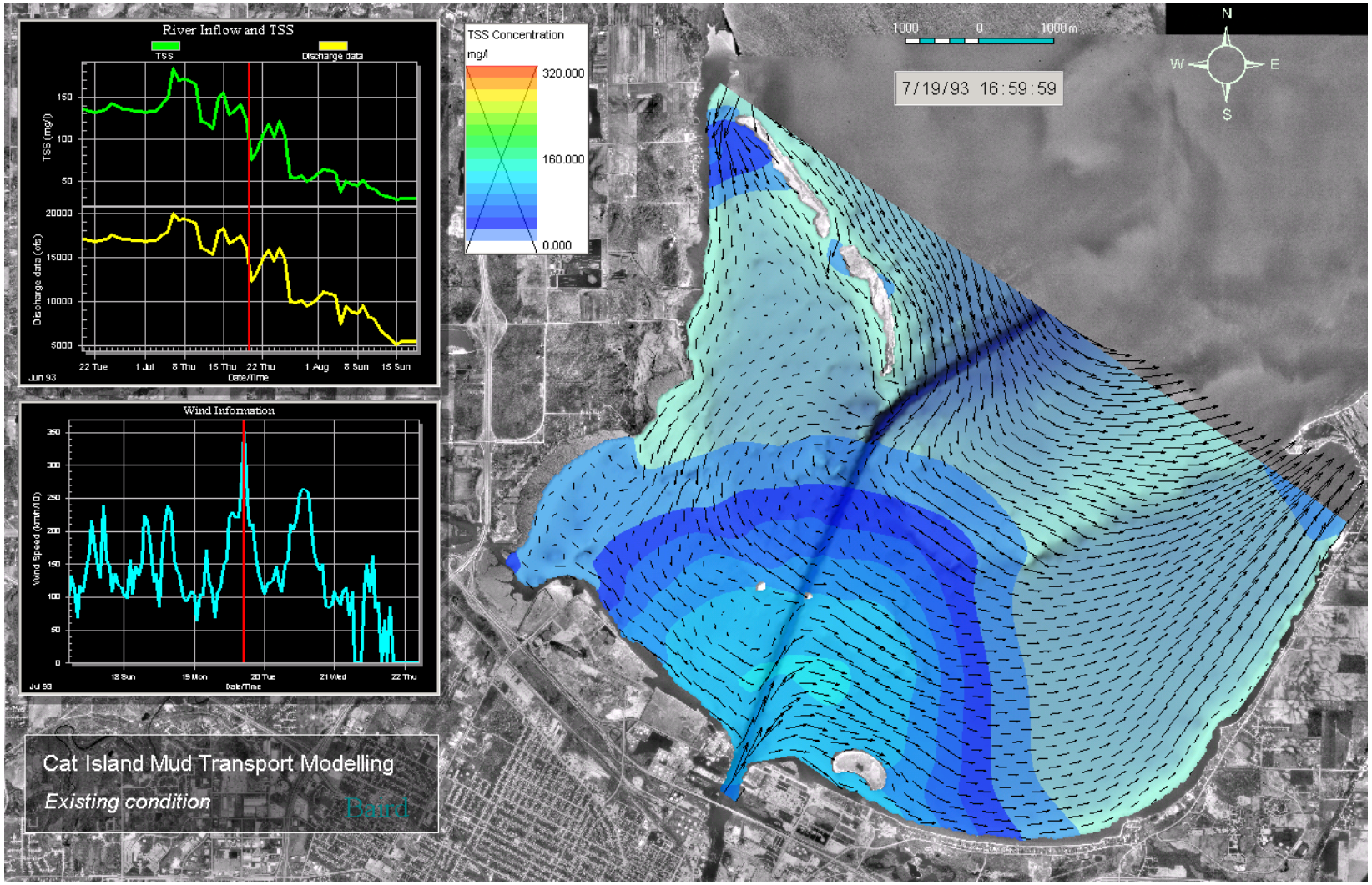

Figure A1 Mud Transport Modeling for Run 1 – Existing Conditions

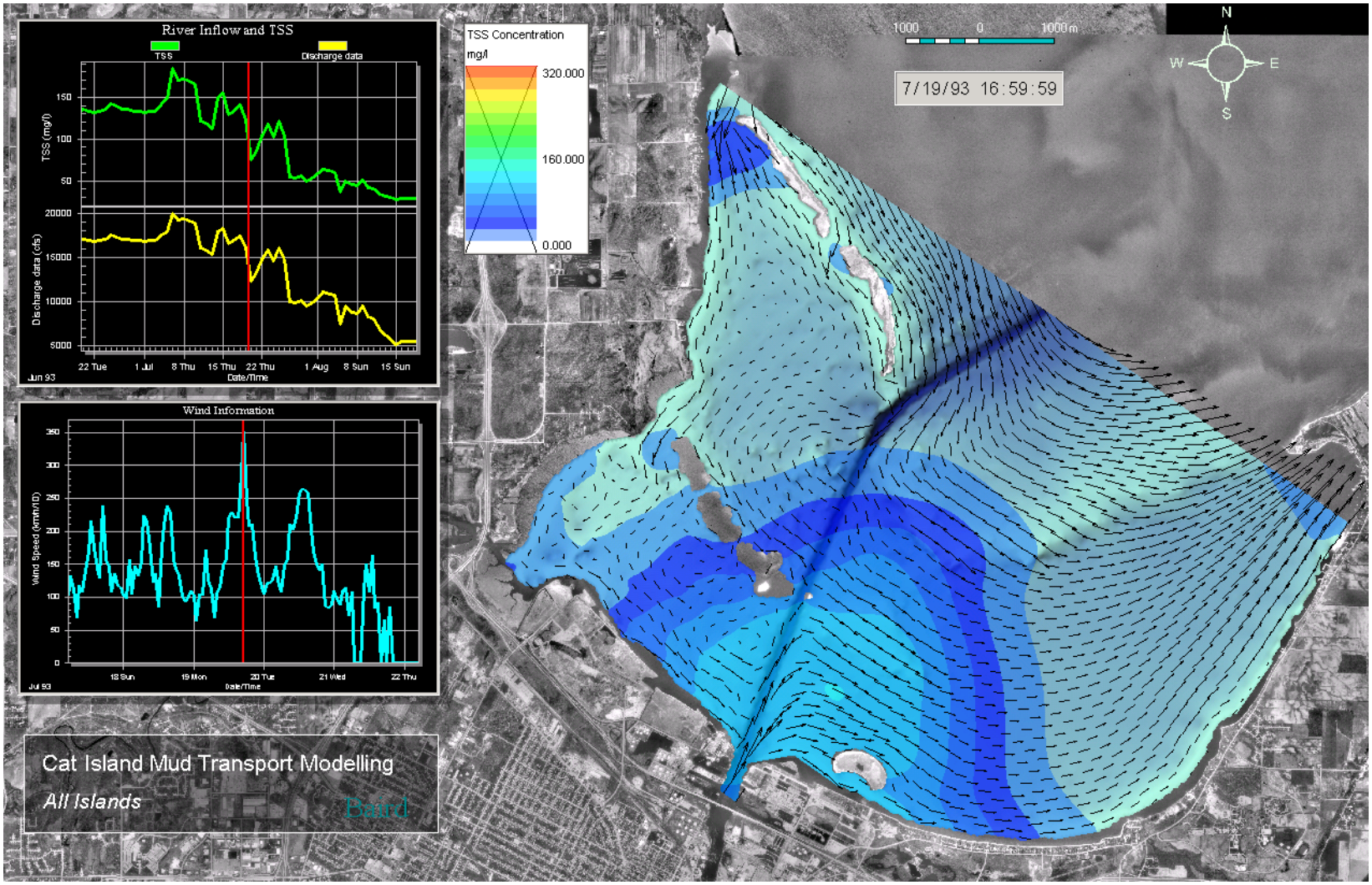

Figure A2 Mud Transport Modeling for Run 1 – All Islands

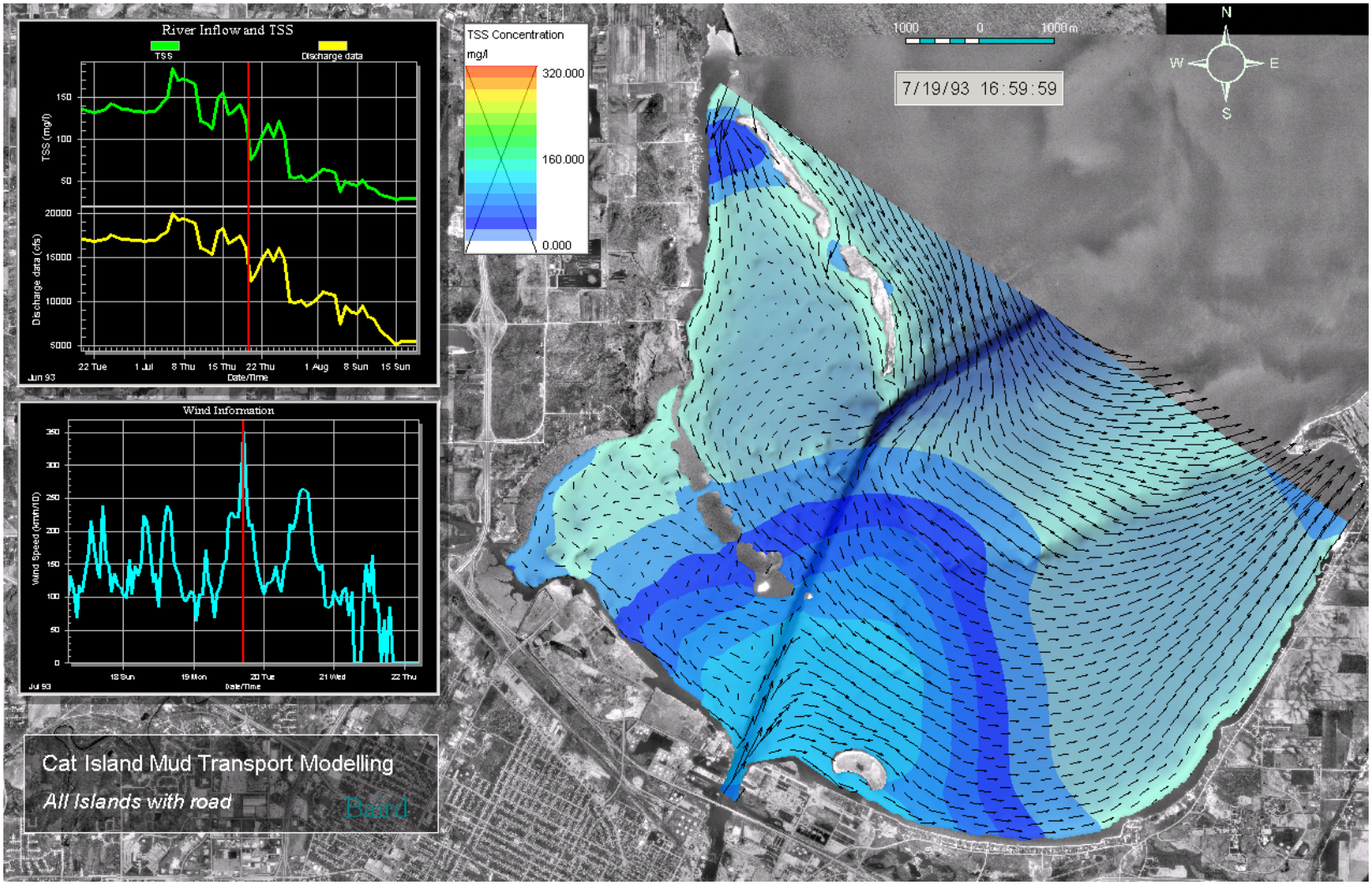

Figure A3 Mud Transport Modeling for Run 1 – All Islands with Road

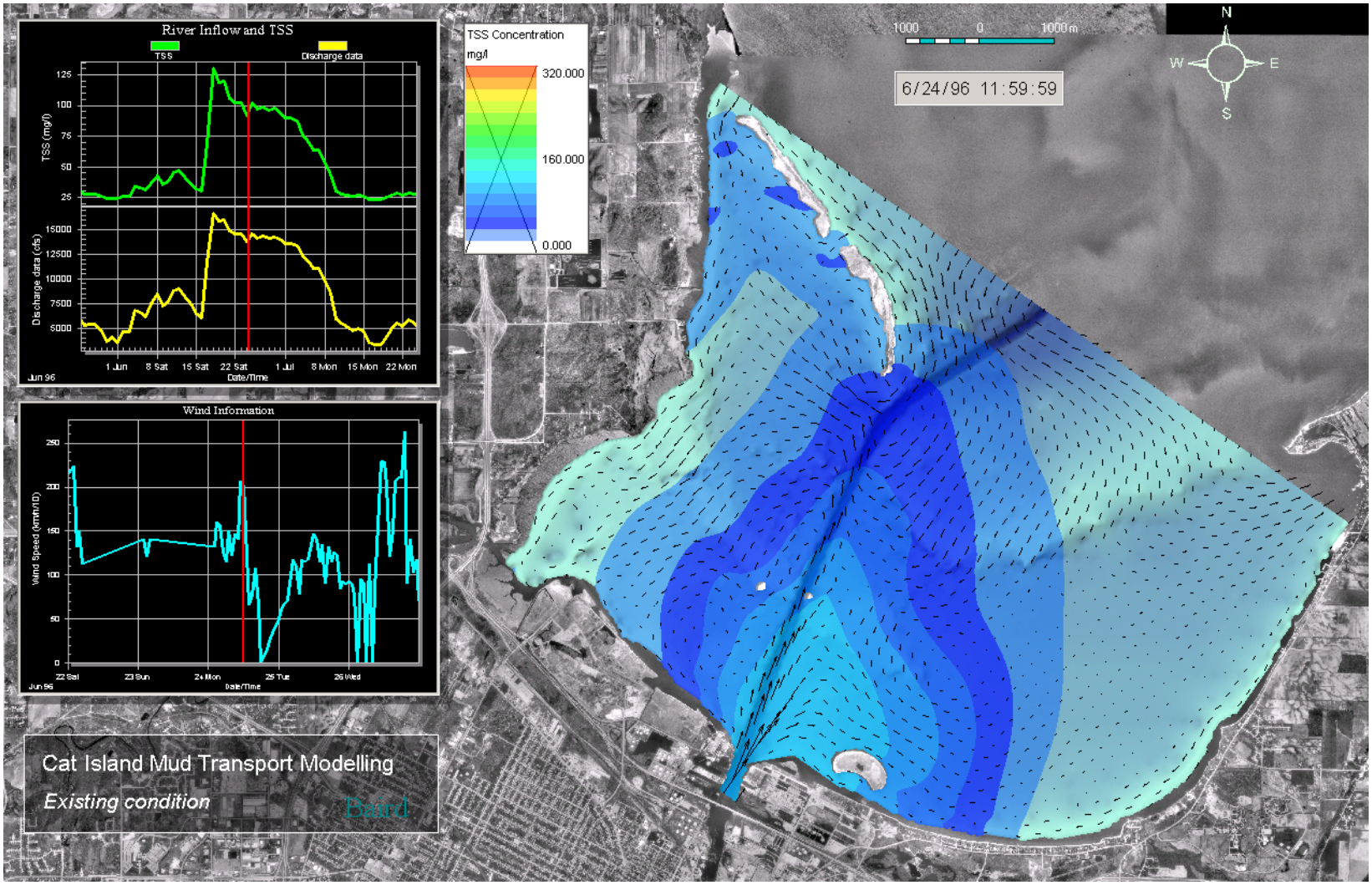

Figure A4 Mud Transport Modeling for Run 2 – Existing Conditions

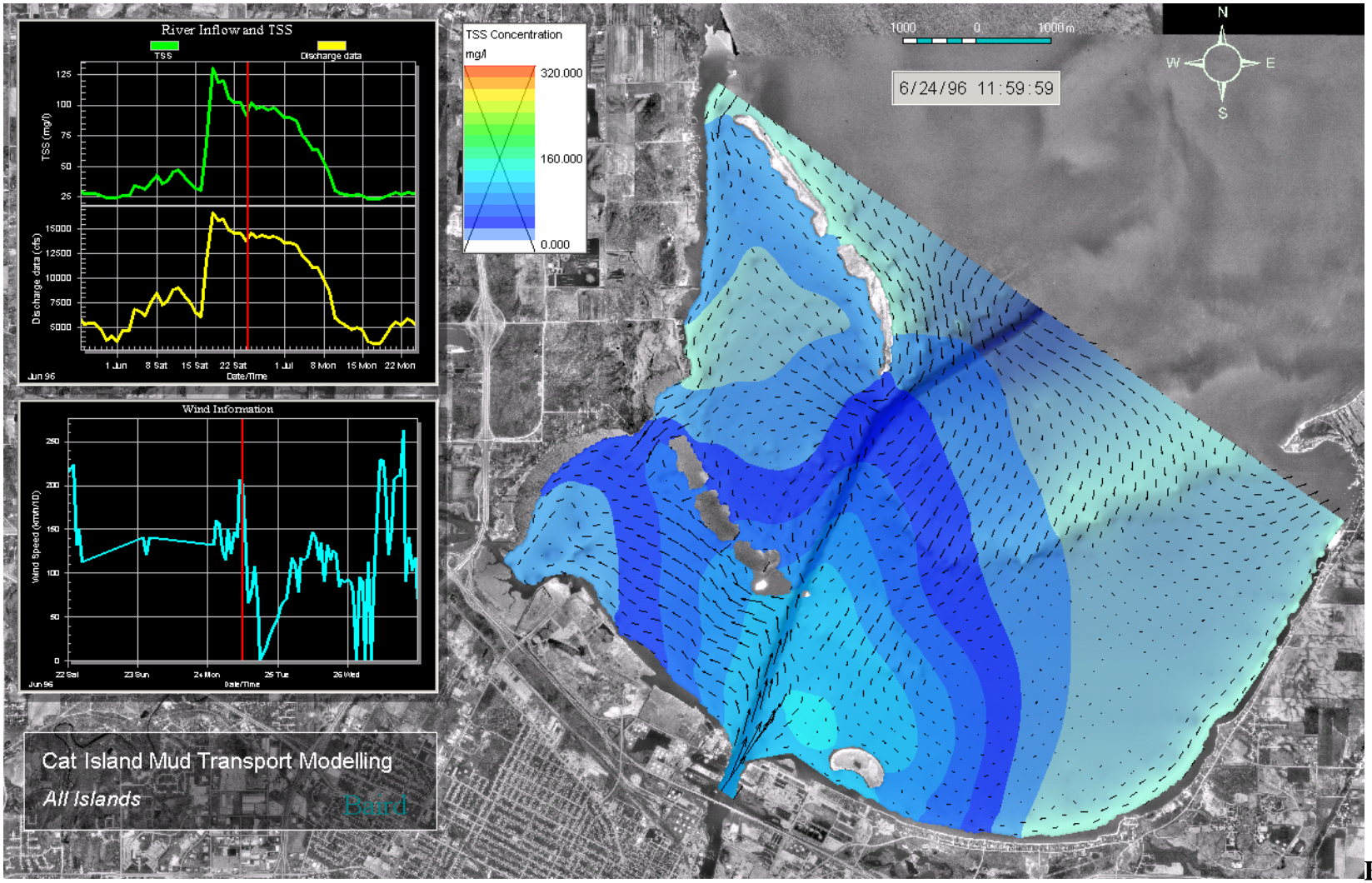

Figure A5 Mud Transport Modeling for Run 2 – All Islands

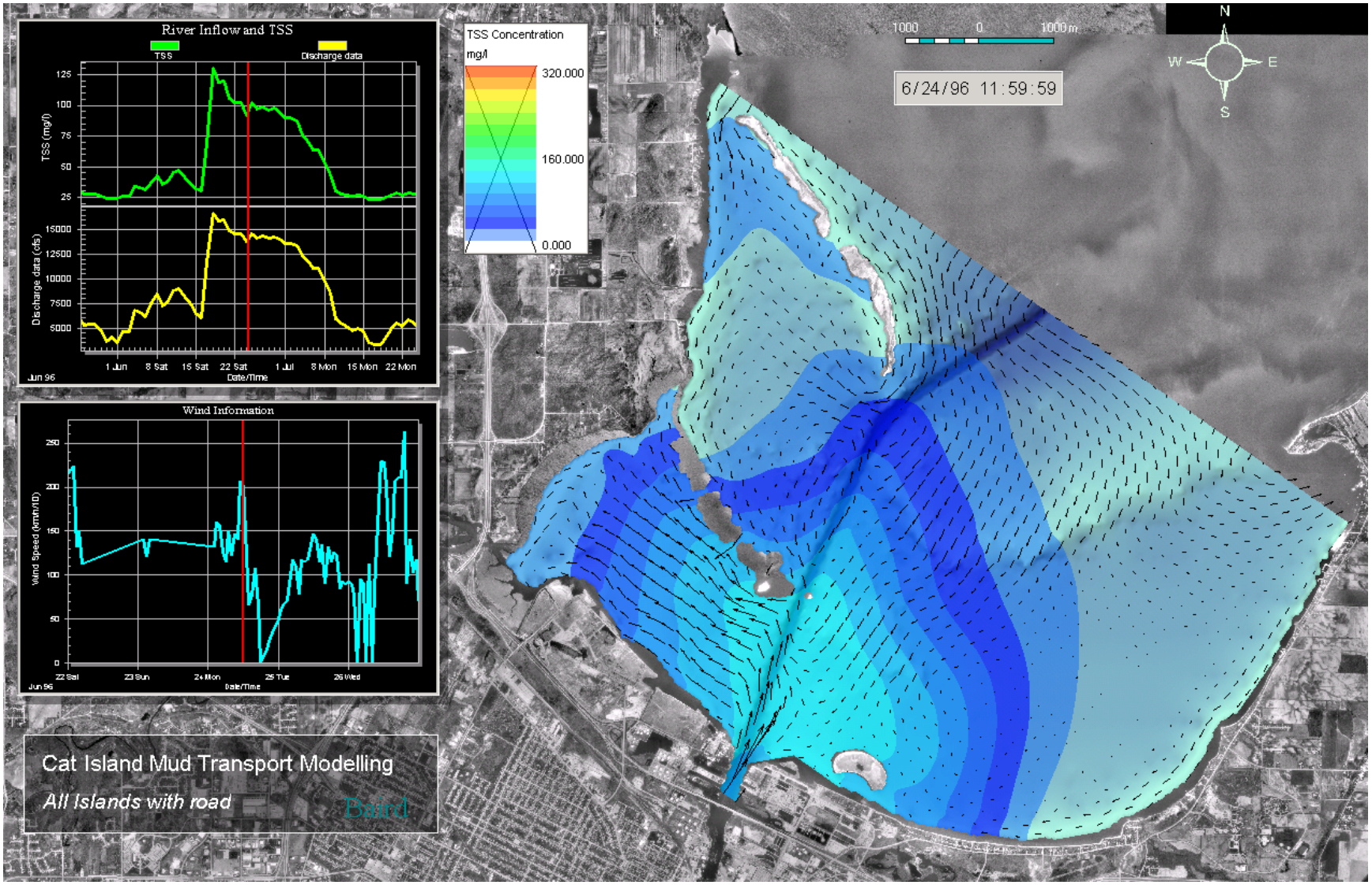

Figure A6 Mud Transport Modeling for Run 2 – All Islands with Road

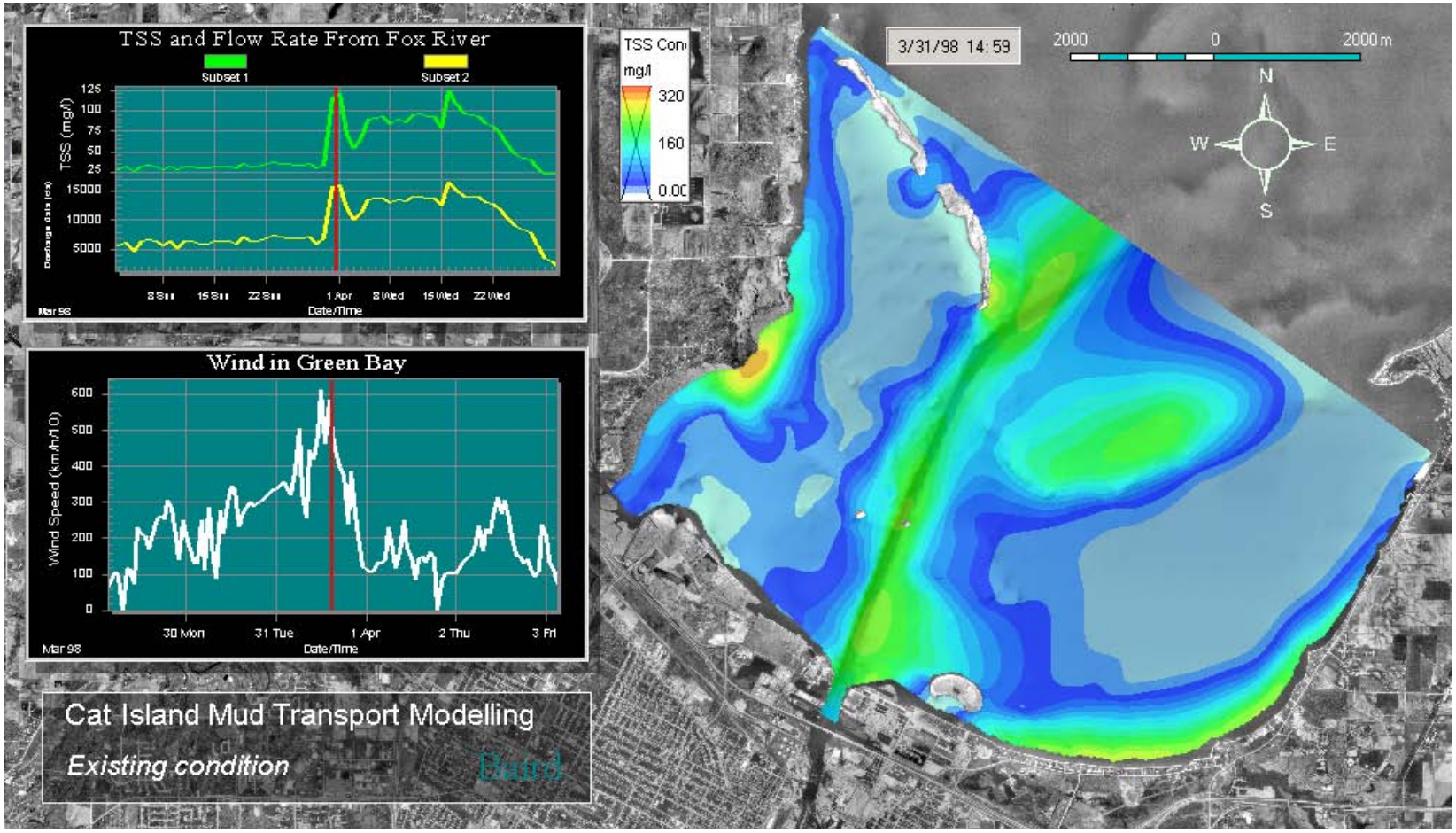

Figure A7 Mud Transport Modeling for Run 3 at Wind Peak – Existing Condtion

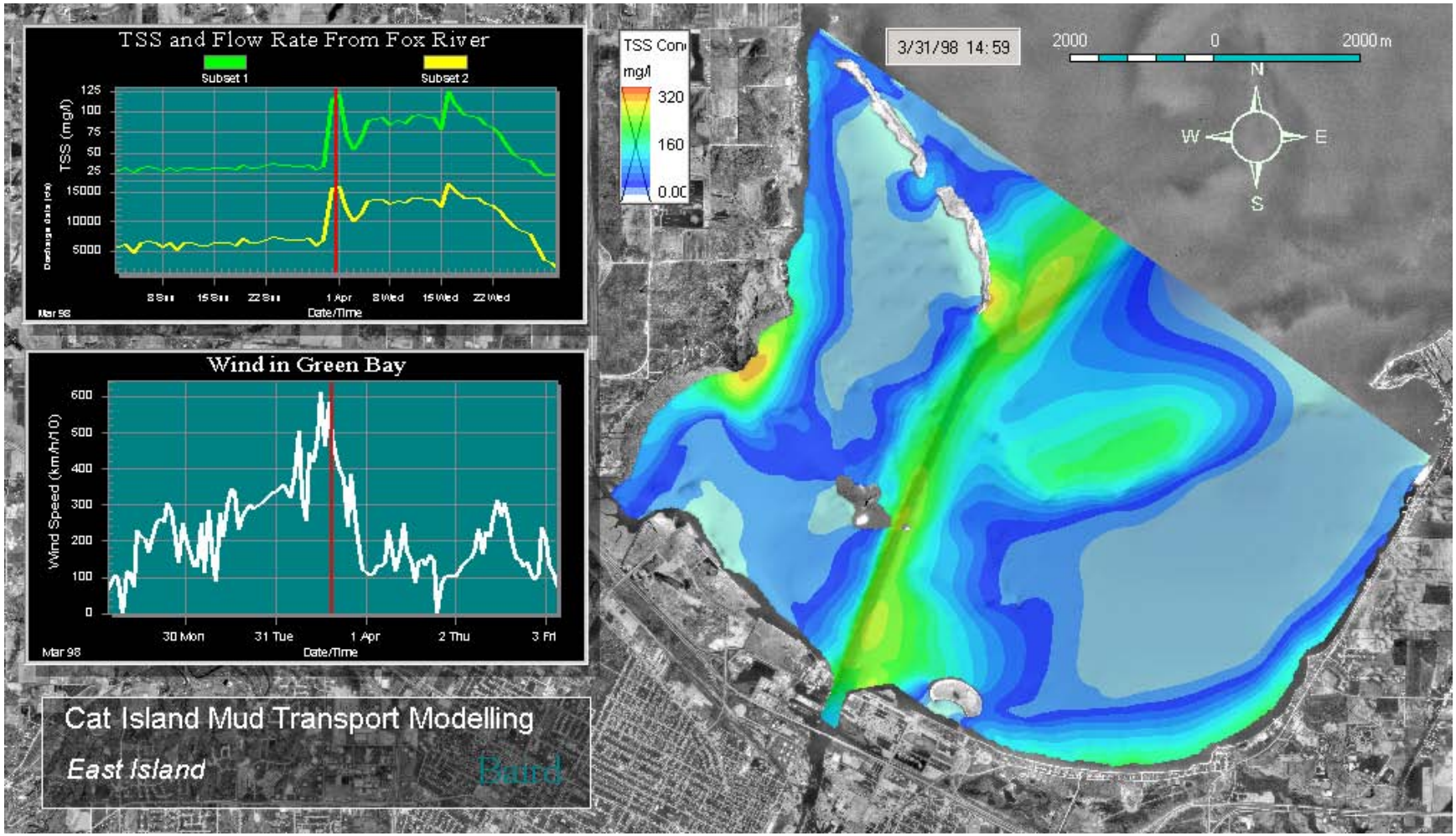

Figure A8 Mud Transport Modeling for Run 3 at Wind Peak – East Island

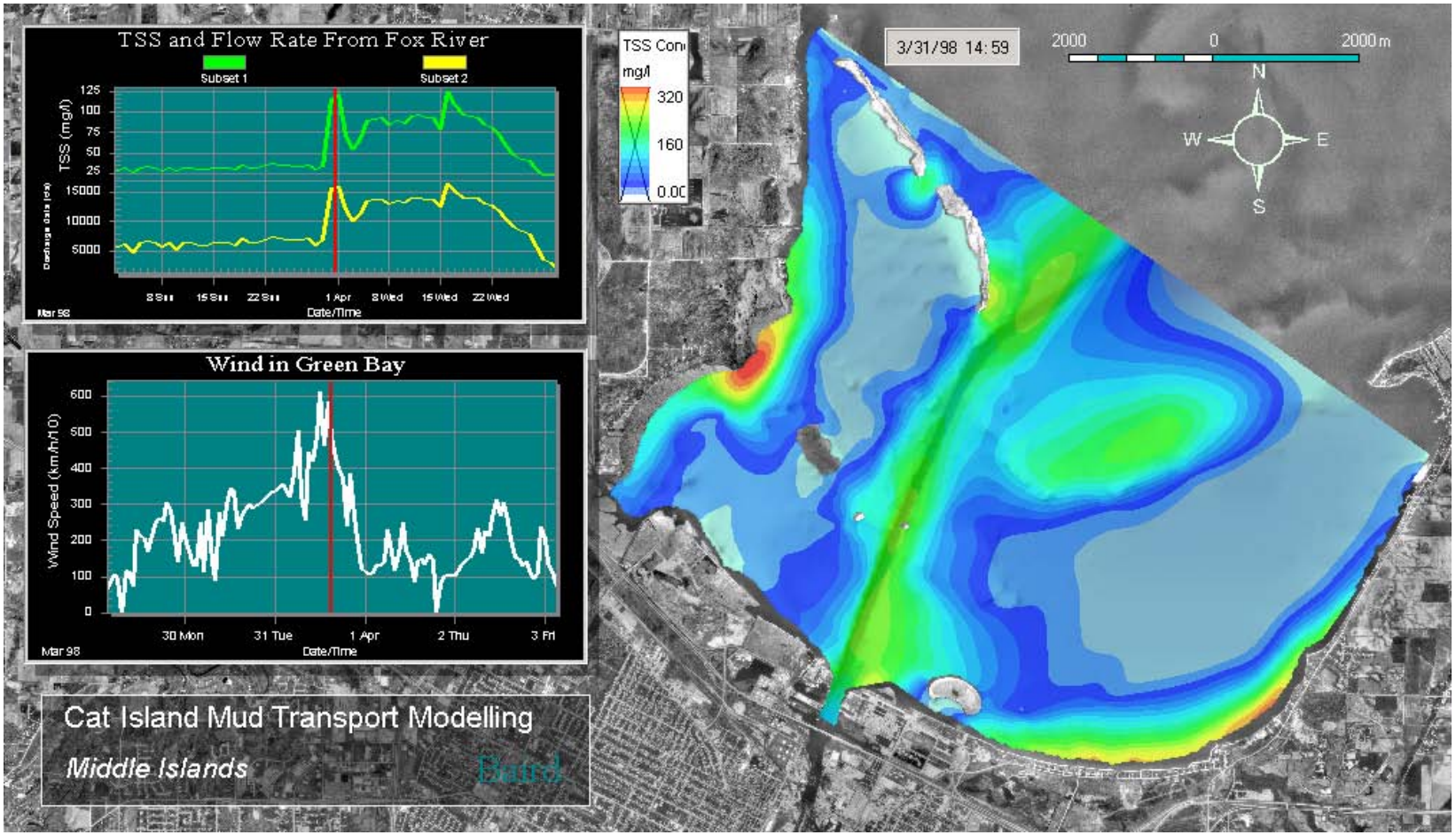

Figure A9 Mud Transport Modeling for Run 3 at Wind Peak – Middle Island

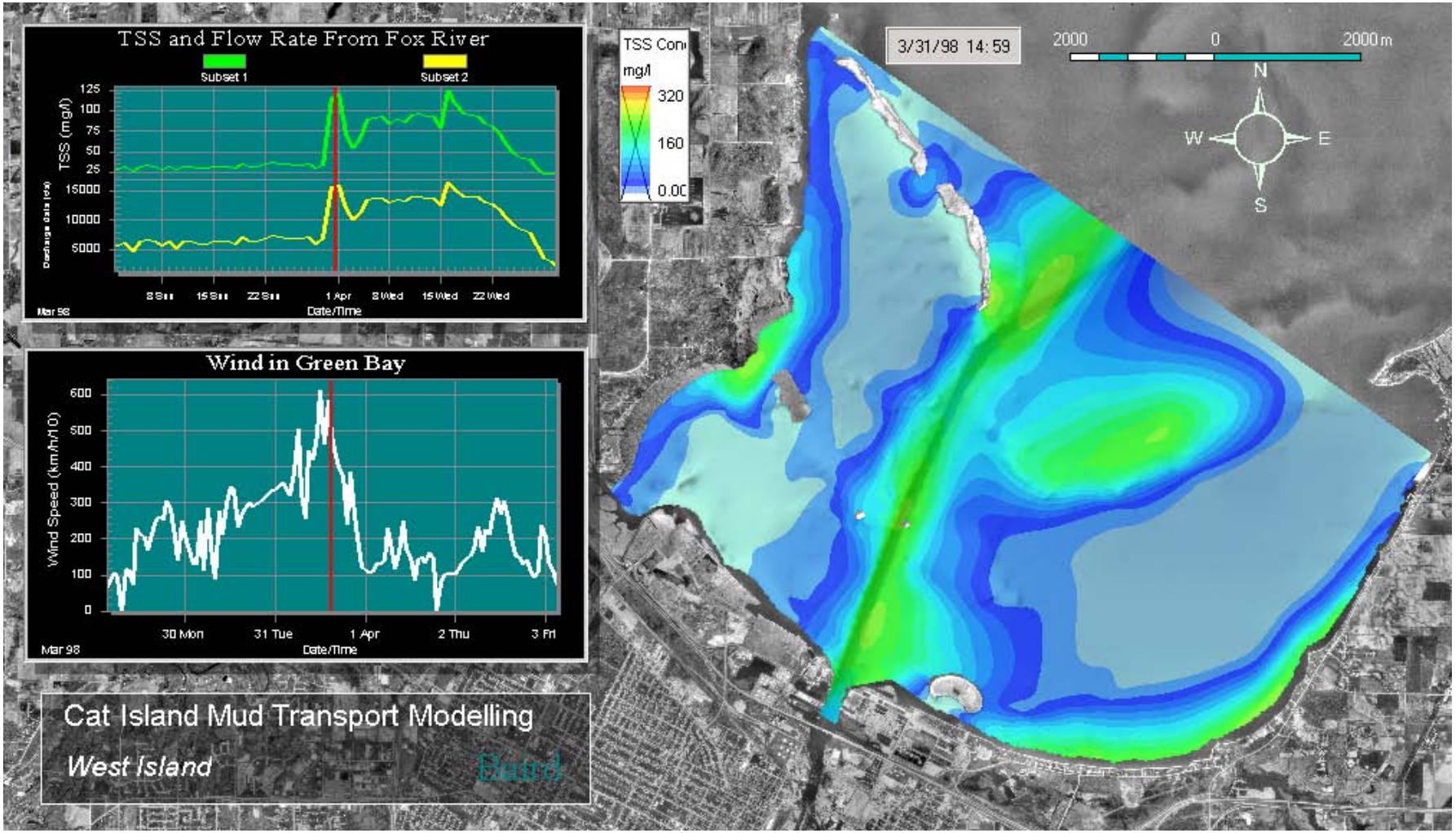

Figure A10 Mud Transport Modeling for Run 3 at Wind Peak – West Island

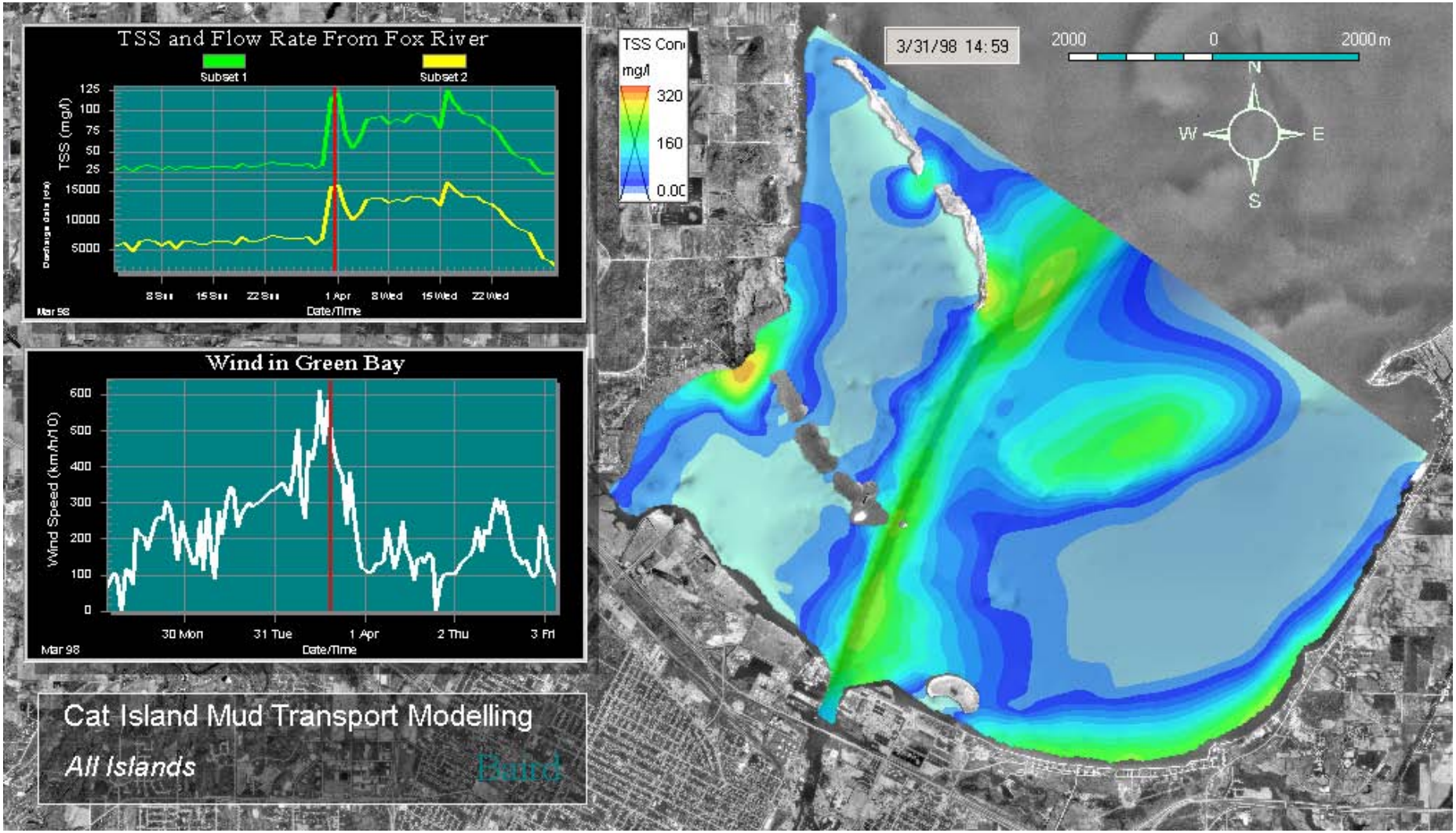

Figure A11 Mud Transport Modeling for Run 3 at Wind Peak – All Island

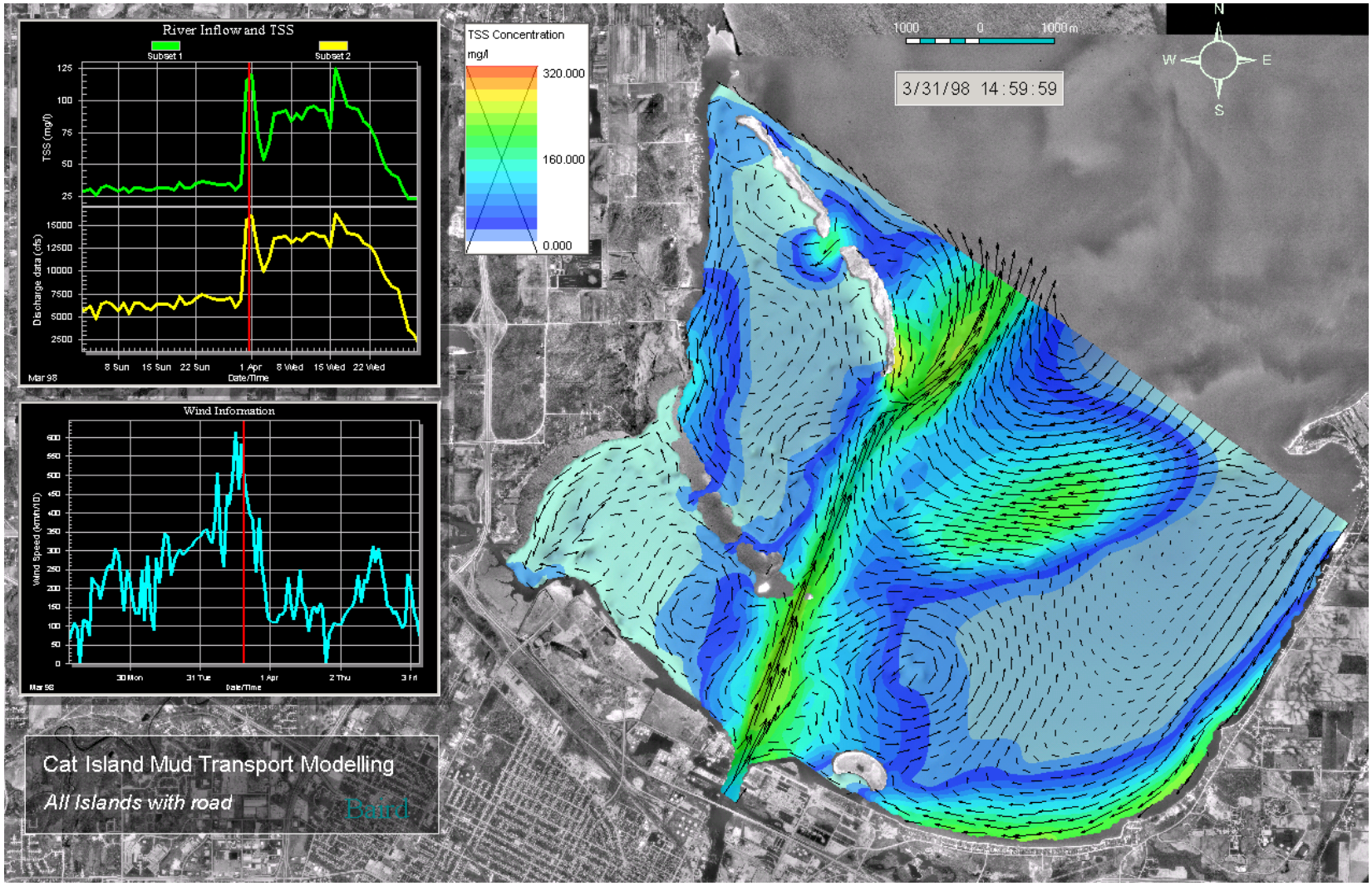

Figure A12 Mud Transport Modeling for Run 3 at Wind Peak – All Island with road

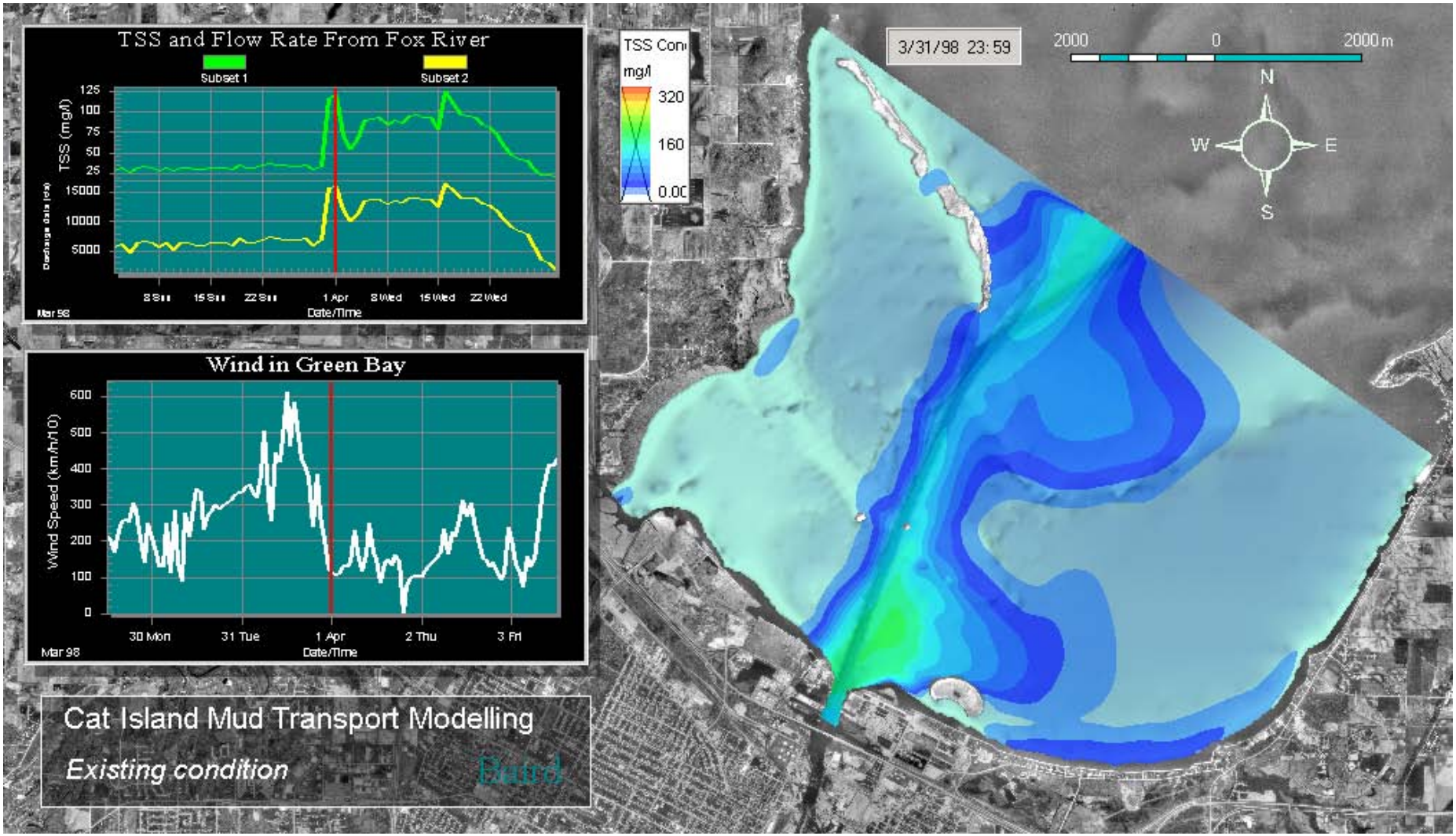

Figure A13 Mud Transport Modeling for Run 3 at Low Wind – Existing Condition

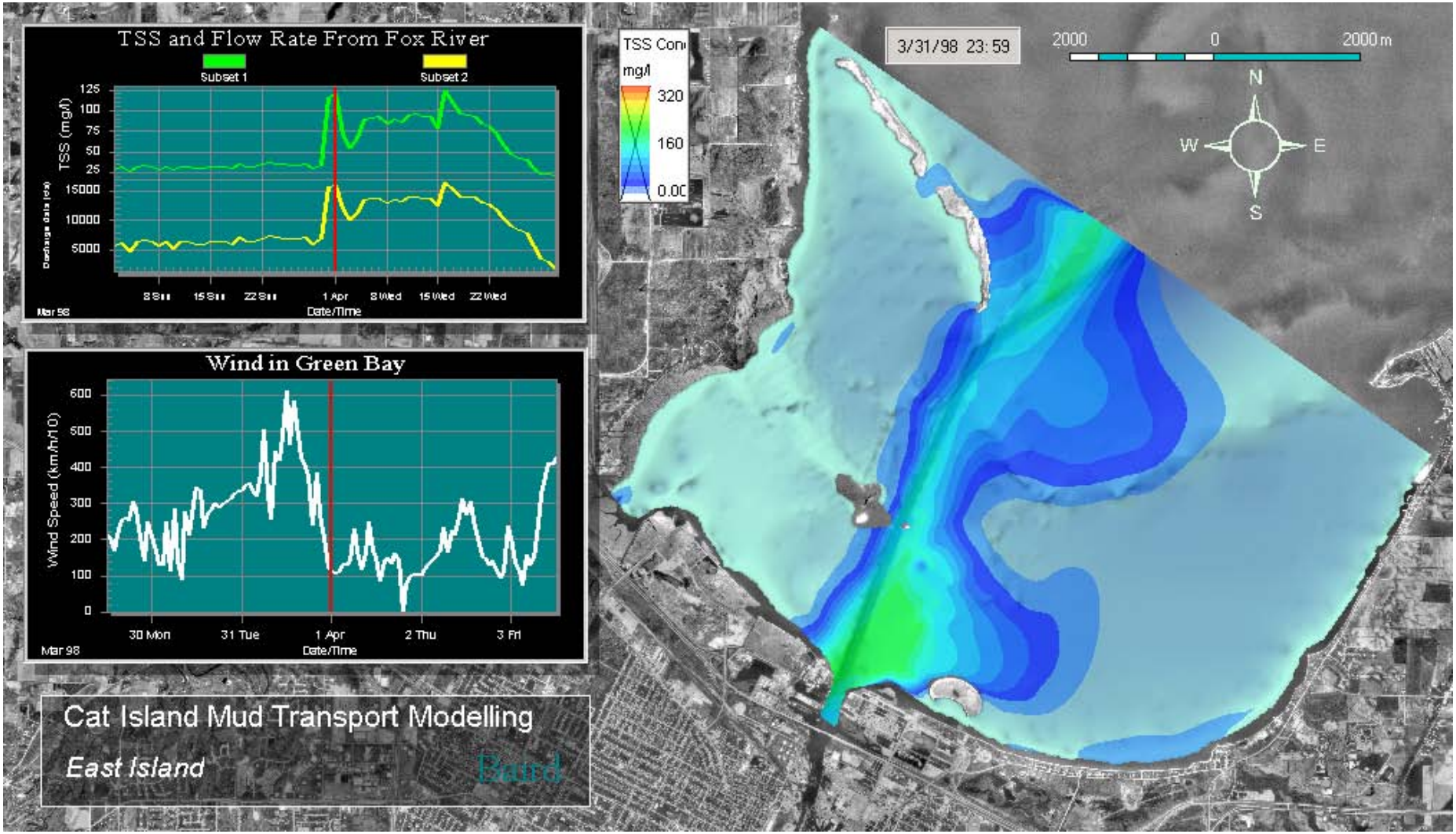

Figure A14 Mud Transport Modeling for Run 3 at Low Wind – East Island

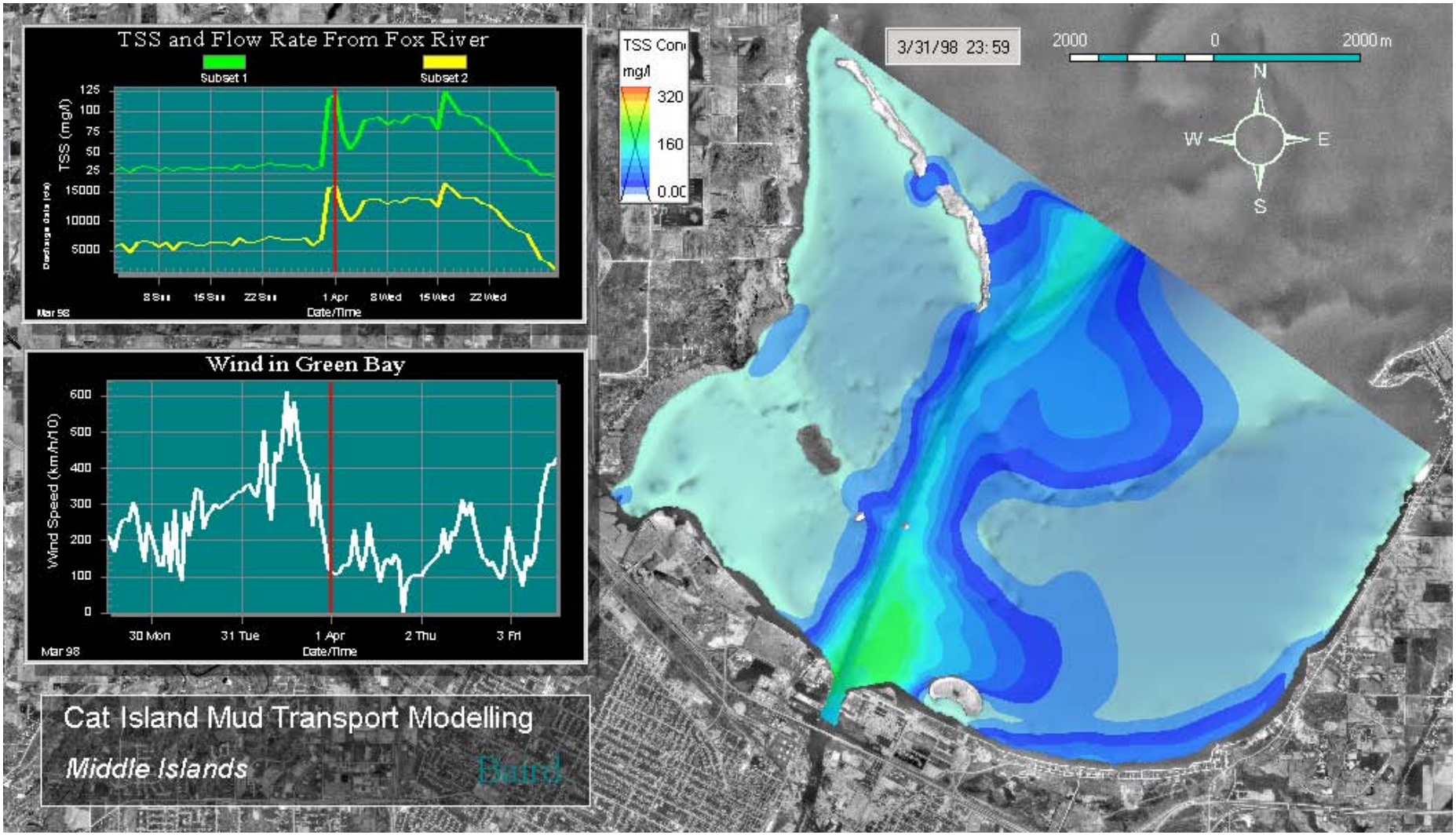

Figure A15 Mud Transport Modeling for Run 3 at Low Wind – Middle Island

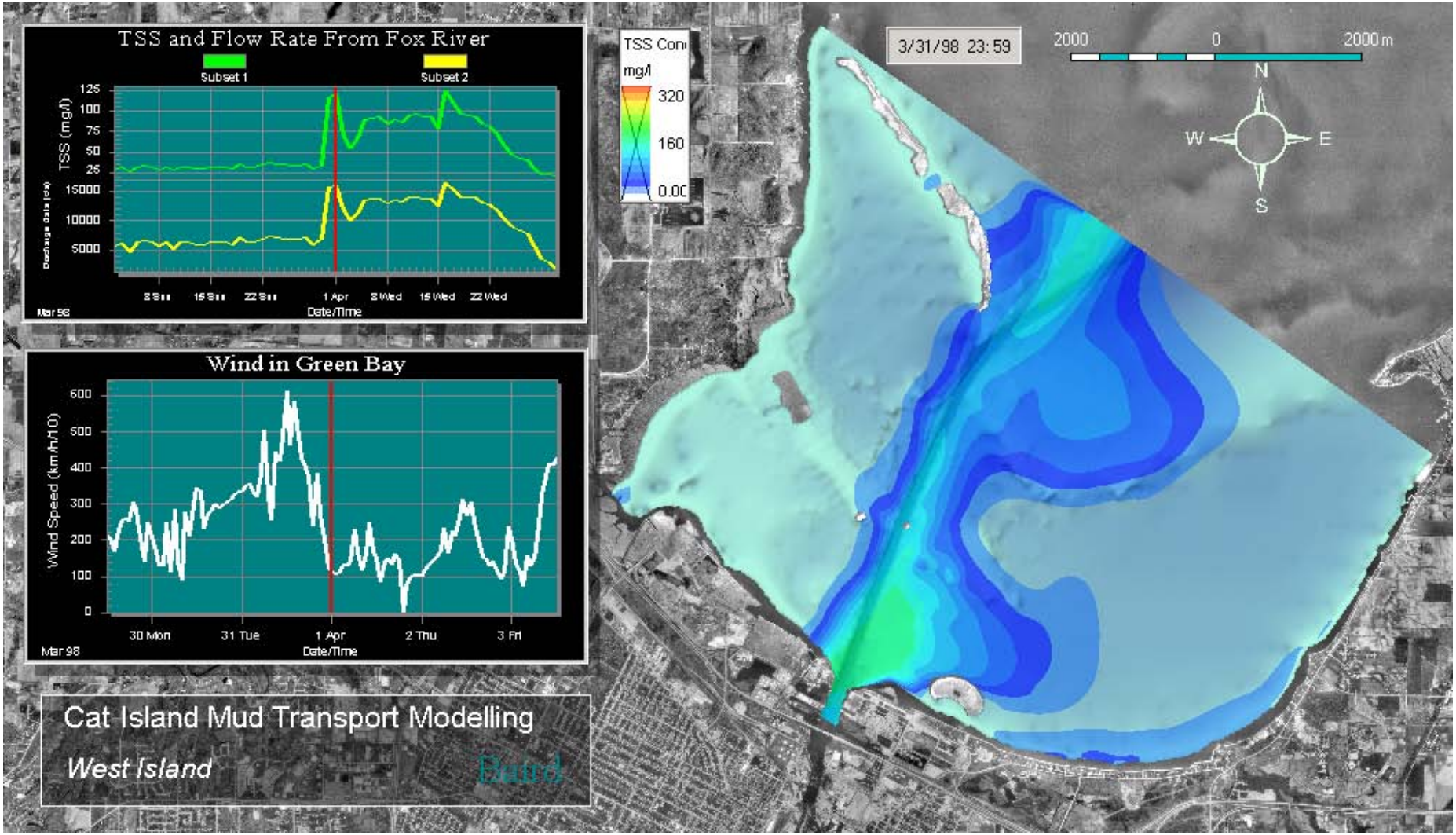

Figure A16 Mud Transport Modeling for Run 3 at Low Wind – West Island

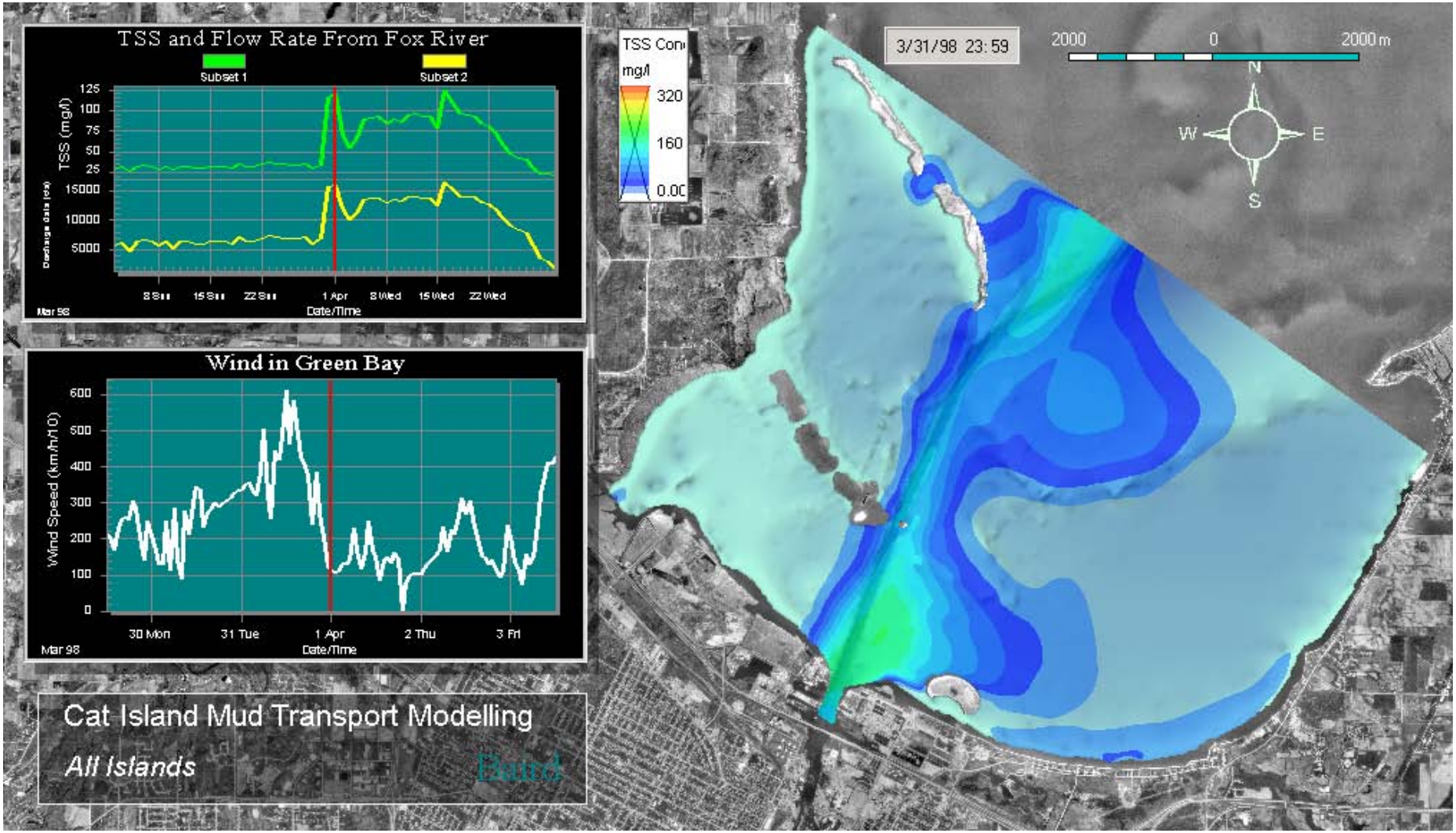

Figure A17 Mud Transport Modeling for Run 3 at Low Wind – All Island

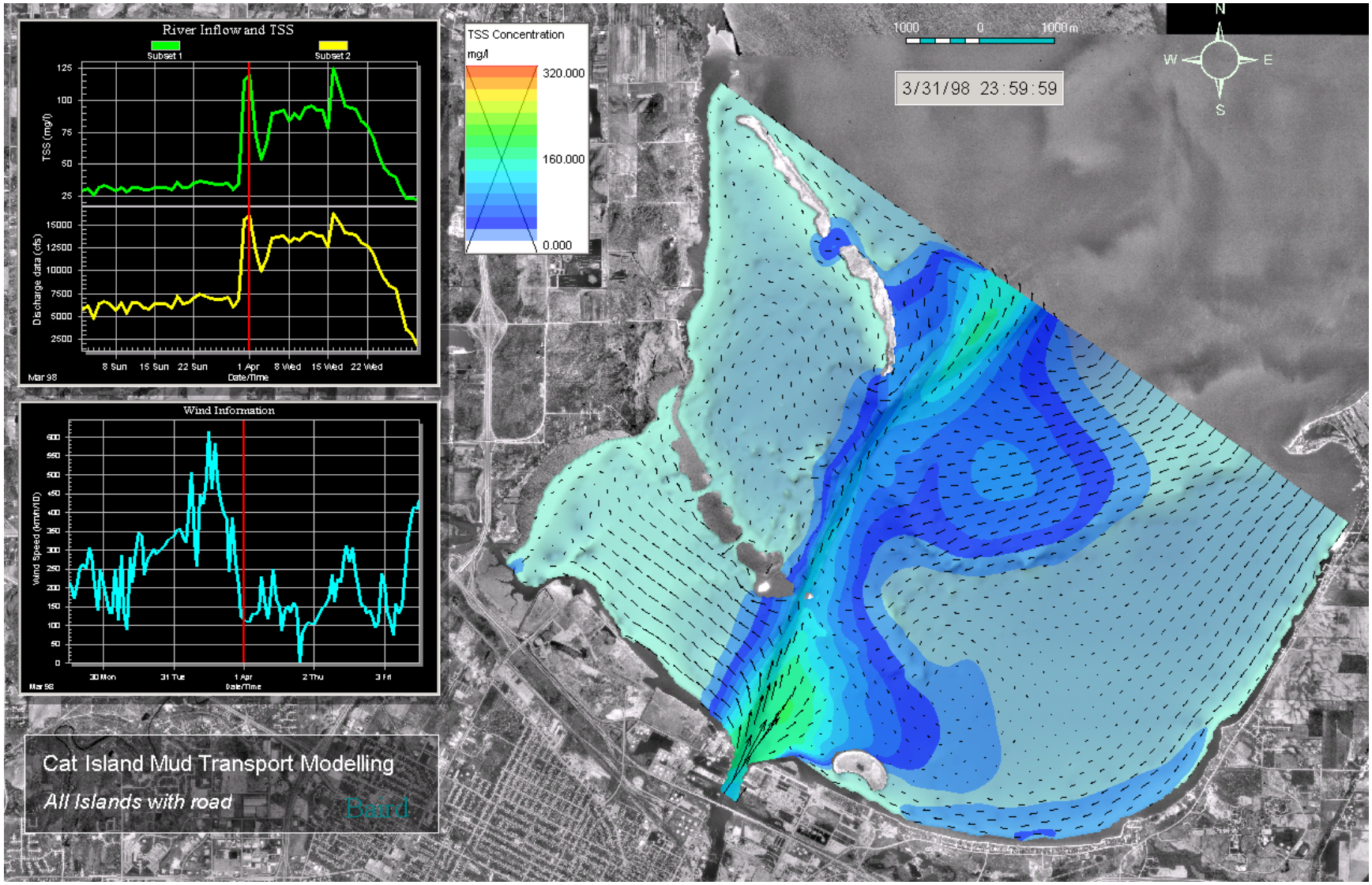

Figure A18 Mud Transport Modeling for Run 3 at Low Wind – All Island with Road

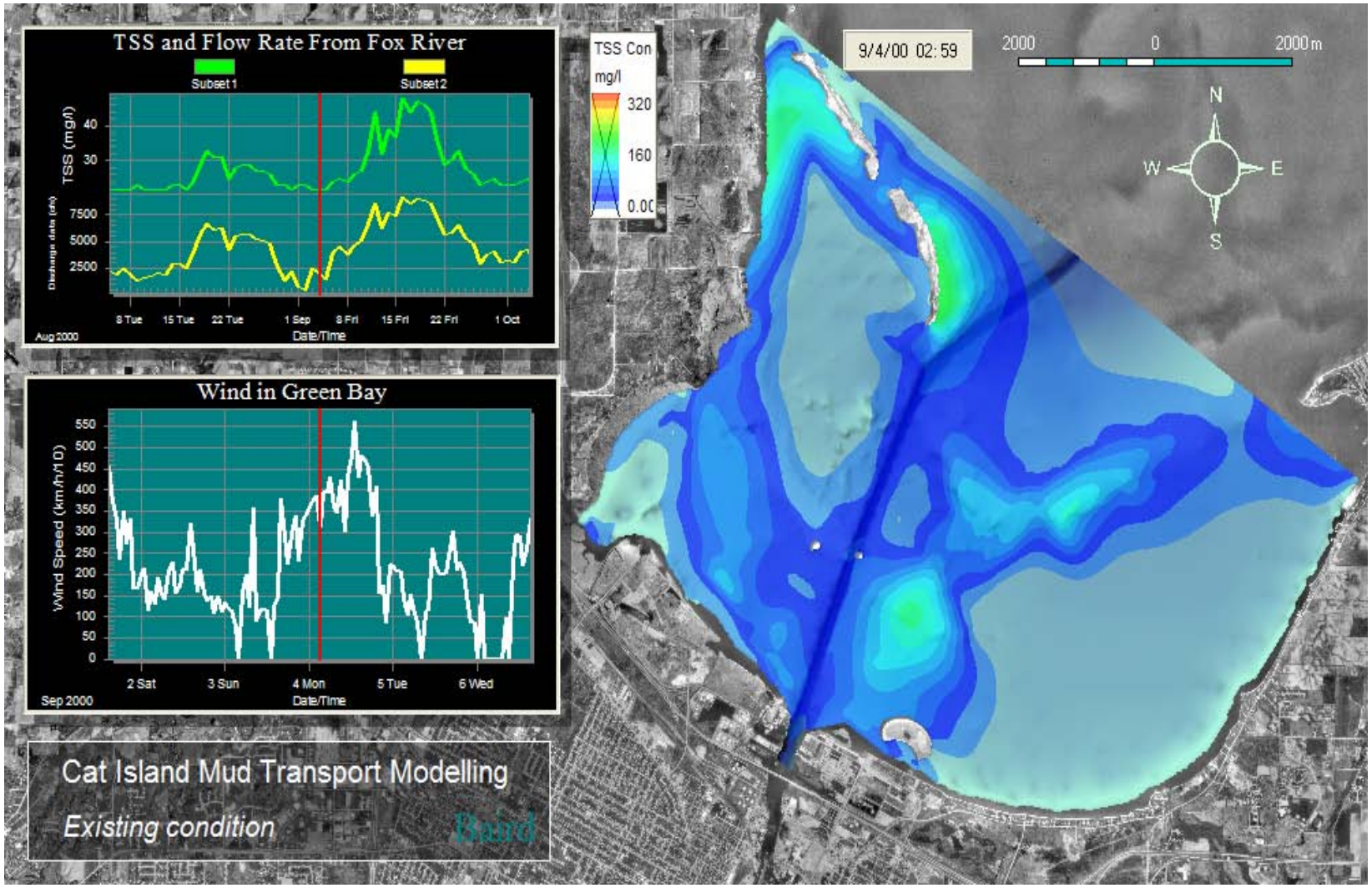

Figure A19 Mud Transport Modeling for Run 4 Storm Developing – Existing Condtion

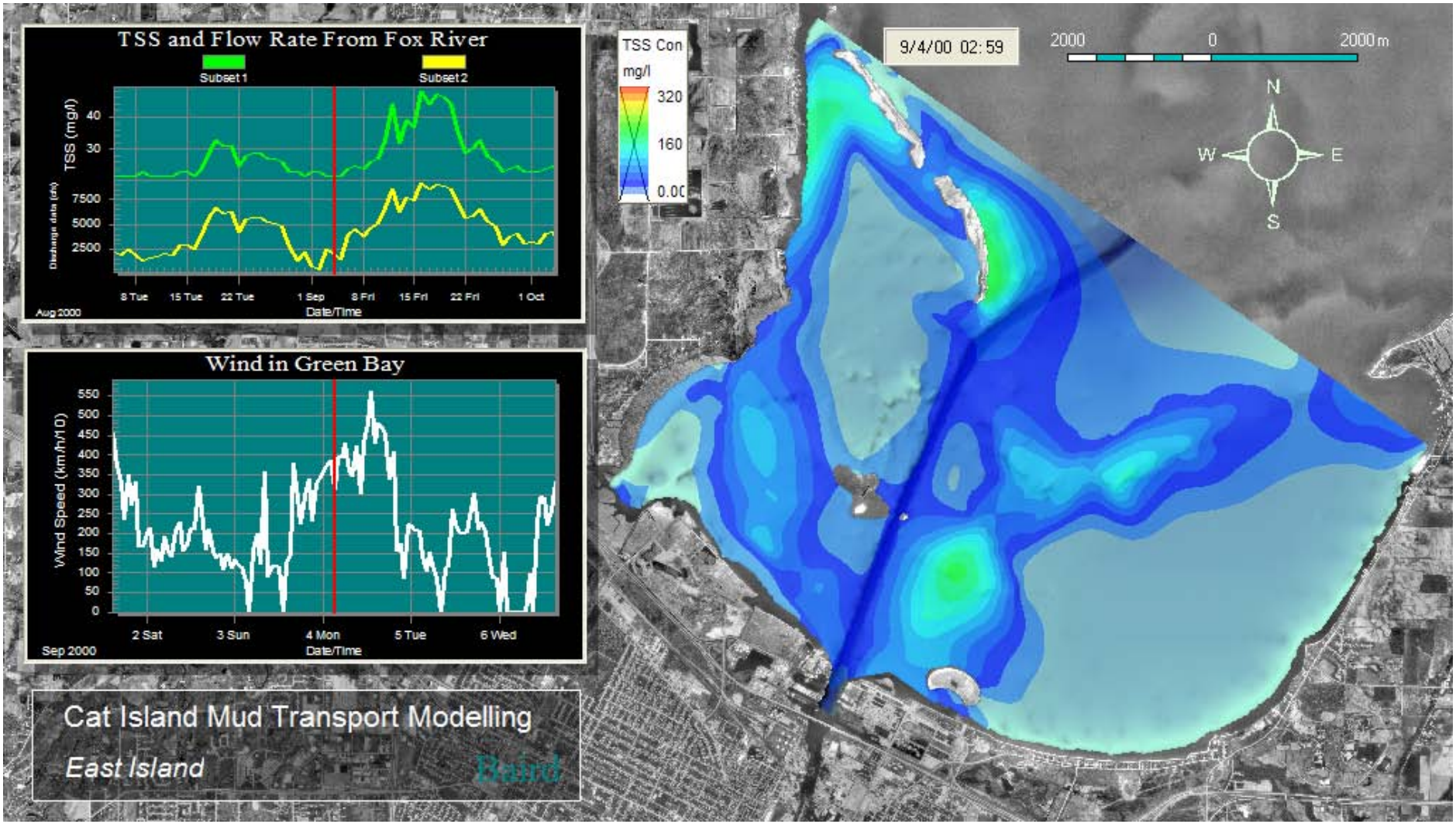

Figure A20 Mud Transport Modeling for Run 4 Storm Developing – East Island

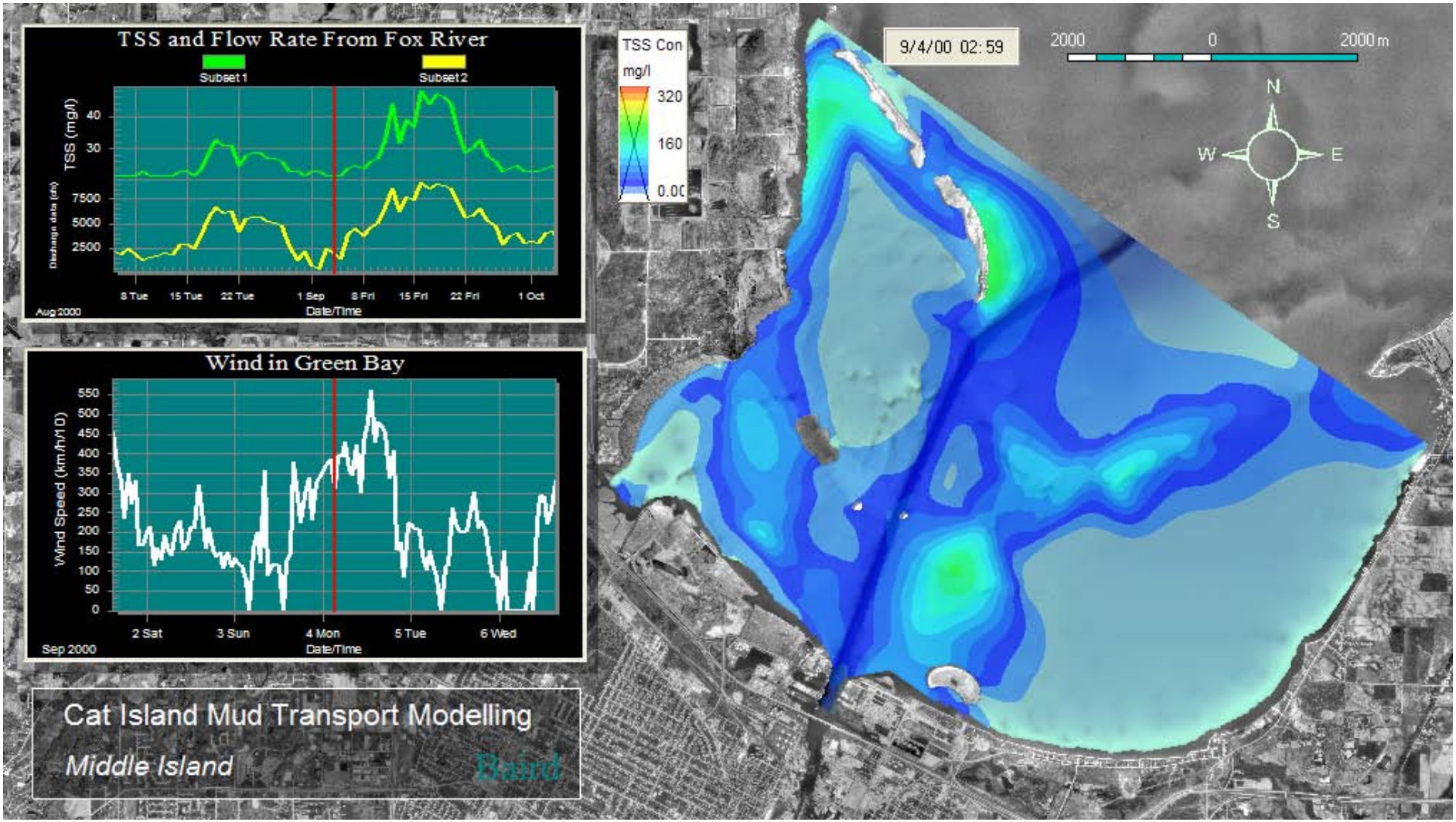

Figure A21 Mud Transport Modeling for Run 4 Storm Developing – Middle Island

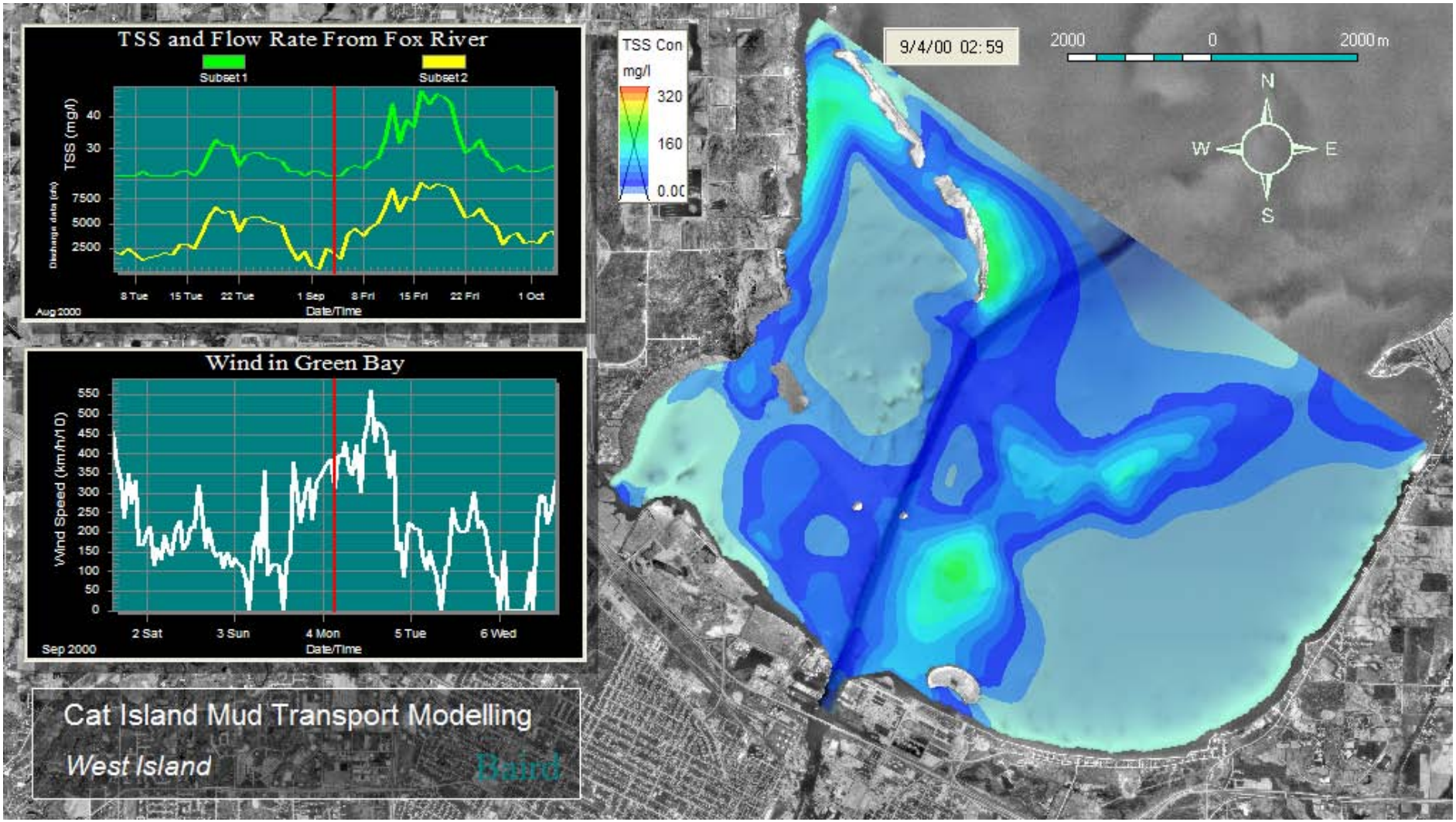

Figure A22 Mud Transport Modeling for Run 4 Storm Developing – West Island

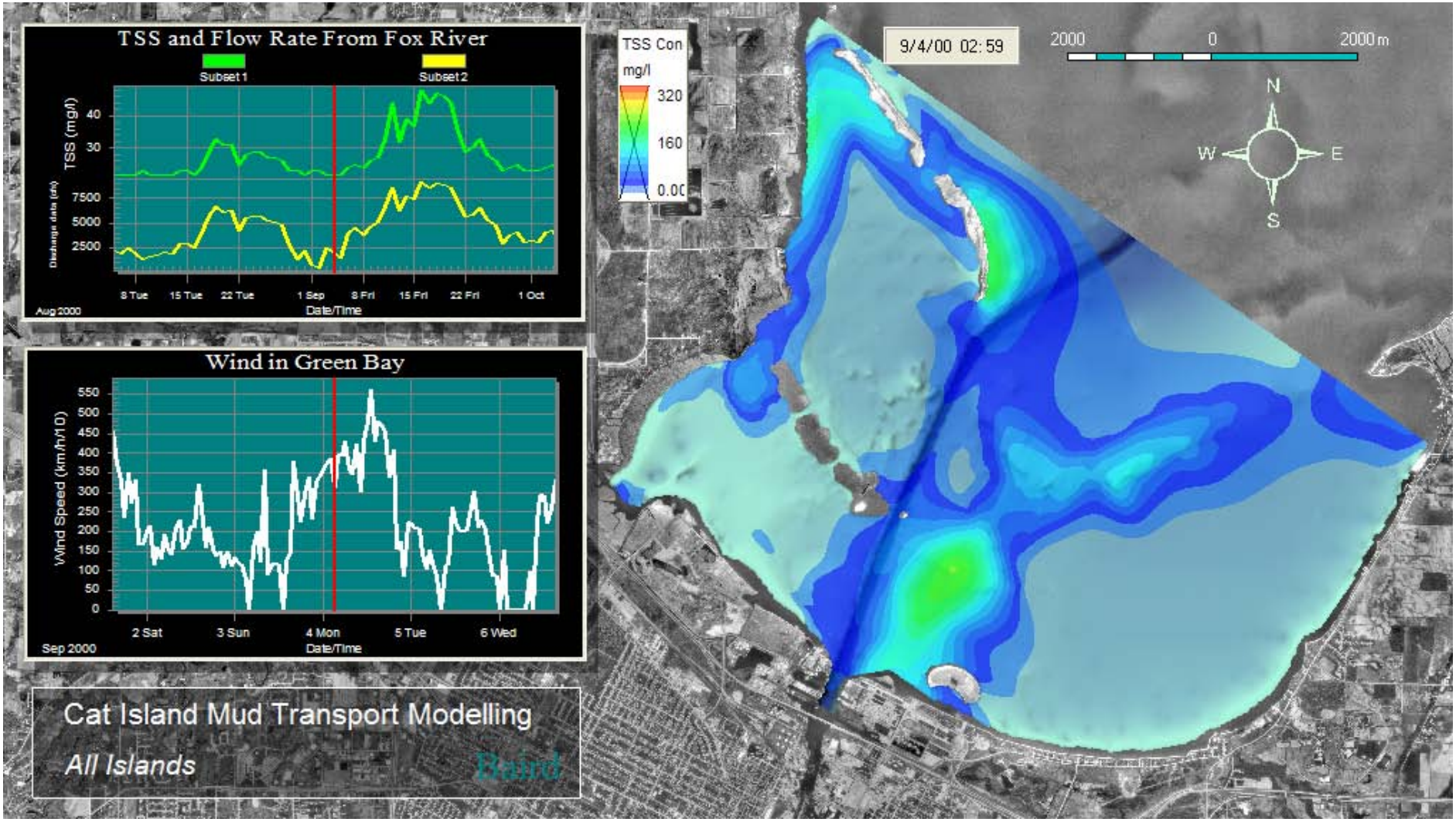

Figure A23 Mud Transport Modeling for Run 4 Storm Developing – All Island

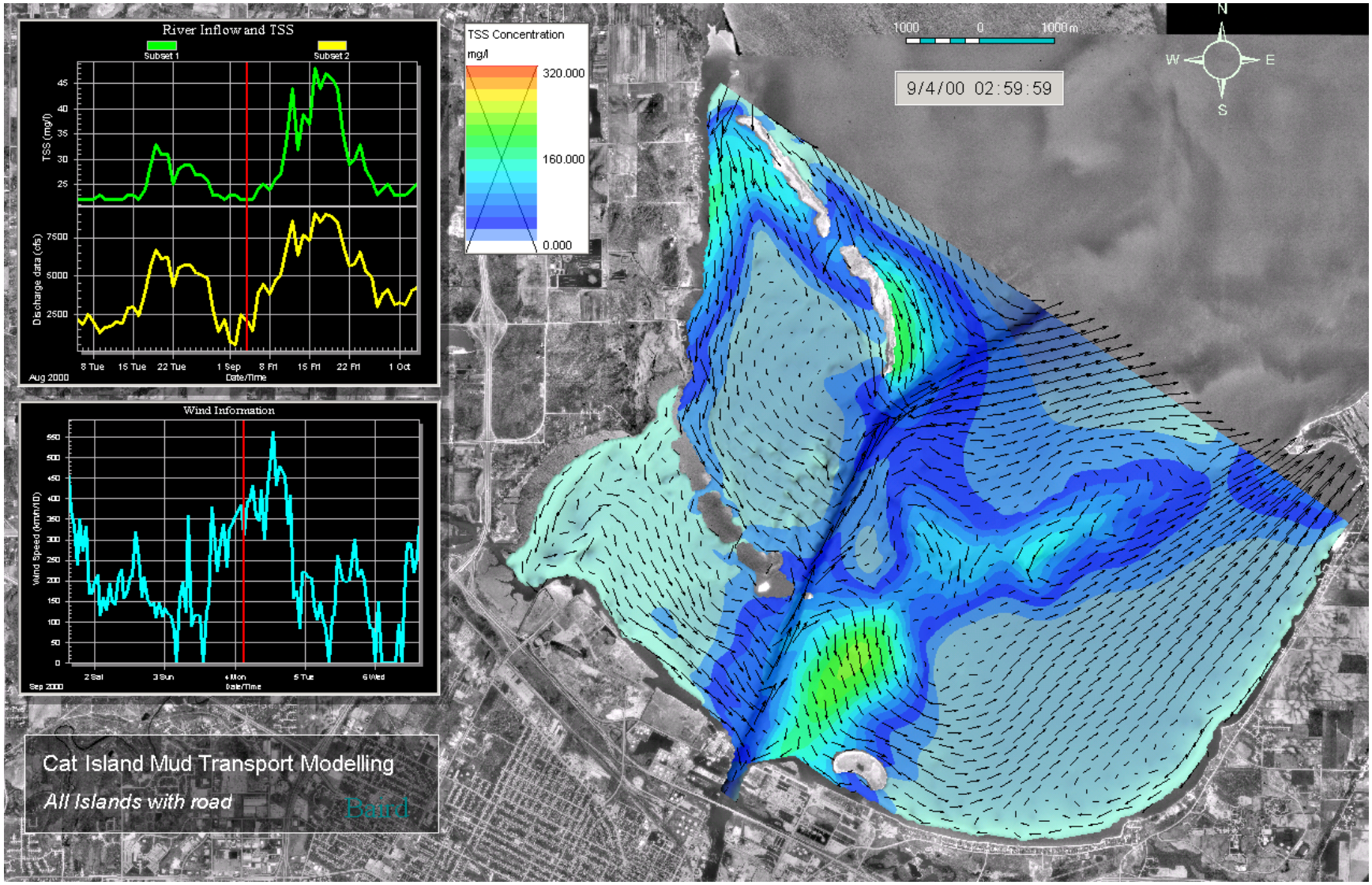

Figure A24 Mud Transport Modeling for Run 4 Storm Developing – All Island with Road

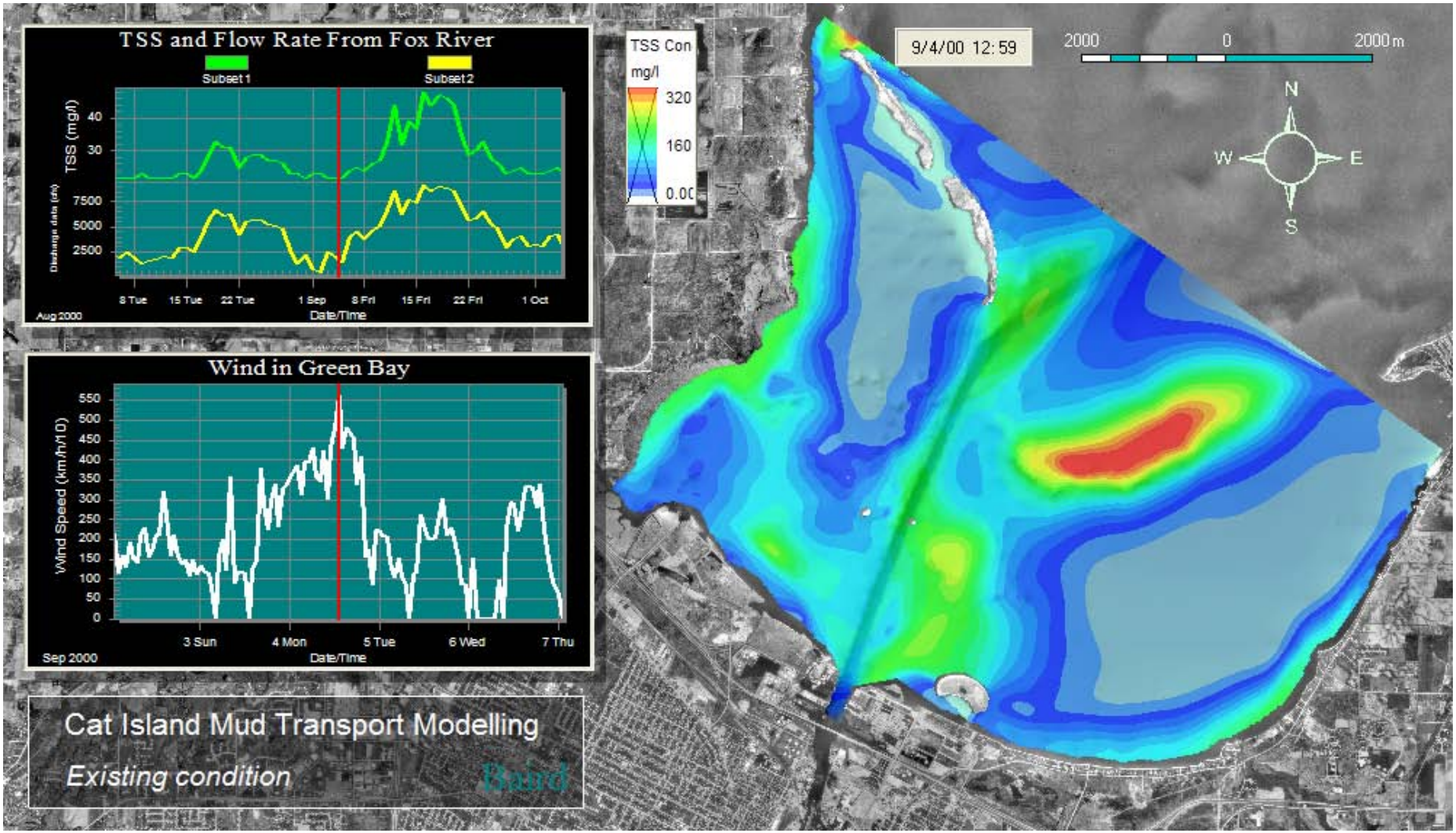

Figure A25 Mud Transport Modeling for Run 4 at Wind Peak – Existing Condition

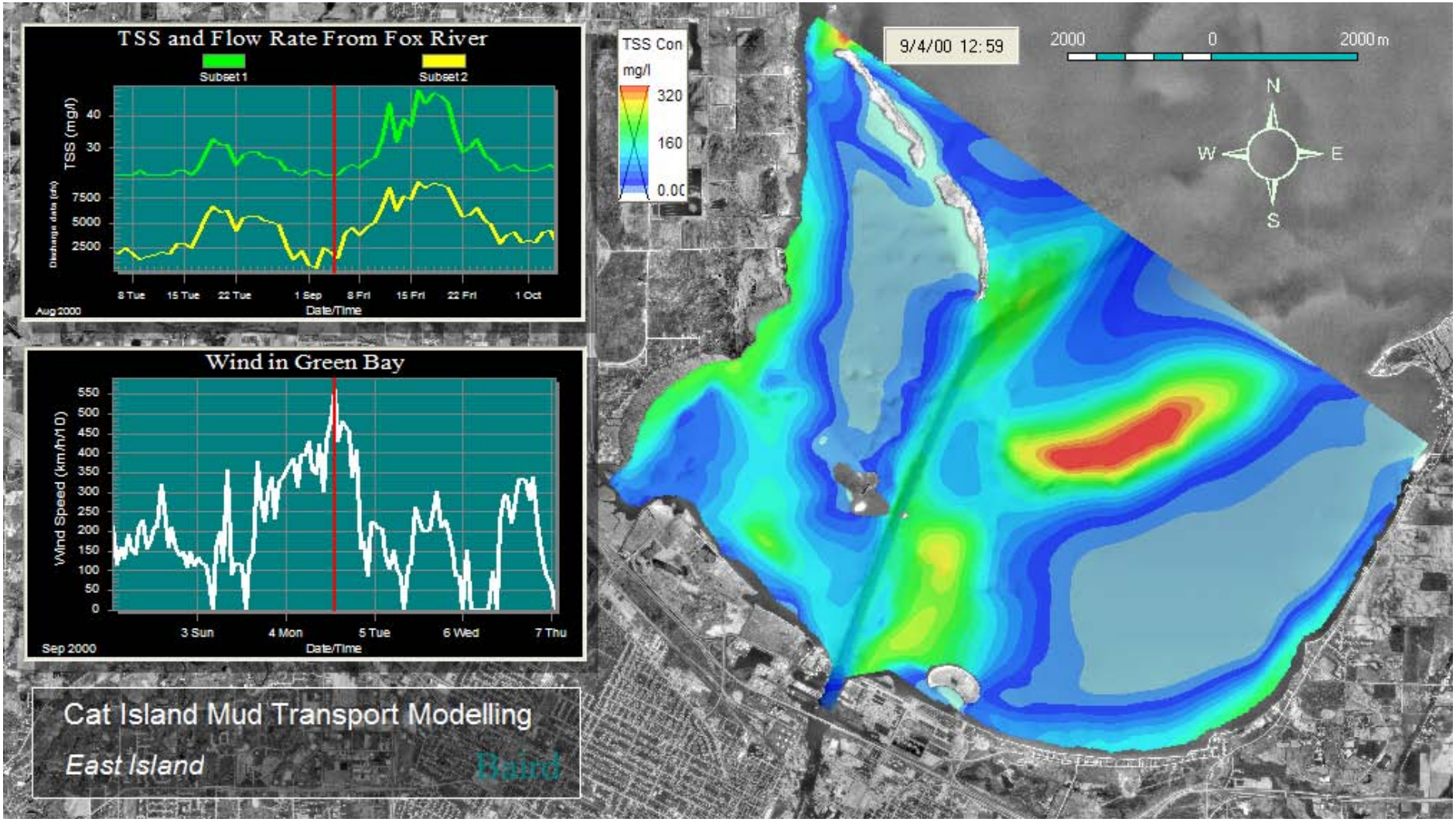

Figure A26 Mud Transport Modeling for Run 4 at Wind Peak – East Island

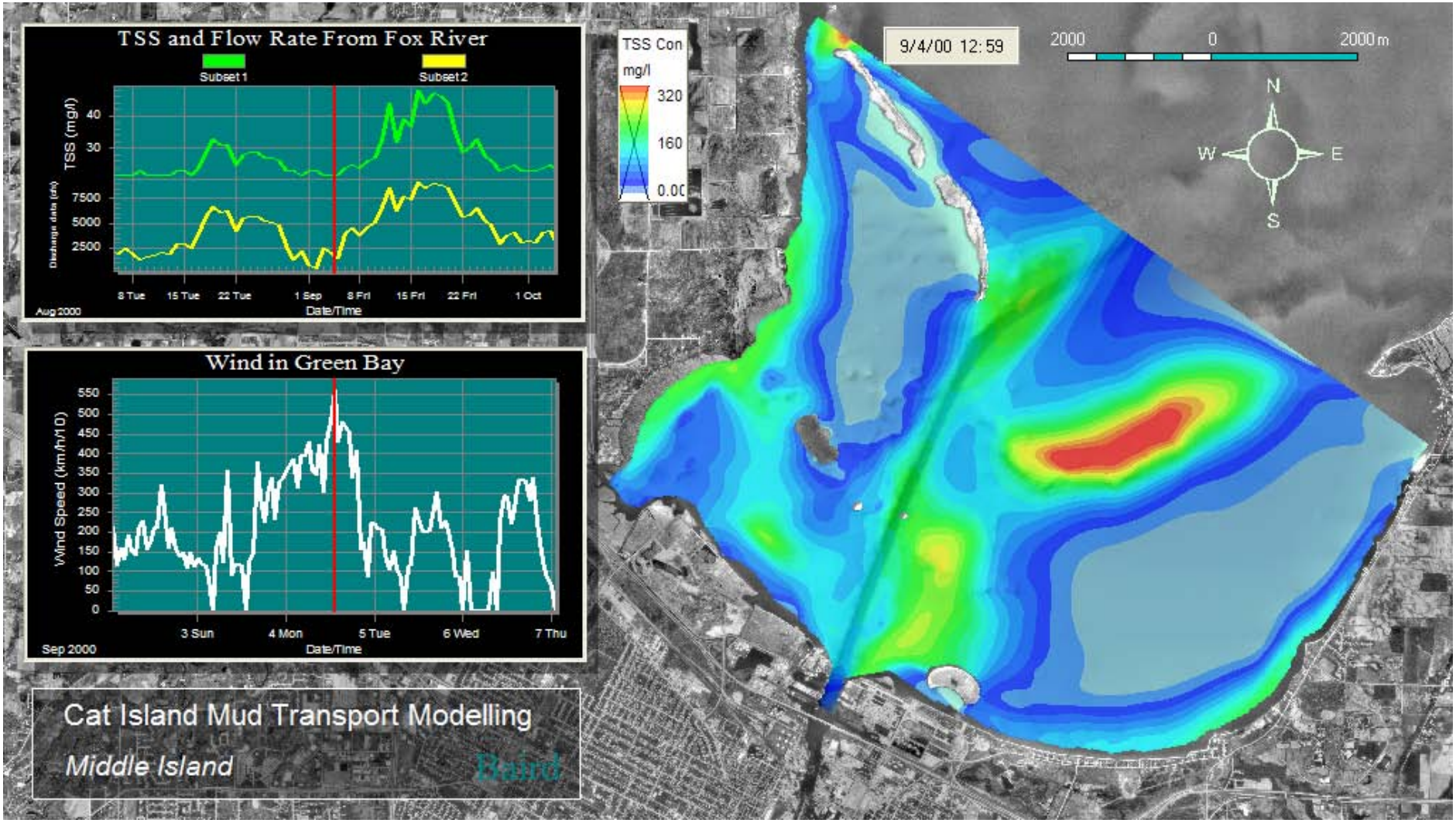

Figure A27 Mud Transport Modeling for Run 4 at Wind Peak – Middle Island

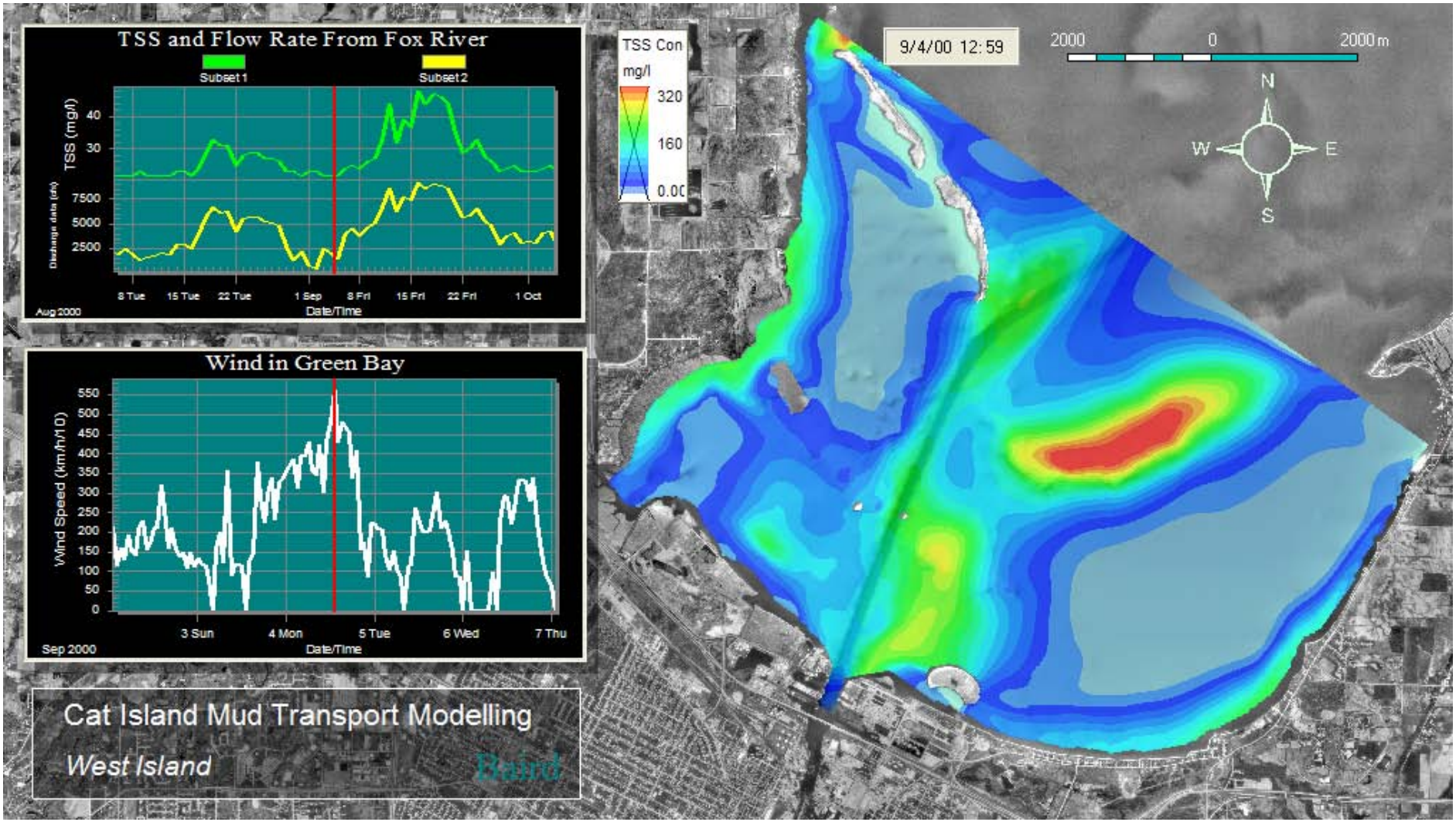

Figure A28 Mud Transport Modeling for Run 4 at Wind Peak – West Island

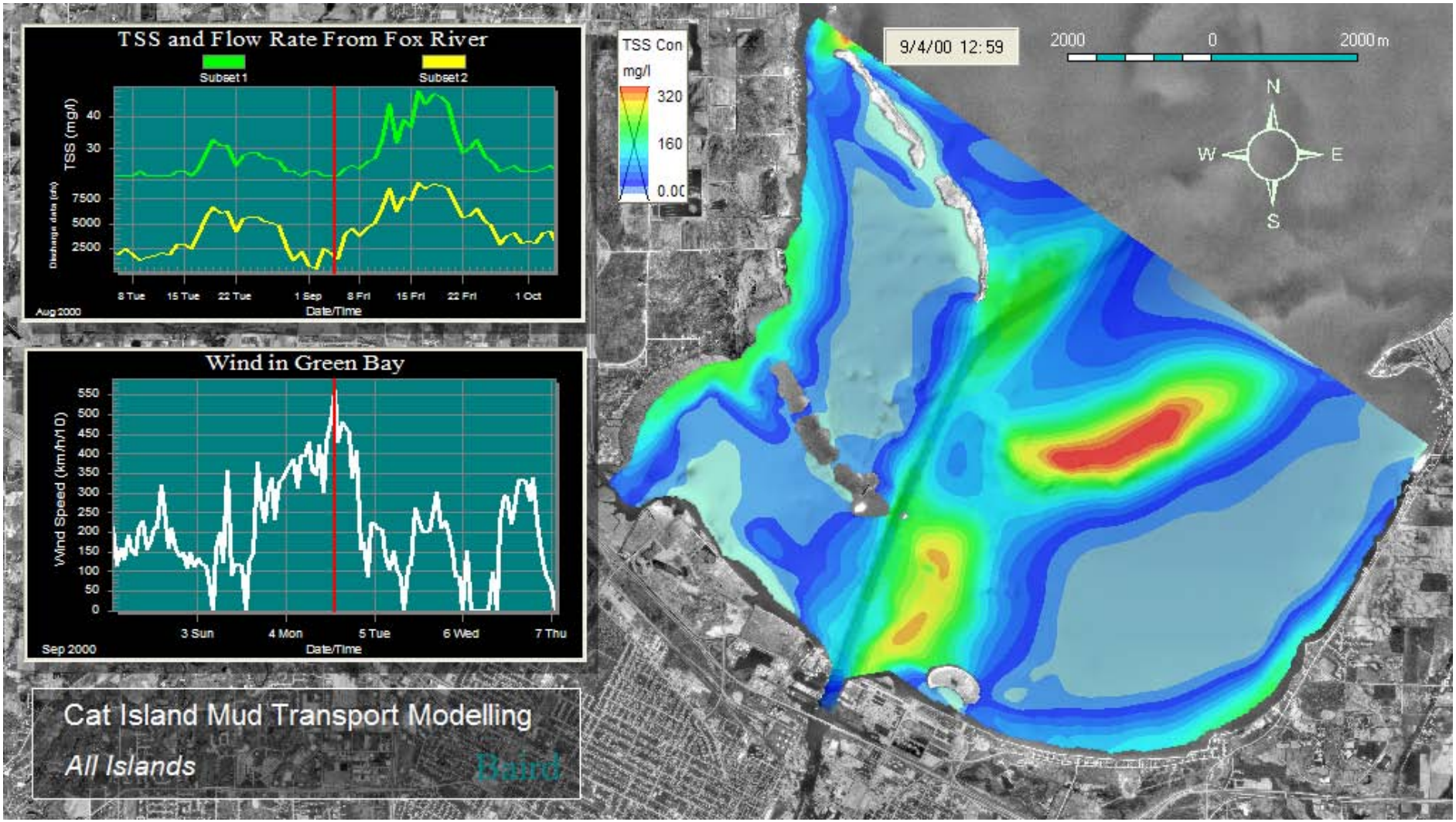

Figure A29 Mud Transport Modeling for Run 4 at Wind Peak – All Island

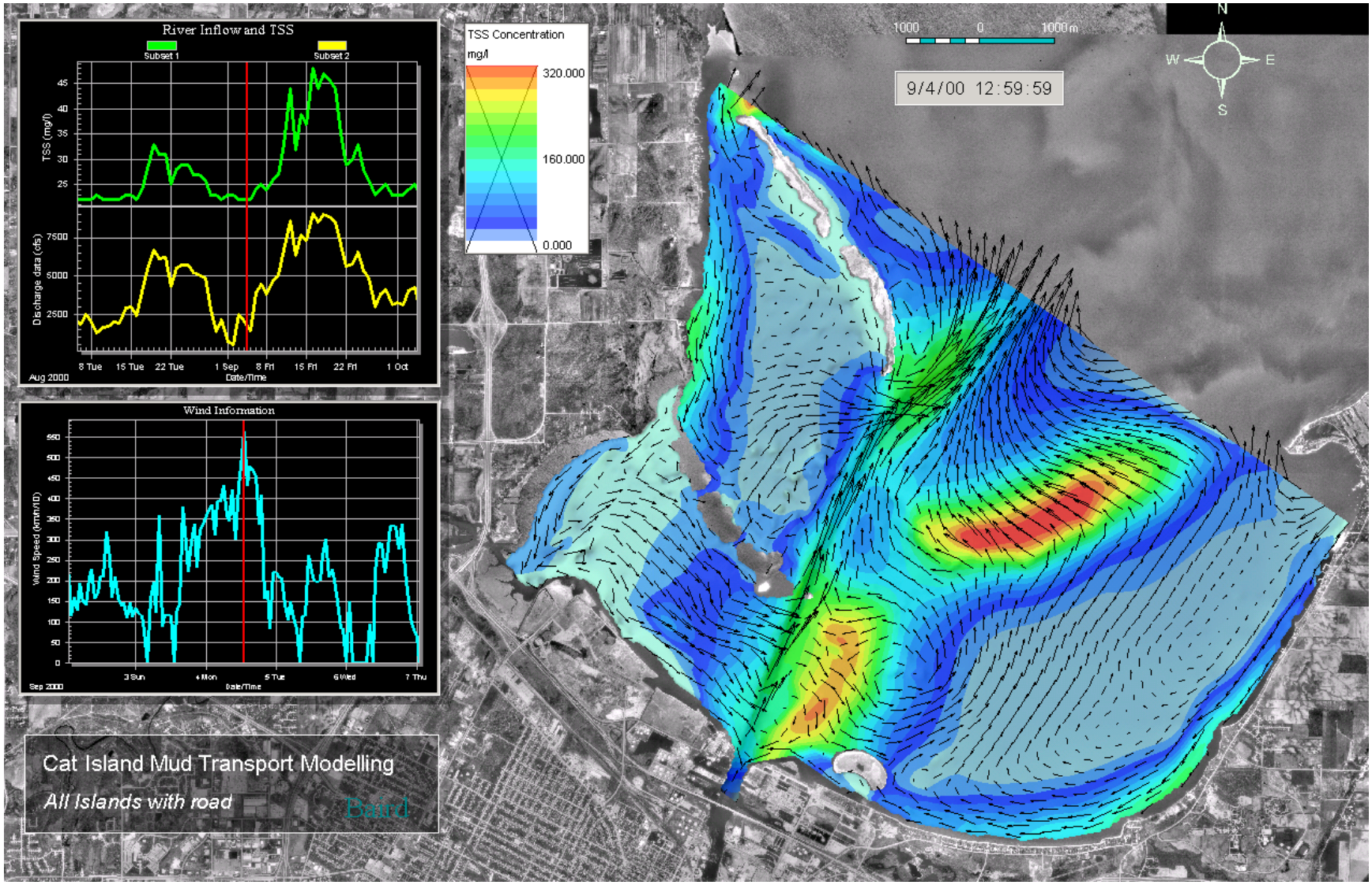

Figure A30 Mud Transport Modeling for Run 4 at Wind Peak – All Island with Road

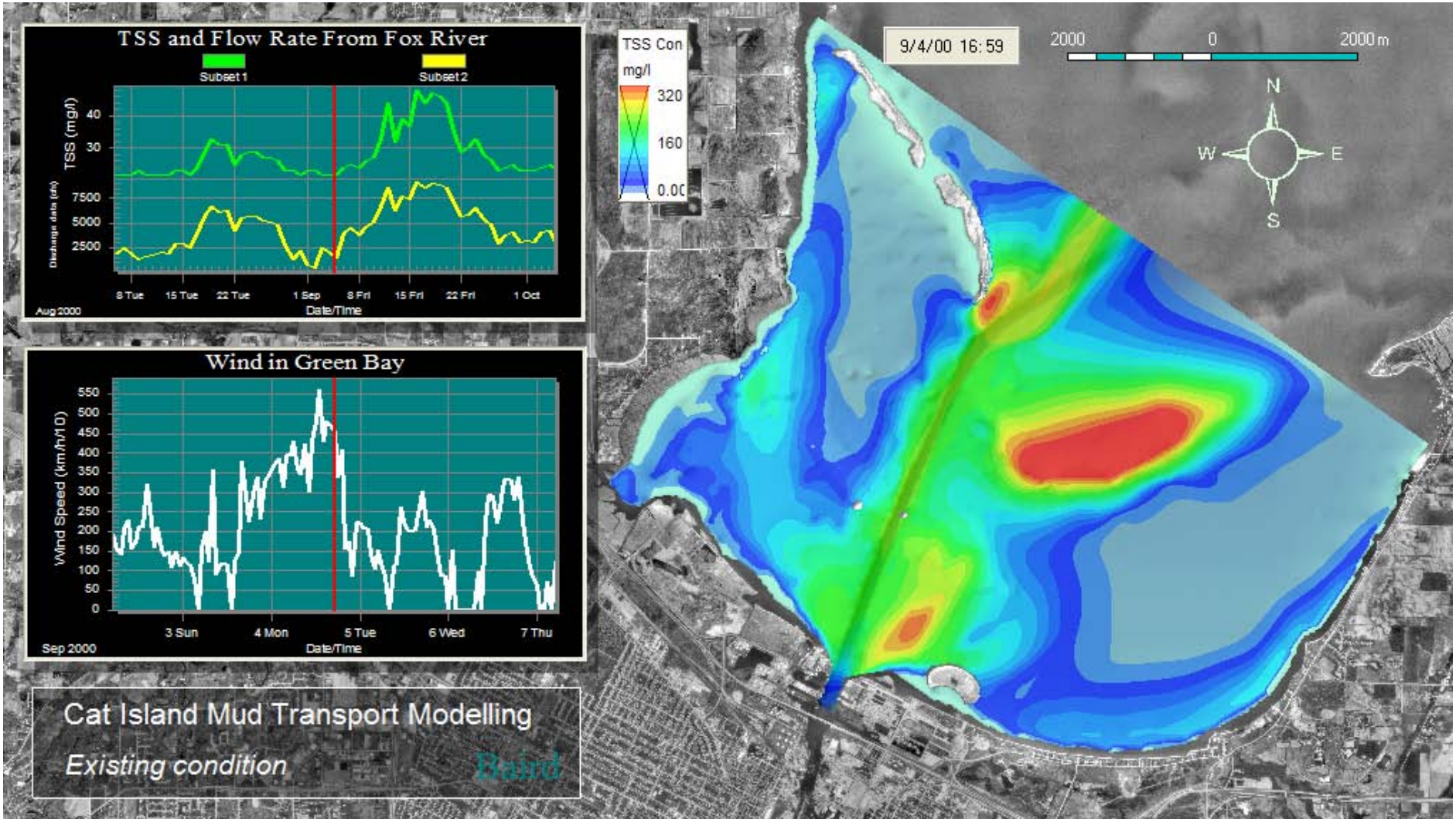

Figure A31 Mud Transport Modeling for Run 4 at TSS Peak – Existing Condition

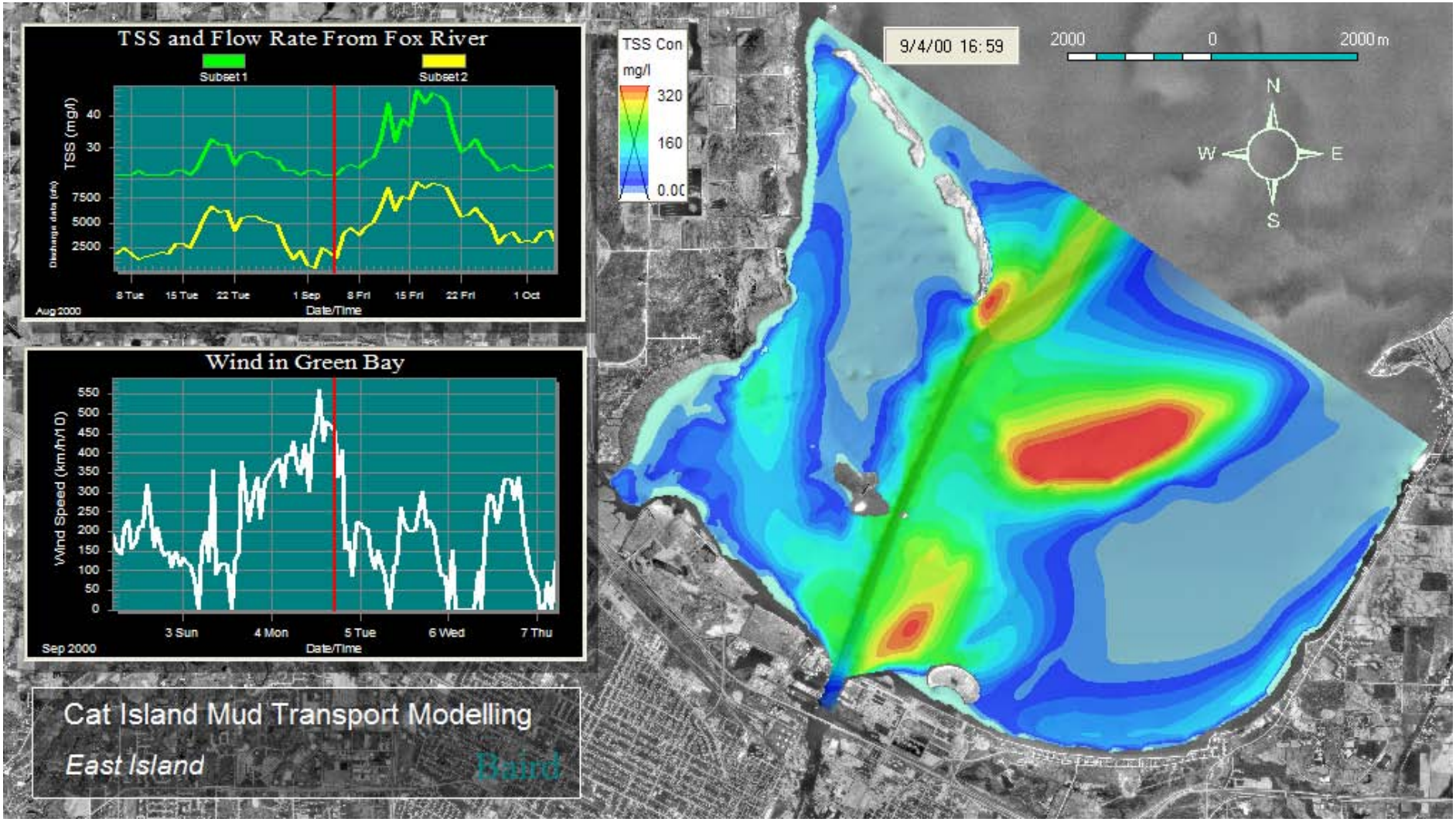

Figure A32 Mud Transport Modeling for Run 4 at TSS Peak – East Island

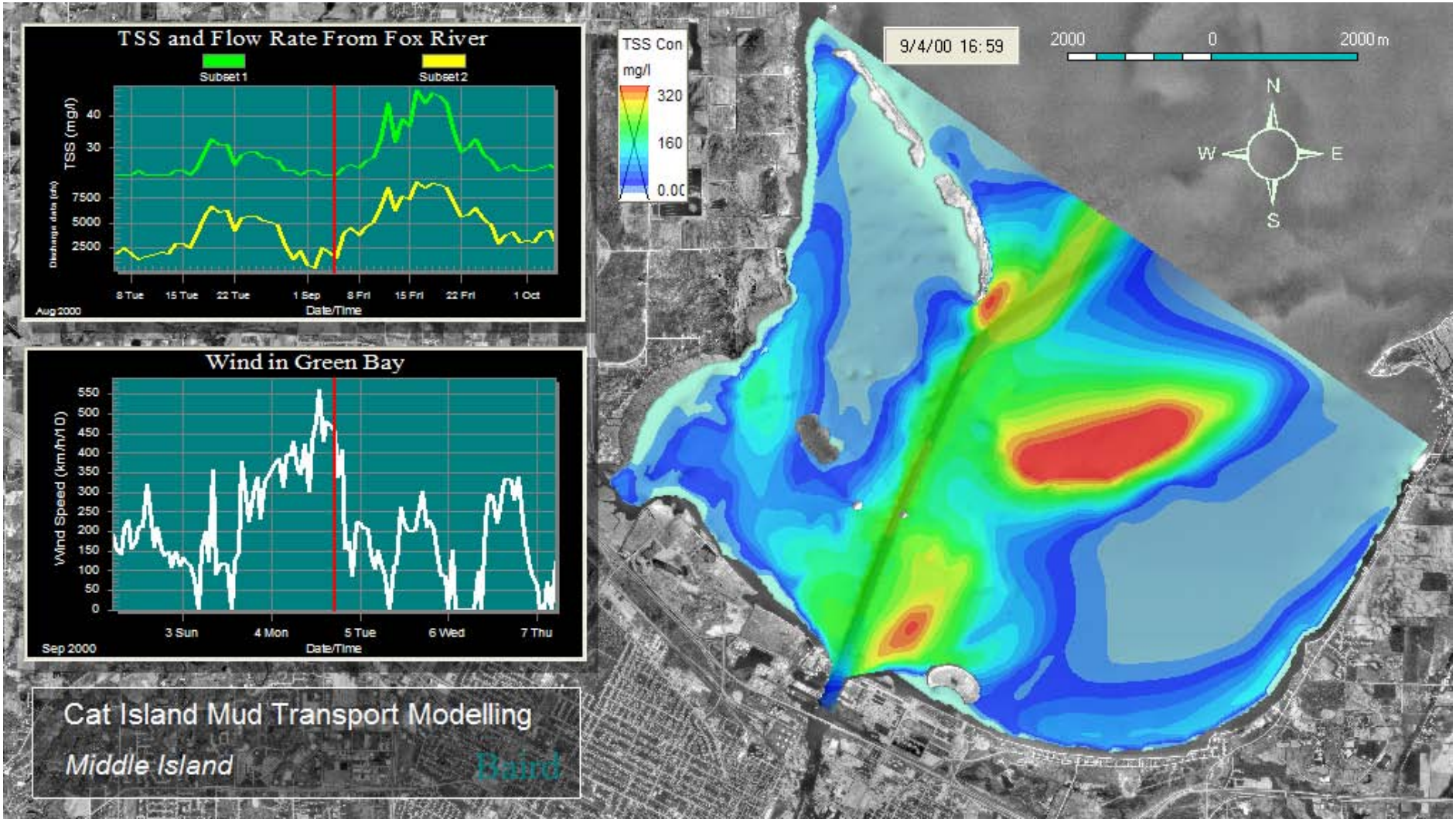

Figure A33 Mud Transport Modeling for Run 4 at TSS Peak - Middle Island

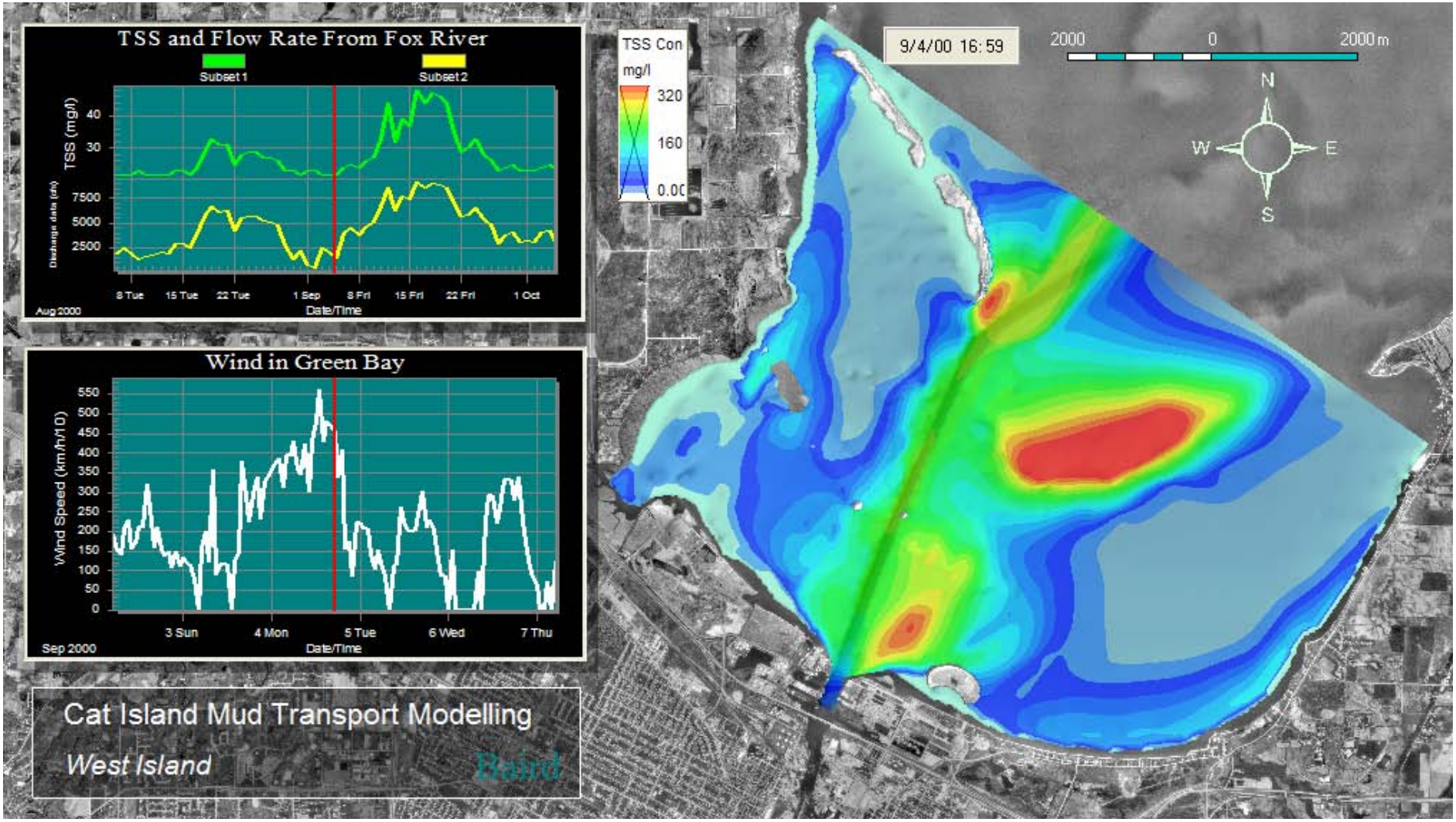

Figure A34 Mud Transport Modeling for Run 4 at TSS Peak - West Island

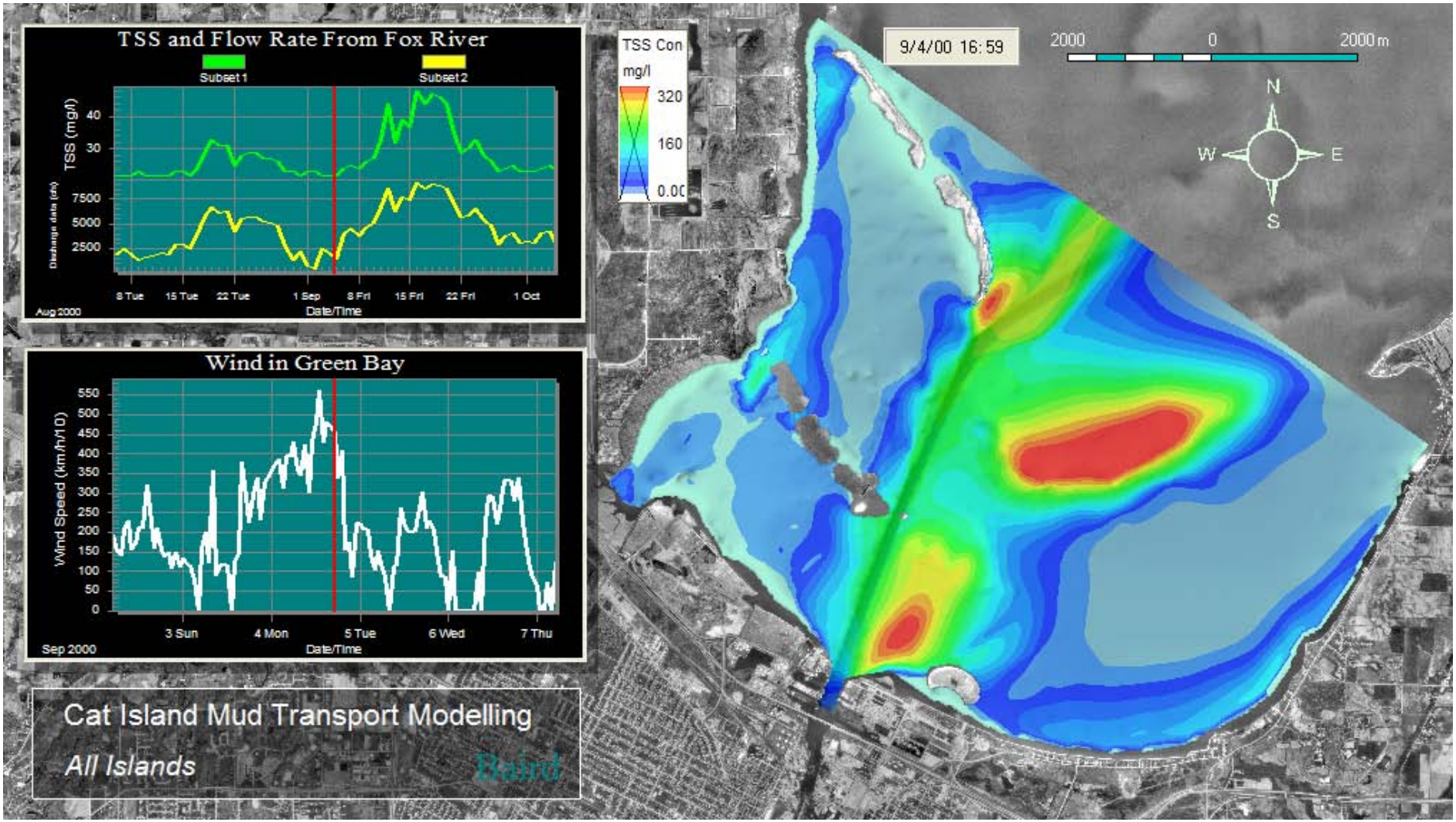

Figure A35 Mud Transport Modeling for Run 4 at TSS Peak - All Island

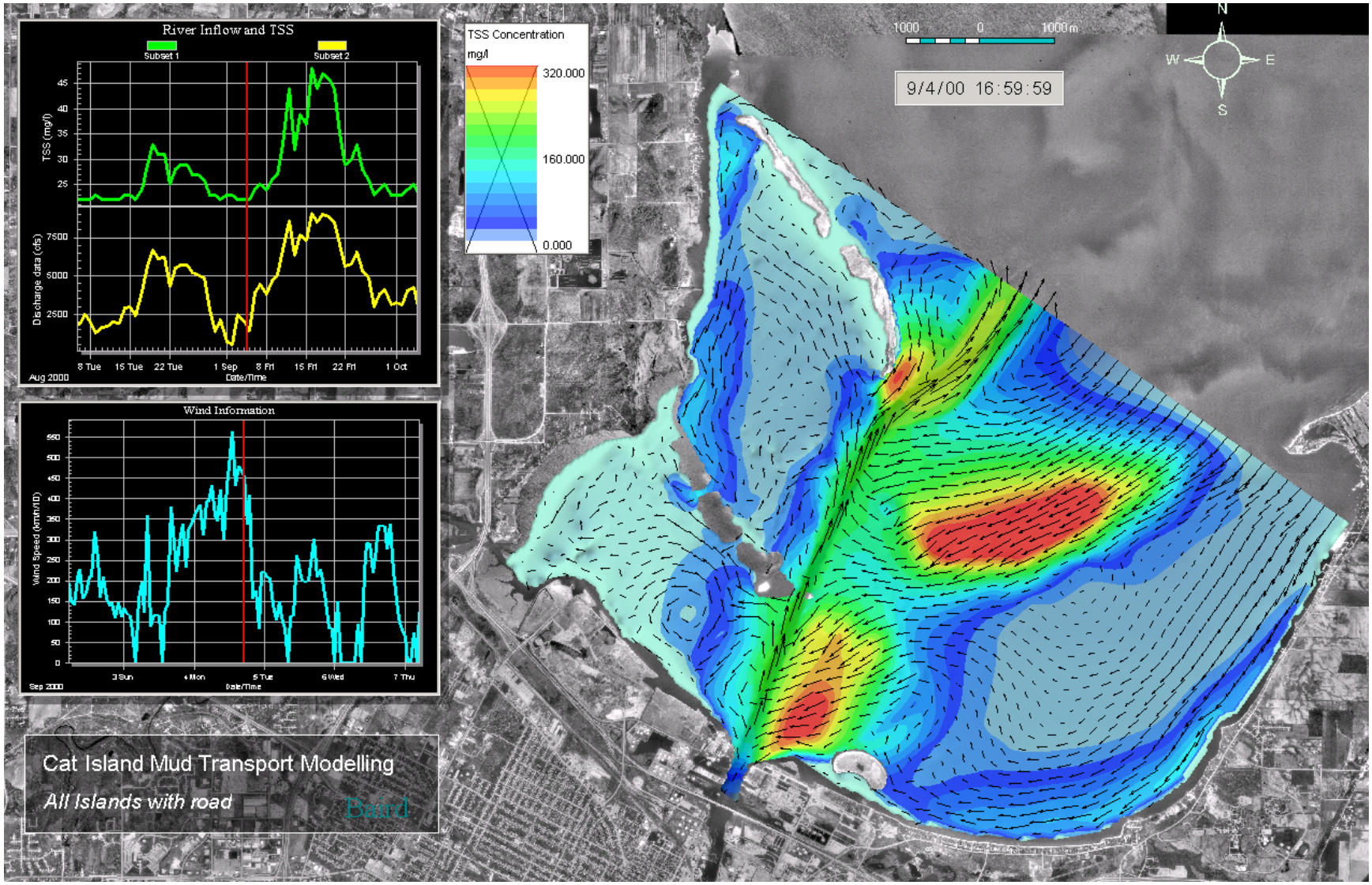

Figure A36 Mud Transport Modeling for Run 4 at TSS Peak - All Island with Road

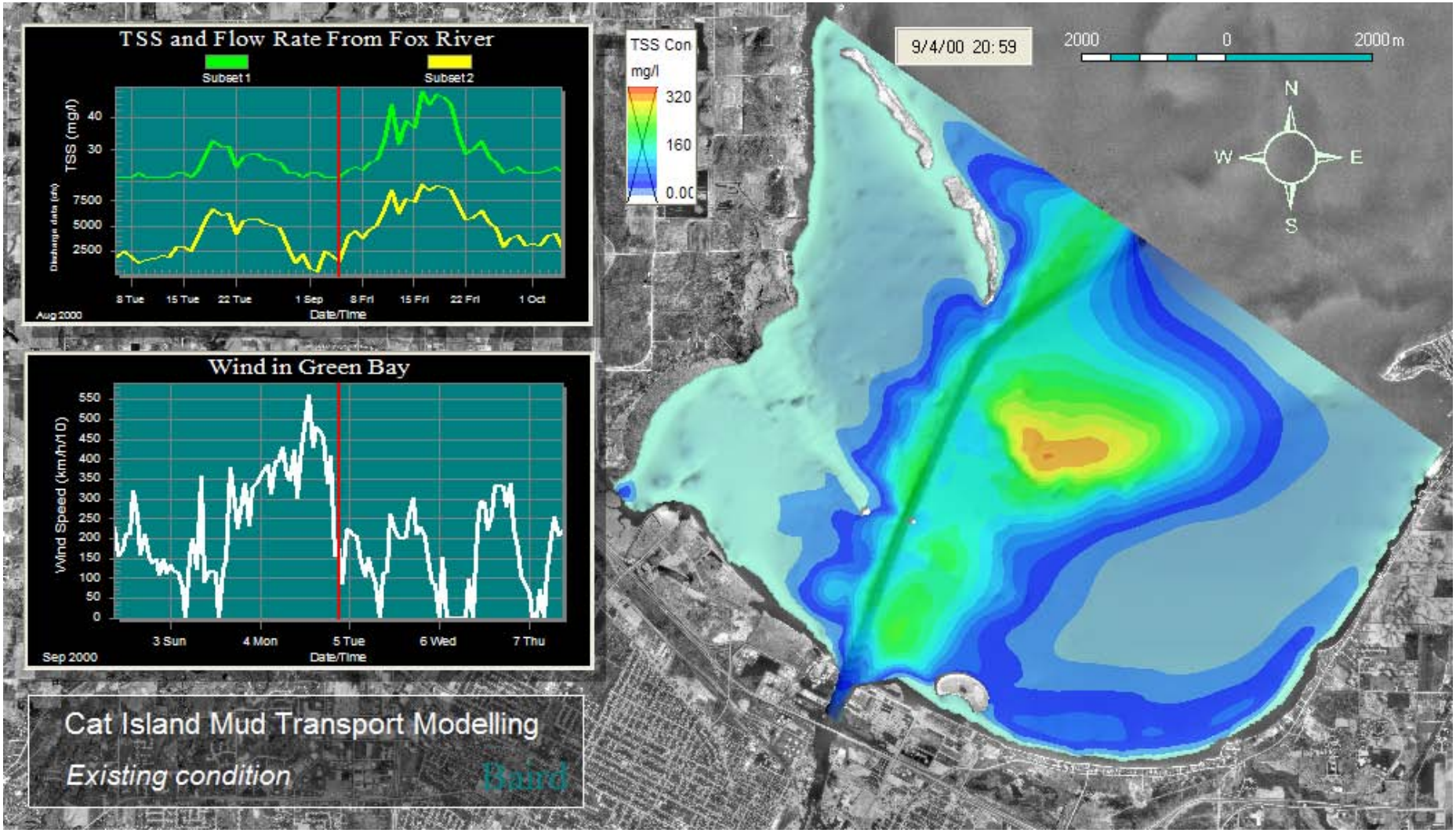

Figure A37 Mud Transport Modeling for Run 4 after Storm – Existing Condtion

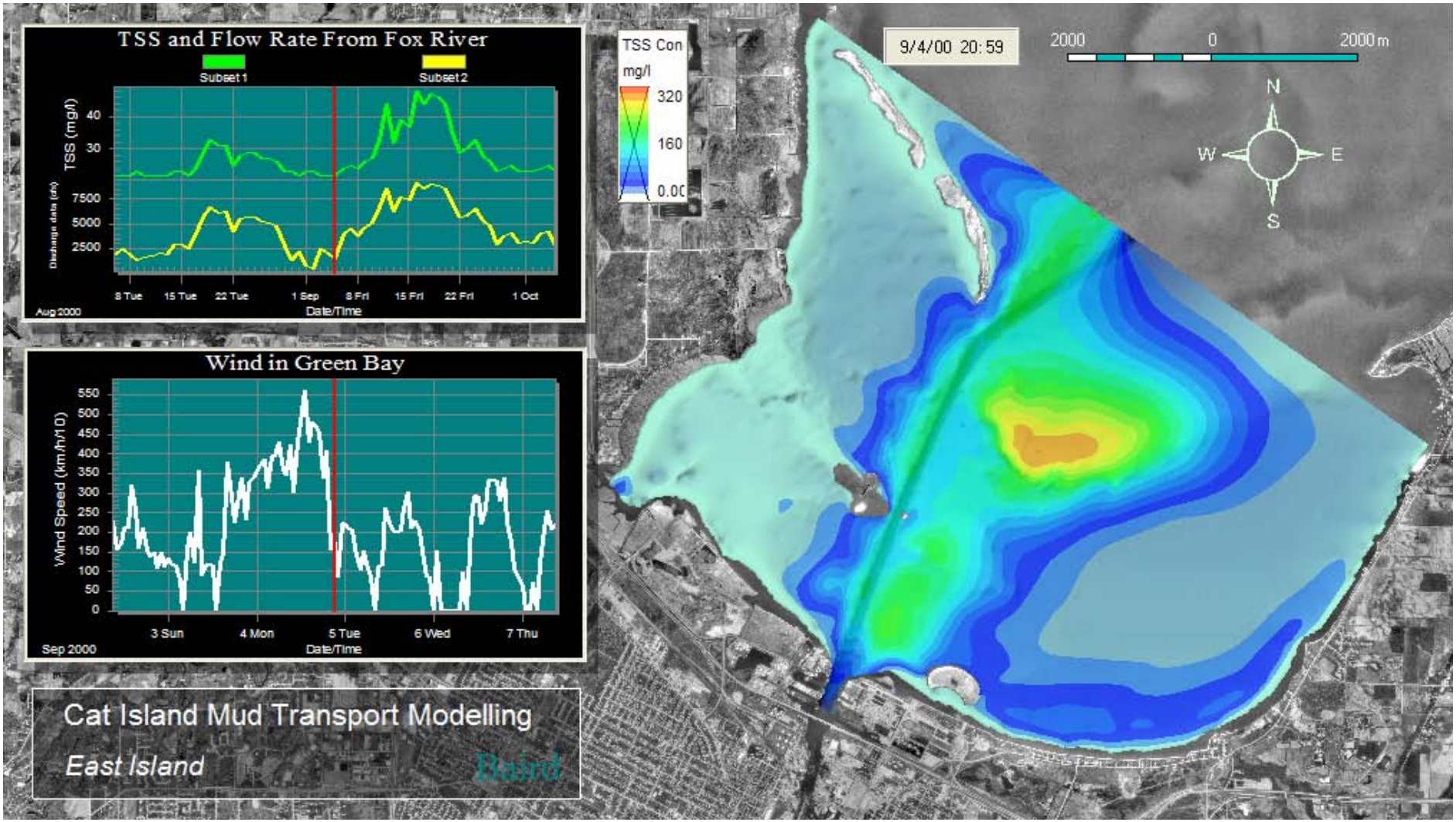

Figure A38 Mud Transport Modeling for Run 4 after Storm – East Island

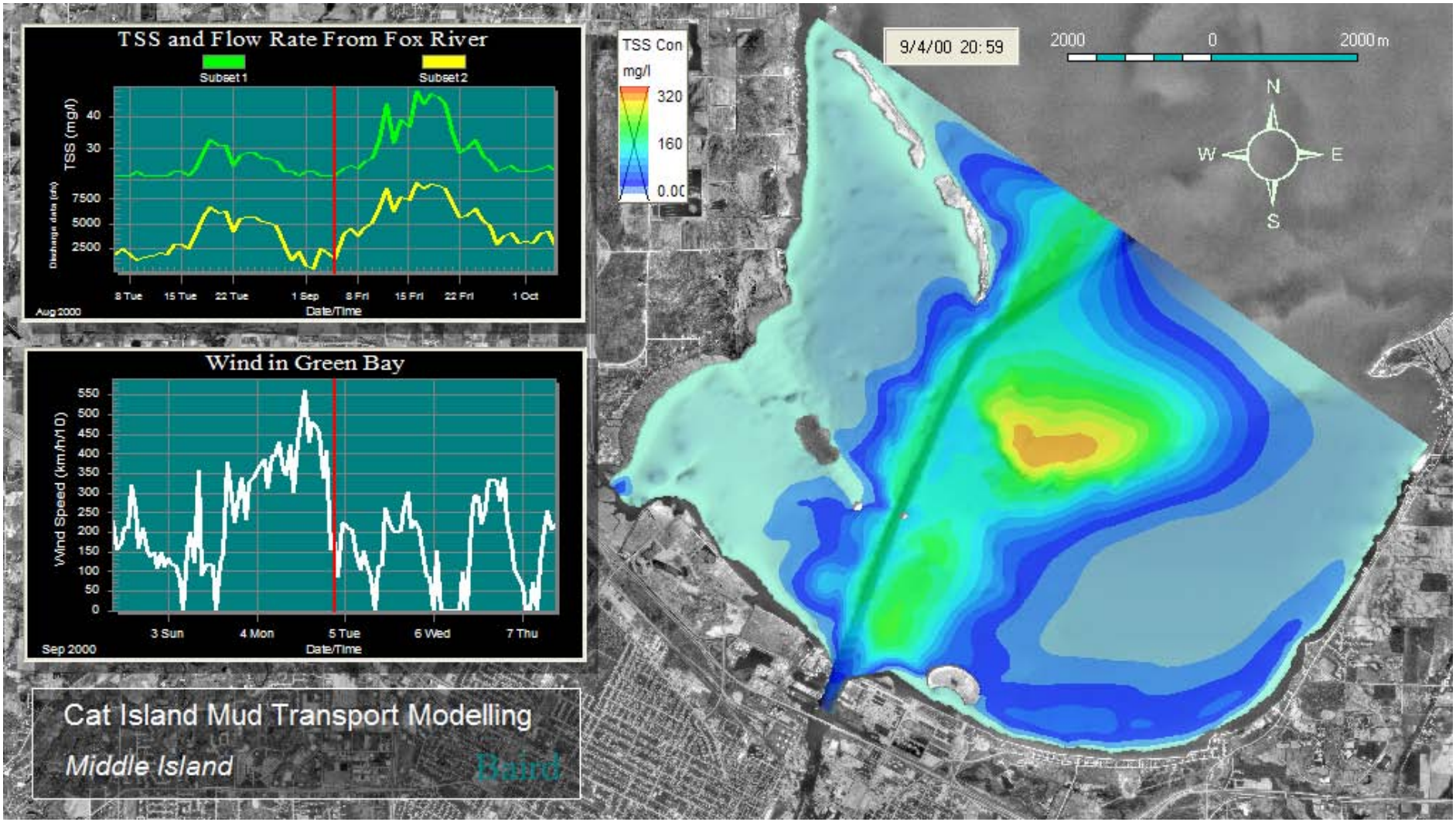

Figure A39 Mud Transport Modeling for Run 4 after Storm –Middle Island

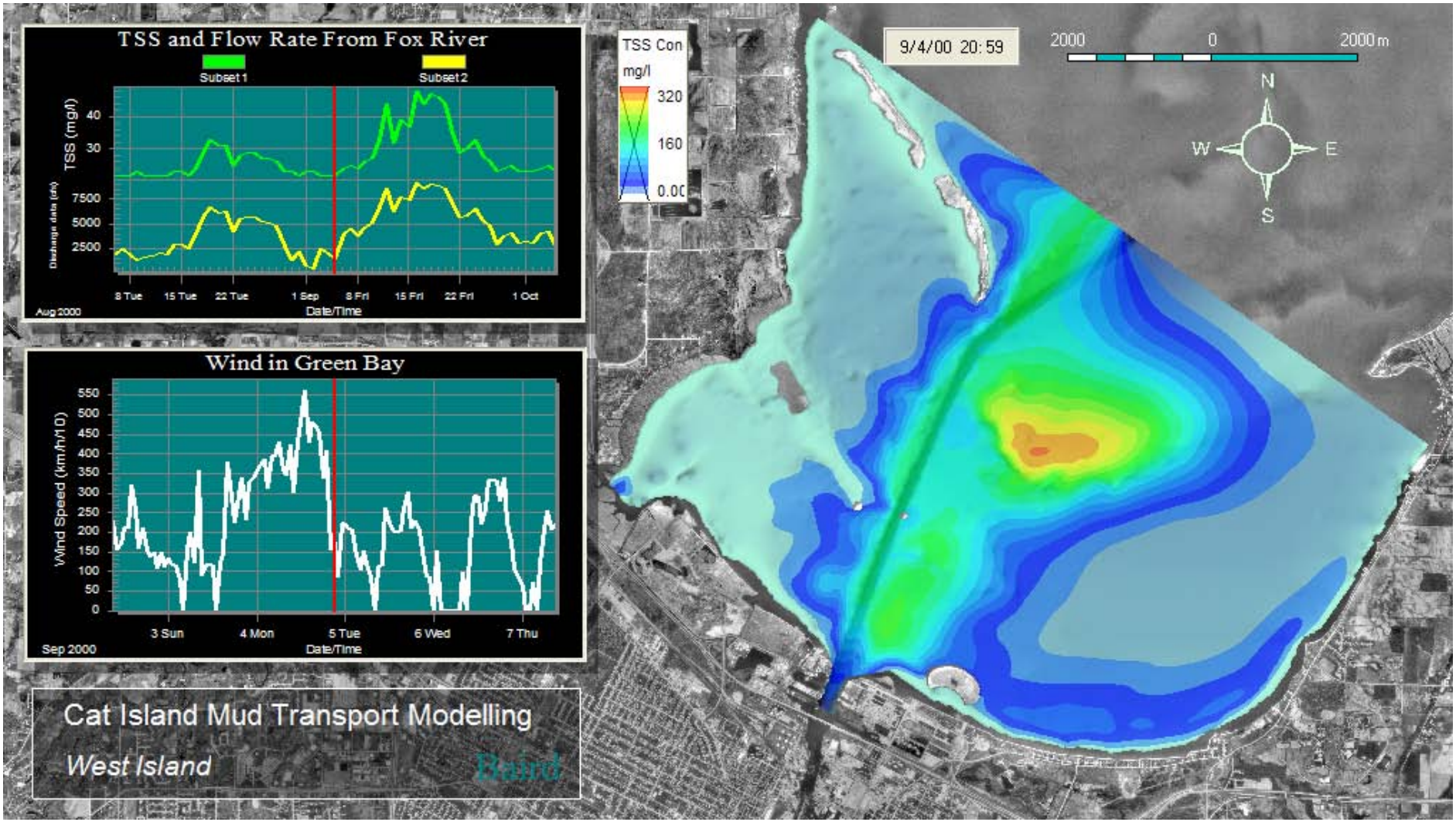

Figure A40 Mud Transport Modeling for Run 4 after Storm – West Island

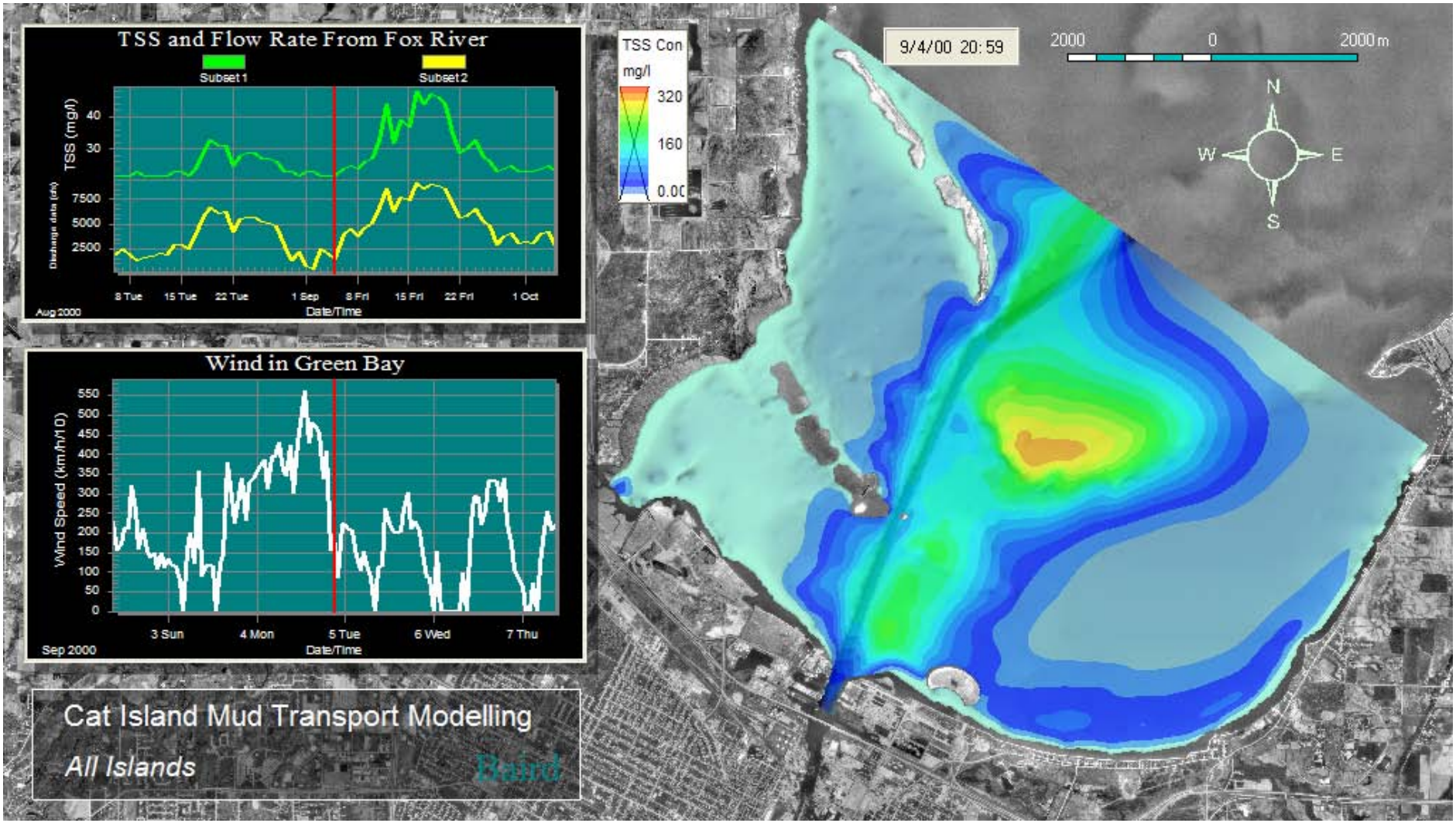

Figure A41 Mud Transport Modeling for Run 4 after Storm – All Island

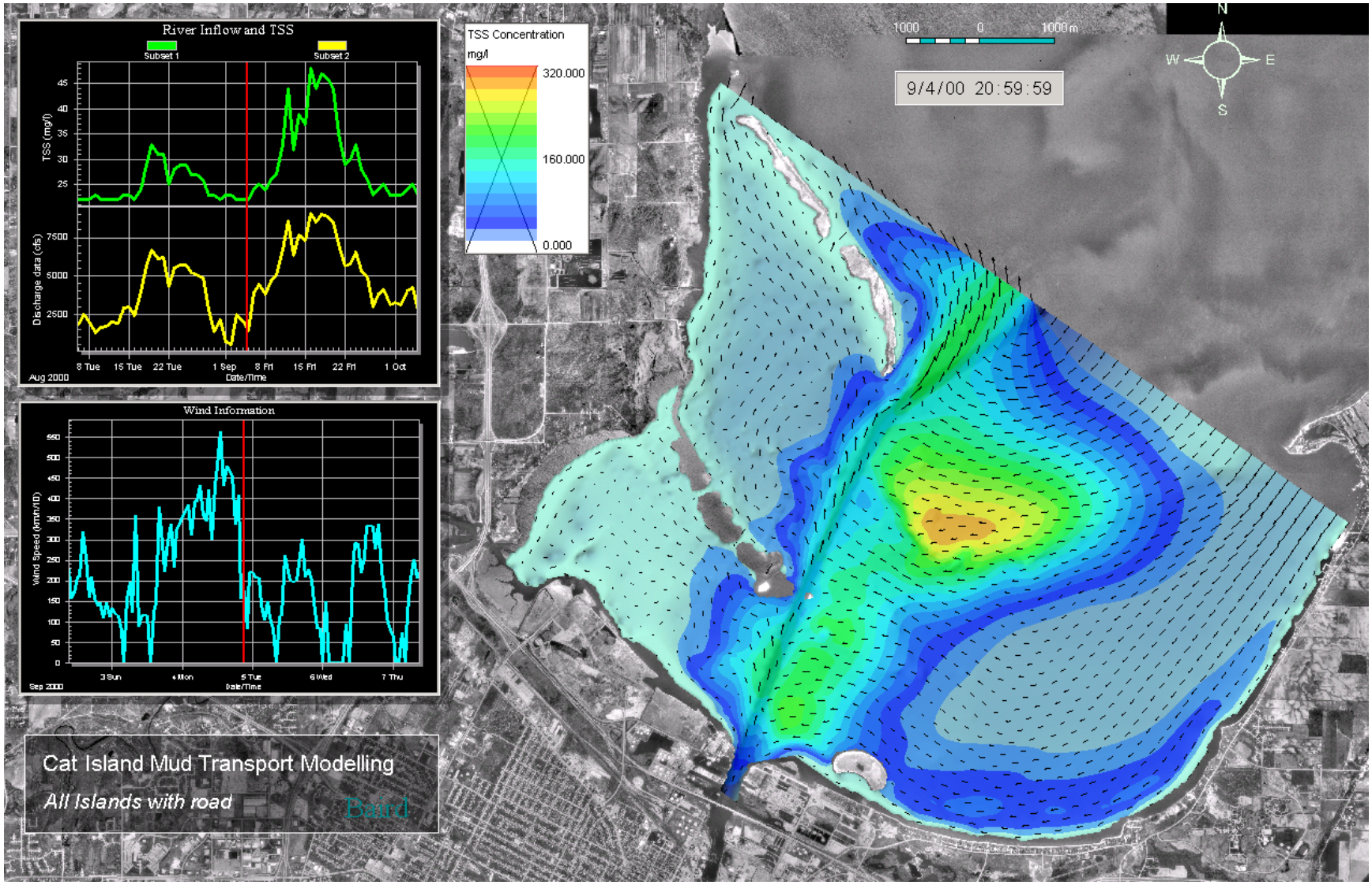

Figure A42 Mud Transport Modeling for Run 4 after Storm – All Island with Road

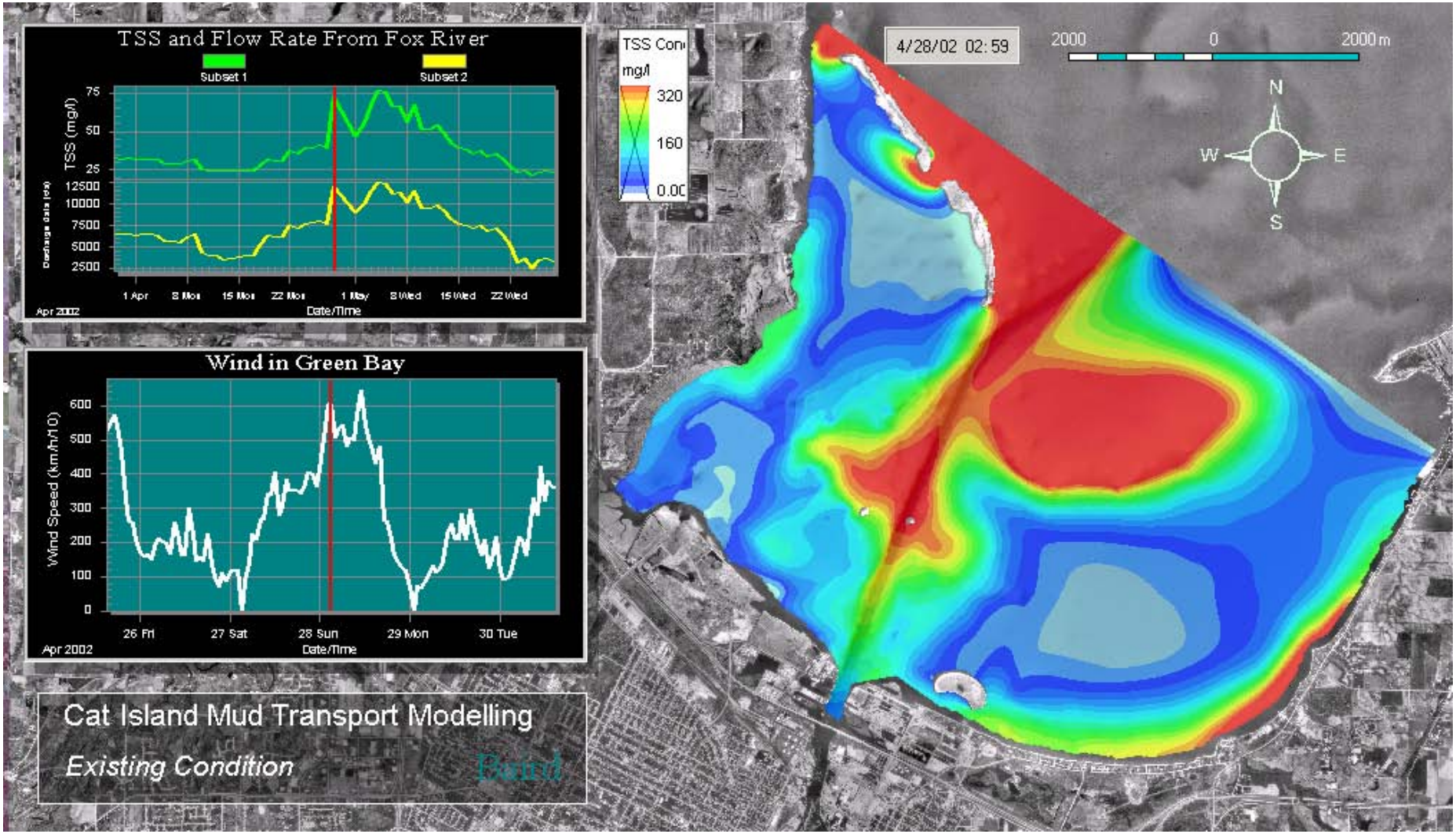

Figure A43 Mud Transport Modeling for Run 5 at TSS Peak – Existing Condition

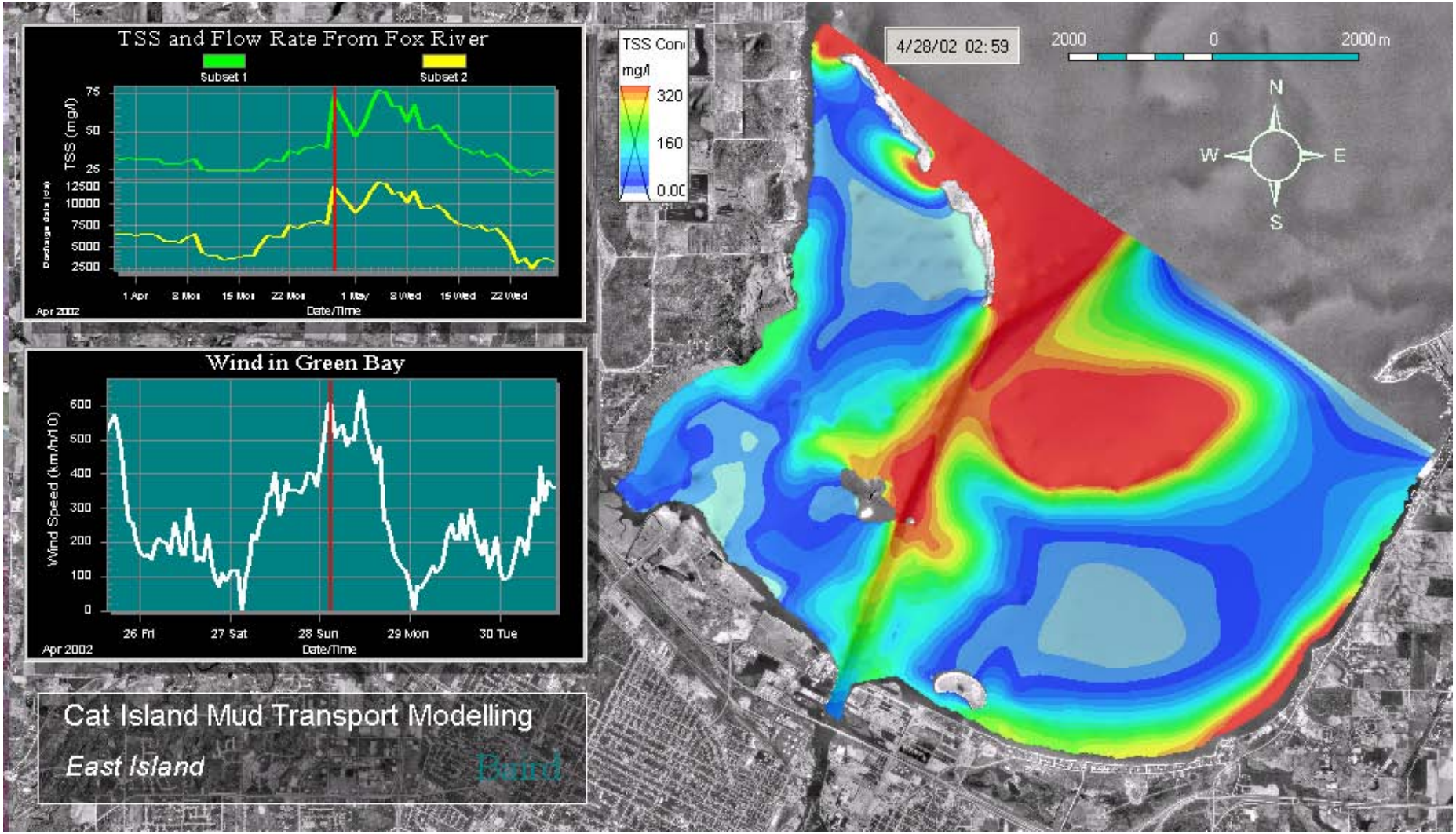

Figure A44 Mud Transport Modeling for Run 5 at TSS Peak – East Island

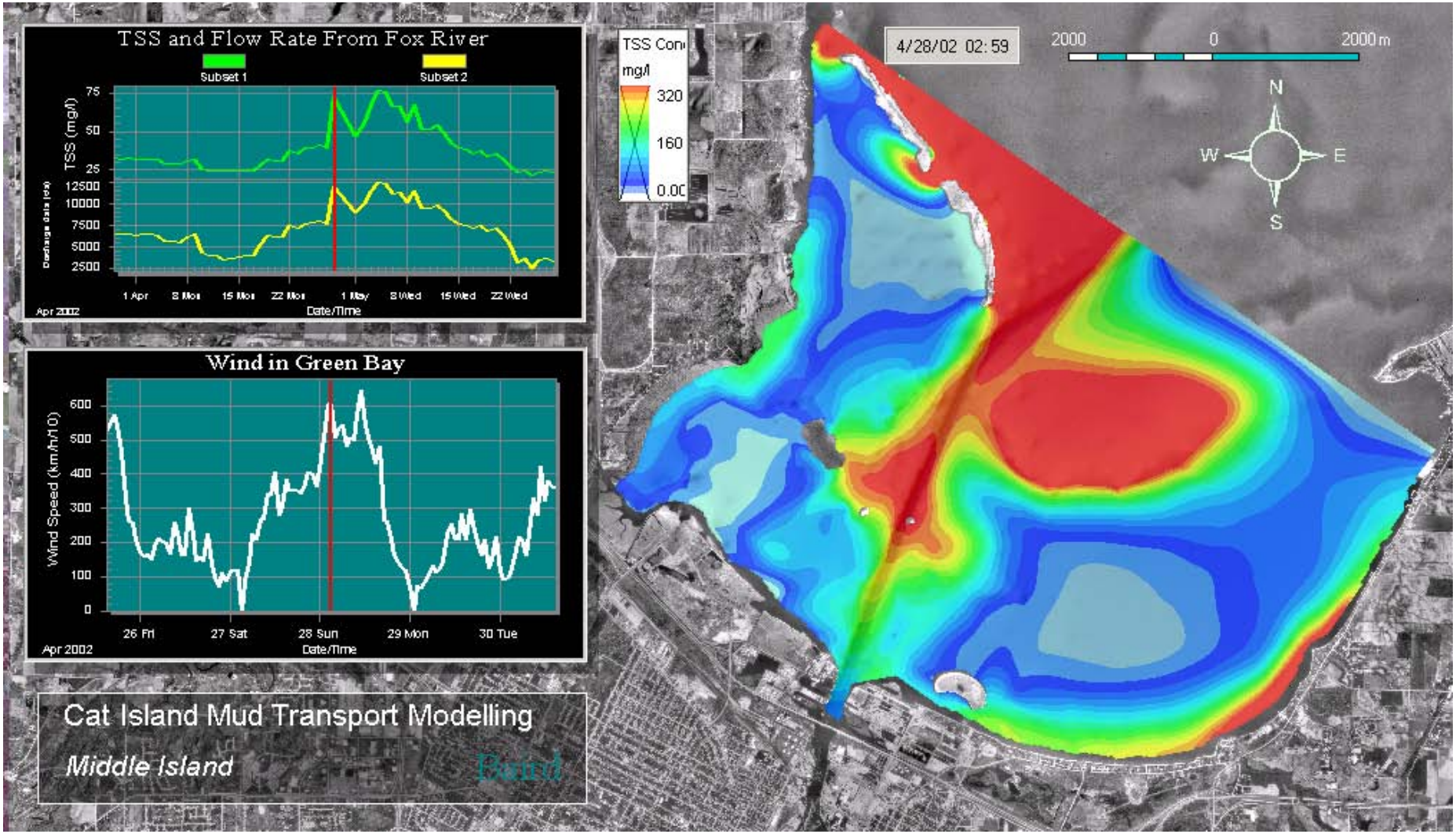

Figure A45 Mud Transport Modeling for Run 5 at TSS Peak – Middle Island

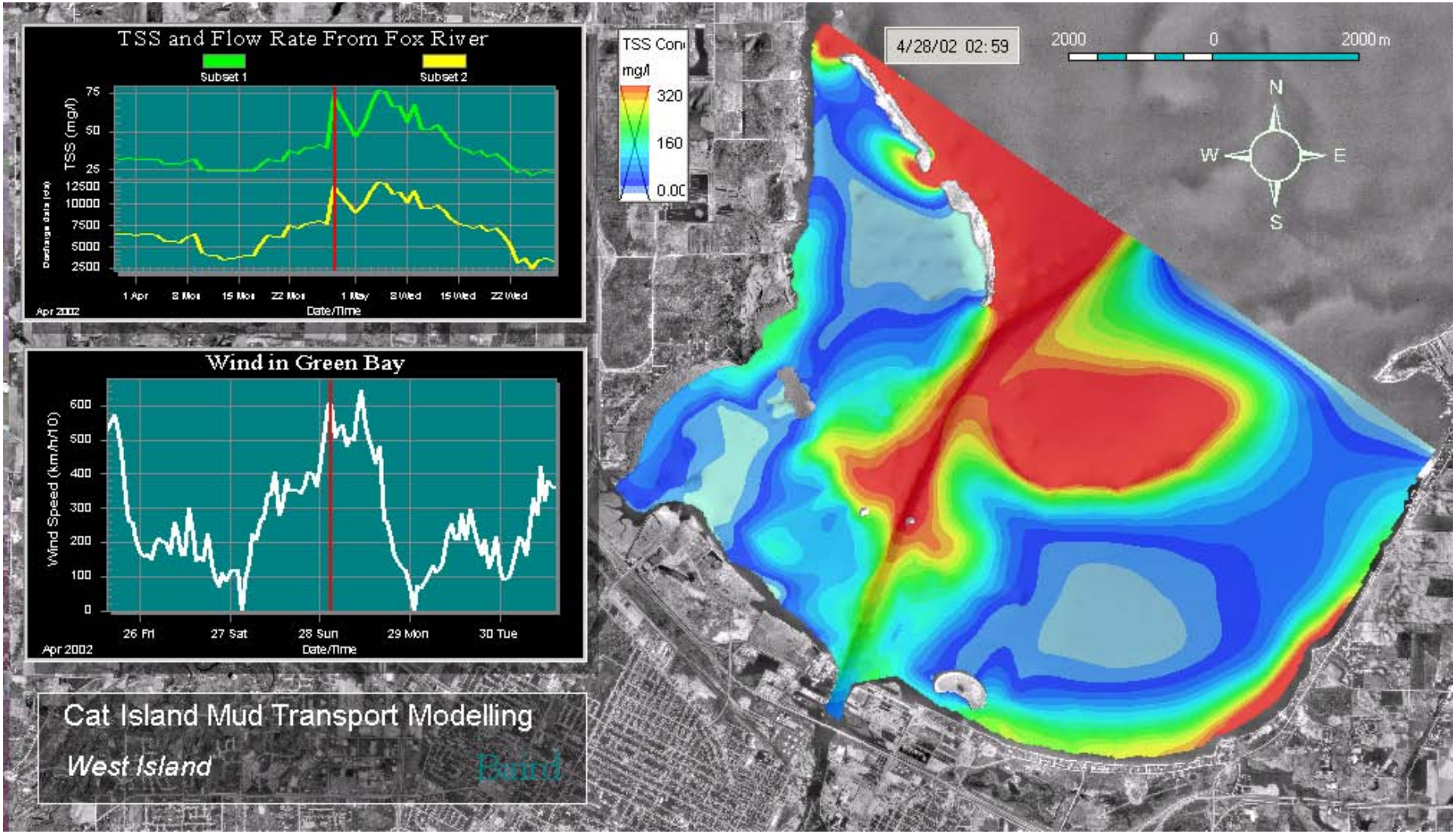

Figure A46 Mud Transport Modeling for Run 5 at TSS Peak – West Island

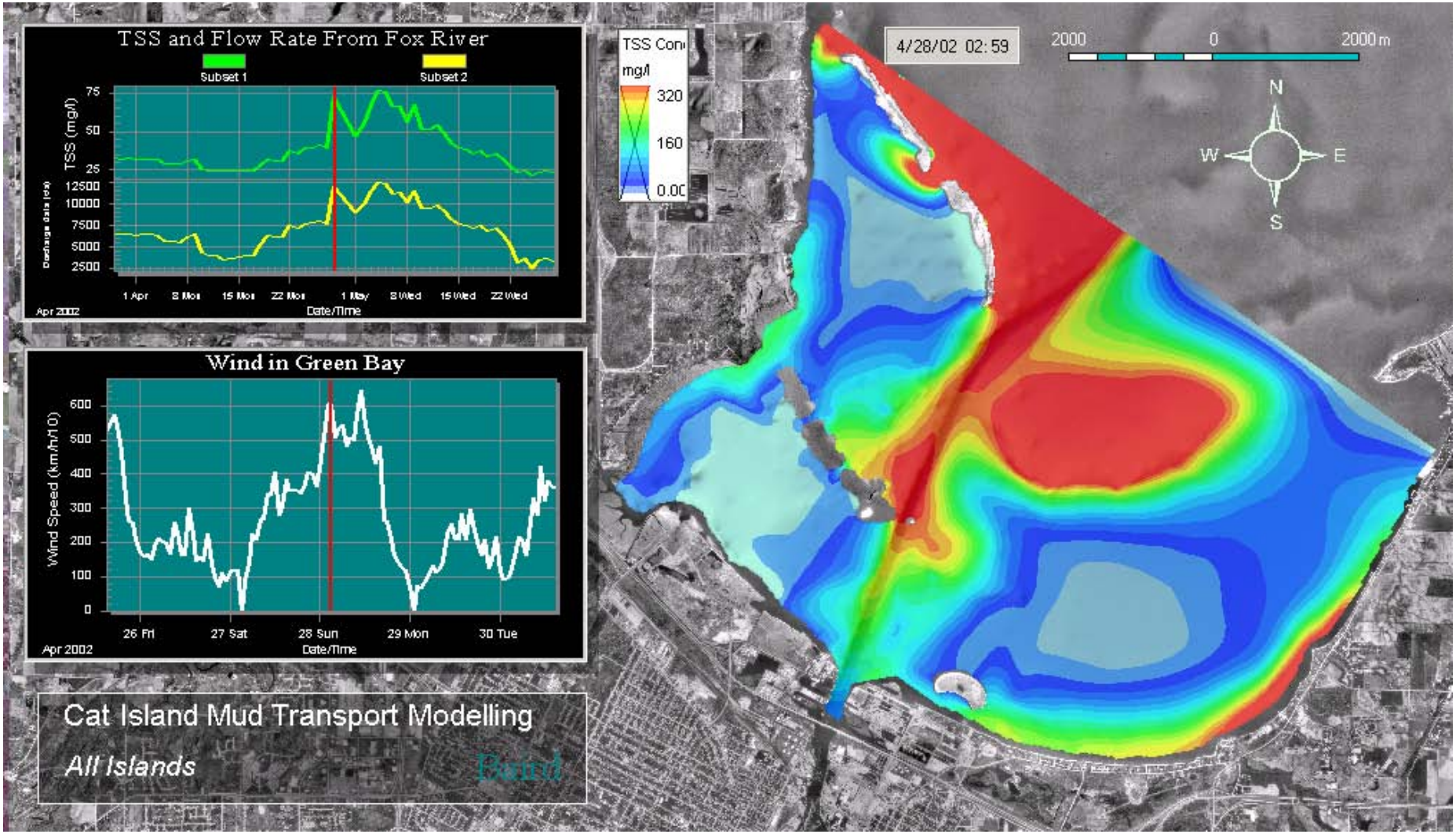

Figure A47 Mud Transport Modeling for Run 5 at TSS Peak – All Island

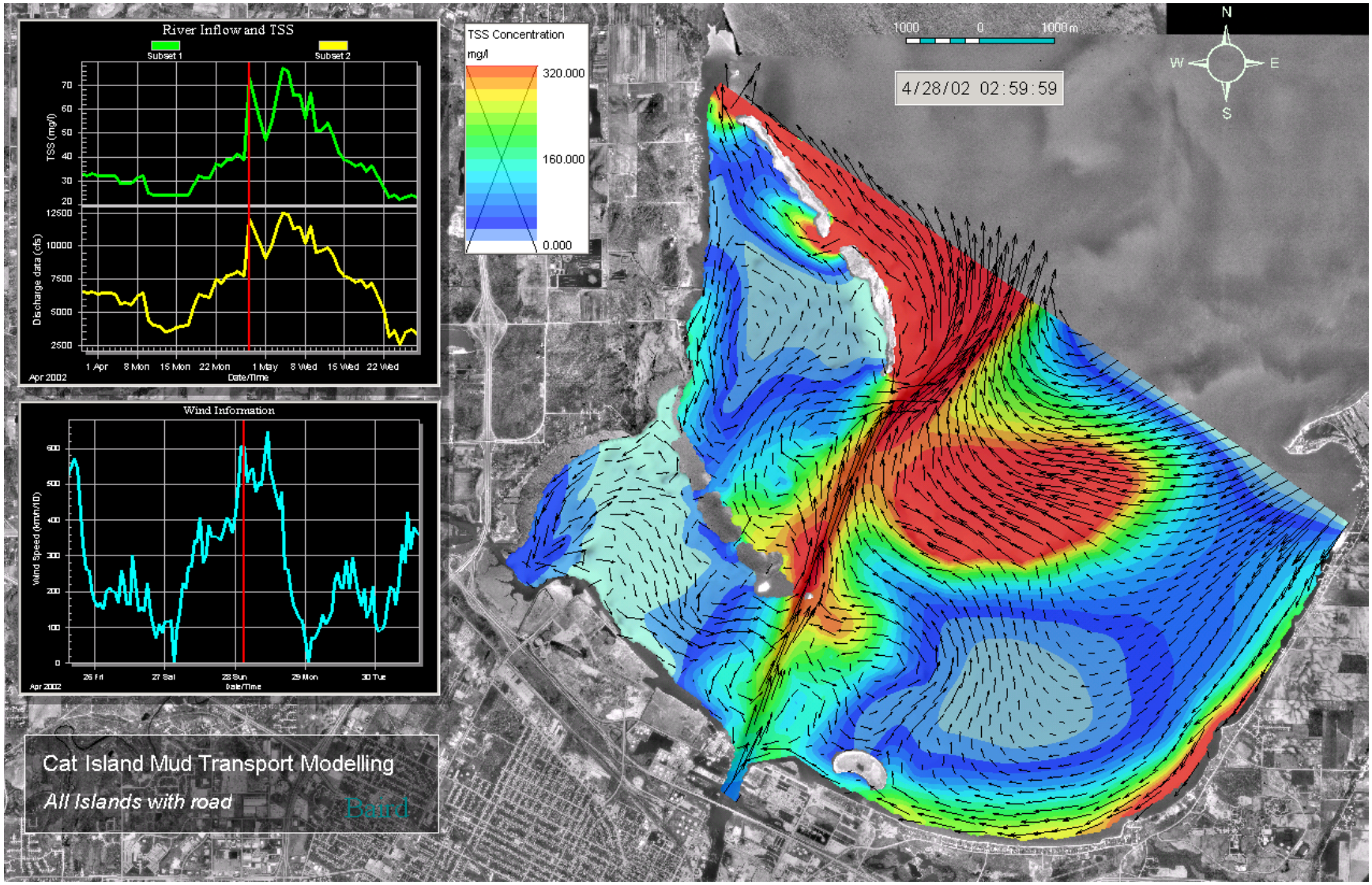

Figure A48 Mud Transport Modeling for Run 5 at TSS Peak – All Island with Road

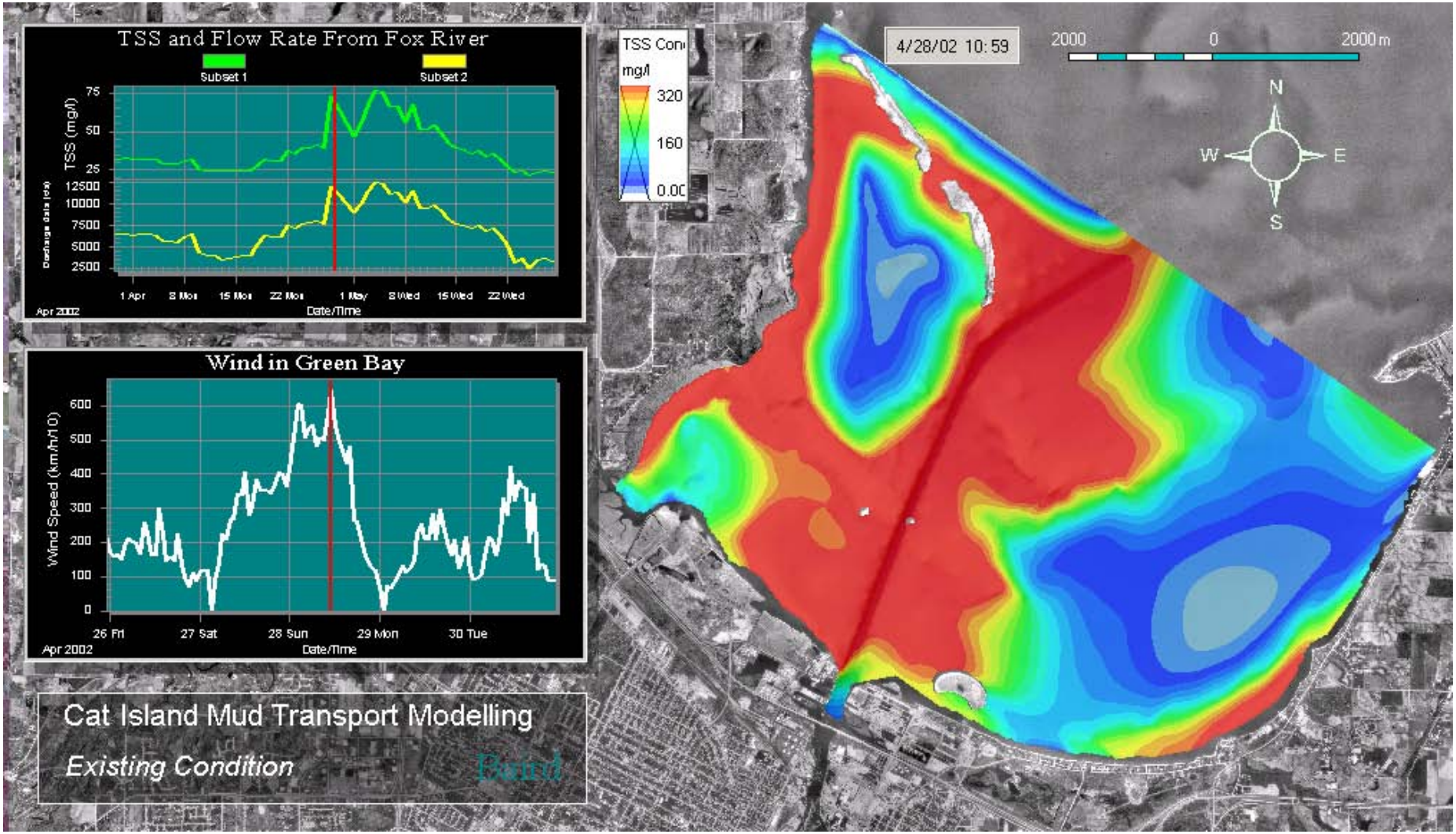

Figure A49 Mud Transport Modeling for Run 5 at Wind Peak – Existing Condition

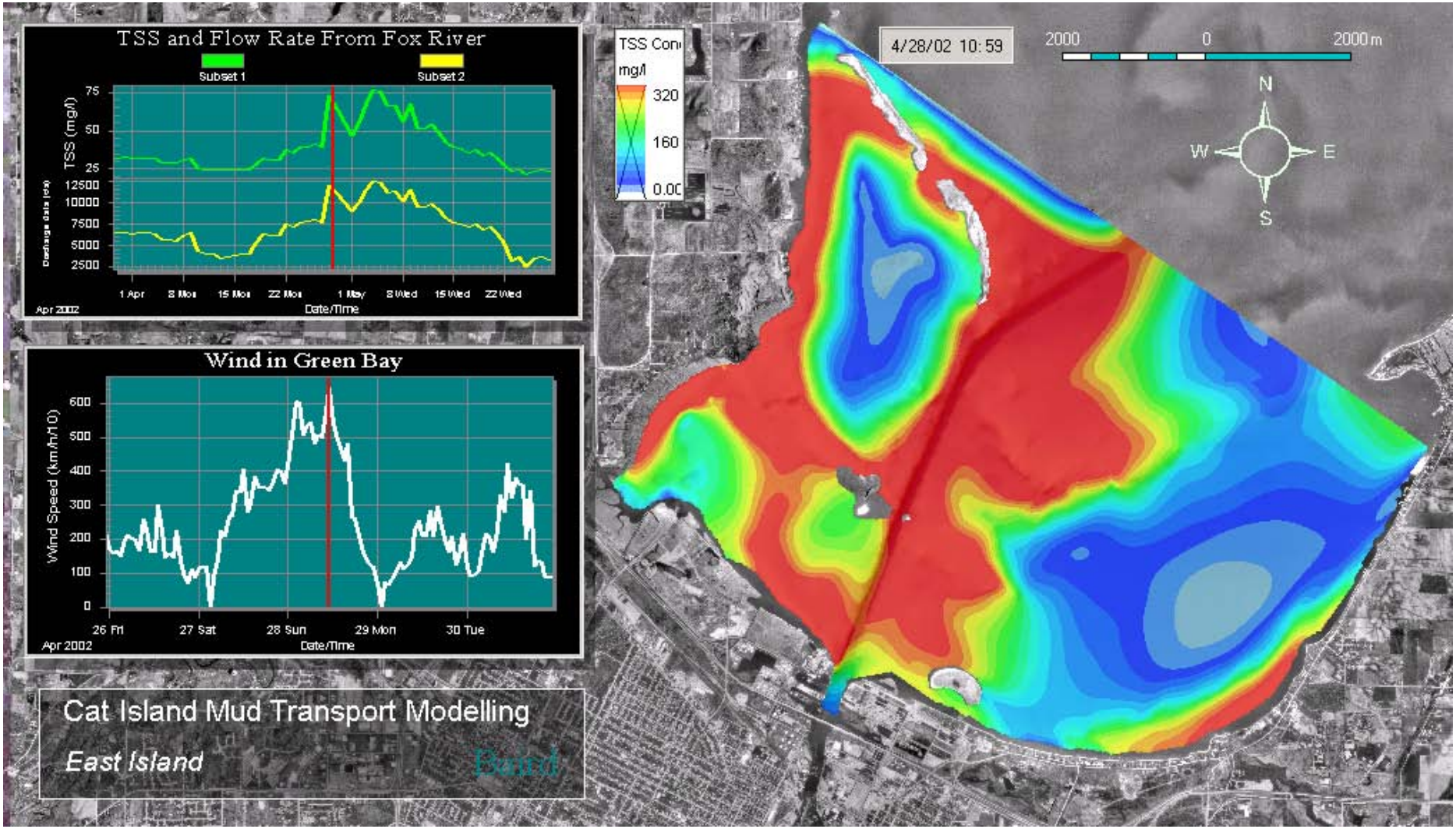

Figure A50 Mud Transport Modeling for Run 5 at Wind Peak – East Island

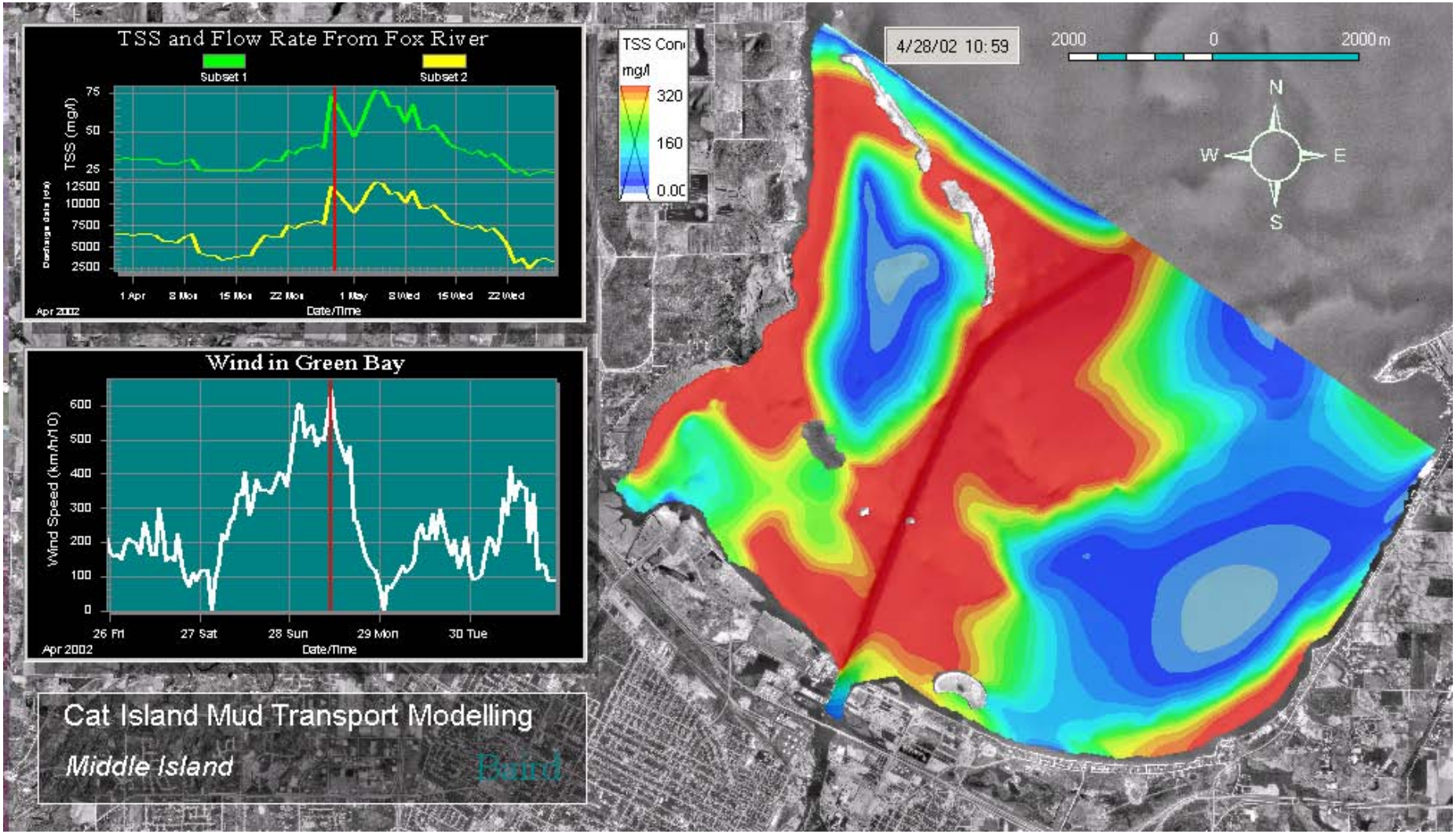

Figure A51 Mud Transport Modeling for Run 5 at Wind Peak – Middle Island

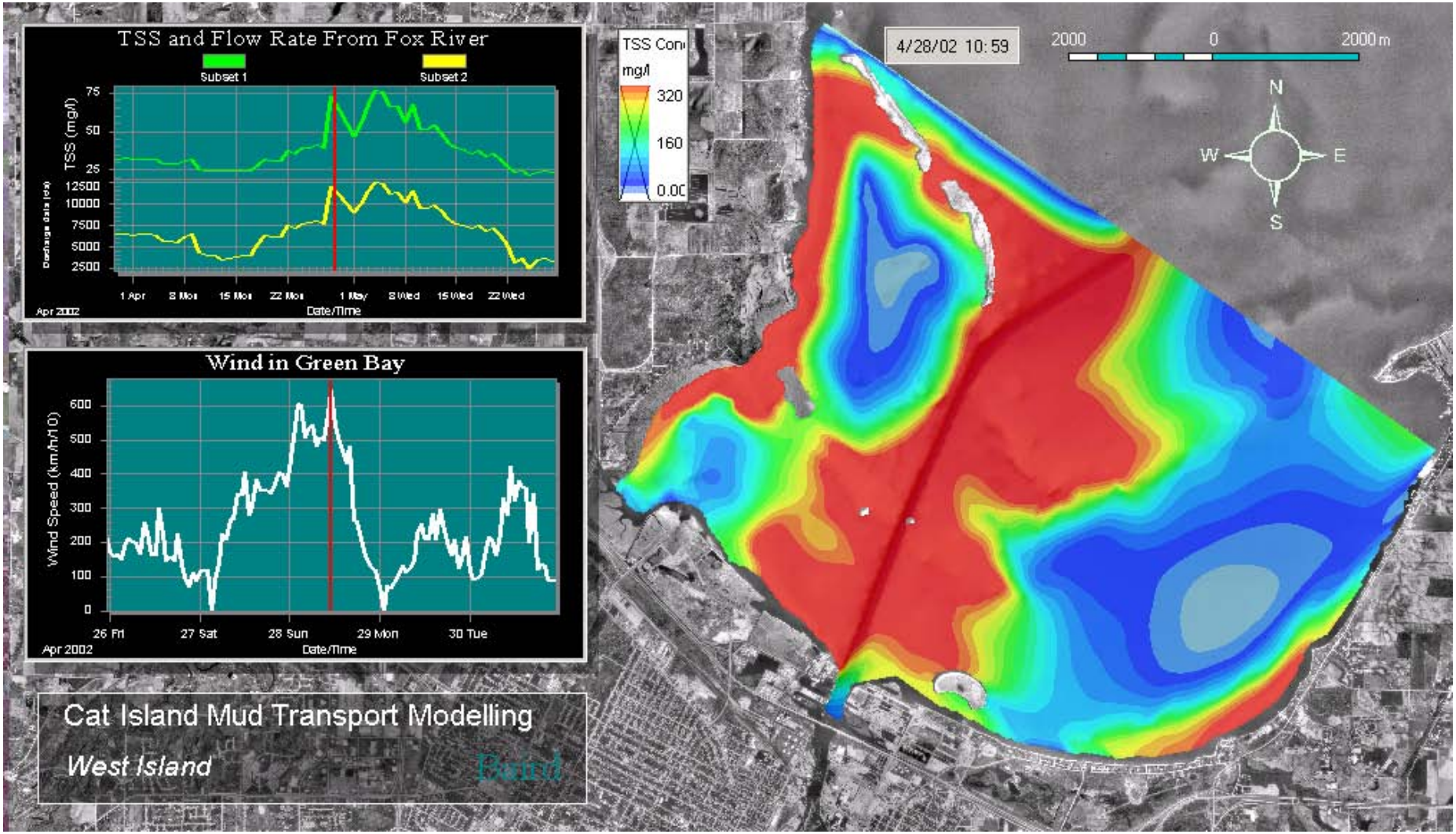

Figure A52 Mud Transport Modeling for Run 5 at Wind Peak – West Island

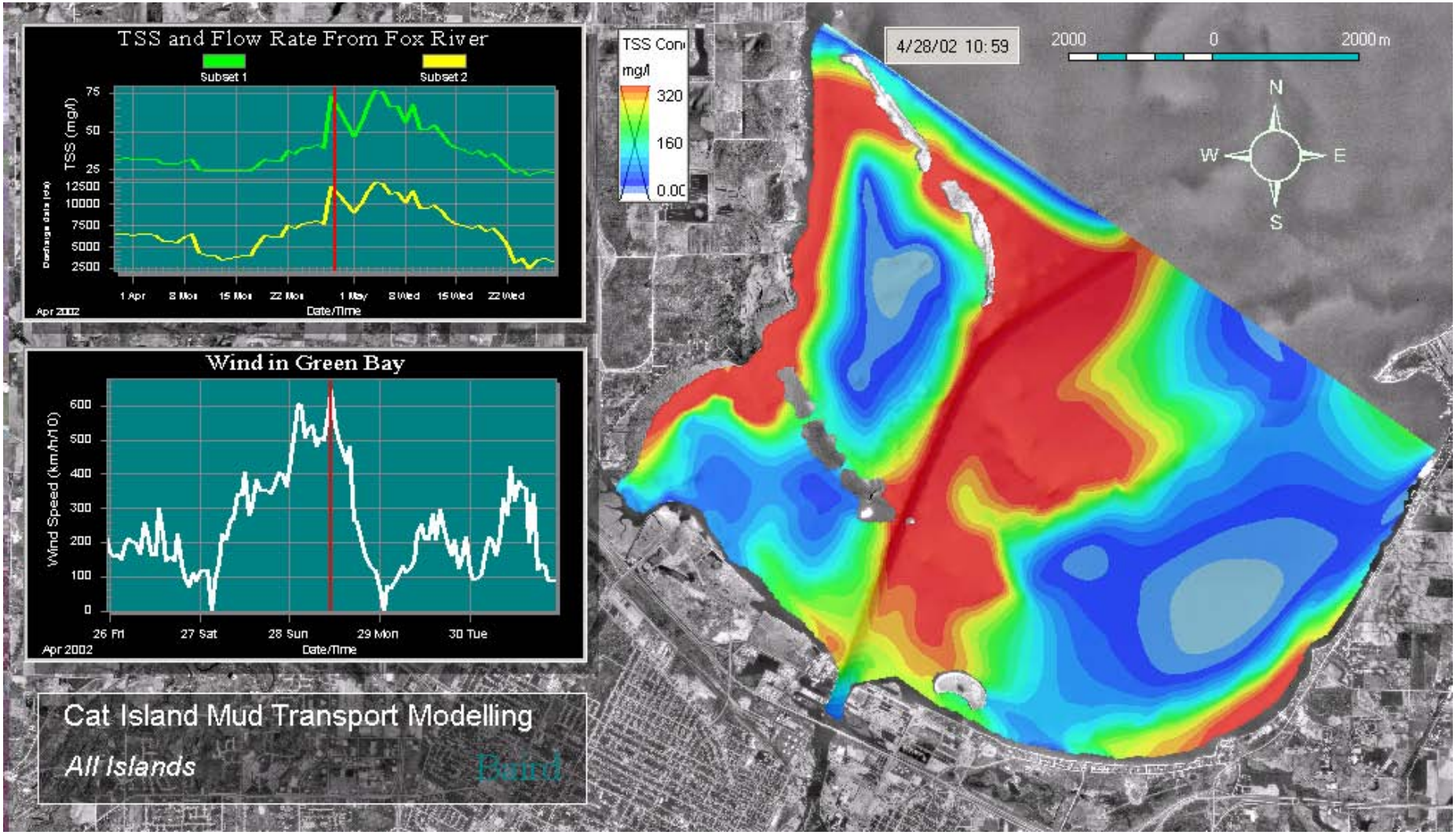

Figure A53 Mud Transport Modeling for Run 5 at Wind Peak – All Island

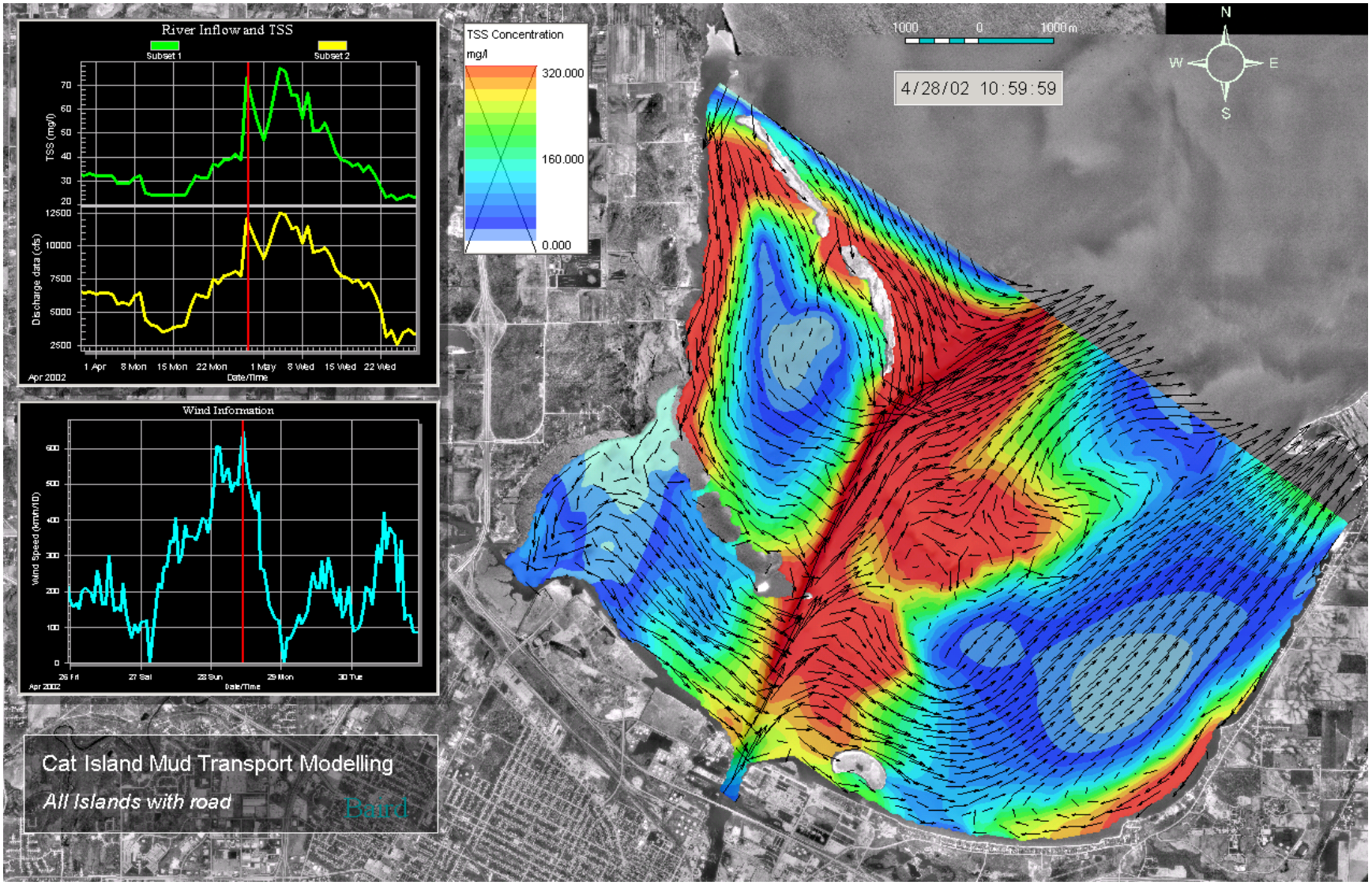

Figure A54 Mud Transport Modeling for Run 5 at Wind Peak – All Island with Road